Die Interaktionsnetzwerke von Ras-Proteinen

Inaugural-Dissertation

zur Erlangung des Doktorgrades
der Mathematisch-Naturwissenschaftlichen Fakultät
der Heinrich-Heine-Universität Düsseldorf

vorgelegt von
Hossein Nakhaeizadeh
aus Mashhad, Iran

Düsseldorf, October 2016

Aus dem Institut für Biochemie und Molekularbiologie II
der Heinrich-Heine-Universität Düsseldorf

Gedruckt mit der Genehmigung der
Mathematisch-Naturwissenschaftlichen Fakultät der
Heinrich-Heine-Universität Düsseldorf

Referent: Prof. Dr. Reza Ahmadian
Prof. Dr. Dieter Willbold
Tag der mündlichen Prüfung: 01 Dec 2016

Table of contents

Summary

Proteins of the Ras family act as molecular switches, cycling between a GTP-bound (active) and a GDP-bound (inactive) state. These molecules sense extracellular signals through activation of transmembrane receptors and intermediate proteins transduce them to downstream targets and trigger, thereby, intracellular responses. Thus, Ras proteins play a key role in various cellular processes, including gene expression, metabolism, cell cycle progression, proliferation, survival, and differentiation. Contrary to the best-investigated Ras isoforms (H-, N- and K-Ras) the individual roles of other members of the Ras family, such as E-Ras or the R-Ras isoforms, have not been fully described. E-Ras, a unique member of the Ras family, is specifically expressed in undifferentiated mouse embryonic stem cells, in several tumor cells, including gastric cancer and neuroblastoma, and also in quiescent hepatic stellate cells, as we have shown recently. E-Ras contains a unique N-terminal extension (38 amino acids) upstream of its GDP/GTP binding domain. However, the function of such an additional region with various motifs remained unclear. We found that the N-terminal extension is essential for E-Ras signaling activity, especially towards PI3K-AKT pathway. Most remarkably, E-Ras revealed a different pattern of interaction with downstream effectors as compared to H-Ras, correlating with amino acid deviations in the effector-binding site. Of all these residues, tryptophan 79 determines the effector selectivity of E-Ras for PI3Ks. A comparative proteome analysis of the N-terminal extension of human and rat E-Ras proteins, which exhibit remarkable sequence deviations, led to the identification of 51 associated proteins (10 with the human E-Ras, 3 with rat E-Ras and 38 with both species). These interactions appear to participate in distinct cellular processes, including cell cycle, transcription, immune response, signal transduction, cell adhesion, cytoskeletal dynamics and metabolism. One of these proteins is the cytosolic Arginase-1, which is known to convert L-arginine to L-ornithine. Interaction studies showed that Arginase-1 physically binds to different E-Ras variants, including isolated E-Ras N-terminus, under cell-free condition using purified proteins and also using lysates of hepatic stellate cells. E-Ras turned out to positively modulate the activity of Arginase-1 and may therefore play a role in the synthesis of polyamines. Equilibrium dissociation constants for the interaction of H-Ras, K-Ras, N-Ras, R-Ras1 and R-Ras2 with both the Ras binding (RB) domain of CRAF and PI3Kα, and the Ras association (RA) domain of RASSF5, RALGDS and PLCε, respectively, were determined using fluorescence polarization. Obtained quantitative data led to the observation of different effector selectivity for Ras and R-Ras isoforms. In combination with detailed in silico analyses we generated a matrix for RAS-effector interactions, on the basis of this interaction matrix we defined five distinct regions, with R1 being central recognition region with mainly intermolecular β-sheet contacts and R3 being a

determinant for isoform specificity. Finally, we revise the current model for the interaction of galectin-1 with H-Ras. Showing that galectin-1 indirectly forms a complex with H-Ras via direct binding to CRAF-RB strongly suggests a new model for H-Ras nanoclustering in plasma membrane. Collectively, data obtained in this thesis provide new insights into protein-protein interaction networks and the physical environment of Ras proteins, and may ultimately open new perspectives in elucidating novel modulatory mechanisms of Ras proteins especially in human diseases.

Zusammenfassung

Proteine der Ras Familie agieren als molekulare Schalter und wechseln zwischen der aktiven, GTP- gebundenen Form und der inaktiven, GDP- gebundenen Form. Diese Moleküle erfassen extrazelluläre Signale durch die Aktivierung von Transmembranrezeptoren, und übermitteln diese Signale mittels dazwischenliegender Proteine an nachgeschaltete Zielproteine für intrazelluläre Antworten. Demzufolge spielen Ras Proteine eine erhebliche Rolle bei verschiedenen zellulären Prozessen, wie Genexpression, Stoffwechselprozessen, Zellzyklusprogression, Proliferation, Überleben der Zelle und Zelldifferenzierung. Im Gegensatz zu den am besten untersuchten Ras Isoformen (H-, N- und K- Ras), sind die Funktionen von anderen Isoformen, wie E- Ras oder R- Ras, bisher nicht vollständig beschrieben. E- Ras, welches ein besonderes Mitglied der Ras Familie darstellt, wird, wie wir kürzlich zeigen konnten, speziell in undifferenzierten, embryonalen Stammzellen der Maus, verschiedenen Tumorzellen, wie Magenkarzinoma und Neuroblastoma, als auch in ruhenden Sternzellen der Leber exprimiert. E- Ras verfügt oberhalb der GDP/GTP- Bindungsdomäne über eine einzigartige N- terminale Verlängerung von 38 Aminosäuren. Die Funktion dieser zusätzlichen Region mit verschiedenen Motiven war bisher unklar. Wir konnten zeigen, dass dieser einmalige N- terminale Verlängerung wesentlich für die E- Ras Signalaktivität ist, vor allem in Richtung des PI3K-AKT Signalweges. Besonders auffallend ist, dass E- Ras im Vergleich zu H- Ras ein unterschiedliches Interaktionsmuster mit nachgeschalteten Effektoren aufweist, welches mit der Abweichung der Aminosäuren in der Effektorbindungsstelle korreliert. Von all diesen Aminosäureresten ist Tryptophan 79 ausschlaggebend für die Effektorselektivität von E- Ras für PI3Ks. Eine proteomische Analyse der N- terminalen Verlängerung bei E-Ras Proteinen des Menschen und der Ratte, welche deutliche Unterschiede in der Sequenz aufweisen, führten zur Identifikation von 51 assoziierenden Proteinen (10 mit dem humanen E- Ras, 3 mit dem E- Ras der Ratte und 38 mit beiden Spezies). Diese Interaktionen ermöglichen verschiedene zelluläre Prozesse, wie Zellzyklus, Transkription, Immunantwort, Signaltransduktion, Zelladhäsion, dynamische Regulation des Zytoskellets und Stoffwechselprozesse. Eines dieser Proteine ist die zytosolische Arginase-1, welche dafür bekannt ist, L-Arginin in L-Ornithin umzuwandeln. Interaktionsstudien haben bewiesen, dass Arginase-1 verschiedene E-Ras Varianten bindet, einschließlich dem isolierten N- Terminus von E- Ras. Diese Interaktionsstudien wurden unter zellfreien Bedingungen sowohl mit aufgereinigten Proteinen, als auch mit Lysaten von Lebersternzellen durchgeführt. Es stellte sich heraus, dass E- Ras die Aktivität von Arginase-1 positiv reguliert und somit eine entscheidene Rolle bei der Synthese von Polyaminen spielt. Die Gleichgewichts-Dissoziationskonstanten für die Interaktionen von H-Ras, K-Ras, N-Ras, R-Ras1 and R-Ras2 sowohl mit den Ras- Bindungsdomänen (RBD) von CRAF und PI3Kα, als auch mit den Ras- Assoziationsdomänen (RAD) von RASSF5, RALGDS und PLCε wurden jeweils mittels Fluoreszenzpolarisation bestimmt. Die gewonnen Daten zeigen unterschiedliche Effektorselektivitäten für Ras und die R-Ras Isoformen. Mittels *in*

silico Analysen wurde eine Matrix für RAS-Effektor Interaktionen entwickelt und auf der Basis dieser fünf verschiedene Regionen definiert, wobei R1 als zentrale Erkennungsregion dient und R3 eine Determinante für Isoformspezifität darstellt. Zusätzlich konnten wir das aktuelle Model für die Interaktion zwischen Galectin-1 und H-Ras überarbeiten und zeigen, dass Galectin-1 durch die direkte Bindung von CRAF-RBD einen Komplex mit H-Ras bildet und somit ein neues Model für das Nanoclustering von H-Ras in Plasmamembranen suggerieren. Insgesamt liefern die gewonnenen Daten dieser Doktorarbeit neue Einblicke sowohl in Protein-Protein Interaktionsnetzwerke, als auch in die physische Umgebung der Ras Proteine, wodurch sich neue Perspektiven in der Erläuterung neuartiger regulierender Mechanismen der Ras Proteine, speziell in menschlichen Erkrankungen, eröffnen.

Table of Figures

Abbreviation

ARG1	Arginase1
CaM	Calmodulin
CR	conserved regions
CRD	cysteine-rich domain
DEP	Dishevelled/Egl-10/Pleckstrin
ECM	extracellular matrix
E-Ras	embryonic stem cell-expressed RAS
ERK	extracellular regulated kinase
FTS	farnesylthiosalicylic acid
FOXO1	forkhead transcription factor 1
Gal-1	Galectin-1
GAP	GTPase-activating protein
GDP	guanosine diphosphate
GEF	guanine nucleotide exchange factor
GFAP	glial fibrillary acidic protein
Grb2	Growth factor receptor-bound protein 2
GTP	guanosine triphosphate
HVR	hypervariable region
HSC	hepatic stellate cell
IQGAPs	IQ-domain GTPase- activating proteins
K-Ras	kirsten rat sarcoma
MAPK	mitogen-activated protein kinase
MAPKAP1	Mitogen-Activated Protein Kinase Associated Protein 1
MEK	MAP/ERK kinase
M-Ras	muscle rat sarcoma
MSC	mesenchymal stem cell
mSin1	mammalian stress-activated MAP kinase-interacting protein 1
Mst	mammalian sterile 20-like kinase
mTOR	mammalian target of rapamycin
mTOR	mammalian target of rapamycin complex
NF	neurofibromin
Nore1	novel RAS effector 1
NOSs	nitric oxide synthases
NPM1	nucleophosmin
N-Ras	neuroblastoma rat sarcoma
PDB	protein data bank
PDK1	3-phosphoinositide-dependent protein kinase 1
PH	pleckstrin homology
PI3K	phosphoinositide 3-kinase
PIP_2	phosphatidylinositol (4,5)-bisphosphate
PIP_3	phosphoinositide 3,4,5-trisphosphate
PLC	phospholipase C
PTM	post-translational modification
RA	Ras association
RAC	RAS-related C3 botulinum toxin substrate
RAF	rapidly accelerated fibrosarcoma
RalA	Ras-related protein Ral-A
RalGDS	guanine nucleotide dissociation stimulator
RalGEF	Ral specific guanine nucleotide exchange factor
RAS	rat sarcoma
RasGEF	Ras specific guanine nucleotide exchange factor
RasGRF	Ras-specific guanine nucleotide-releasing factor
RasGRP	RAS guanyl-releasing protein

RASSF	RAS-association domain family
Rap2A	Ras-related protein2A
RBD	Ras binding domain
REM	Ras exchanger motif
RGL	RALGDS like
RHO	RAS homolog
RTK	Receptor tyrosine kinase
SARAH	Salvador/Rassf/Hippo
SH2	src homology 2
SH3	src homology 3
SIN1	Stress-Activated Map Kinase-Interacting Protein 1
SOS	son of Sevenless

Amino Acids abbreviation

Name	Letter codes	Name	Letter codes	Name	Letter codes	Name	Letter codes
alanine	Ala (A)	glutamic acid	Glu (E)	leucine	Leu (L)	serine	Ser (S)
arginine	Arg (R)	glutamine	Gln (Q)	lysine	Lys (K)	threonine	Thr (T)
asparagine	Asn (N)	glycine	Gly (G)	methionine	Met (M)	tryptophan	Trp (W)
aspartic acid	Asp (D)	histidine	His (H)	phenylalanine	Phe (F)	tyrosine	Tyr (Y)
cysteine	Cys (C)	isoleucine	Ile (I)	proline	Pro (P)	valine	Val (V)

Chapter I

General Introduction

The discovery of the RAS proto-oncogenes

Ras genes were identified in the late 1970s and the early 1980s as oncogenes (Bos, 1989; Der, 1989; Karnoub and Weinberg, 2008). The K-Ras and H-Ras genes were first discovered as the v-K-Ras and v-H-Ras oncogenes of sarcoma viruses (Chien et al., 1979; Shih et al., 1978). Their cellular oncogenes were then identified in human and their mutations were furthermore found in some human carcinomas (Der et al., 1982; Parada et al., 1982; Santos et al., 1982) (Hall et al., 1983; Murray et al., 1983; Shimizu et al., 1983). Ras genes are the most frequently mutated oncogenes in both solid tumors and hematologic neoplasia with single point mutations at codons 12, 13 or 61 (Barbacid, 1990; Beaupre and Kurzrock, 1999; Bos, 1989; Guerrero and Pellicer, 1987; Scheele et al., 2000). The frequency of mutated Ras genes (K-Ras, N-Ras, H-Ras) varies widely depending on the type of cancer. The most commonly mutated gene in solid tumors is the K-Ras gene, with the highest incidence in pancreatic (90%) and colorectal carcinomas (60%) (Almoguera et al., 1988; Burmer and Loeb, 1989). N-Ras, however, is the most frequently mutated gene in wide variety of human leukemias with an incidence of up to 60% in chronic myelomonocytic leukemia and up to 40% in acute myelogenous leukemia (Ahuja et al., 1990; Hirsch-Ginsberg et al., 1990; Janssen et al., 1987).

Ras as the prototype of a superfamily

Ras is the prototype of the superfamily of the small GTP-binding and hydrolyzing proteins (or GTPases), which are monomeric proteins with molecular masses of 20-30 kDa. More than 150 small GTPases have been identified in eukaryotes from yeast to human and they comprise a superfamily (Bourne *et al.*, 1990; Matozaki *et al.*, 2000; Rojas *et al.*, 2012; Wennerberg *et al.*, 2005). The members of Ras superfamily are structurally classified into five major families: Ras, Rho, Rab, Arf and Ran (Figure 1; (Rojas *et al.*, 2012)). The functions of these five families have extensively been elucidated: the Ras family mainly regulates cell growth, differentiation, gene expression and apoptosis; the Rho family regulates both cytoskeletal reorganization and gene expression; the Rab and Arf families regulate intracellular vesicle formation, trafficking and fusion; Ran regulates nucleocytoplasmic transport.

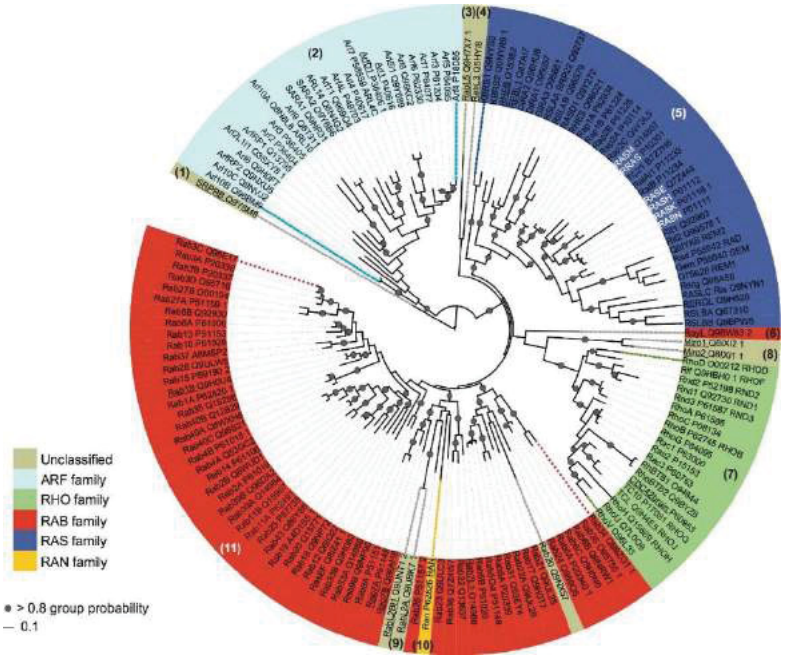

Figure 1: Phylogenetic tree of the human Ras superfamily.
The tree contains 151 sequences that were aligned according to their G-domain. The background colors indicate the original classification of the superfamily in distinct families: blue, Ras family; green, Rho; red, Rab; cyan, Arf; and yellow, Ran. Unclassified members are shown in beige. For more details see the original article of Rojas and colleagues (Rojas *et al.*, 2012).

Structure-function relationship of Ras

In spite of increasing complexity of Ras signaling, its enzymology, however, is very simple; they bind GTP and hydrolyze it to GDP. Therefore, Ras activity is determined by the type of bound nucleotide: Ras is inactive in its GDP-bound state and active in its GTP-bound state. Thus, Ras acts as a molecular switch (Vetter and Wittinghofer, 2001). All members of the Ras superfamily share a GDP/GTP binding (G) domain, which consists of six β-sheets and five α-helices (Figure 2). Although the length and sequence of the G domains are different (*e.g.*, H-Ras residues 1-166), they share a set of conserved GDP/GTP-binding motifs, termed G1-G5 (Figure 2A) (Bourne *et al.*, 1991; Wennerberg *et al.*, 2005): G1 (^{10}GXXXXGKS^{17}; H-Ras numbering) binds the β and γ phosphates of GTP, which also called the phosphate binding (P) loop; G2 (residues 32-40 in H-Ras) is also called the effector binding site or switch I, which coordinates the magnesium ion (Mg^{2+}) and the γ phosphate of GTP, respectively; G3 (^{57}DXXGQ^{61}; H-Ras numbering) is part of the switch II region(residues 60-68 in H-Ras) coordinating the Mg^{2+} ion and γ phosphate of GTP, respectively; G4 (^{116}NKXD^{119}; H-Ras numbering) determines the specificity of the guanine base binding; G5 (^{144}SAK^{146}; H-Ras numbering) specifically stabilizes the guanine ring and the ribose. Switch I and II are

the regions that undergo the conformational changes when Ras cycles between the GTP-bound and GDP-bound states (Vetter and Wittinghofer, 2001). Switch I region (residues 32-40) is located between α1 helix and β2 strand and overlaps with G2 box. Switch II region (residues 60-68) contains part of α2 helix and G3 motif. A GTP-induced conformation change is critical for its molecular switch function, which favors the interaction with the downstream effectors (Vetter and Wittinghofer, 2001).

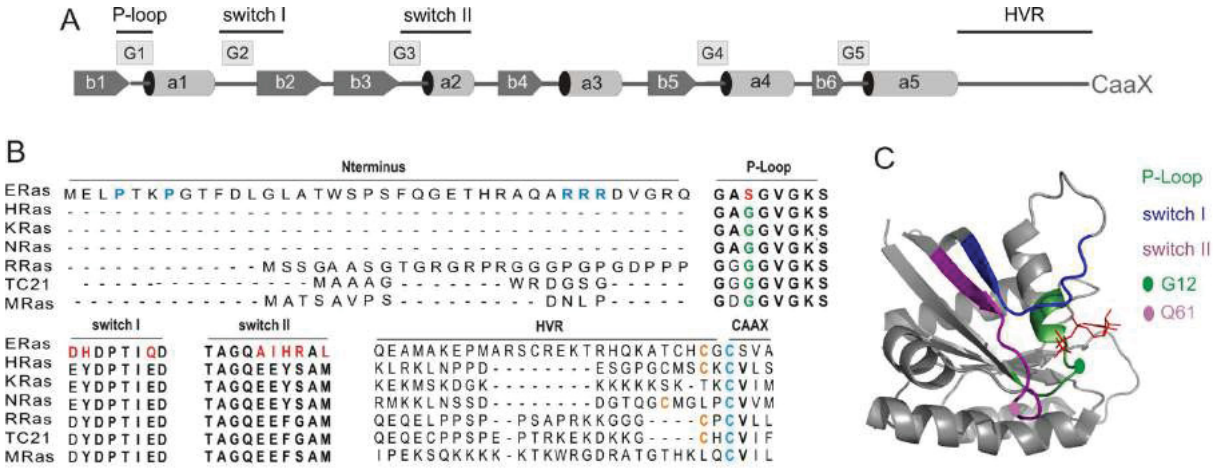

Figure 2: The structure of RAS Protein
A, Primary structure of RAS protein, B, Sequence comparison of switch I, switch II and c-terminus of some RAS proteins, C, crystal structure of Ras (PDB code: 4EFL). P-loop, switch I and switch II labeled with different colors.

Membrane association of Ras

Signaling networks are organized by the specific localization of the signaling molecules to distinct cellular membranes. Posttranslational modifications, including farnesylation and palmitoylation, are essential for plasma membrane localization of Ras proteins (Ahearn *et al.*, 2012). The majority of Ras family proteins consist of a carboxyl terminal CAAX (C is cysteine, A is any aliphatic amino acid, and X is any amino acid) motif (Ahearn *et al.*, 2012).

CAAX motif and its upstream hypervariable region (HVR) contain sites for post-translational modifications and are critical for subcellular localization of Ras proteins (Figure 2) (Ahearn *et al.*, 2012; Takahashi *et al.*, 2005; Wennerberg *et al.*, 2005). Cytosolic Ras proteins are post-translationally modified at their CAAX cysteine successively by the enzymatic activities of farnesyltransferase, endopeptidase and methyltransferase (Takahashi *et al.*, 2005).

The plasma membrane localization of some Ras proteins, such as H-Ras and N-Ras required another lipid modification. Palmitoylation occurs at one or two cysteine residues in the hypervariable region (HVR) of the residues upstream of the CAAX motif

(Rocks *et al.*, 2005). Therefore, four different posttranslational modifications, *e.g.*, farnesylation, endoproteolysis, methylation, and palmitoylation, are necessary for the plasma membrane localization of H-Ras and N-Ras (Takahashi *et al.*, 2005). We have recently proposed that E-Ras, a unique member of the Ras family, is most likely posttranslationally modified by palmitoylation. Substitution of two cysteine residues C226 and C228 in its HVR for serines clearly impaired the plasma membrane localization of E-Ras (Chapter 2).In contrast, farnesylated K-Ras4B instead contains multiple lysine residues upstream of the CAAX motif that stabilize its plasma membrane association via direct interaction with phospholipids (Apolloni *et al.*, 2000).

Regulatory mechanisms of Ras

A hallmark of most small GTPases, like Ras, is their ability to undergo structural changes in response to alternate binding of GDP and GTP (Figure 2). Ras in its GDP-bound `off´ state and the GTP-bound `on´ state interacts with diverse proteins, which regulates its function as a molecular switch in diverse cellular processes (Vetter and Wittinghofer, 2001). Ras activation requires GDP/GTP exchange, an intrinsically very slow process that is accelerated in the cell by a group of proteins called guanine nucleotide exchange factors (GEFs; Figure 3). Activation of Ras proteins occurs in a response to diverse extracellular stimuli leading to recruitment of GEFs to the plasma membrane. Activation of Ras-specific GEFs, like Sos1, is signal transduction-controlled processes. After growth factor stimulation, the tyrosine phosphorylated receptor binds the Grb2-Sos complex, translocating it to the plasma membrane. The principal mechanism used involves formation of complexes of autophosphorylated growth factor receptors with the SH2 and SH3 domain containing adaptor protein GRB2 and the exchange factor Sos1 (Hennig *et al.*, 2015). This is thought to bring Sos into close proximity with Ras, leading to the nucleotide exchange and the activation of Ras.

Activated Ras interacts with multiple, functionally distinct downstream effectors, which act as enzymes or scaffold proteins and control cell proliferation, differentiation, and survival (see below).

Ras inactivation is dependent on a functional intrinsic GTP hydrolysis (or GTPase) reaction, which very slow and requires GTPase-activating proteins (GAPs, Figure 3) (Scheffzek *et al.*, 1998; Vetter and Wittinghofer, 2001). Interestingly in the GTPase reaction of Ras as a molecular drug target stems from the observation that in a large number of human tumors Ras is mutated at codons 12 or 61, more rarely 13. Impaired GTPase activity, even in the presence of GTPase activating proteins (GAPs), has been found to be the biochemical reason behind the oncogenicity of the Gly12/Gln61 mutations, thus preventing Ras from being switched off (Ahmadian, 2002) .Therefore, these oncogenic Ras mutants remain constitutively activated and contribute to the neoplastic phenotype of tumor cells. Ras-specific GAPs, like neurofibromin (NF) and p120RasGAP, are defined by the presence of a conserved catalytic domain, which

supplies a conserved arginine residue and complements an inefficient active site by stabilizing the transition state of the GTPase reaction of Ras (Scheffzek and Ahmadian, 2005; Scheffzek *et al.*, 1998). Neurofibromin and p120 contain a GAP-related domain, which is responsible for a GAP-stimulated GTPase reaction of more than 10^5-fold (Scheffzek and Ahmadian, 2005).

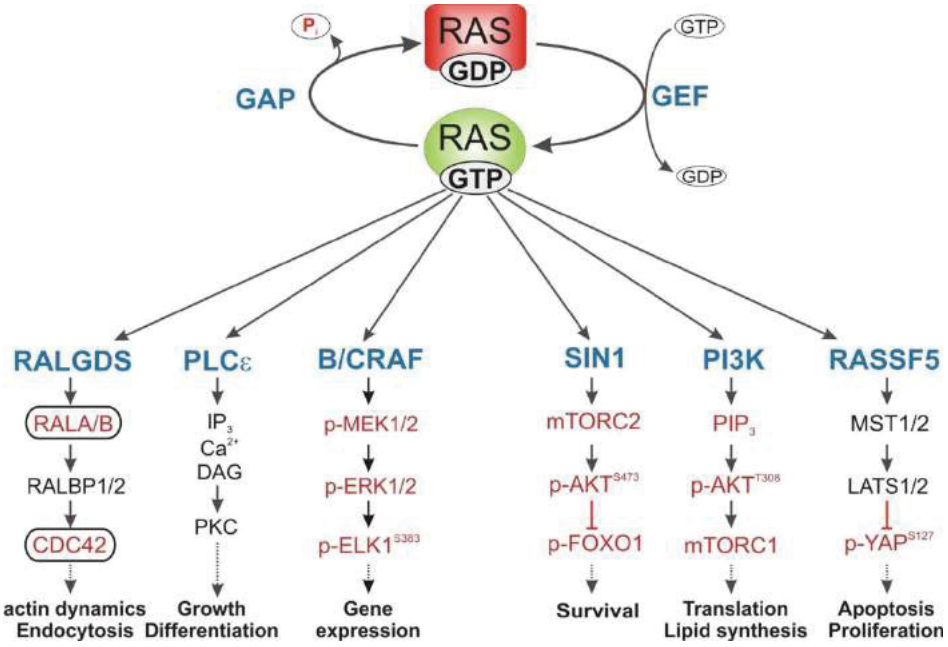

Figure 3: Ras proteins cycling between the active and inactive state
The active state of Ras protein is bound to GTP, the inactive state of Ras protein is bound to GDP. GTP bound form can binds different effectors and triggers different pathways.

Ras effector selection

Ras proteins transmit various signals to downstream effectors and initiates distinct signal transduction pathways responsible for regulation of individual biological processes (Figure 3) (Ayllon and Rebollo, 2000; Cox and Der, 2003; Karnoub and Weinberg, 2008; Matozaki *et al.*, 2000; Nakhaei-Rad *et al.*, 2016) to Ras effectors including the Raf kinase, PI3K, RalGDS, PLCε and Rassf5. They share little homology but all contain either a Ras binding (RBD) or a Ras association (RA) domain (Figure 4) (Chan and Katan, 2013; Repasky *et al.*, 2004b; Wohlgemuth *et al.*, 2005). Effector interaction essentially requires localization of the Ras proteins at the membrane and its activation by specific exchange factors, leading to the formation of the GTP-bound state of Ras proteins (Ahearn *et al.*, 2012). Thereby, they changes their conformation at highly mobile switch regions, to where Effector's RBD or RA specifically associated (Mott and

Owen, 2015; Vetter and Wittinghofer, 2001). Raf1-RBD and RalGDS-RA share a similar ubiquitin-like fold and contact the switch I region *via* a similar binding mode, whereas PI3Kα-RBD, Rassf5-RA and PLCε-RA do not share sequence and structural similarity but commonly bind to both switch regions (Huang *et al.*, 1998; Nassar *et al.*, 1995). The RBD-containing mSin1, an integral component of the mTOR complex 2 (mTORC2), has been reported to bind activated H-Ras and K-Ras in cells (Schroder *et al.*, 2007). A direct interaction between mSIN1 and the Ras proteins has not been reported yet.

Raf kinases

Serine/threonine-protein kinases of the Raf family (A-Raf, B-Raf, and C-Raf/Raf1) act as a link between the membrane-associated Ras proteins and the MEK/ERK cascade. This critical regulatory link functions as a switch determining cell fate decisions, including proliferation, differentiation, apoptosis, survival and oncogenic transformation (Lavoie and Therrien, 2015). Raf activation initiates a mitogen-activated protein kinase (MAPK) cascade that comprises a sequential phosphorylation of the dual-specific MAPK kinases (MEK1 and MEK2) and the extracellular signal-regulated kinases (ERK1 and ERK2). This cascade regulates a large variety of processes including apoptosis, cell cycle progression, differentiation, proliferation, and transformation (Lavoie and Therrien, 2015; Roskoski, 2010).

The Raf isoforms share three different conserved regions (CR) with distinct functions (Desideri *et al.*, 2015; Matallanas *et al.*, 2011). CR1 contains a Ras-binding domain (RBD), which is essential for the interaction with the Ras proteins, and a cysteine-rich domain (CRD), which stabilizes the inactive conformation (Figure 4). CR2 comprises important inhibitory phosphorylation sites participating in the negative regulation of Ras binding and Raf activation, and is required for membrane recruitment of Raf. CR3 contains the kinase domain, including the activation segment, whose phosphorylation is necessary for kinase activation (Matallanas *et al.*, 2011). The regulation of Raf kinase activity is complex and not fully understood (Desideri *et al.*, 2015). In the absence of a cellular stimulus most Raf is in the cytoplasm in a monomeric and closed (inhibited) state, which is achieved through the direct, physical association of its N-terminal CR1 region with the kinase domain. Activated Ras binds to the RBD and translocates Raf to the membrane, and relieves the kinase domain. Thereby, dephosphorylation of CR2 and phosphorylation of CR3 are required to fully activate Raf (Alexa *et al.*, 2010; Matallanas *et al.*, 2011; Desideri *et al.*, 2015). It is important to note that the binding of Raf to Ras can be promoted by the scaffolding protein Sur-8/SHOC2 (Matsunaga-Udagawa *et al.*, 2010). Raf phosphorylates and activates the MEK1/2, that phosphorylates and activates the ERK1/2. Activated ERK1/2 translocate to the nucleus and activate Ets-family transcription factors, which mediate gene expression (Repasky *et al.*, 2004a).

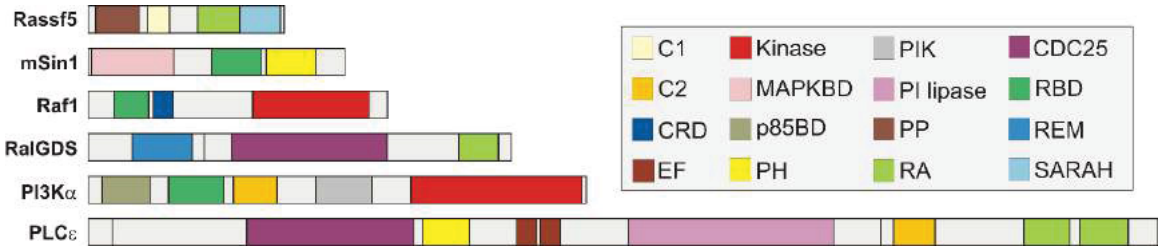

Figure 4: Domain organization of Ras effectors.
Various domains are highlighted, including Ras association (RA) domain and Ras-binding domain (RBD). Other domains are: C1, cysteine-rich lipid binding; C2, calcium-dependent lipid binding; CRD, cysteine rich domains; DEP, Dishevelled/Egl-10/Pleckstrin; EF, EF-hands; kinase, serine/threonine or phosphoinositide kinase; PH, pleckstrin homology; PIK, Phosphoinositide 3-kinase family, accessory *domain;* PP, proline-rich region; RA, Ras association; RalGEF, Ral specific guanine nucleotide exchange factor; RasGEF, Ras specific guanine nucleotide exchange factor; RBD, Ras binding domain; REM, Ras exchanger motif; SARAH, Salvador/Rassf/Hippo.

Phosphatidylinositol 3-kinase (PI3K)

PI3Ks belong to the second best-characterized RAS effector family, which play critical roles in regulating cell growth, cell cycle entry, cell survival, cytoskeleton reorganization, and metabolism (Castellano and Downward, 2011). Activated PI3K converts phosphatidylinositol (4,5)-bisphosphate (PIP_2) into phosphatidylinositol (3,4,5)-trisphosphate (PIP_3), which usually is the target the pleckstrin homology (PH) domains of for example Akt/PKB (Carnero, 2010). Activation of Akt/PKB in turn regulates cell growth, cell cycle entry, and cell survival. PI3K has also the ability to activate Rac1, which is involved in cytoskeleton reorganization (Cantley, 2002). The PI3Ks are heterodimeric lipid kinases, composed of a catalytic and a regulatory subunit, both of which are encoded by separate genes and underlie alternative splicing (Castellano and Downward, 2011; Volinia *et al.*, 1994). The PI3K family is divided into four different classes (Class I-IV) based on primary structure, regulation, and substrate specificity (Leevers *et al.*, 1999). Class I PI3K is the best-characterized class and generally subdivided in two subclasses (IA and IB). The catalytic subunits for class IA are p110α, p110β, and p110δ, which bind to one of five regulatory subunits p85α, p55α, p50α, p85β, and p55γ (Geering *et al.*, 2007). The catalytic subunit for class IB is p110γ that binds to either p101 or p87 as regulatory subunit (Shymanets *et al.*, 2013).The regulatory subunit controls the subcellular location, the interaction with binding partners, and the activity of the catalytic subunit. Under unstimulated conditions, p85 stabilizes the labile p110 protein, while inhibiting its catalytic activity. Recruitment of the p85/p110 complex to receptors, *e.g.*, receptor tyrosine kinases (RTKs), and adaptor proteins, *e.g.*, Grb2, *via* p85 domains leads to PI3K activation and

production of the second messenger PIP_3. PI3K activation is achieved at least in three different modes, either directly by autophosphorylated receptor tyrosine kinases (RTKs), RTK/GRB2 or RTK/Grb2/Sos/Ras. In the mode, Ras directly activates p110 in a p85-independent manner (Geering *et al.*, 2007).The class IB PI3Kγ is activated G protein-coupled receptors and requires physical interaction with Gβγ subunits and Ras for its activation (Kurig *et al.*, 2009).Thereby, the regulatory subunits p87 and p101 are distinct regulators PI3Kγ and determine the specificity of its signaling pathways (Shymanets *et al.*, 2013).

The activation of PI3K results in PIP_3 generation.The activation of PI3K and subsequent production of PIP_3 drive the diverse downstream pathways that regulate a number of cellular functions including those involved in tumor development and progression. The tumor suppressor phosphatase and tensing homolog (PTEN), as a lipid phosphatase antagonizes PI3K and dephosphorylates PIP_3 to PIP_2, thereby terminating PI3K-dependent signaling.

Ral guanine nucleotide dissociation stimulator (RalGDS)

RalGDS was discovered to contain CDC25 domain, which is a signature for a catalytic RasGEF domain (*e.g.*, Sos, RasGRP, RasGRF) (Ferro and Trabalzini, 2010). However, RalGDS turned out to an exchange factor for the Ras-like proteins RalA and RalB rather than for Ras. RalGDS contains a RA domain and is established to be a Ras effector (Neel *et al.*, 2011). Therefore, members of RalGDS family are activated by Ras and activate in turn Ral proteins by promoting their GDP/GTP exchange. The ability of RalGDS proteins to bind GTP-bound Ras and eventually Ras-related proteins is due to their C-terminal RA domain (Ferro and Trabalzini, 2010), which is highly conserved in many different proteins (Wohlgemuth *et al.*, 2005). RalGDS/Ral pathways regulate vesicular trafficking, migration and invasion, tumor formation, metastasis, and gene expression (Gentry *et al.*, 2014).

Ras association domain-containing protein 5 (Rassf5)

Rassf5 (also called novel Ras effector 1 or Nore1) is a downstream effector of Ras. Its complex with mammalian Ste20-like kinase (Mst1), a human ortholog of Hippo, interacts with Ras-GTP and promotes proapoptitic Hippo pathways. Their relative levels of activation balance cell survival or death (Feig and Buchsbaum, 2002). Rassf5, has no detectable catalytic domain. It has SH3-domain-binding sites at the N-terminus followed by a cysteine-rich lipid binding C1 domain, a RA domain and at the very C-terminus a Salvador/Rassf/Hippo or SARAH domain (Figure 4) (Feig and Buchsbaum, 2002). It has been shown that C1 domain of Rassf5 undergoes an intramolecular interaction with the RA domain and represents as such Rassf5 in its autoinhibited state. Ras-GTP binding to RA disrupts this complex and displaces the C1 domain for the

association with phosphatidylinositol 3-phosphate (PI3P) (Harjes *et al.*, 2006). Thereby, SARAH domain of Rassf5 interacts with Mst1 (Makbul *et al.*, 2013).

Phosphatidylinositol 4,5-bisphosphate phosphodiesterase epsilon (PLCε)

Stimulation of PIP_2-hydrolyzing phospholipase C (PLC) is a key signaling even activated by different membrane receptors. It regulates a variety of cellular functions, such as smooth muscle contraction, neuronal signaling, secretion, and cell growth and differentiation (Evellin *et al.*, 2002). PLCβ, PLCγ and PLCδ are differentially regulated by G protein-coupled receptors and the heterotrimeric G protein αq as well as by receptor tyrosine kinases (Gresset *et al.*, 2012). A fourth member of the phospholipases is PLCε, which contains additionally to conserved PLC domains also a CDC25 (RasGEF) domain and two RA domains at the very C-terminus (Figure 4) (Kelley *et al.*, 2001) Both RA domains have been shown to have ubiquitin-like folds (Bunney *et al.*, 2006). Only the second RA domain binds Ras-GTP with high affinity (Kelley *et al.*, 2001).

Stress-activated map kinase-interacting protein 1 (SIN1)

Sin1 (also called Mitogen-Activated Protein Kinase Associated Protein 1 or MAPKAP1) is a member of the mammalian target of rapamycin complex 2 (mTORC2) (Laplante and Sabatini, 2009). Together with Rictor it stabilizes the assembly of mTORC2. SIN1 is essential for mTOR-mediated phosphorylation at Ser-473 Akt/PKB (Frias *et al.*, 2006; Laplante and Sabatini, 2009). Activation of mTORC1 leads to SIN1 phosphorylation at Thr-86 and Thr-398 by S6K1 leading to its dissociation from and inactivation mTORC2 (Liu *et al.*, 2013). SIN1 contains an N-terminal MAPK-binding domain followed RBD and PH domains (Figure 4). It co-localizes with Ras and also interacts with Ras *in vivo* (Schroder *et al.*, 2007). Over-expression of SIN1 can inhibit Ras-mediated activation of ERK1/2, Akt and JNK signaling (Schroder *et al.*, 2007). A direct association of SIN1 with Ras proteins has not been shown yet.

Embryonic stem cell-expressed Ras (E-Ras)

E-Ras, a novel member of the Ras superfamily, has been discovered in mouse embryonic stem cells as a transforming oncogene (Takahashi et al., 2003). A search in mouse genomic databases showed that *E-Ras* gene is located on the X chromosome and contains two exons. The cDNA encodes a protein of 227 amino acids with an average sequence identity of 45% to the Ras isoforms H-Ras, K-Ras and N-Ras,.The five G motives essential for nucleotide binding and hydrolysis are highly conserved (Takahashi et al., 2003). Another characteristic of E-Ras is a Serine (Ser50) instead of a glycine (equivalent to Gly12 in H-Ras), which is frequently mutated in Ras gene in human tumors. Thus, E-Ras constitutes a constitutively active protein in cells (Chapter

2 and Chapter 5). Therefore, E-Ras has the ability to transform cells. Its overexpression induces morphological changes in fibroblasts indicative for the transforming activity of E-Ras (Takahashi et al., 2003). Accordingly, *E-Ras* has been described to be expressed in the early stage of gastric cancer, while no *E-Ras* expression was detected in gastric epithelial cells. Thus, it has been suggested that *E-Ras* is an oncogene and associated with the tumorigenesis of human gastric tumors (Kaizaki et al., 2009). Moreover embryonic stem cells and gastric tumors cells E-RAS specifically expressed in Hepatic stellate cells (HSCs). E-RAS protein was detected in HSCs but not in other liver cell types, including hepatocytes, Kupffer cells and sinusoidal endothelial cells. E-Ras is presence in quiescent HSCs but not in activated HSCs and it was considerably down-regulated during HSC activation (Chapter 5). In quiescent HSCs, E-Ras preferentially interacts with PI3K and activates the PI3K-PDK1-AKT axis and does not show any activity toward the MAPK cascade. The prominent AKT phosphorylation by mTORC2 in quiescent HSCs suggests that mTORC2-AKT acts as a candidate pathway mediates signaling downstream of E-Ras. E-Ras like other Ras proteins should be associated with the lipid membrane to transduced signal. They undergo PMTs at their C-terminus, with the CAAX motif at the farnesylation site, and additional upstream cysteine residues at the palmitoylation site(s) (Chapter 5).

According sequence alignment, human and rat E-Ras proteins show a sequence identity of 71%. Here, major differences are located at the C-terminal HVR and at a unique N-terminal extension, which is missing in the Ras isoforms, such as H-Ras (Chapter 2). The extension of the N-terminus of E-RAS was proposed to modulate its localization through interaction with potential adaptor/scaffold proteins *via* putative PXXP and RRR motifs (Chapter 2). It has been shown that the N-terminal extension is required for the E-Ras association with PI3K and may contribute to a precise activation of the PI3K-AKT-mTORC pathway (Chapter 2). A recent proteome study has shown that the E-Ras N-terminus binds multiple cytosolic and nuclear proteins with different functions (Chapter 4). Interestingly, the majority of the proteins bind both Human and rat E-Ras proteins in spite of large amino acid deviations within their N-terminus. One of these proteins is Arginase 1.

Arginases

Arginase is a manganese-binding enzyme (comprised of 322 amino acids) that catalyzes the conversion of L-arginine to L-ornithine and urea. It is an critical enzyme of the urea cycle and provides cells also with ornithine, which is an essential precursor of proline and polyamine biosynthesis (Curran *et al.*, 2006). There are two isoenzymes. They catalyze the same biochemical reaction but differ in cellular expression, regulation, and localization (Curran *et al.*, 2006) The cytosolic Arginase-1 is primarily expressed in hepatocytes, whereas the mitochondrial arginase-2 is expressed in a variety of tissues, such as kidney, small intestine, prostate, and lactating mammary

gland (Morris, 2009). Arginase-2 is involved in the synthesis of polyamines, the amino acids ornithine, proline, and glutamate and in the inflammatory process and proliferation (Cederbaum *et al.*, 2004). Mammalian arginases are homotrimeric enzyme, but some bacterial arginases are hexameric enzymes (Dowling *et al.*, 2008). High-resolution crystal structures rat Arginase-1 and human Arginase-2 have shown that the trimeric enzymes contain one active site that is located at the bottom of a 15 Å deep cleft (Kanyo *et al.*, 1992; Cama *et al.*, 2003). The two Mn(II) ions are located at the bottom of this cleft, which separated by ∼3.3 Å and bridged by oxygens derived from 2 aspartic acid residues and a solvent-derived hydroxide. This metal bridging hydroxide is supposed to be the nucleophile that attacks the guanidinium carbon of substrate arginine (Ash, 2004).

L-arginine is a common substrate for both Arginases and nitric oxide synthases (NOSs) (Bagi *et al.*, 2013) NOSs catalyze the formation of NO that is involved in a variety of biological functions, for example, it is an established neurotransmitter in the nervous system, it is also secreted by endothelial cells acting as a blood pressure regulator and, produced by macrophages, is a potent anti-microbial, cytotoxic and inflammatory mediator (Heiss *et al.*, 2015) Controlling the relative rates of flux of L-arginine between arginases and NOSs may be a central regulatory switch of cellular growth (Bagi *et al.*, 2013). E-Ras may play a role by directly interacting with and regulating the activity of Arginase-1 for example in hepatic stellate cells (Chapter 5).

Hepatic stellate cells (HSCs)

In a healthy liver, hepatic stellate cells (HSCs; also called Ito cells, lipocytes, fat storing cells, or perisinusoidal cells) remain in a quiescent state. They are located in the space of Disse between the sinusoidal endothelial cells and represent 5-8% of the total number of liver cells. In the quiescent state, they contain numerous vitamin A lipid droplets, constituting the largest reservoir of vitamin A in the body (Kordes and Haussinger, 2013). Research on HSCs within the last 30 years has mainly focused on their contribution to fibrogenesis in chronic liver diseases (Friedman, 2008). A liver injury, through for example viral infection or toxins, results in the HSC activation through signals releases by damaged hepatocytes and immune cells (Kordes *et al.*, 2014; Kordes *et al.*, 2015). Activated HSCs progressively release their vitamin A and increasingly produce extracellular matrix proteins and a temporary scar at the site of injury to protect the liver from further damage (Yin *et al.*, 2013). Liver fibrosis is a reversible reaction to either acute or chronic liver injury that reflects a balance between liver repair and scar formation. During acute injury, the changes in liver construction are temporary and reversible. While chronic injury is a progressive substitution of the liver parenchyma by scar tissue. Despite ongoing injury, the liver has a considerable regenerative capacity, and, as a result, patients often progress slowly to cirrhosis over decades (Lee and Friedman, 2011).Recent data point to

another remarkable characteristic of HSCs that they possess signaling pathways important for maintenance of *stemness* and *cell* differentiation (Kordes *et al.*, 2014; Kordes *et al.*, 2015).

They possess characteristics of stem cells, like the expression of Wnt and NOTCH, which are required for developmental fate decisions. Activated HSCs display an expression profile highly reminiscent of mesenchymal stem cells. Due to typical functions of mesenchymal stem cells, such as differentiation into adipocytes and osteocytes as well as support of hematopoietic stem cells, HSCs were identified as liver-resident mesenchymal stem cells (Kordes *et al.*, 2013). During activation HSCs up-regulate various genes, including smooth muscle actin and collagen type I, and down-regulate GFAP (Kordes and Haussinger, 2013).

The origin of stellate cells is not clear because they express molecular markers of different germ layers (Geerts, 2004) The space of Disse which HSCs localize there has characteristics of stem cell niches (Kordes and Haussinger, 2013) The origin of liver progenitor cells are HSCs and other MSC populations from distance organ that after injury migrate to the liver in order to support regeneration. HSCs can characterize as liver-resident stem cells (Kordes *et al.*, 2014).

Galectin-1

Galectins belong to a family of carbohydrate-binding proteins (lectins). Fifteen different galectins have been described in human, which one or two carbohydrate recognition domain (CRD) (Vasta *et al.*, 2015). This domain contains about 130 amino acids and is responsible for β-galactoside binding. Galectins participates in different biological functions, such as development, differentiation, immunity (Blidner *et al.*, 2015). Galectin-1 (Gal-1) was the first protein discovered to contain one CRD and to be biologically active as homodimers (Camby *et al.*, 2006). It can be found in the cytoplasm, the nucleus, the cell surface and in the extracellular space and is also secreted by an unknown pathway (Seelenmeyer *et al.*, 2008). Gal-1 is differentially expressed by various normal and pathologic tissues and displays a wide range of biological activities (Astorgues-Xerri *et al.*, 2014). In oncology, Gal-1 plays a pivotal role in tumor growth and in the multistep process of invasion, angiogenesis, and metastasis. Evidence indicates that Gal-1 exerts a variety of functions at different steps of tumor progression (Astorgues-Xerri *et al.*, 2014).

The current model for the nanocluster scaffolding activity of Gal-1 (Blazevits *et al.*, 2016) suggests that it directly binds to the C-terminal farnesyl of active H-Ras to modulate its intracellular membrane organization (Rotblat *et al.*, 2004) Augmented nanoclustering then increases effector recruitment thus potentiating MAPK signaling output (Paz *et al.*, 2001). Importantly, the interaction between Gal-1 and the GTP-bound H-Ras is suggested to be the target of the anti-Ras drug Salirasib (developed as farnesylthiosalicylic acid, FTS), which is currently assessed preclinically and in clinical

trials for the treatment of cancer (Laheru *et al.*, 2012). A recent study has demonstrated that Gal-1 does not directly bind to H-Ras, but instead to the RBDs of Ras effectors, such as Raf (Chapter 6). This explains how Gal-1 specifically recognizes active Ras-GTP. This model has entirely revised the mechanism of action of Gal-1 as a nanocluster scaffold and provides additional therapeutic approaches in the future.

Chapeter II

The function of embryonic stem cell-expressed RAS (ERAS), a unique RAS family member, correlates with its additional motifs and its structural properties

Graphical Abstract

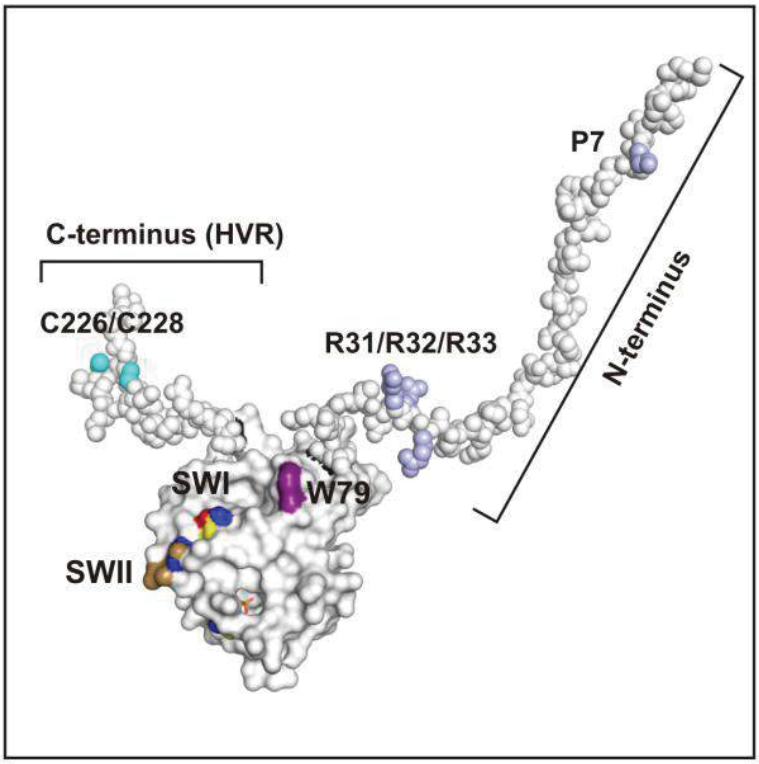

Status: Published in J Biol Chem. 2015 Jun 19

Impact Factor: 4.25

Own Proportion to this work: 10%

Site direct mutagenesis
Cloning
Preparing of the manuscript

THE JOURNAL OF BIOLOGICAL CHEMISTRY VOL. 290, NO. 25, pp. 15892–15903, June 19, 2015

The Function of Embryonic Stem Cell-expressed RAS (E-RAS), a Unique RAS Family Member, Correlates with Its Additional Motifs and Its Structural Properties*[S]

Received for publication, January 28, 2015, and in revised form, April 21, 2015 Published, JBC Papers in Press, May 4, 2015, DOI 10.1074/jbc.M115.640607

Saeideh Nakhaei-Rad[‡], Hossein Nakhaeizadeh[‡], Claus Kordes[§], Ion C. Cirstea[‡¶], Malte Schmick[‖], Radovan Dvorsky[‡], Philippe I. H. Bastiaens[‖], Dieter Häussinger[§], and Mohammad Reza Ahmadian[‡1]

From the [‡]Institute of Biochemistry and Molecular Biology II and [§]Clinic of Gastroenterology, Hepatology, and Infectious Diseases, Medical Faculty of the Heinrich-Heine University, 40255 Düsseldorf, the [¶]Leibniz Institute for Age Research-Fritz Lipmann Institute, 07745 Jena, and the [‖]Department of Systemic Cell Biology, Max Planck Institute of Molecular Physiology, 44227 Dortmund, Germany

Background: E-RAS contains additional motifs and regions with unknown functions.
Results: Biochemical analysis reveals that effector selection of E-RAS significantly differs from H-RAS.
Conclusion: E-RAS selectivity and consequently cellular outcomes depend on its unique switch and interswitch regions.
Significance: E-RAS possesses specific sequence fingerprints and therefore no overlapping function with H-RAS.

E-RAS is a member of the RAS family specifically expressed in embryonic stem cells, gastric tumors, and hepatic stellate cells. Unlike classical RAS isoforms (H-, N-, and K-RAS4B), E-RAS has, in addition to striking and remarkable sequence deviations, an extended 38-amino acid-long unique N-terminal region with still unknown functions. We investigated the molecular mechanism of E-RAS regulation and function with respect to its sequence and structural features. We found that N-terminal extension of E-RAS is important for E-RAS signaling activity. E-RAS protein most remarkably revealed a different mode of effector interaction as compared with H-RAS, which correlates with deviations in the effector-binding site of E-RAS. Of all these residues, tryptophan 79 (arginine 41 in H-RAS), in the interswitch region, modulates the effector selectivity of RAS proteins from H-RAS to E-RAS features.

Small GTPases of the RAS family act as molecular switches within the cell, cycling between a GTP-bound (active) and a GDP-bound (inactive) state (1, 2). These molecules trigger intracellular responses by sensing the extracellular signals through their interacting receptors or intermediate proteins and passing the signal to downstream targets. Therefore, they play a key role in various cellular processes, including gene expression, metabolism, cell cycle progression, proliferation, survival, and differentiation. Somatic or germ line mutations in genes related to members of the RAS family or their regulators are commonly associated with cancer progression or developmental disorders (3–9).

The best investigated RAS proteins are H-, N-, and K-RAS4B, which share overlapping functions, including cell proliferation, differentiation, and apoptosis (10–13). However, different RAS isoforms exhibit a particular pattern of expression, different regulators, and specific microdomains or subcellular localization, indicating their functional specificity as well as redundant roles (10–17). The individual roles of other members of the RAS family, such as R-RAS, TC21, M-RAS, AGS-1, or the embryonic stem cell-expressed RAS (E-RAS), have not been fully described. E-RAS was identified in 2003 as a new member of the RAS family, which is specifically expressed in undifferentiated mouse embryonic stem cells (18). In addition to stem cells, E-RAS has been detected in the several adult cynomolgus tissues (19) and in gastric cancer and neuroblastoma cell lines (20, 21).

Plasma membrane localization of the classical RAS isoforms (H-, N-, and K-RAS4B) has been shown to be critical for their functionality (22–24). The membrane association is achieved by post-translational modifications (PTMs)[2] at the C terminus of RAS proteins. H-RAS and N-RAS undergo two types of PTMs, farnesylation at a cysteine residue in C*AAX* (where C is cysteine, *A* is any aliphatic amino acid, and *X* is any amino acid) motifs and palmitoylation of one or two cysteine residues in the hypervariable region (HVR) (23, 25–27). K-RAS4B lacks the cysteine residues in its HVR; instead it has a basic sequence of six lysines that maintains its strong association with the plasma membrane (24, 28, 29).

RAS proteins are inefficient GTP-hydrolyzing enzymes. Such an intrinsic GTPase reaction requires stimulation through GTPase-activating proteins (GAPs) by orders of magnitude (30–32). However, GDP dissociation is also a very slow

* This work was supported in part by the German Research Foundation through Collaborative Research Center 974 (Grant SFB 974), Communication and Systems Relevance during Liver Injury and Regeneration. The authors declare that they have no conflicts of interest with the contents of this article.
[S] This article contains supplemental Fig. S1.
[1] To whom correspondence should be addressed: Institut für Biochemie und Molekularbiologie II, Medizinische Fakultät der Heinrich-Heine-Universität, Universitätsstr. 1, Gebäude 22.03.03, 40255 Düsseldorf, Germany. Tel.: 49-211-81-12384; Fax: 49-211-81-12726; E-mail: reza.ahmadian@uni-duesseldorf.de.

[2] The abbreviations used are: PTM, post-translational modification; RBD, RAS-binding domain; aa, amino acid; GEF, guanine nucleotide exchange factor; PLC, phospholipase C; PDB, Protein Data Bank; MDCK, Madin-Darby canine kidney cell; HVR, hypervariable region; PIP_3, phosphoinositide 3,4,5-trisphosphate; RA, RAS association; GAP, GTPase-activating protein; EYFP, enhanced YFP.

reaction that needs acceleration by guanine nucleotide exchange factors (GEFs) (33, 34). RAS proteins share a highly conserved GTP-binding (G) domain with five essential motifs, termed G1 to G5 (supplemental Fig. S1) (35, 36). G1 or the P-loop (^{10}G*XXXX*GK(S/T)^{17}; H-RAS numbering) binds the β- and γ-phosphates of GTP (37). Substitution of glycine 12 to any other amino acid (except for proline) is most frequently found in human cancers. These mutations render RAS protein GAP-insensitive and consequently hyperactive (7, 38). G2 and G3, also referred to as switch I and switch II, respectively, are dynamic regions that sense the nucleotide state and provide the regulator and effector-binding sites (1, 39). G4 and G5 are important for determining the guanine base-binding specificity of the G domain (40, 41). Sequence analysis revealed that E-RAS contains a G domain with five fingerprint sequence motifs almost identical to classical RAS proteins indicating that it is a functional GTP-binding protein (supplemental Fig. S1). However, E-RAS contains a serine instead of glycine 12 (H-RAS numbering), making it GAP-insensitive (18).

H-, N-, and K-RAS4B share an identical effector binding regions (switch I and II; supplemental Fig. S1), suggesting that they may share the same downstream effectors. In contrast, E-RAS revealed significant differences in the effector binding regions (supplemental Fig. S1). This implicates that it may utilize other effectors as compared with known H-RAS effectors and may consequently have different cellular functions. However, the downstream effectors selective for E-RAS are not fully identified yet. A known H-RAS effector is phosphoinositide 3-kinase (PI3K) that has also been reported to be activated by E-RAS (18, 27, 42).

In addition to effector binding regions, E-RAS is distinguished from the classical RAS isoforms due to its unique extended N terminus (Fig. 1*A* and supplemental Fig. S1). This may provide a putative interaction site for a new group of proteins, which may determine its subcellular localization. For instance, it contains a P*XX*P motif that may serve as a putative binding motif for interaction with Src homology 3-containing proteins. In this study, we comprehensively investigated human E-RAS and its variants regarding their cellular localization and functional and structural properties in direct comparison with H-RAS wild-type and its G12V hyperactive variant. We found that N-terminal extension of E-RAS is important for E-RAS signaling activity. E-RAS protein most remarkably revealed different effector selectivity as compared with H-RAS, which is influenced by deviations in the effector-binding site of E-RAS. Data presented in this study implicate that in addition to switch regions, the interswitch region of E-RAS also contributes to high affinity binding to PI3Kα and low affinity to other RAS effectors, including RASSF5/Nore1, RAF1, Ral guanine nucleotide dissociation stimulator (RalGDS), and phospholipase Cε (PLCε).

Materials and Methods

Constructs—Human *E-RAS* cDNA was obtained from pCMV6-AC-hsE-RAS (Origene). Human *H-RAS* was obtained from ptacH-RAS (43). $H\text{-}RAS^{Val\text{-}12}$, $E\text{-}RAS^{Ser\text{-}226/Ser\text{-}228}$, $E\text{-}RAS^{Ser\text{-}7}$, and $E\text{-}RAS^{Ala\text{-}31/Ala\text{-}32/Ala\text{-}33}$ were generated by PCR-based site-directed mutagenesis as described (32). The E-RAS with the N-terminal deletion, lacking the first 38 amino acids (aa) ($E\text{-}RAS^{\Delta N}$), was designed using primers to amplify *E-RAS* cDNA starting from aa 39 and ending with aa 233 (supplemental Fig. S1). The same primers were used to generate $E\text{-}RAS^{\Delta N/Ser\text{-}226/Ser\text{-}228}$ (palmitoylation-dead variant of *E-RAS* lacking the N terminus) using $E\text{-}RAS^{Ser\text{-}226/Ser\text{-}228}$ as template. To generate E-RAS constructs with mutations in their effector binding regions, we used $E\text{-}RAS^{WT}$ cDNA as template. First, $E\text{-}RAS^{SwI}$ (H70Y/Q75E; Tyr-32 and Glu-37 in H-RAS), $E\text{-}RAS^{Arg\text{-}79}$ (W79R; Arg-41 in H-RAS), and $E\text{-}RAS^{SwII}$ (A100E/I101E/H102Y/R103S; Glu-62, Glu-63, Tyr-64, and Ser-65 in H-RAS) were generated. These constructs were used to generate $E\text{-}RAS^{SwI/Arg\text{-}79}$, $E\text{-}RAS^{SwI/SwII}$, $E\text{-}RAS^{Arg\text{-}79/SwII}$, and $E\text{-}RAS^{SwI/Arg\text{-}79/SwII}$, respectively. All cDNAs were amplified via PCR and subcloned via BamHI/XhoI in pcDNA 3.1 vector with an N-terminal FLAG tag or EcoRI/BamHI in pEYFP-C1.

Cell Culture and Transfection—MDCK II and COS-7 cells were cultured in Dulbecco's modified Eagle's medium (DMEM) supplemented with 10% fetal calf serum (FCS) and 50 units of penicillin/streptomycin (Gibco® Life Technologies, Inc.). Transfection was performed by using TurboFect transfection reagent, according to manufacturer's protocol (Life Technologies, Inc.).

Immunostaining—Cells were fixed with 4% paraformaldehyde for 20 min at room temperature. After washing with PBS, the cells were permeabilized with 0.25% Triton X-100/PBS for 5 min and washed again. For blocking, the cells were treated 1 h with PBS containing 0.25% Triton X-100 and 3% bovine serum albumin (BSA, Merck) at room temperature, then incubated with primary antibodies for 1 h, then washed three times, followed by incubation with secondary antibodies for 2 h at room temperature. The coverslips were mounted using ProLong® Gold antifade reagent contained DAPI dye (Life Technologies, Inc.). Primary antibodies were rabbit anti-FLAG (1:700, catalog no. F7425 Sigma) and mouse anti-Na^+/K^+-ATPase (1:100, catalog no. A275 Sigma), and secondary antibodies Alexa 488-conjugated goat anti-rabbit IgG (1:500, catalog no. A11008, Life Technologies, Inc.) and Alexa 546-conjugated goat anti-mouse IgG (1:500, catalog no. A11003, Life Technologies, Inc.). The images were taken by using an LSM 510-Meta microscope (Zeiss) at excitation wavelengths of 364, 488, and 546 nm.

Live Cell Imaging—MDCK II cells were seeded on Permanox 8-well chambered slides (Lab-Tek, Nunc). LSM 510-Meta microscope (Zeiss) was equipped with ×63 immersion objective, and fluorescent fusion proteins were excited using lasers with 504 nm (YFP) wavelength. An environmental chamber holds the temperature at 37 °C, and the cells were maintained in imaging medium.

Pulldown Assay and Immunoblotting—The RAS-binding domain (RBD) of RAF1 (aa 51–131), the RAS association (RA) domain of RalGDS (aa 777–872), the RA domain of PLCε (aa 2130–2240), the RBD of p110α (aa 127–314), the catalytic subunit of PI3Kα, and the RA domain of RASSF5 (aa 200–358) were inserted in pGEX-4T vector and expressed in *Escherichia coli* to obtain GST-fused proteins. Bacterial lysates were used to pulldown GTP-bound RAS proteins from total cell lysates. GST pulldown and immunoblotting using rabbit anti-FLAG (1:5000, catalog no. F7425 Sigma) and rat anti-α-tubulin (1:2000, SM 568, Acris) were carried out as described previously (44). In

Functional Properties of E-RAS

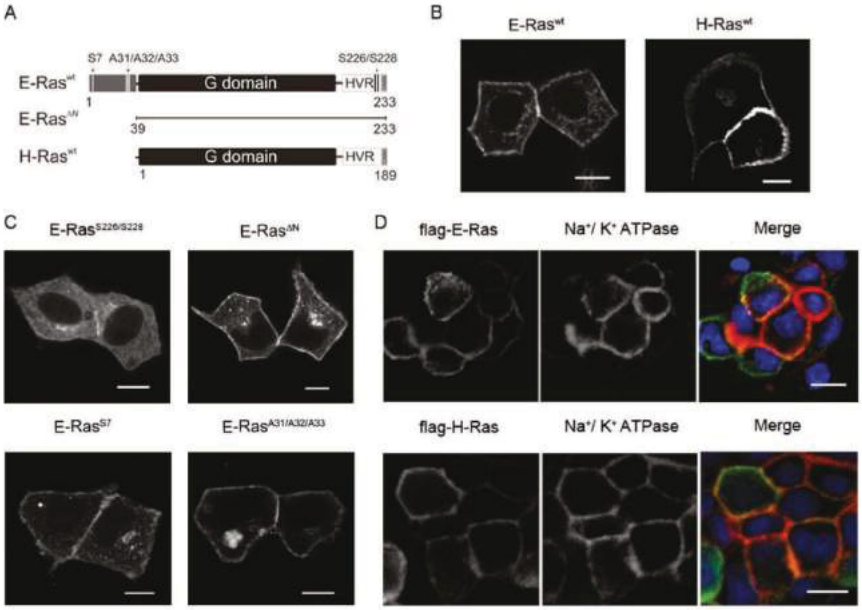

FIGURE 1. **Human E-RAS is largely associated with plasma membrane and some regions of E-RAS modulating its cellular localization.** *A*, different E-RAS variants used in this study, including N-terminal truncated E-RAS$^{\Delta N}$ (aa 39–233), palmitoylation-deficient E-RAS$^{Ser\text{-}226/Ser\text{-}228}$ (aa 1–233), N-terminal putative P*XX*P motif mutant E-RAS$^{Ser\text{-}7}$ (aa 1–233), and an N-terminal triple arginine motif variant E-RAS$^{Ala\text{-}31/Ala\text{-}32/Ala\text{-}33}$ (aa 1–233). *B* and *C*, confocal live images of transiently transfected MDCK II cells with EYFP-tagged E-RAS^{WT}, H-RAS^{WT}, E-RAS$^{Ser\text{-}226/Ser\text{-}228}$, E-RAS$^{\Delta N}$, E-RAS$^{Ser\text{-}7}$, and E-RAS$^{Ala\text{-}31/Ala\text{-}32/Ala\text{-}33}$. *D*, confocal imaging was performed using transiently transfected MDCK II cells with E-RAS and H-RAS. FLAG-tagged E-RAS co-localized with Na^+/K^+-ATPase to the plasma membrane, very similar to H-RAS, which was used as a control. *Scale bar*, 10 μm.

parallel, the cell lysates were used to visualize phospho-MEK1/2, phospho-ERK1/2, and phospho-AKT proteins states, respectively, using antibodies against MEK1/2 (Cell Signaling^{TM}), ERK1/2 (Cell Signaling^{TM}), AKT (Cell Signaling^{TM}), phospho-MEK1/2 (Ser-217/S221, Cell Signaling^{TM}), phospho-ERK1/2 (Thr-202/Thr-204, Cell Signaling^{TM}), and phospho-AKT (Ser-473 and Thr-308, Cell Signaling) in immunoblotting. All antibodies were diluted in 5% nonfat milk (Carl Roth GmbH).

Structural Methods—The structures of H-RAS were used in our study because no E-RAS structure was available to date. The G domains of H-RAS and E-RAS share 48% identity and were originally described to be structurally very similar, if not identical (18). The interactions with potential binding partners were analyzed on the basis of the structures of H-RAS in complexes with p120RASGAP (PDB code 1WQ1) (30), the RASGEF SOS1 (PDB codes 1NVV (45) and 4NYI), and the downstream effectors RAF1-RBD (PDB codes 1C1Y and 3KUD) (46, 47), PI3Kγ (PDB code 1HE8) (48), BYR2-RBD (PDB code 1K8R) (49), RalGDS (PDB code 1LFD) (50), PLC1 (PDB code 2C5L) (51), Grb14 (PDB code 4K81) (52), and RASSF5 (PDB code 3DDCS) (53).

Results

N Terminus Is an Important Factor for E-RAS Function—The cellular localizations of FLAG-tagged and EYFP-tagged wild-type E-RAS (E-RAS^{WT}) were investigated in direct comparison with H-RAS^{WT} in MDCK II cells. Confocal imaging revealed that E-RAS, very similar to H-RAS, is mainly associated with the plasma membrane (Fig. 1*B*) as it is co-localized with the basolateral membrane marker of sodium/potassium-ATPase (Fig. 1*D*). This result clearly suggests that E-RAS undergoes post-translational modifications, *e.g.* farnesylation and palmitoylation, at the very C-terminal cysteines (supplemental Fig. S1). Accordingly, a palmitoylation-deficient E-RAS$^{Ser\text{-}226/Ser\text{-}228}$ variant clearly exhibited a cytoplasmic accumulation, which supports the notion that E-RAS also underlies a palmitoylation/depalmitoylation mechanism as was shown previously for H-RAS (Fig. 1*C*) (25).

Another question addressed in this study was the role of the 38-amino acid unique N-terminal extension in E-RAS, which does not exist in other RAS proteins (Supplemental Fig. S1). This extension contains motifs, which may act either as a P*XX*P motif-binding site for specific Src homology 3-containing proteins or as an electrostatic interaction site (RRR motif) with a negatively charged region of proteins or with a lipid membrane. Thus, one function of the N-terminal extension and its motifs could be providing an additional signal for subcellular localization of E-RAS. Hence, we generated the N-terminal truncated E-RAS$^{\Delta N}$ (aa 39–233), putative P*XX*P motif variant E-RAS$^{Ser\text{-}7}$ (aa 1–233), and a triple arginine motif variant E-RAS$^{Ala\text{-}31/Ala\text{-}32/Ala\text{-}33}$ (aa 1–233) (Fig. 1*A*), and we investigated their localization in transiently transfected MDCK II cells. Confocal imaging of the EYFP-fused E-RAS variants revealed that the N terminus of E-RAS has a slight effect on the E-RAS localization as we observed for the truncated N-terminal variant E-RAS$^{\Delta N}$, putative P*XX*P motif variant E-RAS$^{Ser\text{-}7}$, and E-RAS$^{Ala\text{-}31/Ala\text{-}32/Ala\text{-}33}$-less plasma membrane localization (Fig. 1*C*) but not significant differences.

Effector Selection of E-RAS Significantly Differs from H-RAS—Before investigating the specific function of E-RAS in cells, it was important to gain insights into the E-RAS effector selectiv-

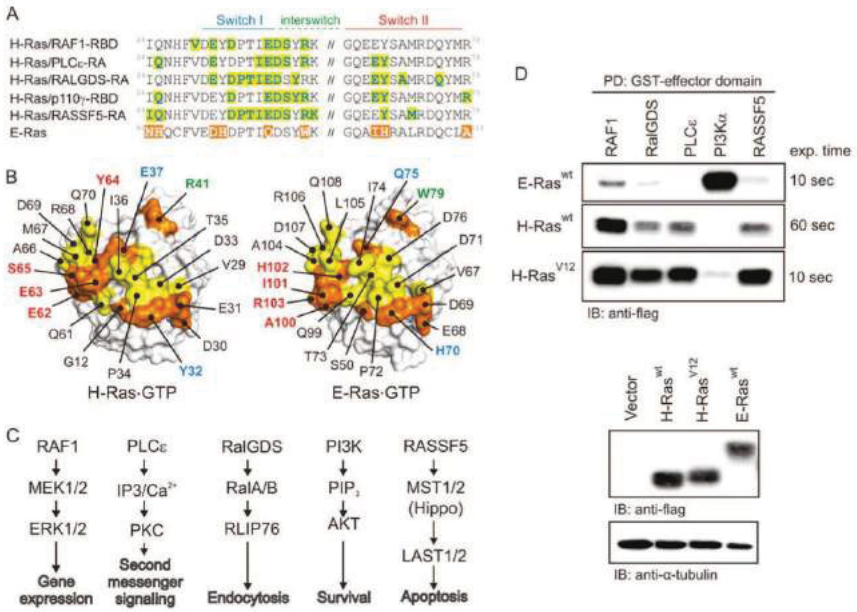

FIGURE 2. **Different effector selection of E-RAS and H-RAS.** *A*, effector-binding residues of H-RAS, obtained from various crystal structures, are highlighted with *blue letters* and *yellow background*, RAF1 (PDB code 1C1Y), PLCε (PDB code 2C5L), RalGDS (PDB code 1LFD), PI3Kγ (PDB code 1HE8), and RASSF5 (PDB code 3DDC). *B*, effector binding regions (in *yellow* and *orange*) of H-RAS and E-RAS were structurally analyzed on the basis of the H-RAS structure in complexes with p120RASGAP (PDB code 1WQ1). The *orange* amino acids indicate the sequence deviation between H-RAS and E-RAS. *C*, schematic view of RAS effector pathways and their cellular functions. *D*, E-RAS and H-RAS pulldown (*PD*) with various RAS effectors using COS-7 cell lysates transiently transfected with FLAG-tagged E-RAS^{WT}, H-RAS^{WT}, and H-RAS^{Val-12} using GST-fused effector proteins, such as RAF1-RBD, RalGDS-RA, PLCε-RA, PI3Kα-RBD, and RASSF5-RA. RAS proteins were analysis by immunoblot using an anti-FLAG antibody. Immunoblots (*IB*) of total cell lysates were used as a control to detect FLAG-RAS. *Exp. time* stands for exposure time. *RAF*, rapidly accelerated fibrosarcoma; *MEK*, mitogen-activated protein kinase/ERK kinase; *ERK*, extracellular signal-regulated kinase; *PLCε*, phospholipase Cε; *PKC*, protein kinase C; *RalGDS*, Ral GDP dissociation stimulator; *RLIP76*, Ral-interacting protein 76 kDa; *PI3K*, phosphoinositide 3-kinase; *PIP_3*, phosphoinositide 3,4,5-trisphosphate; *MST1/2*, mammalian Ste20-like kinases 1.

ity. Effector interactions with H-RAS have been investigated both biochemically and structurally in great detail. Various amino acids of H-RAS undergo selective contacts with the effectors, including RAF1, RalGDS, RASSF5, and PLCε (Fig. 2*A*, *blue residues* with *yellow background*). These residues, mainly switch I, interswitch, and partially in the switch II region, are conserved among common RAS proteins but vary in E-RAS proteins (supplemental Fig. S1). This suggests that classical RAS family members, except the E-RAS, are in principle able to recognize and activate various effectors. Importantly, these effector-binding residues are highly variable between H-RAS and E-RAS (supplemental Fig. S1; Fig. 2*A*). Structural analysis of the effector binding regions of E-RAS was performed according to H-RAS complexes with p120RASGAP (PDB code 1WQ1). In comparison with H-RAS, the exposed residues along the effector-binding surface of E-RAS revealed significant sequence deviations (Fig. 2*B*). This strongly indicates a differential effector selectivity of the RAS proteins.

The members of the RAS family are known to interact with a wide range of effectors (5, 54–61) and therefore stimulate various cellular responses. Regarding their physical interaction with E-RAS and H-RAS proteins, five RAS effectors (RAF1, RalGDS, PLCε, PI3Kα, and RASSF5), with defined cellular functions (Fig. 2*C*), were investigated in this study. In pulldown experiments, GST-fused RAS-binding domain of RAF1 (RAF1-RBD), the RAS association domain of RalGDS (RalGDS-RA), PLCε-RA, PI3Kα-RBD, and RASSF5-RA were used as baits to pulldown FLAG-tagged E-RAS^{WT}, H-RAS^{WT}, and H-RAS^{Val-12} overexpressed in COS-7 cells. We found that H-RAS^{WT} and H-RAS^{Val-12} strongly bind RAF1 and weakly bind to PI3Kα. Importantly, E-RAS^{WT} clearly showed an opposite pattern of these interactions, where it binds very tightly to PI3Kα and very weakly to RAF1, RalGDS, PLCε, and RASSF5 (Fig. 2*D*). These data confirm that the amino acid deviations in effector-binding sites (Fig. 2, *A* and *B*) make E-RAS a unique member of the RAS family and a potent activator of the PI3K-PIP_3-signaling pathways.

Effector Selection by E-RAS Is Largely Determined by Tryptophan 79—To identify the residues determining the specificity for effector binding and activation, we next analyzed the impact of deviating residues in E-RAS on its interaction with different effectors by replacing the E-RAS residues in switch I (His-70 and Gln-75, collectively named here SwI), interswitch (Arg-79), and switch II (Ala-100, Ile-101, His-102, and Arg-103, collectively named here SwII) for the equivalent residues in H-RAS (supplemental Fig. S1). The corresponding variants, E-RAS^{SwI}, E-RAS^{Arg-79}, E-RAS^{SwII}, E-RAS$^{SwI/Arg-79}$, E-RAS$^{Arg-79/SwII}$, RAS$^{SwI/SwII}$, and E-RAS$^{SwI/Arg-79/SwII}$ (Fig. 3*A*), were analyzed for their interaction abilities with different effectors using E-RAS^{WT} and the constitutive active variant of H-RAS^{wt}, H-RAS^{Val-12}, as controls. These constructs were transiently transfected in COS-7 cells, and the GTP-bound forms of these RAS variants were pulled down using GST-fused effector proteins under the same conditions as described above. Data

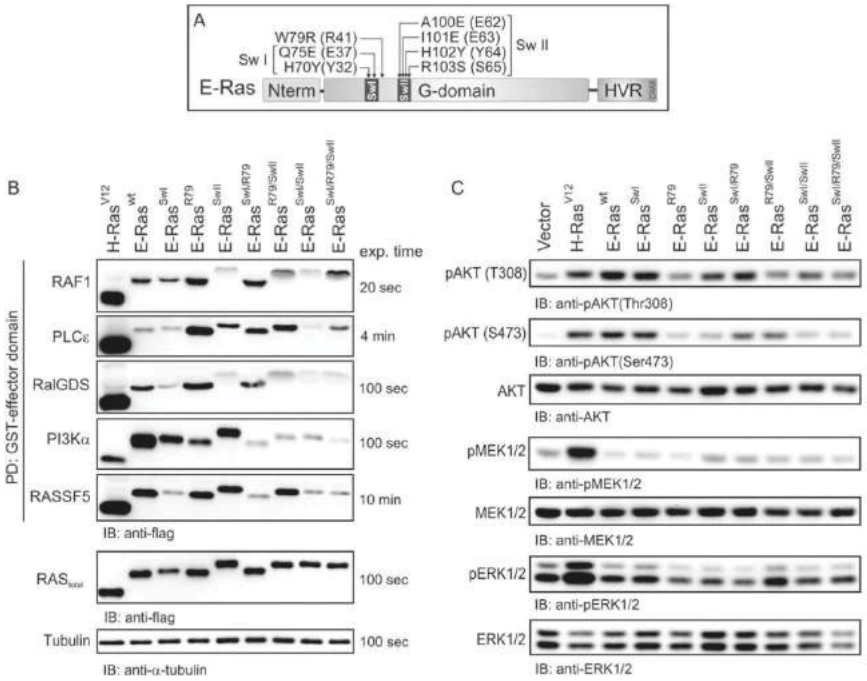

FIGURE 3. **Specificity-determining residues in E-RAS-effector interaction.** *A*, display of different effector binding mutations in E-RAS: E-RAS^{SwI}, H70Y/Q75E (Tyr-32 and Gslu-37 in H-RAS); E-RAS^{Arg-79}, W79R (Arg-41 in H-RAS); E-RAS^{SwII}, A100E/I101E/H102Y/R103S (Glu-62, Glu-63, Tyr-64, and Ser-65 in H-RAS); E-RAS$^{SwI/Arg-79}$, H70Y/Q75E/W79R; E-RAS$^{Arg-79/SwII}$, W79R/A100E/I101E/H102Y/R103S; RAS$^{SwI/SwII}$, H70Y/Q75E/A100E/I101E/H102Y/R103S, and E-RAS$^{SwI/Arg-79/SwII}$, H70Y/Q75E/W79R/A100E/I101E/H102Y/R103S. For details about the amino acid sequences, see supplemental Fig. S1. *B*, pulldown assay of FLAG-fused E-RAS variants carried out with RBD or RA domain of GST-fused effector proteins, including RAF1-RBD, RalGDS-RA, PLCε-RA, PI3Kα-RBD, and RASSF5-RA. The results were analyzed by immunoblot using an anti-FLAG antibody. *Exp. time* stands for exposure time. *C*, total cell lysates were used to monitor the level of phosphorylated AKT (pAKT^{T308} and pAKT^{S473}), MEK1/2 (pMEK1/2), and ERK1/2 (pERK1/2) proteins.

obtained revealed that substitution of Trp-79 for arginine in E-RAS (E-RAS^{Arg-79}) rescued the low affinity of E-RAS for PLCε, RAF1, and RalGDS, and no effect was observed on RASSF5 binding (Fig. 3*B*). In contrast, W79R-containing variants (E-RAS^{Arg-79}, E-RAS$^{SwI/Arg-79}$, E-RAS$^{Arg-79/SwII}$, and E-RAS$^{SwI/Arg-79/SwII}$), when compared with E-RAS^{WT}, exhibited a significant reduction of binding affinity for PI3Kα, which is comparable with the levels with H-RAS^{Val-12}. Collectively, all mutations in three regions, especially W79R, affected E-RAS interaction for PI3Kα (Fig. 3*B*). Mutations in the switch I region (E-RAS^{SwI}, E-RAS$^{SwI/Arg-79}$, RAS$^{SwI/SwII}$, and E-RAS$^{SwI/Arg-79/SwII}$) exclusively compromised E-RAS interaction with RASSF5. However, switch II variants (E-RAS^{SwII}, E-RAS$^{Arg-79/SwII}$, and RAS$^{SwI/SwII}$) more strongly diminished affinity for RalGDS and RAF1 (Fig. 3*B*).

These results raised the following question. How does the Trp-79 interaction with effectors affect the binding affinity of E-RAS for these proteins? To address this question, we inspected available H-RAS structures in complexes with investigated effector proteins and created corresponding structural models of E-RAS with particular focus on Trp-79 in E-RAS (Arg-41 in H-RAS). Data obtained pointed to an unexpected and potentially significant role of Glu-3 (Glu-41 in E-RAS) in effector selection by RAS proteins (Fig. 4; supplemental Fig. S1). Arg-41 is stabilized by intramolecular interactions with Glu-3 (Glu-41 in E-RAS) and side-chain contacts directly at Lys-65 of RAF1 among the analyzed H-RAS effector complexes but not PI3K. Tryptophan replacing Arg-41 in E-RAS would, because of its hydrophobic nature, be expelled from Glu-41, Glu-54, and Asn-92. This generates new conformation in the effector region of E-RAS and accounts for a shift in effector selectivity. The highest probability for such adopting provides an empty space around the Arg-41 in the case of the PI3K complex thus yielding higher affinity of PI3K to E-RAS^{WT}. Trp-79 interacts best in a hydrophobic environment with PI3K as compared with RAF1. Reciprocal scenario applies in the case of RAF1 and PLCε causing lower affinity of these effectors to E-RAS^{WT}. One example is the repulsion of Lys-65 of RAF1 by the W79R mutation that might be responsible for a weak reconstitution of E-RAS^{Arg-79} binding to RAF1.

We next examined the consequences of the affected effector interaction of the E-RAS variants regarding activation of the corresponding downstream cascades (see Fig. 3*C*). Interestingly, impaired PI3Kα binding of E-RAS variants, particularly W79R and SwII, also strongly influenced downstream signals of PI3K monitored by pAKT levels but not that of RAF1 analyzed by pMEK/pERK levels (Fig. 3*C*). Remarkably, AKT phosphorylation at both sides, Thr-308 (PDK1) and Ser-473 (mTORC2), were impaired (see below). The E-RAS^{Arg-79} variant lost its ability to signal via the PI3K/AKT cascade almost completely, indicating a key role of tryptophan 79 in E-RAS and E-RAS-like proteins in effector association and activation. An interesting observation is that a gain of RAF1 binding to E-RAS variants, especially SwI and W79R, did not result in RAF1 activation and

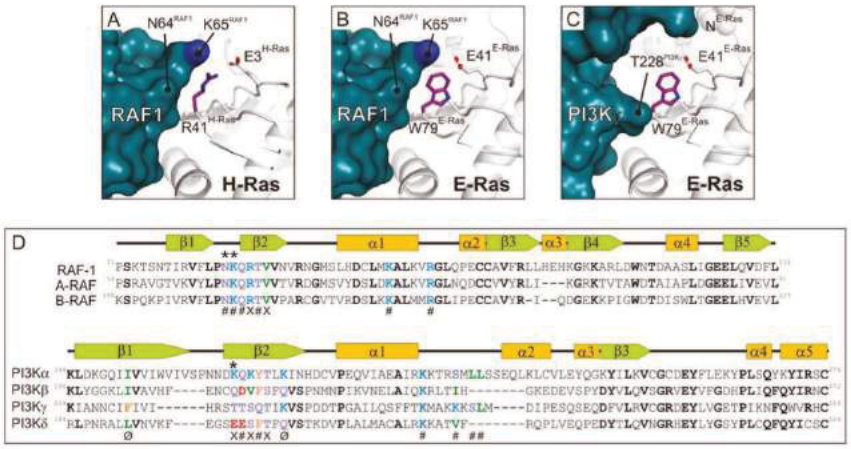

FIGURE 4. **Glutamate 41 function and its role in effector selection is discharged in E-RAS.** *A*, in H-RAS-GTP, Arg-41 (Trp-79 in E-RAS) is intramolecularly stabilized by Glu-3 (Glu-41 in E-RAS), attracted by backbone oxygen of Asn-64, and repulsed by Lys-65 in RAF1. *B*, in E-RAS, Trp-79 is expelled from Glu-41 and cannot adopt favorable conformation because of the close presence of Asn-64 and Lys-65 of RAF1. The conformation of arginine at the place of Trp-79 in E-RAS^{Arg-79} would be restored due to its interaction with Glu-41 similarly to H-RAS, thus increasing the binding affinity of RAF1. *C*, PI3K does not contact E-RAS tightly in the vicinity of Trp-79 leaving enough space for proper reorientation of tryptophan side chain expelled from Glu-41 and not disfavoring the affinity of their complex. Moreover, orientation of Thr-228 enables tight hydrophobic contact with Trp-79. In E-RAS^{Arg-79}, arginine attracted by Glu-41 would not contribute to the interaction with PI3K weakening its affinity to E-RAS^{Arg-79}. *D*, selectivity-determining amino acids in RAS effectors. Multiple amino acid sequence alignments of the RBD of human RAF isoforms and the catalytic subunits of human PI3K isoforms are illustrated with major focus on the some RAS-binding residues. The corresponding sequences are RAF-1 (P04049; aa 51–131), A-RAF (P10398; aa 14–91), B-RAF (P15056; aa 105–227), PI3Kα (P42336; aa 184–276), PI3Kβ (P42338; aa 191–272), PI3Kγ (P48736; aa 214–296), and PI3Kδ (O00329; aa 184–226). *X* highlights residues interacting in β-β manner with switch I. # highlights additional residues interacting with switch I. Ø shows residues interacting with Tyr-64 in switch II. * shows residues close to Arg-41 in H-RAS or Trp-79 in E-RAS.

in turn phosphorylation of MEK1/2 and ERK1/2 (Fig. 3, *B* and *C*).

Distinct Downstream Signaling Pathways of E-RAS via PI3K—The data presented above shed light on the specificity determining residues for direct E-RAS-effector interaction and the consequent activation of downstream pathways. The next question we addressed was to understand the role of additional motifs within the N-terminal extension and HVR of E-RAS (see Fig. 1*A*) as potential molecular and cellular determinants required for signal transduction through PI3K-AKT-mTORC and RAF1-MEK1/2-ERK1/2. Therefore, we first investigated the ability of E-RAS variants to directly interact with PI3Kα and RAF1. In this experiment, FLAG-tagged E-RAS variants, H-RAS^{WT} and H-RAS^{Val-12}, transiently transfected in COS-7 cells, were pulled down with GST-fused PI3Kα-RBD and RAF1-RBD from the cell lysates (Fig. 5*A*). Similar to E-RAS^{WT}, the interactions of E-RAS variants were much stronger with PI3Kα-RBD as compared with RAF1-RBD, although hyperactive H-RAS^{Val-12} mainly bound to RAF1-RBD. Moreover, this assay was used to visualize the amounts of the GTP-bound state of the E-RAS variants. Fig. 5*A* shows that all E-RAS variants exist in the active, GTP-bound forms.

To provide further insights to the downstream signaling activity of the above-mentioned E-RAS variants, we investigated the phosphorylation status of AKT (Thr-308 and Ser-473), MEK1/2 (Ser-217/Ser-221), and ERK1/2 (Thr-202/Thr-204), which are representative cellular targets of PI3K and RAF1 (Fig. 5*B*). Although the pulldown showed almost no significant difference between E-RAS variants in binding to RAS effectors, we found E-RAS$^{\Delta N}$, E-RAS$^{Ser-226/Ser-228}$, and E-RAS$^{\Delta N/Ser-226/Ser-228}$ were strongly impaired in the activation of the PI3K-AKT-mTORC axis and clearly exhibited lower phosphorylation levels for AKT, especially at Thr-308. All E-RAS variants, including E-RAS$^{\Delta N}$, were inefficient in stimulation of MEK1/2 and ERK1/2 phosphorylation in comparison with H-RAS^{WT} and H-RAS^{Val-12} that actively contributed to activation of the RAF1-MEK1/2-ERK1/2 axis.

Next, we aimed to determine the cellular co-localization of E-RAS with PI3Kα and RAF1. Transiently transfected MDCK II cells with FLAG-tagged E-RAS and H-RAS were incubated with recombinant GST-fused RBDs of PI3Kα and RAF1 and stained with antibodies against GST and FLAG, respectively. We observed that PI3Kα but not RAF1 localized with E-RAS mainly at the plasma membrane (Fig. 6*A*). In contrast, RAF1, and to a lower extent also PI3Kα, co-localized with H-RAS at the plasma membrane (Fig. 6*B*). These data suggest that both the N-terminal extension of E-RAS and its palmitoylation are essential and critical for the cellular activation of the PI3K-AKT-mTORC cascade, although the formation of the GTP-bound state and the interaction with PI3K were not affected.

Discussion

In this study, we have investigated cellular localization and the signaling activity of human E-RAS regarding its physical interaction with RAS effectors and the roles of both its unique features, the N terminus and PTM by palmitoylation in direct comparison with human H-RAS. The structure-function relationship of the effector interaction sites of E-RAS resulted in the identification of tryptophan 79 as a specificity-determining amino acid of E-RAS, which is critical for its strong association with PI3K. In the cell, this interaction additionally requires the presence of both a functional N-terminal extension and palmitoylation at cysteines 226 and 228 that collectively lead to the precise activation of the PI3K-AKT-mTORC pathway.

Functional Properties of E-RAS

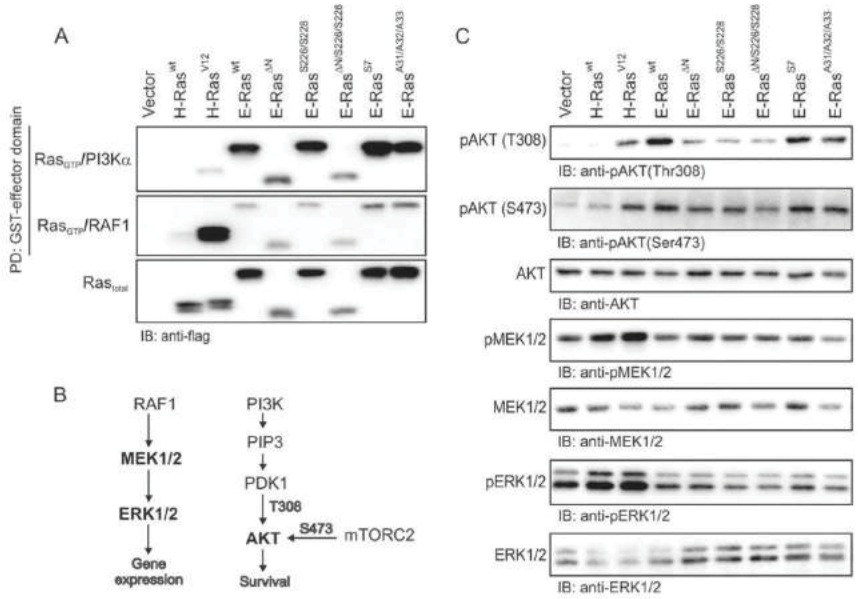

FIGURE 5. **E-RAS signaling activities in COS-7 cells.** Pulldown (*PD*) experiments and immunoblot (*IB*) analysis of total cell lysates were derived from transfected COS-7 cells with FLAG-tagged E-RAS variants H-RAS^{WT} and H-RAS^{Val-12}. *A*, pulldown analysis revealed that E-RAS variants like E-RAS^{WT} most strongly bind to GST-fused PI3Kα-RBD than RAF1-RBD, whereas hyperactive H-RAS^{Val-12} mainly bound to GST-fused RAF1-RBD. In addition, PI3Kα-RBD PD showed that all E-RAS variants are in the GTP-bound state and consequently in their activated forms. Total amounts of the RAS proteins were detected as a control using anti-FLAG antibody. *B*, schematic view of MAPK and PI3K-AKT cascades. *C*, total cell lysates were analyzed for the phosphorylation level of AKT (pAKT308 and pAKT473), MEK1/2 (pMEK1/2) and ERK1/2 (pERK1/2). Total amounts of AKT, MEK1/2, and ERK1/2 were applied as loading controls.

Palmitoylation Modification and E-RAS Trafficking—To transduce signals, RAS proteins should be associated with the lipid membranes. They are compartmentalized by PTMs at their C terminus, with the *CAAX* motif at the farnesylation site, and additional upstream cysteine residues at the palmitoylation site(s) in the case of H- and N-RAS (supplemental Fig. S1) (23–25, 29). We found that like the mouse E-RAS (42), substitution of two cysteine residues Cys-226/Cys-228 in HVR of human E-RAS with serines clearly impaired the plasma membrane localization of protein. This is a strong indication that human E-RAS undergoes palmitoylation at these sites, as described for the first time for H-RAS (62). Yamanaka and co-workers (42) reported that these cysteine residues are important for endomembrane localization of mouse E-RAS and only signals if HVR of H-RAS can rescue endomembrane localization of E-RAS$^{Ser-226/Ser-228}$. Our confocal microscopy data revealed that in contrast to plasma membrane localization of E-RAS^{WT}, palmitoylation-deficient E-RAS$^{Ser-226/Ser-228}$ is mainly localized, with a clear pattern, in cytoplasm and also in endomembranes. Our data clearly support proposed reports demonstrating that H-RAS and N-RAS cycle between Golgi and the plasma membrane via reversible and dynamic palmitoylation-depalmitoylation reactions (25, 63, 64).

N-terminal Extension and C-terminal Insertion of E-RAS—A sequence comparison between E-RAS and other RAS isoforms highlighted additional regions and motifs, such as the unique N terminus of E-RAS that is not present in other RAS-like proteins. We propose that the N-terminal extension of E-RAS might modulate its localization through interaction with potential adaptor/scaffold proteins via putative P*XX*P and RRR motifs. With our co-localization studies, we did not observe significant differences in localization of the N-terminal mutants of E-RAS. However, considering our results, we cannot exclude the role of the E-RAS N terminus as a putative protein interaction site, because E-RAS is not expressed endogenously in the MDCK II cells, and therefore its binding partner may not be available in this cell line. To confirm our hypothesis, we need to study a different cell line, like embryonic stem cells (42), gastric tumors (65), neuroblastoma cells (20), and also hepatic stellate cells,[3] where E-RAS is endogenously expressed (unpublished data).

Imaging methods used in this study did not allow visualizing microdomain localization of E-RAS variants. The plasma membrane is not a homogeneous lipid bilayer and includes a set of microdomains, such as lipid raft and caveolae (66, 67). The HVR at the C-terminal end of RAS proteins is critical for lateral sorting and is divided into two separate domains, membrane-targeting domain and linker domain (68). Membrane targeting domain contains a *CAAX* box and one or two upstream cysteines that are palmitoylation sites. Palmitoylated proteins can be targeted to lipid rafts. Because H-, N-, and K-RAS are dipalmitoylated, monopalmitoylated, and nonpalmitoylated, respectively, they exhibit different lateral segregation across the plasma membrane microdomains (69). GDP-bound H-RAS is associated with the lipid raft, but when it is activated and GTP-loaded, it moves laterally to nonlipid raft regions (68, 70, 71). E-RAS, like H-RAS, is dipalmitoylated suggesting that it may favor the lipid rafts. On the contrary, E-RAS is mainly GTP-

[3] S. Nakhaei-Rad, C. Kordes, H. Nakhaeizadeh, R. Dvorsky, I. C. Cirstea, I. Sawitza, S. Götze, Ro. P. Piekorz, B. Görg, D. Haussinger, and M. R. Ahmadian, unpublished data.

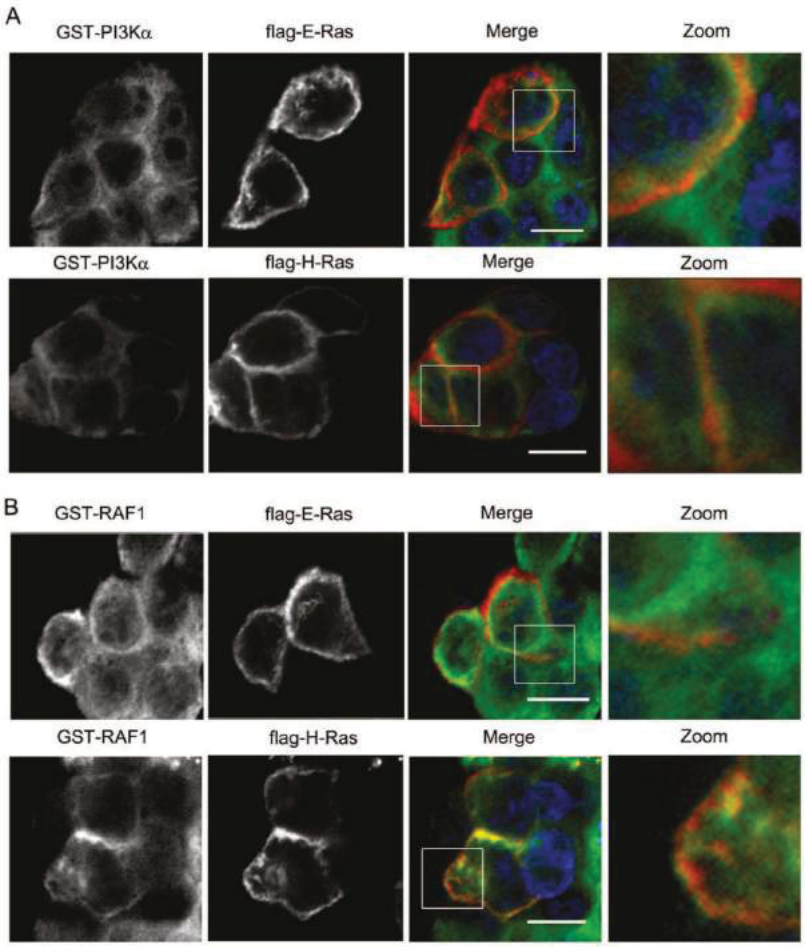

FIGURE 6. **Co-localization of E-RAS with PI3Kα.** Transfected MDCKII cells with FLAG-tagged E-RAS were incubated with bacterial lysates, containing GST-RBDs of PI3Kα and RAF1 proteins and stained with antibodies raised against GST and FLAG to investigate their co-localization with GTP-bound H-RAS and E-RAS proteins. E-RAS co-localized with PI3Kα. *Scale bar,* 10 μm.

loaded, which makes it difficult to compare it with wild-type H-RAS. It is reported that the active GTP-loaded H-RAS^{Val-12} variant occupies the nonlipid rafts so the constitutively active E-RAS may also be clustered in this region. The second domain in HVR, termed linker domain, releases GTP-loaded H-RAS from the lipid rafts. Linker domain can be divided in N- and C-terminal regions in a way that the C-terminal region is a spacer, which seems not to be important (68). Human E-RAS has an insertion in this C-terminal spacer (aa 173–179, H-RAS numbering) that may also affect microdomain migration of E-RAS. Taken together, we propose that three factors most likely modulate the microdomain targeting of E-RAS, such as an extended N terminus, a C-terminal insertion, and the GTP-loaded state due to a prominent deviation at position Ser-50 (Gly-12 in H-RAS).

Our cell-based studies revealed that the N-terminal extension of E-RAS is critical for PI3K-AKT-mTORC activation, and N-terminal truncated E-RAS variants (E-RAS$^{\Delta N}$ and E-RAS$^{\Delta N/Ser-226/Ser-228}$) remarkably had a lower signaling activity. One explanation may be the role of the unique N terminus in the lateral segregation of E-RAS across the membrane that consequently specifies association with and activation of its effectors in a manner reminiscent to microdomain localization of H-RAS that regulates its interaction with effector proteins of RAF1 and PI3K (68). In addition, E-RAS was found in membrane ruffles (data not shown), which may be induced by Rac1 activated by the E-RAS-PI3K-PIP_3-RacGEF axis (72–74). Such a scenario has been reported for the R-RAS N-terminal 26-amino acid extension, which has been proposed to positively regulate Rac activation and cell spreading (75).

Constitutively Active Form—GAPs accelerate the GTP hydrolysis reaction of RAS proteins by orders of magnitude by supplying a highly conserved, catalytic arginine finger (31, 32). H-RAS glycine 12 mutations to any other amino acid interfere with insertion of arginine finger in the GTPase active site and therefore make the enzyme GAP-insensitive (30). Interestingly, E-RAS has a deviation in the corresponding position and carries a serine instead of a glycine indicating that E-RAS is hyperactive and GAP-insensitive. Our stopped-flow data revealed that p120RASGAP was not able to accelerate the GTP hydrolysis

reaction of E-RAS, although it can act on H-RAS and convert it to the GDP-bound inactive form (data not shown). We have shown that all E-RAS variants exist mostly in GTP-bound forms as shown by a pulldown experiment with PI3K and RAF1. This and the fact that E-RAS is GAP-insensitive suggest that E-RAS may underlie a different and yet undefined control mechanism that negatively regulates E-RAS activity and thus its signal transduction.

It seems that expression of E-RAS is highly regulated at the transcriptional levels and rather limited to special cell types, such as embryonic stem cells (42), gastric tumors (65), neuroblastoma cells (20), and also hepatic stellate cells.[5] Moreover, the unique N terminus of E-RAS may provide specialized protein-protein interaction sites resulting in E-RAS sequestration, degradation, or membrane microdomain localization as shown for R-RAS (75, 76). E-RAS could interact with specific scaffolding proteins that bring it close to its effectors and regulate its activities. It is tempting to speculate that E-RAS may underlie a similar mechanism via serine/threonine phosphorylation and 14-3-3 binding as described for Rnd3 (75, 76), a constitutively active member of the Rho protein family (77). However, there is as yet no evidence for an E-RAS phosphorylation particularly at its N terminus that contains 4 threonines and 2 serines (supplemental Fig. S1).

Effector Binding Regions—RAS proteins transduce extracellular signals to a variety of intracellular signaling pathways through the interaction with a wide spectrum of effector proteins. Upon GDP to GTP exchange, RAS proteins undergo conformational changes in two critical regions, switch I and switch II. Notably, the GTP-bound form of RAS interacts with their target effectors through switch regions and thereby activates various pathways (5). A detailed study of structure-sequence relationships revealed a distinctive effector binding region for E-RAS in comparison with RAS isoforms (H-, N-, and K-RAS). Subsequent interaction analysis with five different RAS effectors revealed that effector binding profile of E-RAS significantly differs from H-RAS. E-RAS^{WT} tightly bound to PI3Kα and revealed very low affinity for other RAS effectors. In contrast, H-RAS showed an opposite pattern with the highest affinity for RAF1. These data were confirmed by investigating the respective downstream signaling cascades (PI3K-AKT-mTORC and RAF1-MEK1/2-ERK1/2) at the level of phosphorylated AKT, MEK1/2, and ERK1/2. Our results are consistent with a previous study of Yamanaka and co-workers (18), who applied another PI3K isoform (PI3Kδ) and observed differences between H-RAS and E-RAS. It seems probable that E-RAS and H-RAS possess a different affinity for distinct PI3K isoforms, α, β, γ, and δ, and this may account for their specific biological outputs (78). Consistently, the catalytic subunit of the PI3Kγ isoform, PI3Kγ, interacts with switch I of H-RAS in anti-parallel β-sheet fashion (48), also approaching RAS-conserved Asp-33 by two lysines. Residues in H-RAS contacting β-strand of PI3Kγ and preceding amino acids differ significantly among the PI3K isoforms regarding the primary structures (Fig. 4*D*). Although PI3Kγ has four hydroxyl-containing amino acid side chains at this place, PI3Kβ possesses one and PI3Kδ isoform two negatively charged residues whereby both have in addition two amino acid insertions. In contrast, the PI3Kα isoform has insertion of six residues, and the hydroxyl-containing amino acids are replaced by one asparagine and two lysines (Fig. 4*D*). We hypothesize that these differences in PI3K isoforms are of particular importance due to the stabilization of intermolecular β-sheet interaction and especially because the contact site of the crucial Trp-79 in E-RAS (Arg-41 in H-RAS) is highly variable (Lys, Gln, Thr, and Glu; see Fig. 4*D*).

Substitutions for E-RAS residues in the switch I and II and interswitch regions with corresponding residues in H-RAS provided several interesting aspects and new insights (Fig. 3). One is a shift in effector selection. Strikingly, and in contrast to other investigated effectors, RAF1-RBD undergoes contacts with the switch I and the interswitch regions (Fig. 2*A*) (46, 47). However, E-RAS^{SwI}, which has an almost identical switch I when compared with H-RAS, showed a reduced binding to RAF1 that was clearly elevated when this was combined with the interswitch mutation W79R (E-RAS$^{SwI/Arg\text{-}79}$) (Fig. 3*B*). Consistently, the major difference was observed with E-RAS$^{Arg\text{-}79}$, where a tryptophan was replaced by an arginine (Arg-41 in H-RAS). This variant led to increase in RAF1 binding and partly rescued the low affinity of the wild type and the switch variants (E-RAS$^{SwI/Arg\text{-}79}$ and E-RAS$^{SwI/Arg\text{-}79/SwII}$). According to the crystal structure (46), Arg-41 in H-RAS (Trp-79 in E-RAS) interestingly forms a hydrogen bond with the backbone oxygen of Asn-64 in RAF1-RBD that very likely enabled E-RAS$^{Arg\text{-}79}$ to make additional electrostatic contacts with RAF1 (Fig. 4, *A* and *B*). In addition, E-RAS shares a glutamate (Glu-41) with H-RAS (Glu-3) (supplemental Fig. S1). Glu-3 interacts in intermolecular fashion with Arg-41 and stabilizes the H-RAS·RAF1 complex formation (Fig. 4*A*). Accordingly, mutation of W79R in E-RAS reconstitutes such intermolecular interaction between Glu-41 and Arg-79, thus increasing significantly the interaction between E-RAS$^{Arg\text{-}79}$ and RAF1 (Fig. 3*B*). Another important contribution to effector binding concerning Trp-79 originates very likely in its expulsion from the above-mentioned Glu-41 and the ability of bound effector protein to accommodate altered conformation of Trp-79. As mentioned before, Arg-41 of H-RAS is contacted by RAF1 in its complex structure. The space where the tryptophan can be accommodated and hydrophobically interact with the effector is thus limited resulting in diminished affinity of these effectors to E-RAS^{WT}. Moreover, switch II quadruple mutation of E-RAS (E-RAS^{SwII}; see Fig. 3*A*) showed the largest impairment in RAF1 binding. This was not expected especially because the structural data, reported previously (46, 47), have shown that RAF1-RBD does not physically contact the switch II of RAS. Again, E-RAS$^{Arg\text{-}79/SwII}$ partially restored the loss of RAF1 binding but most remarkably not the E-RAS$^{SwI/SwII}$ variant that actually is almost identical to H-RAS regarding the amino acid sequence of its switch I and II regions (see Fig. 3*A*). Even though E-RAS$^{Arg\text{-}79}$ binds more tightly to RAF1, it still does not activate the MAPK pathway like E-RAS^{WT}. Note that there was no increase in MEK and ERK phosphorylation, and we detected even the opposite, namely a significant decrease in pMEK1/2 and pERK1/2 as compared with the vector control (Fig. 3*C*; see *E-RAS^{WT}* and *E-RAS$^{Arg\text{-}79}$ lanes*). An explanation for the absence of E-RAS$^{Arg\text{-}79}$ signaling toward the MAPK pathway is that most probably the additional component, including scaffold proteins such as SHOC2 (79–

81), may not exist in the E-RAS^{Arg-79}·RAF1 complex. This provides the assumption that E-RAS localizes to a different membrane region then, for example, the H-RAS, RAF1, and the components of the MAPK pathway.

PLCϵ contains two RAS association domains, RA1 and RA2. RA2 forms a complex with H-RAS in a GTP-dependent manner by contacting nine different residues of the switch I and II regions, and also Gln-25 and Arg-41 (51), from which four (Glu-37, Arg-41, Glu-63, and Tyr-63) deviate in E-RAS (Fig. 3*A*). This explains why we observed an extremely weak E-RAS-PLCϵ interaction as compared with H-RAS^{Val-12}. Most interestingly, the W79R mutation of E-RAS resulted in a strong gain of binding activity (Fig. 3*B*; see *E-RAS^{WT}* and *E-RAS^{Arg-79} lanes*). Notably, this effect was not so strong in the case of the switch II mutation (E-RAS^{SwII}), and the switch I mutation (E-RAS^{SwI}) did not show any change in the E-RAS association with PLCϵ. A combination of the mutations (E-RAS$^{SwI/SwII}$) was hardly detectable and the combinations with W79R (E-RAS$^{Arg-79/SwI}$, E-RAS$^{Arg-79/SwII}$, and RAS$^{SwI/Arg-79/SwII}$) rather counteracted the gain of binding activity of RAS^{Arg-79}. On a molecular level, Trp-79 in wild-type E-RAS can be hydrophobically attracted to Pro-2149 of PLCϵ but not intramolecularly to Glu-41 (data not shown), and the space for its conformational relaxation is limited similarly to RAF1 as mentioned above. We propose that W79R mutation generates stronger intramolecular contact between Glu-41 and Arg-79 and consequently stabilizes the protein complex with PLCϵ. Katan and co-workers (51) have discussed that the H-RAS residues Tyr-64, Ile-36, and Met-67 (His-102, Ile-74, and Leu-105 in E-RAS) in combination with Phe-2138 and Val-2152 from PLCϵ-RA2, provide a hydrophobic clusters. Introduction of another hydrophobic residue in E-RAS as demonstrated with a single point mutation at Trp-79 (E-RAS^{Arg-79}) has obviously created an additional and distinct binding site for RAS association domains, such as RA2 of PLCϵ and most likely also RA of RalGDS. The latter, a GEF for Ral, links two RAS family members, RAS and Ral (82). Although the crystal structure of H-RAS/RalGDS-RA has not reported an involvement of Arg-41 (50), our structural analysis predicted a close hydrophobic contact of Arg-41 with Met-819 of RalGDS (3.2 Å). Notably, data obtained from the interaction of RalGDS and RAF1 with E-RAS variants appear similar as compared with that for PLCϵ.

PI3K is a well known effector of classical RAS proteins and promotes cellular survival (78). In comparison with H-RAS, E-RAS interacts more strongly with PI3Kα-RBD and activates the PI3K-AKT-mTORC cascade. Mutagenesis at switch and interswitch regions (E-RAS^{SwI}, E-RAS^{Arg-79}, and E-RAS^{SwII}), attenuated binding of E-RAS to PI3Kα-RBD, demonstrating the role of critical E-RAS residues at effector binding regions. These data are consistent with a previous study that has shown that PI3Kγ-RBD contacts both switch I and switch II regions of H-RAS (48). Interestingly, W79R mutation of E-RAS (Arg-41 H-RAS), which has increased binding to RAF1, PLCϵ, and RalGDS, dramatically reduced the binding to PI3Kα. The affinity of this E-RAS mutant (E-RAS^{Arg-79}) for PI3Kα-RBD appears similar to that of H-RAS^{Val-12} (Fig. 3*B*; see *H-RAS^{Val-12}* and *E-RAS^{Arg-79} lanes*). We think that the strong interaction between E-RAS and PI3K stems from the ability of structure to accommodate altered conformation of Trp-79 and from its hydrophobic contact to PI3K (Fig. 4*C*). In contrast, W79R mutation in E-RAS enables Glu-41 to attract Arg-79 and to interfere with this hydrophobic interaction, resulting in a significant reduction of the binding affinity between PI3K and E-RAS (Fig. 4*C*). In the same line of evidence, we also observed E-RAS^{Arg-79} deficient at the activation of RAS-PI3K-AKT-mTORC2 pathway (9) as monitored with Ser-473 phosphorylation of AKT (see result Fig. 3*C*). Thus, Trp-79 in E-RAS represents a specificity-determining residue for the proper binding to and activation of PI3K.

RASSF members are known as a RAS effector with tumor suppressor functions. RASSF5 have two splice variants NORE1A and RAPL, which share same RBD (53). We applied the RASSF5-RA domain to analyze the interaction of E-RAS variants with this RAS effector. As shown for RAF1 and RalGDS, switch I H70Y/Q75E mutation of E-RAS (E-RAS^{SwI}) also attenuated the binding to RASSF5, and this was the case for all E-RAS variants harboring switch I mutations (E-RAS$^{SwI/Arg-79}$, E-RAS$^{SwI/SwII}$, and E-RAS$^{SwI/Arg-79/SwII}$). Switch II and W79R mutations did not affect the binding affinity for RASSF5, emphasizing the importance of the more conserved switch I region in the complex formation of the RAS proteins with RASSF5 (53). It remains to be investigated whether E-RAS is an activator of RASSF5 and thus a regulator of the Hippo pathway.

In summary, we conclude that switch regions of E-RAS act as core effector binding regions that form an E-RAS-specific interaction interface for its effectors, such as PI3K. The PI3K isoform specificity in E-RAS-expressing cells remains to be investigated. Trp-79 of E-RAS appears to determine the effector selectivity. E-RAS binding to other RAS effectors, such as RASSF5, RalGDS, and RAF1, is weak but may still be of physiological relevance. Improvement of the interaction with RAF1 by mutagenesis, for example, rather exhibited an inhibitory impact on the MAPK pathway. It remains unclear whether protein phosphatases specific for MAPKs were activated. The N terminus of E-RAS is unique and may play a critical role in the interaction with its accessory proteins for positioning E-RAS to subcellular microdomains of the plasma membrane.

Acknowledgments—We are grateful to Ehsan Amin, Hedyeh Amintoosi, Silke Götze, Lothar Gremer, Ilse Meyer, Kazem Nouri, Björn Papke, Roland P. Piekorz, Georg Rosenberger, Claudia Rupprecht, Iris Sawitza, Jürgen Scheller, Madhurendra Singh, Nachiket Vartak, and Si-Cai Zhang for their helpful advice, stimulating discussions, and for sharing reagents.

Note Added in Proof—Supplemental Fig. 1 comparing mammalian E-RAS and classical RAS sequences was inadvertently omitted from the version of this article that was published May 4, 2015 as a Paper in Press. Supplemental Fig. 1 is now available on line.

References

1. Vetter, I. R. (2001) The guanine nucleotide-binding switch in three dimensions. *Science* **294,** 1299–1304
2. Boguski, M. S., and McCormick, F. (1993) Proteins regulating Ras and its relatives. *Nature* **366,** 643–654
3. Ahmadian, M. R., Wittinghofer, A., and Schmidt, G. (2002) The actin filament architecture: tightly regulated by the cells, manipulated by patho-

gens. International Titisee Conference on the actin cytoskeleton: from signalling to bacterial pathogenesis. *EMBO Rep.* **3,** 214–218
4. Gremer, L., Merbitz-Zahradnik, T., Dvorsky, R., Cirstea, I. C., Kratz, C. P., Zenker, M., Wittinghofer, A., and Ahmadian, M. R. (2011) Germ line KRAS mutations cause aberrant biochemical and physical properties leading to developmental disorders. *Hum. Mutat.* **32,** 33–43
5. Karnoub, A. E., and Weinberg, R. A. (2008) Ras oncogenes: split personalities. *Nat. Rev. Mol. Cell Biol.* **9,** 517–531
6. Pylayeva-Gupta, Y., Grabocka, E., and Bar-Sagi, D. (2011) RAS oncogenes: weaving a tumorigenic web. *Nat. Rev. Cancer* **11,** 761–774
7. Tidyman, W. E., and Rauen, K. A. (2009) The RASopathies: developmental syndromes of Ras/MAPK pathway dysregulation. *Curr. Opin. Genet. Dev.* **19,** 230–236
8. Flex, E., Jaiswal, M., Pantaleoni, F., Martinelli, S., Strullu, M., Fansa, E. K., Caye, A., De Luca, A., Lepri, F., Dvorsky, R., Pannone, L., Paolacci, S., Zhang, S. C., Fodale, V., Bocchinfuso, G., *et al.* (2014) Activating mutations in RRAS underlie a phenotype within the RASopathy spectrum and contribute to leukaemogenesis. *Hum. Mol. Genet.* **23,** 4315–4327
9. Cirstea, I. C., Gremer, L., Dvorsky, R., Zhang, S. C., Piekorz, R. P., Zenker, M., and Ahmadian, M. R. (2013) Diverging gain-of-function mechanisms of two novel KRAS mutations associated with Noonan and cardio-facio-cutaneous syndromes. *Hum. Mol. Genet.* **22,** 262–270
10. Castellano, E., and Santos, E. (2011) Functional specificity of Ras isoforms: so similar but so different. *Genes Cancer* **2,** 216–231
11. Ichise, T., Yoshida, N., and Ichise, H. (2010) H-, N- and Kras cooperatively regulate lymphatic vessel growth by modulating VEGFR3 expression in lymphatic endothelial cells in mice. *Development* **137,** 1003–1013
12. Omerovic, J., Laude, A. J., and Prior, I. A. (2007) Ras proteins: paradigms for compartmentalised and isoform-specific signalling. *Cell. Mol. Life Sci.* **64,** 2575–2589
13. Potenza, N., Vecchione, C., Notte, A., De Rienzo, A., Rosica, A., Bauer, L., Affuso, A., De Felice, M., Russo, T., Poulet, R., Cifelli, G., De Vita, G., Lembo, G., and Di Lauro, R. (2005) Replacement of K-Ras with H-Ras supports normal embryonic development despite inducing cardiovascular pathology in adult mice. *EMBO Rep.* **6,** 432–437
14. Leon, J., Guerrero, I., and Pellicer, A. (1987) Differential expression of the ras gene family in mice. *Mol. Cell. Biol.* **7,** 1535–1540
15. Johnson, L., Greenbaum, D., Cichowski, K., Mercer, K., Murphy, E., Schmitt, E., Bronson, R. T., Umanoff, H., Edelmann, W., Kucherlapati, R., and Jacks, T. (1997) K-ras is an essential gene in the mouse with partial functional overlap with N-ras. *Genes Dev.* **11,** 2468–2481
16. Nakamura, K., Ichise, H., Nakao, K., Hatta, T., Otani, H., Sakagami, H., Kondo, H., and Katsuki, M. (2008) Partial functional overlap of the three ras genes in mouse embryonic development. *Oncogene* **27,** 2961–2968
17. Lau, K. S., and Haigis, K. M. (2009) Nonredundancy within the RAS oncogene family: insights into mutational disparities in cancer. *Mol. Cells* **28,** 315–320
18. Takahashi, K., Mitsui, K., and Yamanaka, S. (2003) Role of ERas in promoting tumour-like properties in mouse embryonic stem cells. *Nature* **423,** 541–545
19. Tanaka, Y., Ikeda, T., Kishi, Y., Masuda, S., Shibata, H., Takeuchi, K., Komura, M., Iwanaka, T., Muramatsu, S., Kondo, Y., Takahashi, K., Yamanaka, S., and Hanazono, Y. (2009) ERas is expressed in primate embryonic stem cells but not related to tumorigenesis. *Cell Transplant.* **18,** 381–389
20. Aoyama, M., Kataoka, H., Kubota, E., Tada, T., and Asai, K. (2010) Resistance to chemotherapeutic agents and promotion of transforming activity mediated by embryonic stem cell-expressed Ras (ERas) signal in neuroblastoma cells. *Int. J. Oncol.* **37,** 1011–1016
21. Kubota, E., Kataoka, H., Aoyama, M., Mizoshita, T., Mori, Y., Shimura, T., Tanaka, M., Sasaki, M., Takahashi, S., Asai, K., and Joh, T. (2010) Role of ES cell-expressed Ras (ERas) in tumorigenicity of gastric cancer. *Am. J. Pathol.* **177,** 955–963
22. Willumsen, B. M., Christensen, A., Hubbert, N. L., Papageorge, A. G., and Lowy, D. R. (1984) The p21 ras C-terminus is required for transformation and membrane association. *Nature* **310,** 583–586
23. Ahearn, I. M., Haigis, K., Bar-Sagi, D., and Philips, M. R. (2012) Regulating the regulator: post-translational modification of RAS. *Nat. Rev. Mol. Cell Biol.* **13,** 39–51
24. Schmick, M., Vartak, N., Papke, B., Kovacevic, M., Truxius, D. C., Rossmannek, L., and Bastiaens, P. I. (2014) KRas localizes to the plasma membrane by spatial cycles of solubilization, trapping and vesicular transport. *Cell* **157,** 459–471
25. Rocks, O., Peyker, A., Kahms, M., Verveer, P. J., Koerner, C., Lumbierres, M., Kuhlmann, J., Waldmann, H., Wittinghofer, A., and Bastiaens, P. I. (2005) An acylation cycle regulates localization and activity of palmitoylated Ras isoforms. *Science* **307,** 1746–1752
26. Takahashi, K., Murakami, M., and Yamanaka, S. (2005) Role of the phosphoinositide 3-kinase pathway in mouse embryonic stem (ES) cells. *Biochem. Soc. Trans.* **33,** 1522–1525
27. Yu, Y., Liang, D., Tian, Q., Chen, X., Jiang, B., Chou, B.-K., Hu, P., Cheng, L., Gao, P., Li, J., and Wang, G. (2014) Stimulation of somatic cell reprogramming by ERas-Akt-FoxO1 signaling axis. *Stem Cells* **32,** 349–363
28. Lerner, E. C., Qian, Y., Blaskovich, M. A., Fossum, R. D., Vogt, A., Sun, J., Cox, A. D., Der, C. J., Hamilton, A. D., and Sebti, S. M. (1995) Ras CAAX peptidomimetic FTI-277 selectively blocks oncogenic Ras signaling by inducing cytoplasmic accumulation of inactive Ras-Raf complexes. *J. Biol. Chem.* **270,** 26802–26806
29. Apolloni, A., Prior, I. A., Lindsay, M., Parton, R. G., and Hancock, J. F. (2000) H-ras but not K-ras traffics to the plasma membrane through the exocytic pathway. *Mol. Cell. Biol.* **20,** 2475–2487
30. Scheffzek, K., Ahmadian, M. R., Kabsch, W., Wiesmüller, L., Lautwein, A., Schmitz, F., and Wittinghofer, A. (1997) The Ras-RasGAP complex: structural basis for GTPase activation and its loss in oncogenic Ras mutants. *Science* **277,** 333–338
31. Ahmadian, M. R., Hoffmann, U., Goody, R. S., and Wittinghofer, A. (1997) Individual rate constants for the interaction of Ras proteins with GTPase-activating proteins determined by fluorescence spectroscopy. *Biochemistry* **36,** 4535–4541
32. Ahmadian, M. R., Stege, P., Scheffzek, K., and Wittinghofer, A. (1997) Confirmation of the arginine-finger hypothesis for the GAP-stimulated GTP-hydrolysis reaction of Ras. *Nat. Struct. Biol.* **4,** 686–689
33. Lenzen, C., Cool, R. H., Prinz, H., Kuhlmann, J., and Wittinghofer, A. (1998) Kinetic analysis by fluorescence of the interaction between Ras and the catalytic domain of the guanine nucleotide exchange factor Cdc25Mm. *Biochemistry* **37,** 7420–7430
34. Buday, L., and Downward, J. (2008) Many faces of Ras activation. *Biochim. Biophys. Acta* **1786,** 178–187
35. Bourne, H. R., Sanders, D. A., and McCormick, F. (1990) The GTPase superfamily: a conserved switch for diverse cell functions. *Nature* **348,** 125–132
36. Bourne, H. R., Sanders, D. A., and McCormick, F. (1991) The GTPase superfamily: conserved structure and molecular mechanism. *Nature* **349,** 117–127
37. Saraste, M., Sibbald, P. R., and Wittinghofer, A. (1990) The P-loop–a common motif in ATP- and GTP-binding proteins. *Trends Biochem. Sci.* **15,** 430–434
38. Bos, J. L. (1989) ras oncogenes in human cancer: a review. *Cancer Res.* **49,** 4682–4689
39. Herrmann, C. (2003) Ras-effector interactions: after one decade. *Curr. Opin. Struct. Biol.* **13,** 122–129
40. Schmidt, G., Lenzen, C., Simon, I., Deuter, R., Cool, R. H., Goody, R. S., and Wittinghofer, A. (1996) Biochemical and biological consequences of changing the specificity of p21ras from guanosine to xanthosine nucleotides. *Oncogene* **12,** 87–96
41. Wittinghofer, A., and Vetter, I. R. (2011) Structure-function relationships of the G domain, a canonical switch motif. *Annu. Rev. Biochem.* **80,** 943–971
42. Takahashi, K., Nakagawa, M., Young, S. G., and Yamanaka, S. (2005) Differential membrane localization of ERas and Rheb, two Ras-related proteins involved in the phosphatidylinositol 3-kinase/mTOR pathway. *J. Biol. Chem.* **280,** 32768–32774
43. Tucker, J., Sczakiel, G., Feuerstein, J., John, J., Goody, R. S., and Wittinghofer, A. (1986) Expression of p21 proteins in *Escherichia coli* and stereochemistry of the nucleotide-binding site. *EMBO J.* **5,** 1351–1358
44. Cirstea, I. C., Kutsche, K., Dvorsky, R., Gremer, L., Carta, C., Horn, D.,

Roberts, A. E., Lepri, F., Merbitz-Zahradnik, T., König, R., Kratz, C. P., Pantaleoni, F., Dentici, M. L., Joshi, V. A., Kucherlapati, R. S., *et al.* (2010) A restricted spectrum of NRAS mutations causes Noonan syndrome. *Nat. Genet.* **42,** 27–29

45. Margarit, S. M., Sondermann, H., Hall, B. E., Nagar, B., Hoelz, A., Pirruccello, M., Bar-Sagi, D., and Kuriyan, J. (2003) Structural evidence for feedback activation by Ras. GTP of the Ras-specific nucleotide exchange factor SOS. *Cell* **112,** 685–695
46. Nassar, N., Horn, G., Herrmann, C., Block, C., Janknecht, R., and Wittinghofer, A. (1996) Ras/Rap effector specificity determined by charge reversal. *Nat. Struct. Biol.* **3,** 723–729
47. Filchtinski, D., Sharabi, O., Rüppel, A., Vetter, I. R., Herrmann, C., and Shifman, J. M. (2010) What makes Ras an efficient molecular switch: a computational, biophysical, and structural study of Ras-GDP interactions with mutants of Raf. *J. Mol. Biol.* **399,** 422–435
48. Pacold, M. E., Suire, S., Perisic, O., Lara-Gonzalez, S., Davis, C. T., Walker, E. H., Hawkins, P. T., Stephens, L., Eccleston, J. F., and Williams, R. L. (2000) Crystal structure and functional analysis of Ras binding to its effector phosphoinositide 3-kinase γ. *Cell* **103,** 931–943
49. Scheffzek, K., Grünewald, P., Wohlgemuth, S., Kabsch, W., Tu, H., Wigler, M., Wittinghofer, A., and Herrmann, C. (2001) The Ras-Byr2RBD complex: structural basis for Ras effector recognition in yeast. *Structure* **9,** 1043–1050
50. Huang, L., Hofer, F., Martin, G. S., and Kim, S. H. (1998) Structural basis for the interaction of Ras with RalGDS. *Nat. Struct. Biol.* **5,** 422–426
51. Bunney, T. D., Harris, R., Gandarillas, N. L., Josephs, M. B., Roe, S. M., Sorli, S. C., Paterson, H. F., Rodrigues-Lima, F., Esposito, D., Ponting, C. P., Gierschik, P., Pearl, L. H., Driscoll, P. C., and Katan, M. (2006) Structural and mechanistic insights into ras association domains of phospholipase Cε. *Mol. Cell* **21,** 495–507
52. Qamra, R., and Hubbard, S. R. (2013) Structural basis for the interaction of the adaptor protein grb14 with activated ras. *PLoS One* **8,** e72473
53. Stieglitz, B., Bee, C., Schwarz, D., Yildiz, O., Moshnikova, A., Khokhlatchev, A., and Herrmann, C. (2008) Novel type of Ras effector interaction established between tumour suppressor NORE1A and Ras switch II. *EMBO J.* **27,** 1995–2005
54. Vavvas, D., Li, X., Avruch, J., and Zhang, X. F. (1998) Identification of Nore1 as a potential Ras effector. *J. Biol. Chem.* **273,** 5439–5442
55. González-García, A., Pritchard, C. A., Paterson, H. F., Mavria, G., Stamp, G., and Marshall, C. J. (2005) RalGDS is required for tumor formation in a model of skin carcinogenesis. *Cancer Cell* **7,** 219–226
56. Castellano, E., and Downward, J. (2011) RAS interaction with PI3K: more than just another effector pathway. *Genes Cancer* **2,** 261–274
57. Bunney, T. D., and Katan, M. (2006) Phospholipase Cε: linking second messengers and small GTPases. *Trends Cell Biol.* **16,** 640–648
58. Yan, J., Roy, S., Apolloni, A., Lane, A., and Hancock, J. F. (1998) Ras isoforms vary in their ability to activate Raf-1 and phosphoinositide 3-kinase. *J. Biol. Chem.* **273,** 24052–24056
59. Song, C., Hu, C. D., Masago, M., Kariyai, K., Yamawaki-Kataoka, Y., Shibatohge, M., Wu, D., Satoh, T., and Kataoka, T. (2001) Regulation of a novel human phospholipase C, PLC, through membrane targeting by Ras. *J. Biol. Chem.* **276,** 2752–2757
60. Kuriyama, M., Harada, N., Kuroda, S., Yamamoto, T., Nakafuku, M., Iwamatsu, A., Yamamoto, D., Prasad, R., Croce, C., Canaani, E., and Kaibuchi, K. (1996) Identification of AF-6 and canoe as putative targets for Ras. *J. Biol. Chem.* **271,** 607–610
61. Lambert, J. M., Lambert, Q. T., Reuther, G. W., Malliri, A., Siderovski, D. P., Sondek, J., Collard, J. G., and Der, C. J. (2002) Tiam1 mediates Ras activation of Rac by a PI(3)K-independent mechanism. *Nat. Cell Biol.* **4,** 621–625
62. Hancock, J. F., Magee, A. I., Childs, J. E., and Marshall, C. J. (1989) All ras proteins are polyisoprenylated but only some are palmitoylated. *Cell* **57,** 1167–1177
63. Matallanas, D., Sanz-Moreno, V., Arozarena, I., Calvo, F., Agudo-Ibáñez, L., Santos, E., Berciano, M. T., and Crespo, P. (2006) Distinct utilization of effectors and biological outcomes resulting from site-specific Ras activation: Ras functions in lipid rafts and Golgi complex are dispensable for proliferation and transformation. *Mol. Cell. Biol.* **26,** 100–116
64. Goodwin, J. S., Drake, K. R., Rogers, C., Wright, L., Lippincott-Schwartz, J., Philips, M. R., and Kenworthy, A. K. (2005) Depalmitoylated Ras traffics to and from the Golgi complex via a nonvesicular pathway. *J. Cell Biol.* **170,** 261–272
65. Kaizaki, R., Yashiro, M., Shinto, O., Yasuda, K., Matsuzaki, T., Sawada, T., and Hirakawa, K. (2009) Expression of ERas oncogene in gastric carcinoma. *Anticancer Res.* **29,** 2189–2193
66. Simons, K., and Toomre, D. (2000) Lipid rafts and signal transduction. *Nat. Rev. Mol. Cell Biol.* **1,** 31–39
67. Iwabuchi, K., Handa, K., and Hakomori, S. (1998) Separation of "glycosphingolipid signaling domain" from caveolin-containing membrane fraction in mouse melanoma B16 cells and its role in cell adhesion coupled with signaling. *J. Biol. Chem.* **273,** 33766–33773
68. Jaumot, M., Yan, J., Clyde-Smith, J., Sluimer, J., and Hancock, J. F. (2002) The linker domain of the Ha-Ras hypervariable region regulates interactions with exchange factors, Raf-1 and phosphoinositide 3-kinase. *J. Biol. Chem.* **277,** 272–278
69. Prior, I. A., Muncke, C., Parton, R. G., and Hancock, J. F. (2003) Direct visualization of Ras proteins in spatially distinct cell surface microdomains. *J. Cell Biol.* **160,** 165–170
70. Prior, I. A., and Hancock, J. F. (2001) Compartmentalization of Ras proteins. *J. Cell Sci.* **114,** 1603–1608
71. Rotblat, B., Prior, I. A., Muncke, C., Parton, R. G., Kloog, Y., Henis, Y. I., and Hancock, J. F. (2004) Three separable domains regulate GTP-dependent association of H-ras with the plasma membrane. *Mol. Cell. Biol.* **24,** 6799–6810
72. Innocenti, M., Frittoli, E., Ponzanelli, I., Falck, J. R., Brachmann, S. M., Di Fiore, P. P., and Scita, G. (2003) Phosphoinositide 3-kinase activates Rac by entering in a complex with Eps8, Abi1, and Sos-1. *J. Cell Biol.* **160,** 17–23
73. Inabe, K., Ishiai, M., Scharenberg, A. M., Freshney, N., Downward, J., and Kurosaki, T. (2002) Vav3 modulates B cell receptor responses by regulating phosphoinositide 3-kinase activation. *J. Exp. Med.* **195,** 189–200
74. Dillon, L. M., Bean, J. R., Yang, W., Shee, K., Symonds, L. K., Balko, J. M., McDonald, W. H., Liu, S., Gonzalez-Angulo, A. M., Mills, G. B., Arteaga, C. L., and Miller, T. W. (2014) P-REX1 creates a positive feedback loop to activate growth factor receptor, PI3K/AKT and MEK/ERK signaling in breast cancer. *Oncogene* **6,** 328
75. Holly, S. P., Larson, M. K., and Parise, L. V. (2005) The unique N-terminus of R-ras is required for Rac activation and precise regulation of cell migration. *Mol. Biol. Cell* **16,** 2458–2469
76. Riou, P., Kjær, S., Garg, R., Purkiss, A., George, R., Cain, R. J., Bineva, G., Reymond, N., McColl, B., Thompson, A. J., O'Reilly, N., McDonald, N. Q., Parker, P. J., and Ridley, A. J. (2013) 14-3-3 proteins interact with a hybrid prenyl-phosphorylation motif to inhibit G proteins. *Cell* **153,** 640–653
77. Jaiswal, M., Dvorsky, R., and Ahmadian, M. R. (2013) Deciphering the molecular and functional basis of Dbl family proteins: a novel systematic approach toward classification of selective activation of the Rho family proteins. *J. Biol. Chem.* **288,** 4486–4500
78. Vanhaesebroeck, B., Guillermet-Guibert, J., Graupera, M., and Bilanges, B. (2010) The emerging mechanisms of isoform-specific PI3K signalling. *Nat. Rev. Mol. Cell Biol.* **11,** 329–341
79. Matsunaga-Udagawa, R., Fujita, Y., Yoshiki, S., Terai, K., Kamioka, Y., Kiyokawa, E., Yugi, K., Aoki, K., and Matsuda, M. (2010) The scaffold protein Shoc2/SUR-8 accelerates the interaction of Ras and Raf. *J. Biol. Chem.* **285,** 7818–7826
80. Cordeddu, V., Di Schiavi, E., Pennacchio, L. A., Ma'ayan, A., Sarkozy, A., Fodale, V., Cecchetti, S., Cardinale, A., Martin, J., Schackwitz, W., Lipzen, A., Zampino, G., Mazzanti, L., Digilio, M. C., Martinelli, S., *et al.* (2009) Mutation of SHOC2 promotes aberrant protein N-myristoylation and causes Noonan-like syndrome with loose anagen hair. *Nat. Genet.* **41,** 1022–1026
81. Rodriguez-Viciana, P., Oses-Prieto, J., Burlingame, A., Fried, M., and McCormick, F. (2006) A phosphatase holoenzyme comprised of Shoc2/Sur8 and the catalytic subunit of PP1 functions as an M-Ras effector to modulate Raf activity. *Mol. Cell* **22,** 217–230
82. Ferro, E., and Trabalzini, L. (2010) RalGDS family members couple Ras to Ral signalling and that's not all. *Cell. Signal.* **22,** 1804–1810

Supplementary Data

The function of embryonic stem cell-expressed Ras (E-Ras), a unique Ras family member, correlates with its additional motifs and its structural properties

Saeideh Nakhaei-Rad[1], Hossein Nakhaeizadeh[1], Claus Kordes[2], Ion C. Cirstea[1,3], Malte Schmick[4], Radovan Dvorsky[1], Philippe I. H. Bastiaens[4], Dieter Häussinger[2], Mohammad Reza Ahmadian[1@]

[1]Institute of Biochemistry and Molecular Biology II, Medical Faculty of the Heinrich-Heine University, Düsseldorf, Germany; [2]Clinic of Gastroenterology, Hepatology and Infectious Diseases, Medical Faculty of the Heinrich-Heine University, Düsseldorf, Germany; [3]Leibniz Institute for Age Research - Fritz Lipmann Institute, 07745 Jena, Germany; [4]Department of Systemic Cell Biology, Max Planck Institute of Molecular Physiology, Dortmund, Germany.

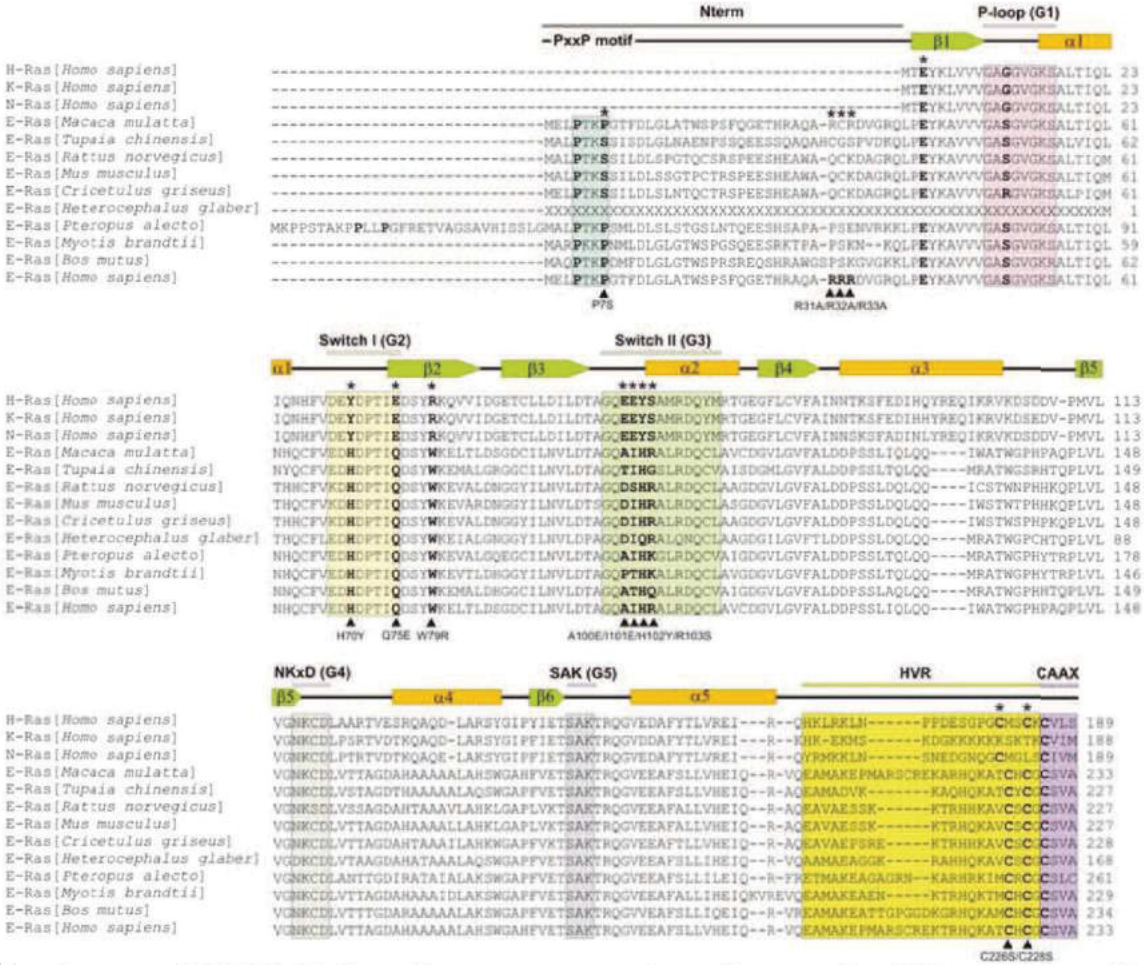

Supplementary FIGURE S1. **Overall sequence comparison of mammalian E-Ras proteins with classical Ras proteins.** E-Ras contains an extended N-terminus (aa 1-38), missing in H-, K-, and N-Ras, with a putative SH3-binging motif (PxxP). G1 to G5 boxes indicate the presence of five essential GDP/GTP binding (G) motifs. The P-loop (G1) of E-Ras contains a serine instead of a glycine (codon 12, H-Ras numbering), a frequently mutated site within *RAS* genes in human cancer (Fasano *et al.*, 1984). Several residues in switch I (G2) and switch II (G2) regions that are responsible for effector recognition are different between E-Ras and H-Ras (bold letters). E-Ras contains, like H-Ras, a CAAX motif and two cysteines at the C-terminal hypervariable region (HVR), which is the sites for PTMs by farnesylation and palmitoylation, respectively. The incomplete, N-terminal sequence of *Heterocephalus glaber* E-Ras is shown by X letters. The secondary structure elements, the α helices (orange) and β sheets (green), of the G domain were deduced from the H-Ras crystal structure (Pai *et al.*, 1990) (PDB code: 5p21). The mutation sites of E-Ras variants, which are used in this study, are highlighted by arrowheads below and asterisk above the sequence.

Chapter III

The RAS-effector interface: Isoform-specific differences in the effector binding regions

Graphica Abstract

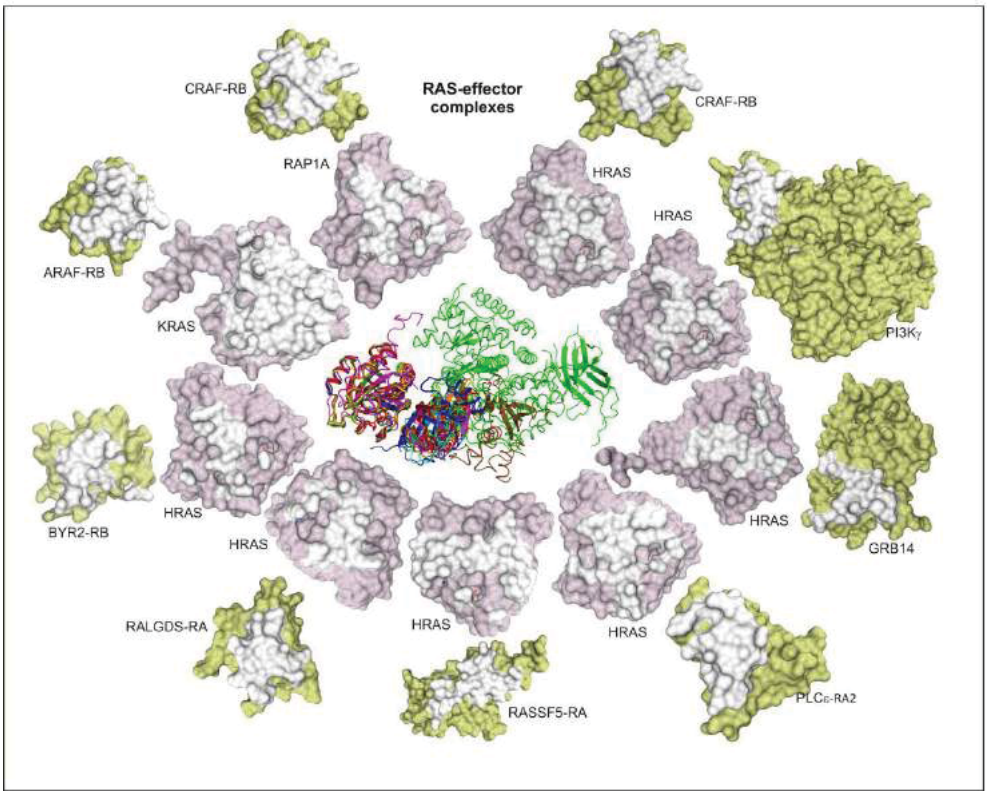

Status: Published in PLOS ONE 9 Dec 2016

Impact Factor: 3.23

Own Proportion to this work: 65%

Cloning

Proteins purification

Nucleotide exchange

Fluorecensce polarization

Prepare figures

Preparing of the manuscript

PLOS | ONE

RESEARCH ARTICLE

The RAS-Effector Interface: Isoform-Specific Differences in the Effector Binding Regions

Hossein Nakhaeizadeh, Ehsan Amin, Saeideh Nakhaei-Rad, Radovan Dvorsky, Mohammad Reza Ahmadian*

Institute of Biochemistry and Molecular Biology II, Medical Faculty of the Heinrich-Heine University, Düsseldorf, Germany

* reza.ahmadian@uni-duesseldorf.de

OPEN ACCESS

Citation: Nakhaeizadeh H, Amin E, Nakhaei-Rad S, Dvorsky R, Ahmadian MR (2016) The RAS-Effector Interface: Isoform-Specific Differences in the Effector Binding Regions. PLoS ONE 11(12): e0167145. doi:10.1371/journal.pone.0167145

Editor: Laszlo Buday, Hungarian Academy of Sciences, HUNGARY

Received: September 28, 2016

Accepted: November 9, 2016

Published: December 9, 2016

Data Availability Statement: All relevant data are within the paper and its Supporting Information files.

Funding: This study was supported in part by the German Research Foundation (Deutsche Forschungsgemeinschaft or DFG) through the Collaborative Research Center 974 (SFB 974) "Communication and Systems Relevance during Liver Injury and Regeneration", the International Research Training Group 1902 (IRTG 1902) "Intra- and interorgan communication of the cardiovascular system", the German Federal Ministry of Education and Research (BMBF) -

Abstract

RAS effectors specifically interact with the GTP-bound form of RAS in response to extracellular signals and link them to downstream signaling pathways. The molecular nature of effector interaction by RAS is well-studied but yet still incompletely understood in a comprehensive and systematic way. Here, structure-function relationships in the interaction between different RAS proteins and various effectors were investigated in detail by combining our *in vitro* data with *in silico* data. Equilibrium dissociation constants were determined for the binding of HRAS, KRAS, NRAS, RRAS1 and RRAS2 to both the RAS binding (RB) domain of CRAF and PI3Kα, and the RAS association (RA) domain of RASSF5, RALGDS and PLCε, respectively, using fluorescence polarization. An interaction matrix, constructed on the basis of available crystal structures, allowed identification of hotspots as critical determinants for RAS-effector interaction. New insights provided by this study are the dissection of the identified hotspots in five distinct regions (R1 to R5) in spite of high sequence variability not only between, but also within, RB/RA domain-containing effectors proteins. Finally, we propose that intermolecular β-sheet interaction in R1 is a central recognition region while R3 may determine specific contacts of RAS *versus* RRAS isoforms with effectors.

Introduction

RAS family proteins, including HRAS, KRAS, NRAS, RRAS1, RRAS2 (or TC21), RRAS3 (or MRAS) and ERAS, act as signaling nodes and regulate the function of various effectors with divergent biochemical functions in all eukaryotes [1,2,3]. Signal transduction implies physical association of these proteins with a spectrum of functionally diverse downstream effectors, *e.g.*, CRAF, PI3Kα, RALGDS, PLCε and RASSF5, and their activation [1,4,5,6,7,8,9,10]. CRAF, a serine/threonine kinase, activates the MEK-ERK axis and controls gene expression and cell proliferation [11]. PI3Kα generates phosphatidylinositol (3,4,5)-trisphosphate (PIP_3) and regulates cell growth, cell survival, cytoskeleton reorganization, and metabolism [12]. RALGDS links RAS with RAL, a RAS-related protein, and regulates cellular processes, such as vesicular trafficking and migration [13]. PLCε generates two second messengers of diacylglycerol (DAG) and inositol trisphosphate (IP_3) leading to an intracellular increase of calcium levels,

German Network of RASopathy Research (GeNeRARe; fund number 01GM1519D), and the European Network on Noonan Syndrome and Related Disorders (NSEuroNet; fund number 01GM1602B).

Competing Interests: The authors have declared that no competing interests exist.

which controls endocytosis, exocytosis, and cytoskeletal reorganization [14]. RASSF5 forms a complex with MST1/2 kinases, human orthologues of Hippo, and WW45 which promote apoptosis and cell cycle arrest [15].

Gain-of-function RAS mutations are frequently found in human cancers, (*e.g.*, pancreatic cancer [16]) and developmental disorders, including Noonan syndrome [17,18,19]. Whereas the latter is thought to be commonly caused by dysregulation of mainly one pathway, the RAS-MAPK pathway [19], RAS-mediated cancer progression involves activation of several pathways, *e.g.*, PI3K-AKT [3,20], RALGDS-RAL [9,13], PLCε-second messengers [14] or Hippo-YAP [21] as well as RAS-MAPK [22]. Understanding how effectors selectively recognize RAS-GTP is an attractive approach to functionalize peptides and peptidomimetics capable of inhibiting RAS interactions and signaling.

RAS effectors contain either a RAS binding (RB) or a RAS association (RA) domain (among other domains; Fig 1) [7,23,24]. RAS-effector interaction essentially requires RAS association with membranes [25] and its activation by specific regulatory proteins (*e.g.*, guanine nucleotide exchange factors or GEFs), leading to the formation of GTP-bound, active RAS [26,27,28]. Notably, RAS proteins change their conformation mainly at two highly mobile regions, designated as switch I (residues 30–40) and switch II (residues 60–68) [29,30]. Only in GTP-bound form, the switch regions of the RAS proteins provide a platform for the association with effector proteins, especially through their RB or RA domains, respectively. This interaction appears to be a prerequisite for effector activation [24,31,32,33]. RB/RA associations with RAS proteins do not exhibit the same mode of interaction among different RAS effectors [24,34,35,36]. However, CRAF-RB and RALGDS-RA domains share a similar ubiquitin-like fold and contact the switch I region *via* a similar binding mode. In contrast, PI3Kα-RB, RASSF5-RA and PLCε-RA domains do not share sequence and structural similarity but commonly associate with the switch regions, especially switch I [34,35,36,37,38]. Early cell-based studies have shown that distinct amino acids in switch I, *e.g.*, Thr-35, Glu-37, Asp-38 or Tyr-40) dictate effector specificity [39,40,41,42]. However, there is no clear explanation for such a differential selection of the switch I region by various effectors.

To date, various methods and different conditions for measuring the binding affinity between different effectors and RAS proteins, especially HRAS, have been used in many laboratories (reviewed in [4,24,43]), as summarized in Table 1. In this study, the interactions of five different RAS proteins with both the RB domains of CRAF and PI3Kα, and the RA domains of RALGDS, PLCε and RASSF5 were reinvestigated under comparable conditions

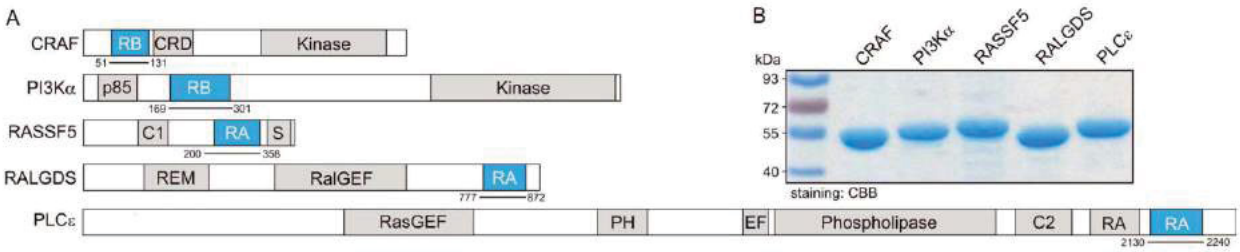

Fig 1. Domain organization of RAS effectors and different proteins used in this study. (A) Various domains are highlighted, including RAS association domain (RA) and RAS-binding (RB) domain in blue. The numbers indicate the N- and C-terminal amino acids of the respective effector domain used in this study. Other domains are: C1, cysteine-rich lipid binding; C2, calcium-dependent lipid binding; CRD, cysteine rich domains; DEP, Dishevelled/Egl-10/Pleckstrin; EF, EF-hand; kinase, serine/threonine or phosphoinositide kinase; PH, pleckstrin homology; PI3K, Phosphoinositide 3-kinase family, accessory *domain;* PP, proline-rich region; RA, RAS association; RALGEF, RAL specific guanine nucleotide exchange factor; RASGEF, RAS specific guanine nucleotide exchange factor; RB, RAS binding; REM, RAS exchanger motif; SARAH, Salvador/RASSF/Hippo. (B) Coomassie brilliant blue (CBB) stained SDS-PAGE of purified MBP fusion proteins used in this study.

doi:10.1371/journal.pone.0167145.g001

using fluorescence polarization. In addition, available complex structures and sequence alignments were utilized to construct an interaction matrix and systematically assess the association of investigated effector domains with various RAS proteins. The dissociation constants (K_d values) obtained were combined with the interaction matrix enabling us to determine common hotspots as critical specificity-determining residues and to predict selectivity of five RB- and RA-containing proteins.

Materials and Methods

Constructs

Fragments of human genes encoding both RBs of CRAF (accession number P04049; amino acids or aa 51–131), PI3Kα (P42336; aa 169–301), and RAs of RALGDS (Q12967; aa 777–872), PLCε (Q9P212; aa 2130–2240), RASSF5 (Q8WWW0; aa 200–358) were cloned into pMal-c5X-His vector. Constructs for the expression of human HRAS, KRAS, NRAS, RRAS1 and RRAS2 isoforms were described previously [5].

Proteins

All RAS and the effector proteins were expressed in *Escherichia coli* using the pGEX and pMAL-His expression systems and prepared using glutathione and Ni-NTA based affinity chromatography as described previously [18]. RAS-mGppNHp was prepared as described [18].

Fluorescence polarization

RAS-effector interaction was performed in 50 mM Tris/HCl pH 7.5, 100 mM NaCl, 5 mM $MgCl_2$ and 3 mM dithiothreitol at 25˚C using a Fluoromax 4 fluorimeter in polarization mode as described [18]. Increasing amounts of MBP-tagged effector proteins (0.05–100 μM) titrated to 1 μM RAS-mGppNHp resulted in an increase of polarization. Equilibrium dissociation constants (K_d) were calculated by fitting the concentration dependent binding curve using a quadratic ligand binding equation.

Sequence and structural analysis

Sequence alignments were performed with Bioedit program using the ClustalW algorithm [44]. Chimera was used to adjust sequence alignments with superimposed structures [45]. A python code was written to match sequence alignments with complex structures (S1 Table) and calculate intermolecular contacts in the form of an interaction matrix. The intermolecular contacts were defined as pairs residues with a distance $\leq$4.0 Å between effectors and RAS proteins in available complex structures in the protein data bank (http://www.pdb.org). Biopython modules [46] were also used to elucidate corresponding residues in all available complex structures. All structural representations were generated using PyMol viewer [47].

Results

A general approach for quantitative study of RAS-effector interaction

As previous studies focused mainly on HRAS interaction with effectors, there is a lack of information for other RAS proteins (Table 1). Dissociation constants (K_d values) have been invaluable in providing insights into particular RAS-effector interactions. However, they have been obtained under various conditions using diverse experimental techniques (see Table 1) and cannot be used as such for a comparative evaluation of the interaction of different RAS proteins with various effectors. For this reason, we set out to analyze the interaction of HRAS,

Table 1. Register of dissociation constants (K_d) determined for the RAS-effector interactions.

RAS	Nnucleotide[a]	Effectors[b]	K_d (μM)	Method[c]	T (°C)	Reference
HRAS	mGTPγS	CRAF-RB	0.005	GDI	37	[102]
	mGDP	CRAF-RB	24.0	GDI	37	[102]
	[^{3}H]GTP	CRAF-RB	0.065	SPA	37	[103]
	[γ^{32}P]GTP	CRAF-N275	0.029	CPA	4	[104]
	[γ^{32}P]GTP	RALSGDS-C127	0.028	CPA	4	[104]
	mGppNHp	AF6-RA1	2.4	GDI	37	[105]
		AF6-RA1	2.4	FK	10	[106]
		AF6-RA1	2.8	FK	25	[107]
		CRAF-RB	0.16	FK	25	[107]
		CRAF-RB	0.14	FP	25	[108]
		CRAF-RB	0.22	FP	25	[18]
		CRAF-RB	0.018	GDI	37	[102]
		CRAF-RB	0.16	GDI	25	[109]
		CRAF-RB	0.33	GDI	25	[110]
		RALGDS-RA	2.70	FP	25	[108]
		RALGDS-RA	1.30	FK	25	[107]
		RALGDS-RA	3.50	GDI	37	[111]
		RASSF5-RA	5.20	FP	25	[108]
		RASSF5-RA	0.8	GDI	37	[35]
		RASSF5-RA	0.08	FK	37	[35]
		PLCε-RA2	5.20	FP	25	[108]
	GppNHp	CRAF-RB	0.08	ITC	25	[112]
		AF6-RA1	3.00	ITC	25	[112]
		AF6-RA1	2.20	ITC	25	[24]
		RALGDS-RA	1.0	ITC	25	[112]
		RALGDS-RA	1.0	ITC	25	[24]
		RASSF1-C1-RA	39.0	ITC	25	[24]
		RASSF5-C1-RA	0.40	ITC	25	[113]
		RASSF5-RA	0.21	ITC	25	[113]
		PLCε-RA2	0.82	ITC	25	[24]
		PLCε-RA1/2	0.98	ITC	25	[24]
		AF6-RA1(Y32W)	0.58	WF	10	[106]
KRAS	mGppNHp	CRAF-RB	0.04	GDI	37	[102]
		CRAF-RB	0.102	ITC	25	[17]
	GppNHp	CRAF-RB	0.056	BBA	25	[114]
NRAS	mGppNHp	RAF-RB	0.04	GDI	37	[102]
		PI3Kγ-RB	2.90	FP	20	[36]
RRAS1	mGppNHp	CRAF-RB	252.9	FP	25	[115]
		RALGDS-RA	376.7	FP	25	[115]
		RASSF5-RA	54.6	FP	25	[115]
		PLCε-RA1	306.6	FP	25	[115]
		PI3Kα-RB	330.5	FP	25	[115]
		CRAF-RB	1.10	GDI	37	[116]

(*Continued*)

Table 1. (*Continued*)

RAS	Nnucleotide[a]	Effectors[b]	K_d (μM)	Method[c]	T (˚C)	Reference
RRAS3	GppNHp	AF6-RA1	2.80	ITC	25	[24]
		RALGDS-RA	3.70	ITC	25	[24]
		PLCε-RA1/2	7.50	ITC	25	[24]

[a] Different GTP or GDP analogs bound to HRAS have been used: GppNHp, Guanosine-5'- [(β,γ) -imido]triphosphate; mGDP, N-methylanthraniloyl-guanosine-5'-diphosphate; mGppNHp, N-methylanthraniloyl-GppNHp; mGTPγS, N-methylanthraniloyl-guanosine 5'-[gamma-thio-]triphosphate; [^{3}H]GTP, tritium-labeled GTP; [γ^{32}P]GTP, gamma 32-phosphate-labeled GTP.

[b] RAS binding (RB) and RAS association (RA) of various effectors were used; CRFA-N275 contains the N-terminal 275 aa encompassing RB domain; RALGDS-C127 contains the C-terminal 127 aa encompassing RA domain. PI3Kγ-RB consists of aa 144–1102.

[c] BBA, bead–based assay; CPA, co-precipitation assay; FK, fluorescence kinetics; FP, fluorescence polarization; GDI, guanine nucleotide dissociation inhibition; ITC, isothermal titration calorimetry; SPA, scintillation proximity assay; SPR, surface plasmon resonance.

doi:10.1371/journal.pone.0167145.t001

KRAS, NRAS, RRAS1 and RRAS2, with five distinct RB- and RA-containing effectors (Fig 1) under the same conditions. Since the kinetic analysis using stopped-flow spectrofluorometric method was not applicable to all isolated effector proteins, we utilized the fluorescence polarization approach [48].

Therefore, we prepared both, the RAS proteins in complex with mant (m) GppNHp, a non-hydrolysable fluorescent GTP analog, and the effector proteins fused to maltose-binding protein (MBP, 42 kDa). We chose the MBP because it increases the molecular mass of small-sized RB or RA domains, leads to an amplified fluorescence signal (Fig 2A) and ensures a

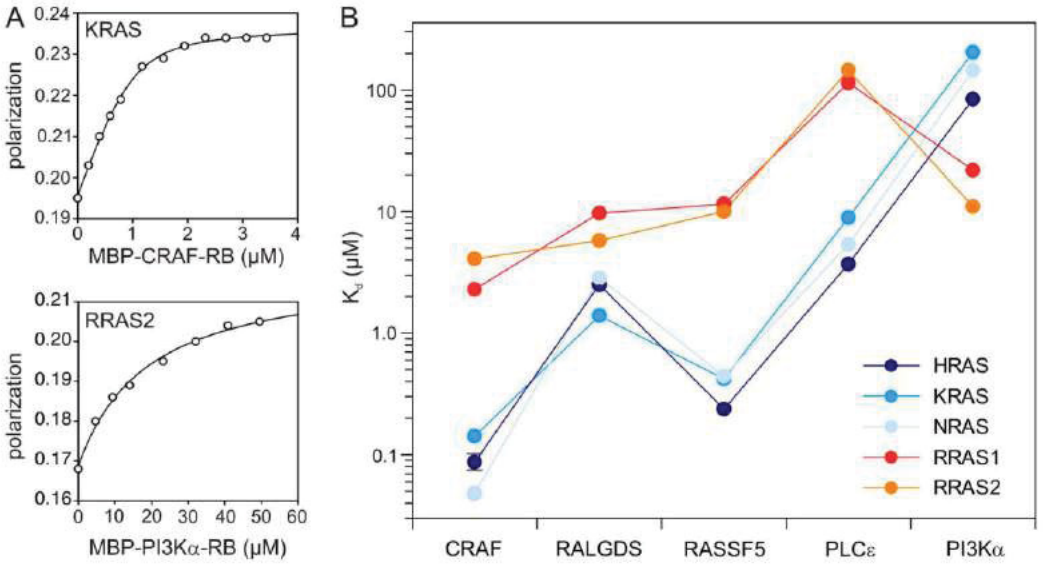

Fig 2. Equilibrium dissociation constants for RAS-effector interaction determined Fluorescence polarization. (A) Fluorescence polarization experiments were conducted by titrating mGppNHp-bound, active forms of RAS proteins (1 μM, respectively) with increasing concentrations of the respective effector domains as MBP fusion proteins. Data of two representative experiments for the interaction of KRAS (upper panel) and RRAS2 (lower panel) with CRAF-RB and PI3Kα-RB, respectively, are shown. All other data are illustrated in S1 Fig (B) Evaluated equilibrium dissociation constants (K_d) in μM shown as data points illustrate a significant difference in the binding properties of the effector proteins with both RAS and RRAS isoforms, respectively. A mean value of 0.94 ± 0.014 μM has been determined for the interaction between HRAS and CRAF to exemplify the reproducibility of this approach.

doi:10.1371/journal.pone.0167145.g002

Table 2. Dissociation constants (K_d) in μM for the interaction between RAS proteins and effectors.

Effector domains[a]	HRAS	KRAS	NRAS	RRAS1	RRAS2
CRAF-RB	0.094	0.142	0.048	2.29	4.09
RASSF5-RA	0.238	0.421	0.442	11.5	10.00
RALGDS-RA	2.50	1.39	2.84	9.71	5.78
PLCε-RA2	3.70	8.90	5.36	114.4	145.4
PI3Kα-RB	84.3	204.7	145.0	11.00	18.10

[a] The effector domain were used in these fluorescence polarization measurement as MBP fusion.

doi:10.1371/journal.pone.0167145.t002

homogeneous monomeric form of the fusion proteins. GST-fusion protein in contrast yielded a mixture of dimeric and monomeric species (data not shown). Equilibrium titration experiments revealed sufficient signal changes upon binding and guaranteed comparable experimental conditions for all measurements. By taking advantages of this method, complexes formed between these two types of proteins provided distinct polarized signals (Fig 2A and S1 Fig) that enabled us to determine K_d values for RAS-effector interactions (Table 2).

The affinities determined for the interaction between RAS proteins and individual effector domains vary between 48 nM for the NRAS–CRAF interaction and 205 μM for the interaction between KRAS and PI3Kα (Fig 2B; Table 2). In general, the tested RAS proteins can be nicely divided according to their affinities into two distinctive groups, the first comprising HRAS, KRAS, NRAS and the second the RRAS proteins. Highest affinities were obtained for CRAF, which were roughly 3–8 fold higher when compared to those for RASSF5, followed by RALGDS and PLCε with K_d values in the lower micromolar ranges (Fig 2B; Table 2). In contrast, RRAS1 and RRAS2 have similar micromolar affinities for the effectors and, interestingly, also for PI3Kα but not for PLCε. Our data clearly support previous findings (see Table 1) that isolated effector domains, such as RB or RA, represent functional units, capable of recognizing and tightly binding to RAS proteins. Exceptions are the low affinity of PLCε RA domain for the RRAS proteins and PI3Kα RB domain for HRAS, KRAS and NRAS.

Identification of hotspots within protein interfaces

To date eleven complex structures of RAS proteins and their effectors has been determined (S1 Table). Since some of them contain more than one complex in the unit cell, there were altogether sixteen complex structures available for the analysis. In order to map atomic interactions responsible for observed variable affinities, we have extracted information about interacting interface from all these complex structures and combined them with their sequence alignments (S2 and S3 Figs). Interestingly, effectors show low sequence similarity (S2A Fig), but their mode of interaction appears to be well conserved as can be seen after a superposition of the complex structures on the RAS structure (Fig 3 and S4 Fig). However, some amino acids aligned according to the sequence were quite distant in the space. Therefore, we edited the sequence alignment to synchronize it with structural alignment (S2A Fig). Our python code finally took sequence alignments with PDB files of complex structures as inputs and calculated all interaction pairs in analyzed complex structures in the form of a matrix (Fig 4A).

Interaction matrix and binding regions

An interaction matrix relates, in a comprehensive manner, the interacting residues on both sides of complexes, with RAS isoforms as rows and effector proteins as columns (Fig 4A). All numbering in this study is based on HRAS and CRAF proteins. Each element of the matrix

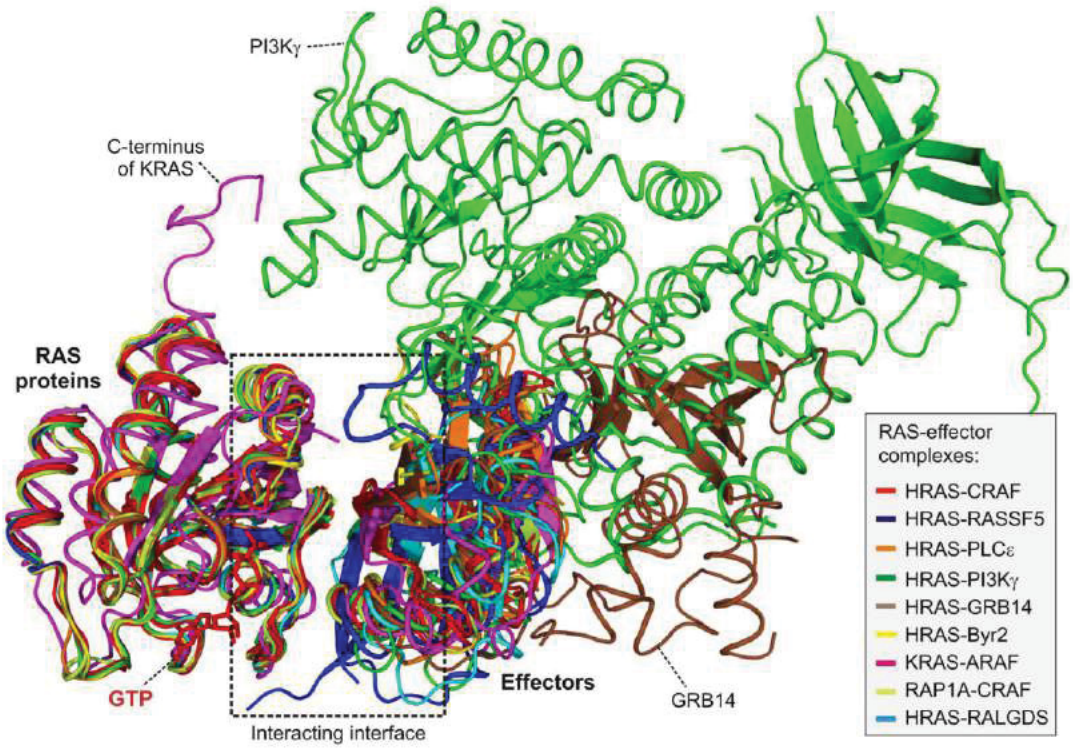

Fig 3. Superposition of all available RAS–effector complex structures. Nine structures of RAS-effector domain complexes, found in a PDB search, including HRAS-CRAF (PDB code: 4g0n, 4g3x, 3kud; red), HRAS-BYR2 (PDB code: 1k8r; yellow), RAP1A-CRAF (PDB code: 1gua; lime), KRAS-ARAF (PDB code: 2mse; magenta), HRAS-RALGDS (PDB code: 1lfd; cyan), HRAS-PI3K (PDB code: 1he8; green), HRAS-PLCε (PDB code: 2c5l; orange), HRAS-RASSF (PDB code: 3ddc; blue), HRAS-GRAB14 (PDB code: 4k81; brown), were overlaid in ribbon presentation. Additional properties outside the interaction interface (box) are indicated.

doi:10.1371/journal.pone.0167145.g003

accounts for the number of contacts between corresponding residues in all analyzed structures. Residues, involved in at least one interaction, were considered to represent a general interaction interface between RAS proteins and their effectors. Interacting amino acids form continuous patches on both sides of the complexes. Particular modes of interactions between parts of these two patches correspond to regions in the interacting matrix. We identified five such distinct regions (denoted from R1 to R5) in the matrix which had the highest number of interactions. These are separately highlighted in Fig 4.

Most pronounced is R1, located in the middle of matrix. Inspection of the particular interactions corresponding to this region clearly shows an arrangement of intermolecular β-sheet interactions in an anti-parallel fashion (Fig 4B). As many of these contacts in R1 are mediated by main-chain/main-chain interactions, we divided each element of R1 in the matrix into four categories of interactions (main-chain–main-chain, main-chain–side-chain, side-chain–main-chain and side-chain–side-chain; S5 Fig). Main-chain–main-chain interactions typically involve hydrogen bonds between the N-H group and the carbonyl oxygen. We found three interaction hotspots in all RAS-effector complexes, which represent a central recognition site in R1. These amino acids are Glu-37, Asp-38 and Ser-39 from the RAS side and positions 66 to 69 from the effector side (Fig 4A, red box). However, side-chain interactions are also highly

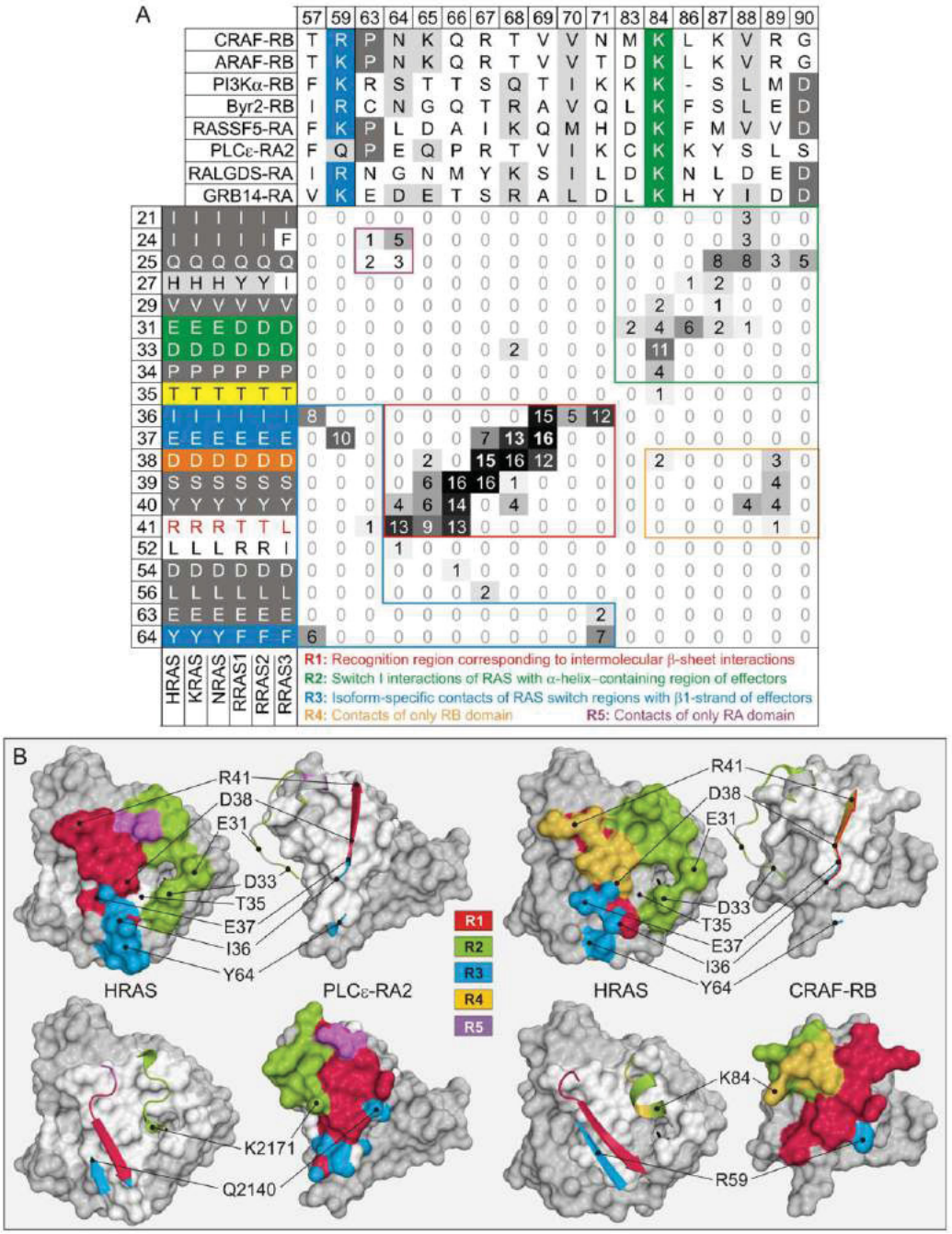

Fig 4. RAS-effector interaction hotspots. (A) Interaction matrix of RAS isoforms and effector proteins. Interaction matrix is launched to demonstrate interaction residues in all available structures (see Fig 3 and S4 Fig). Left and upper parts comprise the amino acid sequence alignments of the RAS proteins and the effector domains, respectively. Each element corresponds to a possible interaction of RAS (row; HRAS numbering) and effector (column; CRAF numbering) residues. As indicated, interaction matrix represents five main regions, which cover the main interacting interfaces. (B) The five main regions, comprising the main hotspot for the RAS-effector interaction, are highlighted as ribbon and surface representations in the corresponding colors for the structures of HRAS-PLCε (PDB code: 2C5L) and HRAS-CRAF (PDB code: 4G0N). Key amino acids which are highlighted by colored background in A are indicated on the structures as well.

doi:10.1371/journal.pone.0167145.g004

populated in these spots indicating that the nature of amino acids in R1 region also influences the RAS-effector association (S5 Fig).

Another distinct region is R2, which corresponds to the interactions between the residues 21 to 34 of RAS, including the N-terminal half of switch I, and an elongated loop containing an α helix (in the case of PLCε and PI3Kα) and two α helices covering positions 83 to 90 (Fig 4). However, the overall shape of corresponding amino acids as well as the spatial orientation of α-helical structures is very diverse (Fig 4B). These structural diversities not only cause widely dispersed interactions in R2, but are also responsible for the interactions in the frames of region R4. The capability of RB domains in R2 to interact also with the β-strand in switch I of RAS simultaneously involves the recognition region R1 and gives rise to the region R4 (Fig 4B; upper panel). On the other hand, the spatial position of the N-terminal residues of RA domains in R1 is similar to the position of the C-terminal residues RB domains in R2 resulting in the interactions established in the region R5. Remarkably, the interaction matrix gives the hints for a region R3 (Fig 4) that could not be defined as a general interaction patch from a direct pair-wise comparison of individual complex structures. This region comprises critical residues, including Ile-36, Glu-37 and Tyr-64 on the RAS side, and positions 57, 59 and 71 on effector side. R3 very likely determines the selectivity of RAS-effector interaction, especially because of sequence deviations at this region (Arg-41 and Tyr-64) when comparing HRAS, KRAS and NRAS with RRAS1, RRAS2, RRAS3. Strikingly, the binding affinities between these two groups of RAS subfamilies are indeed different.

Discussion

Since the discovery of the first RAS effector [49,50,51,52], inhibition of RAS signaling by blocking RAS-effector interactions has been an ever-evolving and challenging venture [53,54,55,56]. Biochemical and biophysical studies providing insights into the interaction of the downstream effectors with RAS proteins and their variants established the basic principles for drug design and development [31,43,53,57,58]. There is, however, a quite significant gap in our understanding of how RAS proteins specifically bind to, and activate, their diverse effectors. Rigorous understanding of this RAS-effector interplay would require an investigation of larger fragments or full-length effector proteins that was so far been accomplished in only a few studies [36,59,60]. For several reasons, isolated effector domains have been used in the vast majority of biochemical and structural studies for the investigation of their interactions with RAS proteins, predominantly with HRAS (Table 1 and S1 Table). However, interaction characteristics obtained for the same proteins differ considerably. For example, K_d values for the interaction of HRAS-GTP with CRAF or RALGDS vary from 5 to 330 nM and 80 nM to 39 μM, respectively (Table 1). Another major difference of more than two orders of magnitude was observed for the interaction between RRAS1 and CRAF. Such a large variation of K_d values (summarized in Table 1), which in addition have been determined by different groups using different methods and experimental conditions, made a comprehensive analysis of sequence-structure-function relationships practically impossible. Thus, we have quantitatively analyzed the interaction between five effector domains and five RAS proteins, covering for the first time RRAS2, under the same conditions (Table 2).

Our measurements reveal that the RAS isoforms (HRAS, KRAS and NRAS) behave similarly toward each effector but very differently as compared to RRAS isoforms (RRAS1 and RRAS2), in spite of their high sequence identity. A previous study has reported that RAS isoforms much more strongly activate the MAPK pathway *via* the RAF kinase as compared to RRAS isoforms [60]. These data are consistent with K_d values determined in this study for RAS (ranging 0.048 to 0.142 μM) and RRAS (2.29 to 4.09 μM) isoforms. Notably, RRAS

isoforms bind, except for PLCε, similarly to all tested effector domains with an up to 4-fold difference in binding affinities compare to RAS isoforms. Interestingly, they significantly interacted with PI3Kα but not with PLCε (Table 2), which is in agreement with the cell-based data reported previously [60].

In particular, the RAS isoforms, which exhibit high selectivity for CRAF followed by RASSF5, RALGDS and PLCε, appeared not to retain affinity for PI3Kα. It could be argued that the isolated RB domain of PI3Kα (consisting of the amino acids 169–301) may lack additional binding determinants, when compared to the 50-fold higher affinity obtained with the isolated RB domain of PI3Kγ (amino acids 144–1102) (Tables 1 and 2) [36]. A recent cell-based study has shown that RB domain of PI3Kα (aa 127–314) is sufficient to bind to ERAS, a newly discovered member of the RAS family, but obviously not to HRAS [5,61]. However, the immunoprecipitation studies have revealed the endogenous PI3K isoforms α and γ interact with almost same affinity with both ERAS and HRAS [5]. These data suggest that RB domain of PI3K is sufficient for a tight interaction with ERAS but clearly requires additional capacity to properly associate with HRAS. Sequence deviations in effector binding regions may be critical for determining the minimal binding regions of RAS/effectors. It is, therefore, hypothesized that ERAS and RRAS isoforms but not RAS isoforms efficiently interact with RB domain of PI3Ks and that RAS isoforms need a second binding region or alternatively a scaffold protein.

Considering the affinities of RAS isoforms compared to RRAS isoforms, these are very similar for both groups regardless of the effector protein. Correspondingly, the RAS isoforms have identical effector binding regions and RRAS isoforms, also including RRAS3, revealed a very high sequence identity in these regions (S3 Fig). Considering differences in affinities between them, residues outside the interacting interface may play a role in the association *via* indirect long-range interactions, electrostatic steering or allosteric modulation. However, direct interacting residues that differ between these two classes of proteins are most likely to be responsible for observed differences. Noteworthy, there are only two such amino acids in the region R3 with significant occurrence in the interaction at position 41 (Arg/Thr in RAS isoforms compared to RRAS isoforms) and 64 (Tyr/Phe). R41 in RAS isoforms interacts favorably with asparagine and aspartic acid in CRAF respectively RASSF5, most likely stabilizing the high affinity interactions with the effector proteins. These interactions appear to be much weaker if Arg-41 is replaced by a threonine in RRAS isoforms. This explains, thus, huge differences in K_d between the RAS isoforms and the RRAS isoforms. The same arginine does not make such favorable contact with RALGDS or PLCε, contributing to lower affinities. Its interaction with counter residues in PI3K is loose in all analyzed complexes corresponding to higher K_d values for this effector. Interaction at this spot may determine effector selectivity between these isoforms, as confirmed for ERAS that has a tryptophan (Trp-79) at the corresponding position of Arg-41 in HRAS and has exhibited a higher selectivity for PI3K than CRAF [61]. Another crucial hotspot at position 64 of the RAS proteins very likely also plays an important role in the interaction with effectors. In accordance with the interaction matrix, it is in the vicinity of residues at effector positions 57 and 71, respectively. The mode of interaction between these residues, however, is not pronounced as in the case of Arg-41. Substitution of Tyr-64 for Phenylalanine may have very diverse impacts on the binding affinity.

The RB and RA domains share higher sequence homologies if they are aligned individually. However, there is no common consensus sequence for RAS binding if they are aligned together, particularly in the RAS binding regions R1 to R5 (S2 Fig; see arrowheads). Previous studies dealing with the interaction of small GTPases with their regulators have shown that there are patches of identical or highly homologous hotspots on both sides of protein surfaces that interact with each other [62,63,64]. Such interaction is evolutionary conserved and responsible for the recognition of counter proteins. Our finding that there is no patch of

identical amino acids in RAS effector proteins (Fig 4 and S2 Fig) seemed to break this rule. However, intermolecular β-sheet interactions between RAS proteins and their effectors are conserved and seem to supply the role of such critical patch (or in this special case, a stretch) of homologous amino acid residues. The analysis of complex structures showed that these interactions, covered by the recognition region R1 in the interaction matrix, are prevalent and occur in almost all structures. A β-sheet homodimer interface has been recently reported for the structures of KRAS-GTP that overlaps the binding site of the effectors within R1 [65]. Therefore, we have analyzed the proximity of effector binding residues in different RAS isoforms in the same way as of residues involved in β-sheet interactions and summarized the results as matrices (Fig 4A and S5 Fig). Introduction of four different interaction types in the matrix with high scores that separated main-chain and side-chain RAS-effector interactions allowed a detailed inspection of the central R1 region. Strikingly, there are three hotspots, which largely undergo main-chain/main-chain interactions (Glu-37 of RAS proteins with effector residues at position 68 and 69, respectively Asp-38 with residues at position 67; S5 Fig). These observations confirm the central role of R1 in the association of RAS proteins with their effectors and strongly suggest that the main-chain/main-chain interactions within this region are crucial for the recognition of these classes of proteins. Finally, we note that interactions in R1 also dependent, to a certain extent, on side chains of accompanying amino acids. They indirectly support the formation of β-sheet on both sides of complexes. However, they also utilize their side chains in another intramolecular interactions significantly contributing to the complex formation. In this way, Asp-38 interacts *via* its side chain exclusively with the effector residues at positions 68 and 69 within R1. Side chains of Glu-37 and Ile-37 undergo contacts with residues at positions 57 and 59 outside of the effector β-strand within the region R3. On the effector side of complexes, there are only two positions that contain identical or highly homologous amino acids, namely the position 59 and 84 (Fig 4A). In both cases they are populated by positively charged residues, with exception of PLCε that has a Gln at position 59. These residues interact with negatively charged residues on RAS proteins (Glu-37 and Asp-33) and strongly contribute to the formation of complexes. However, no unique and/or particular residue of effectors can be considered to cause the overall differences observed for their association with RAS proteins. Effector interacting residues are so variable at almost all interacting spots that only their concerted action is likely to explain the observed diversity.

Previous studies have shown that RAS variants (at residues Thr-35, Glu-37, Asp-38 and Tyr-40 and including also residues mentioned above) preferentially interact with some effectors but not others [39,40,41,42]. However, to date there is no clear explanation for the variable selections of these mutants of RAS by specific effectors. The invariant Thr-35 of RAS was not located in one of the three main regions in the matrix as it is mainly involved in RAS structure and does not directly interact with RAF1. However, Spoerner and colleagues have shown that T35S mutation drastically reduces HRAS affinity for effectors, including CRAF-RB (60-fold) and RALGDS-RA (>100-fold) [66]. They suggest that minor changes, such as truncating Thr-35 by a methyl group, strongly affect dynamic behavior of the switch 1 region and, in turn, its interaction with effectors. However, an early cell-based study has shown that HRAS T35S mutant interacts only with CRAF but not PI3K, BYR2, RALGDS or RASSF5, and activates the MAPK pathway [39]. One explanation may be that Gal1 scaffolds the $HRAS^{T35S}$-CRAF [67]. On the other hand, the E37G mutation results in loss of PI3K and CRAF binding, but is able to interact with RA domain-containing effectors, such as RALGDS, RASSF5 and BYR2 [39]. Our interaction matrix shows contacts between E37G of HRAS and positively charged residues 61 and 69, and main-chain interactions with residue 69, and 70 of effectors. D38A mutation has been shown to retain CRAF binding but to lose interaction with PI3K, RALGDS and RASSF5 [42,68]. Among different effector binding mutants, Y40C selectively activates PI3K

but is unable to activate other effectors, such as RAF1, RALGDS, RASSF5 and BYR2 [69]. $HRAS^{G12V/Y40C}$ and $HRAS^{G12V/E37G}$ have been reported to cooperatively induce cell transformation *via* PI3K and RALGDS, respectively, but not *via* CRAF [40]. Vandal and colleagues have observed that $KRAS^{G12V/Y40C}$-PI3K has the largest impact on an increase in tumor size whereas $KRAS^{G12V/E38G}$-CRAF resulted in a decrease in tumor size but an increase of the number of tumors when combined with $BRAF^{V600E}$ [70]. Being central elements of R1, R3 and R4, our analysis not only confirms a prominent role of Glu-37, Asp-38 and Tyr-40 in effector binding but also gives hints for the mode of their interaction, which relies on the main-chain-main-chain interaction. As this interaction is largely independent of associated side chains, it can be considered as conserved in effectors. Consequently, it supplies the role of homologous residues found to be essential for the recognition of regulator proteins by Rho GTPases. Hence, we state that these RAS residues are responsible with their main-chain atoms for the recognition of effectors. On the other hand, side chains of these residues are still influential on the binding with effectors, either indirectly by affecting the structure of RAS switch I or directly by interacting with effector residues within the regions R3 and R4 of our interaction matrix.

In conclusion, our data collectively support previous observations that the specificity in the signaling properties and biological functions of the various RAS proteins arises from the specific combination of effector pathways they regulate in each cell type. Considering the identity of interacting residues of different types of isoforms, a uniform association of RAS isoforms or rather RRAS isoforms can be expected with a particular effector. This raises the questions of how does the cell selects between respective RAS proteins and maintains respective effector activation. There are several review articles illustrating the current state of the art regarding the activation mechanism of various effectors [9,11,12,13,21,71,72,73]. HRAS, KRAS and NRAS exhibit remarkable differences beyond their common interaction interfaces for regulators and effectors [74,75,76], especially at their C-terminal hypervariable region (S3 Fig), which has different features, including protein-protein interaction [77,78]. An interesting issue, which is increasingly appreciated, is a RAS-membrane interaction that appears to generate RAS isoform specificity with respect to effector interactions [79,80,81]. This is likely achieved by RAS-specific scaffold proteins, including CaM, GAL1, GAL3, IQGAPs, NPM1, NCL, SHOC2/SUR8 [78,82], which may modulate isoform specificity at specific site of the cell. Hence, elucidation of the RAS signal transduction requires not only RAS-effector interactions but also additional structures and interplay of multiprotein complexes [25]. Another critical aspect is sorting/trafficking of the isoforms [83,84] that has recently been shown to be highly specific for the respective RAS proteins and dependents on specific posttranslational modifications, including prenylation and acylation [85,86], phosphorylation [87,88], ubiquitination [89,90,91,92] and acetylation [93,94,95]. Similar characteristics have been reported for the RRAS isoforms, including protein-protein interaction required for subcellular localization, e.g., at focal adhesion or recycling endosomes,[96,97], and posttranslational modifications [98,99,100]. In addition, they contain extended N-termini (S3 Fig) that have been shown to be critical for RRAS1 in cell migration [101]. The N-terminus of ERAS, which undergoes multiple interaction with other proteins (Nakhaeizadeh *et al.*, unpublished), contains (like RRAS1) putative SH3-binding motifs. These motifs may provide additional mechanisms for sorting and trafficking to specific subcellular sites.

An issue, that remained to be elucidated in more detail, is the mechanism of effector activation. Notably, identification of additional components of the RAS signal transduction is a critical step towards understanding the relationship between the RAS proteins and the selective activation of respective effectors. Functional reconstitution of RAS interaction networks by using appropriate liposomes and full-length effector proteins may eventually provide

fundamental insights into the functional characterization of multiprotein complexes of RAS and the complete identification of regulatory mechanisms.

Supporting Information

S1 Table. Published structures of the RAS and Effector protein complexes.
(DOCX)

S1 Fig. Equilibrium dissociation constants for RAS-effector interaction. Fluorescence polarization experiments were conducted to determine the dissociation constants (K_d) by titrating mGppNHp-bound, active forms of RAS proteins (1 μM, respectively) with increasing concentrations of the respective effector domains, as indicated. The y-axis represents fluorescence polarization and the x-axis the concentration of the effector domain as MBP fusion proteins in μM. Evaluated equilibrium K_d values are illustrated as bar charts in Fig 2 and summarized in Table 2.
(DOCX)

S2 Fig. Sequence Alignment of the RAS effector domains. The overall amino acid alignment of RB and RA domains (A) was adjusted with structure alignment to increase the identity score. The latter was clearly increased when we separated RB domains of RAF isoforms (B) and the catalytic subunits of PI3K isoforms (C) from the RA domains (D). The five regions, described in Fig 3, are highlighted as arrowheads: R1 in red, R2 in green, R3 in blue, R4 in orange and R5 in purple. The secondary structure elements, the α helices and β sheets, from the RA domains were deduced from the crystal structures of HRAS complexes with RALGDS (PDB code: 1LFD) [37], RASSF5 (PDB code: 3DDC) [117], PLCε (PDB code: 2C5L) [34], and GRB14 (PDB code: 4K81) [118], respectively.
(DOCX)

S3 Fig. Overall sequence comparison of human RAS proteins. Multiple amino acid sequence alignment of RAS proteins with high similarities has been determined by ClustalW. Interaction regions, R1 to R5, at interface with the RB and RA effector domains are illustrated by arrowhead (color-coding is the same as in Fig 4: R1 in red; R2 in green; R3 in blue; R4 in purple; R4 in orange). The secondary structure elements, the α helices and β sheets, of the G domain were deduced from the HRAS crystal structure (PDB code: 5P21) [119]. G1 to G5 boxes indicate the presence of five essential GDP/GTP binding (G) motifs. The three amino acid deviations between RAS and RRAS isoforms that are critical selectivity-determining residues for effector binding are highlighted in red.
(DOCX)

S4 Fig. Known structures of the RAS-effector complexes. Nine structures of RAS-effector domain complexes were found in a PDB search, including HRAS-CRAF-RB (PDB code: 4g0n, 4G3X, 3kud), HRAS-BYR2-RB (PDB code: 1k8r), RAP1A-CRAF-RB (PDB code: 1GUA), KRAS-ARAF-RB (PDB code: 2mse), HRAS-RALGDS (PDB code: 1lfd), HRAS-PI3Kγ (PDB code: 1he8), HRAS-PLCε (PDB code: 2c5l), HRAS-RASSF (PDB code: 3ddc), HRAS-GRAB14 (PDB code: 4k81). An overlaid structure in ribbon presentation (central panel) illustrates the overall contacts of these structures (see also Fig 3). The contact sites (with distances of 4 Å or less) were calculated by Pymol and colored in white. RAS proteins are shown in orchid and the effector domains in olive as indicated.
(DOCX)

S5 Fig. Intermolecular β sheet-β sheet interactions covered by the recognition region R1. Intermolecular β sheet interactions between RAS proteins and their effectors is covered by the

recognition region R1 in the interaction matrix, which is launched to demonstrate interaction residues in all available structures. Left and upper panels comprises the amino acid sequence alignment of RAS and effector proteins, respectively. Each element corresponds a possible interaction of RAS (row) and effectors (column) residues. Besides, each element involves four sub-elements, which show a combination of main-chain and side-chain interactions, as indicated. Main-chain–main-chain contacts are shown in red.
(DOCX)

S1 File. Supporting References.
(DOCX)

Acknowledgments

The authors thank D. J. Timson for critical reading of the manuscript, Christian Herrmann, Mathilda Katan, Claus Kordes, Roland P. Piekorz, and Alfred Wittinghofer for plasmids, reagents and valuable discussions, and Ilse Meyer for technical assistance.

Author Contributions

Conceptualization: MRA RD.

Data curation: RD.

Formal analysis: HN EA RD.

Funding acquisition: MRA.

Investigation: HN SNR EA.

Methodology: HN EA SNR RD.

Project administration: MRA.

Software: EA RD.

Supervision: MRA.

Validation: HN EA RD.

Visualization: HN MRA.

Writing – original draft: HS EA RD.

Writing – review & editing: MRA SNR RD EA.

References

1. Wittinghofer A, Herrmann C (1995) Ras-effector interactions, the problem of specificity. FEBS Lett 369: 52–56. PMID: 7641884
2. Gutierrez-Erlandsson S, Herrero-Vidal P, Fernandez-Alfara M, Hernandez-Garcia S, Gonzalo-Flores S, Mudarra-Rubio A, et al. (2013) R-RAS2 overexpression in tumors of the human central nervous system. Mol Cancer 12: 127. doi: 10.1186/1476-4598-12-127 PMID: 24148564
3. Karnoub AE, Weinberg RA (2008) Ras oncogenes: split personalities. Nature reviews Molecular cell biology 9: 517–531. doi: 10.1038/nrm2438 PMID: 18568040
4. Herrmann C (2003) Ras-effector interactions: after one decade. Curr Opin Struct Biol 13: 122–129. PMID: 12581669
5. Nakhaei-Rad S, Nakhaeizadeh H, Gotze S, Kordes C, Sawitza I, Hoffmann MJ, et al. (2016) The Role of Embryonic Stem Cell-expressed RAS (ERAS) in the Maintenance of Quiescent Hepatic Stellate

Cells. The Journal of biological chemistry 291: 8399–8413. doi: 10.1074/jbc.M115.700088 PMID: 26884329

6. Castellano E, Downward J (2010) Role of RAS in the regulation of PI 3-kinase. Curr Top Microbiol Immunol 346: 143–169. doi: 10.1007/82_2010_56 PMID: 20563706
7. Chan JJ, Katan M (2013) PLCvarepsilon and the RASSF family in tumour suppression and other functions. Advances in biological regulation 53: 258–279. doi: 10.1016/j.jbior.2013.07.008 PMID: 23958207
8. Bunney TD, Katan M (2011) PLC regulation: emerging pictures for molecular mechanisms. Trends Biochem Sci 36: 88–96. doi: 10.1016/j.tibs.2010.08.003 PMID: 20870410
9. Ferro E, Trabalzini L (2010) RalGDS family members couple Ras to Ral signalling and that's not all. Cellular signalling 22: 1804–1810. doi: 10.1016/j.cellsig.2010.05.010 PMID: 20478380
10. Rajalingam K, Schreck R, Rapp UR, Albert S (2007) Ras oncogenes and their downstream targets. Biochimica et biophysica acta 1773: 1177–1195. doi: 10.1016/j.bbamcr.2007.01.012 PMID: 17428555
11. Desideri E, Cavallo AL, Baccarini M (2015) Alike but Different: RAF Paralogs and Their Signaling Outputs. Cell 161: 967–970. doi: 10.1016/j.cell.2015.04.045 PMID: 26000477
12. Castellano E, Downward J (2011) RAS Interaction with PI3K: More Than Just Another Effector Pathway. Genes & cancer 2: 261–274.
13. Gentry LR, Martin TD, Reiner DJ, Der CJ (2014) Ral small GTPase signaling and oncogenesis: More than just 15minutes of fame. Biochimica et biophysica acta 1843: 2976–2988. doi: 10.1016/j.bbamcr.2014.09.004 PMID: 25219551
14. Bunney TD, Katan M (2006) Phospholipase C epsilon: linking second messengers and small GTPases. Trends Cell Biol 16: 640–648. doi: 10.1016/j.tcb.2006.10.007 PMID: 17085049
15. Feig LA, Buchsbaum RJ (2002) Cell signaling: life or death decisions of ras proteins. Curr Biol 12: R259–261. PMID: 11937045
16. Bryant KL, Mancias JD, Kimmelman AC, Der CJ (2014) KRAS: feeding pancreatic cancer proliferation. Trends Biochem Sci 39: 91–100. doi: 10.1016/j.tibs.2013.12.004 PMID: 24388967
17. Cirstea IC, Gremer L, Dvorsky R, Zhang SC, Piekorz RP, Zenker M, et al. (2013) Diverging gain-of-function mechanisms of two novel KRAS mutations associated with Noonan and cardio-facio-cutaneous syndromes. Human molecular genetics 22: 262–270. doi: 10.1093/hmg/dds426 PMID: 23059812
18. Gremer L, Merbitz-Zahradnik T, Dvorsky R, Cirstea IC, Kratz CP, Zenker M, et al. (2011) Germline KRAS mutations cause aberrant biochemical and physical properties leading to developmental disorders. Human mutation 32: 33–43. doi: 10.1002/humu.21377 PMID: 20949621
19. Lissewski C, Kant SG, Stark Z, Schanze I, Zenker M (2015) Copy number variants including RAS pathway genes-How much RASopathy is in the phenotype? Am J Med Genet A 167A: 2685–2690. doi: 10.1002/ajmg.a.37155 PMID: 25974318
20. McCormick F (2015) KRAS as a Therapeutic Target. Clin Cancer Res 21: 1797–1801. doi: 10.1158/1078-0432.CCR-14-2662 PMID: 25878360
21. Donninger H, Schmidt ML, Mezzanotte J, Barnoud T, Clark GJ (2016) Ras signaling through RASSF proteins. Seminars in cell & developmental biology.
22. Dhillon AS, Hagan S, Rath O, Kolch W (2007) MAP kinase signalling pathways in cancer. Oncogene 26: 3279–3290. doi: 10.1038/sj.onc.1210421 PMID: 17496922
23. Repasky GA, Chenette EJ, Der CJ (2004) Renewing the conspiracy theory debate: does Raf function alone to mediate Ras oncogenesis? Trends Cell Biol 14: 639–647. doi: 10.1016/j.tcb.2004.09.014 PMID: 15519853
24. Wohlgemuth S, Kiel C, Kramer A, Serrano L, Wittinghofer F, Herrmann C (2005) Recognizing and defining true Ras binding domains I: biochemical analysis. Journal of molecular biology 348: 741–758. doi: 10.1016/j.jmb.2005.02.048 PMID: 15826668
25. Nussinov R, Tsai CJ, Muratcioglu S, Jang H, Gursoy A, Keskin O (2015) Principles of K-Ras effector organization and the role of oncogenic K-Ras in cancer initiation through G1 cell cycle deregulation. Expert Rev Proteomics 12: 669–682. doi: 10.1586/14789450.2015.1100079 PMID: 26496174
26. Ahearn IM, Haigis K, Bar-Sagi D, Philips MR (2012) Regulating the regulator: post-translational modification of RAS. Nature reviews Molecular cell biology 13: 39–51.
27. Hennig A, Markwart R, Esparza-Franco MA, Ladds G, Rubio I (2015) Ras activation revisited: role of GEF and GAP systems. Biol Chem 396: 831–848. doi: 10.1515/hsz-2014-0257 PMID: 25781681
28. Fischer A, Hekman M, Kuhlmann J, Rubio I, Wiese S, Rapp UR (2007) B- and C-RAF display essential differences in their binding to Ras: the isotype-specific N terminus of B-RAF facilitates Ras binding.

The Journal of biological chemistry 282: 26503–26516. doi: 10.1074/jbc.M607458200 PMID: 17635919

29. Mott HR, Owen D (2015) Structures of Ras superfamily effector complexes: What have we learnt in two decades? Critical Reviews in Biochemistry and Molecular Biology 50: 85–133. doi: 10.3109/10409238.2014.999191 PMID: 25830673
30. Vetter IR, Wittinghofer A (2001) The guanine nucleotide-binding switch in three dimensions. Science 294: 1299–1304. doi: 10.1126/science.1062023 PMID: 11701921
31. Athuluri-Divakar SK, Vasquez-Del Carpio R, Dutta K, Baker SJ, Cosenza SC, Basu I, et al. (2016) A Small Molecule RAS-Mimetic Disrupts RAS Association with Effector Proteins to Block Signaling. Cell 165: 643–655. doi: 10.1016/j.cell.2016.03.045 PMID: 27104980
32. Thapar R, Williams JG, Campbell SL (2004) NMR characterization of full-length farnesylated and non-farnesylated H-Ras and its implications for Raf activation. Journal of molecular biology 343: 1391–1408. doi: 10.1016/j.jmb.2004.08.106 PMID: 15491620
33. Drugan JK, Khosravi-Far R, White MA, Der CJ, Sung YJ, Hwang YW, et al. (1996) Ras interaction with two distinct binding domains in Raf-1 may be required for Ras transformation. The Journal of biological chemistry 271: 233–237. PMID: 8550565
34. Bunney TD, Harris R, Gandarillas NL, Josephs MB, Roe SM, Sorli SC, et al. (2006) Structural and Mechanistic Insights into Ras Association Domains of Phospholipase C Epsilon. Molecular Cell 21: 495–507. doi: 10.1016/j.molcel.2006.01.008 PMID: 16483931
35. Stieglitz B, Bee C, Schwarz D, Yildiz O, Moshnikova A, Khokhlatchev A, et al. (2008) Novel type of Ras effector interaction established between tumour suppressor NORE1A and Ras switch II. EMBO J 27: 1995–2005. doi: 10.1038/emboj.2008.125 PMID: 18596699
36. Pacold ME, Suire S, Perisic O, Lara-Gonzalez S, Davis CT, Walker EH, et al. (2000) Crystal structure and functional analysis of Ras binding to its effector phosphoinositide 3-kinase gamma. Cell 103: 931–943. PMID: 11136978
37. Huang L, Hofer F, Martin GS, Kim SH (1998) Structural basis for the interaction of Ras with RalGDS. Nat Struct Biol 5: 422–426. PMID: 9628477
38. Nassar N, Horn G, Herrmann C, Scherer A, McCormick F, Wittinghofer A (1995) The 2.2 A crystal structure of the Ras-binding domain of the serine/threonine kinase c-Raf1 in complex with Rap1A and a GTP analogue. Nature 375: 554–560. doi: 10.1038/375554a0 PMID: 7791872
39. White MA, Nicolette C, Minden A, Polverino A, Van Aelst L, Karin M, et al. (1995) Multiple Ras functions can contribute to mammalian cell transformation. Cell 80: 533–541. PMID: 7867061
40. Khosravi-Far R, White MA, Westwick JK, Solski PA, Chrzanowska-Wodnicka M, Van Aelst L, et al. (1996) Oncogenic Ras activation of Raf/mitogen-activated protein kinase-independent pathways is sufficient to cause tumorigenic transformation. Mol Cell Biol 16: 3923–3933. PMID: 8668210
41. Khwaja A, Rodriguez-Viciana P, Wennstrom S, Warne PH, Downward J (1997) Matrix adhesion and Ras transformation both activate a phosphoinositide 3-OH kinase and protein kinase B/Akt cellular survival pathway. EMBO J 16: 2783–2793. doi: 10.1093/emboj/16.10.2783 PMID: 9184223
42. Vavvas D, Li X, Avruch J, Zhang XF (1998) Identification of Nore1 as a potential Ras effector. J Biol Chem 273: 5439–5442. PMID: 9488663
43. Erijman A, Shifman JM (2016) RAS/Effector Interactions from Structural and Biophysical Perspective. Mini Rev Med Chem 16: 370–375. PMID: 26423700
44. Hall TA (1999) BioEdit: a user-friendly biological sequence alignment editor and analysis program for Windows 95/98/NT. Nucleic Acids Symposium Series 41: 95–98.
45. Pettersen EF, Goddard TD, Huang CC, Couch GS, Greenblatt DM, Meng EC, et al. (2004) UCSF Chimera—A visualization system for exploratory research and analysis. Journal of Computational Chemistry 25: 1605–1612. doi: 10.1002/jcc.20084 PMID: 15264254
46. Cock PJ, Antao T, Chang JT, Chapman BA, Cox CJ, Dalke A, et al. (2009) Biopython: freely available Python tools for computational molecular biology and bioinformatics. Bioinformatics 25: 1422–1423. doi: 10.1093/bioinformatics/btp163 PMID: 19304878
47. DeLano WL (2002) The PyMOL Molecular Graphics System.
48. Raines RT (2015) Fluorescence polarization assay to quantify protein-protein interactions: an update. Methods Mol Biol 1278: 323–327. doi: 10.1007/978-1-4939-2425-7_19 PMID: 25859958
49. Kolch W, Heidecker G, Lloyd P, Rapp UR (1991) Raf-1 protein kinase is required for growth of induced NIH/3T3 cells. Nature 349: 426–428. doi: 10.1038/349426a0 PMID: 1992343
50. Warne PH, Viciana PR, Downward J (1993) Direct interaction of Ras and the amino-terminal region of Raf-1 in vitro. Nature 364: 352–355. doi: 10.1038/364352a0 PMID: 8332195

51. Zhang XF, Settleman J, Kyriakis JM, Takeuchi-Suzuki E, Elledge SJ, Marshall MS, et al. (1993) Normal and oncogenic p21ras proteins bind to the amino-terminal regulatory domain of c-Raf-1. Nature 364: 308–313. doi: 10.1038/364308a0 PMID: 8332187

52. Moodie SA, Willumsen BM, Weber MJ, Wolfman A (1993) Complexes of Ras.GTP with Raf-1 and mitogen-activated protein kinase kinase. Science 260: 1658–1661. PMID: 8503013

53. Lu S, Jang H, Gu S, Zhang J, Nussinov R (2016) Drugging Ras GTPase: a comprehensive mechanistic and signaling structural view. Chem Soc Rev.

54. Shima F, Yoshikawa Y, Matsumoto S, Kataoka T (2013) Discovery of small-molecule Ras inhibitors that display antitumor activity by interfering with Ras.GTP-effector interaction. Enzymes 34 Pt. B: 1–23.

55. Beeram M, Patnaik A, Rowinsky EK (2003) Regulation of c-Raf-1: therapeutic implications. Clin Adv Hematol Oncol 1: 476–481. PMID: 16258435

56. Beeram M, Patnaik A, Rowinsky EK (2005) Raf: a strategic target for therapeutic development against cancer. J Clin Oncol 23: 6771–6790. doi: 10.1200/JCO.2005.08.036 PMID: 16170185

57. Ostrem JM, Shokat KM (2016) Direct small-molecule inhibitors of KRAS: from structural insights to mechanism-based design. Nat Rev Drug Discov.

58. Cromm PM, Spiegel J, Grossmann TN, Waldmann H (2015) Direct Modulation of Small GTPase Activity and Function. Angew Chem Int Ed Engl 54: 13516–13537. doi: 10.1002/anie.201504357 PMID: 26470842

59. Kurig B, Shymanets A, Bohnacker T, Prajwal, Brock C, Ahmadian MR, et al. (2009) Ras is an indispensable coregulator of the class IB phosphoinositide 3-kinase p87/p110gamma. Proc Natl Acad Sci U S A 106: 20312–20317. doi: 10.1073/pnas.0905506106 PMID: 19906996

60. Rodriguez-Viciana P, Sabatier C, McCormick F (2004) Signaling specificity by Ras family GTPases is determined by the full spectrum of effectors they regulate. Mol Cell Biol 24: 4943–4954. doi: 10.1128/MCB.24.11.4943-4954.2004 PMID: 15143186

61. Nakhaei-Rad S, Nakhaeizadeh H, Kordes C, Cirstea IC, Schmick M, Dvorsky R, et al. (2015) The Function of Embryonic Stem Cell-expressed RAS (E-RAS), a Unique RAS Family Member, Correlates with Its Additional Motifs and Its Structural Properties. The Journal of biological chemistry 290: 15892–15903. doi: 10.1074/jbc.M115.640607 PMID: 25940089

62. Dvorsky R, Ahmadian MR (2004) Always look on the bright site of Rho: structural implications for a conserved intermolecular interface. EMBO Rep 5: 1130–1136. doi: 10.1038/sj.embor.7400293 PMID: 15577926

63. Jaiswal M, Dvorsky R, Ahmadian MR (2013) Deciphering the molecular and functional basis of Dbl family proteins: a novel systematic approach toward classification of selective activation of the Rho family proteins. The Journal of biological chemistry 288: 4486–4500. doi: 10.1074/jbc.M112.429746 PMID: 23255595

64. Amin E, Jaiswal M, Derewenda U, Reis K, Nouri K, Koessmeier KT, et al. (2016) Deciphering the molecular and functional basis of RhoGAP family proteins: A systematic approach towards selective inactivation of Rho family proteins. The Journal of biological chemistry.

65. Muratcioglu S, Chavan TS, Freed BC, Jang H, Khavrutskii L, Freed RN, et al. (2015) GTP-Dependent K-Ras Dimerization. Structure 23: 1325–1335. doi: 10.1016/j.str.2015.04.019 PMID: 26051715

66. Spoerner M, Herrmann C, Vetter IR, Kalbitzer HR, Wittinghofer A (2001) Dynamic properties of the Ras switch I region and its importance for binding to effectors. Proc Natl Acad Sci U S A 98: 4944–4949. doi: 10.1073/pnas.081441398 PMID: 11320243

67. Elad-Sfadia G, Haklai R, Ballan E, Gabius HJ, Kloog Y (2002) Galectin-1 augments Ras activation and diverts Ras signals to Raf-1 at the expense of phosphoinositide 3-kinase. J Biol Chem 277: 37169–37175. doi: 10.1074/jbc.M205698200 PMID: 12149263

68. Katz ME, McCormick F (1997) Signal transduction from multiple Ras effectors. Curr Opin Genet Dev 7: 75–79. PMID: 9024640

69. Rodriguez-Viciana P, Warne PH, Khwaja A, Marte BM, Pappin D, Das P, et al. (1997) Role of phosphoinositide 3-OH kinase in cell transformation and control of the actin cytoskeleton by Ras. Cell 89: 457–467. PMID: 9150145

70. Vandal G, Geiling B, Dankort D (2014) Ras effector mutant expression suggest a negative regulator inhibits lung tumor formation. PloS one 9: e84745. doi: 10.1371/journal.pone.0084745 PMID: 24489653

71. Wing MR, Bourdon DM, Harden TK (2003) PLC-epsilon: a shared effector protein in Ras-, Rho-, and G alpha beta gamma-mediated signaling. Mol Interv 3: 273–280. doi: 10.1124/mi.3.5.273 PMID: 14993441

72. Wellbrock C, Karasarides M, Marais R (2004) The RAF proteins take centre stage. Nature reviews Molecular cell biology 5: 875–885. doi: 10.1038/nrm1498 PMID: 15520807

73. Baljuls A, Kholodenko BN, Kolch W (2013) It takes two to tango—signalling by dimeric Raf kinases. Mol Biosyst 9: 551–558. doi: 10.1039/c2mb25393c PMID: 23212737

74. Ahmadian MR, Hoffmann U, Goody RS, Wittinghofer A (1997) Individual rate constants for the interaction of Ras proteins with GTPase-activating proteins determined by fluorescence spectroscopy. Biochemistry 36: 4535–4541. doi: 10.1021/bi962556y PMID: 9109662

75. Scheffzek K, Ahmadian MR, Wittinghofer A (1998) GTPase-activating proteins: helping hands to complement an active site. Trends Biochem Sci 23: 257–262. PMID: 9697416

76. Castellano E, Santos E (2011) Functional specificity of ras isoforms: so similar but so different. Genes & cancer 2: 216–231.

77. Chavan TS, Jang H, Khavrutskii L, Abraham SJ, Banerjee A, Freed BC, et al. (2015) High-Affinity Interaction of the K-Ras4B Hypervariable Region with the Ras Active Site. Biophys J 109: 2602–2613. doi: 10.1016/j.bpj.2015.09.034 PMID: 26682817

78. Abraham SJ, Nolet RP, Calvert RJ, Anderson LM, Gaponenko V (2009) The hypervariable region of K-Ras4B is responsible for its specific interactions with calmodulin. Biochemistry 48: 7575–7583. doi: 10.1021/bi900769j PMID: 19583261

79. Parker JA, Mattos C (2015) The Ras-Membrane Interface: Isoform-specific Differences in The Catalytic Domain. Molecular cancer research: MCR 13: 595–603. doi: 10.1158/1541-7786.MCR-14-0535 PMID: 25566993

80. Abankwa D, Hanzal-Bayer M, Ariotti N, Plowman SJ, Gorfe AA, Parton RG, et al. (2008) A novel switch region regulates H-ras membrane orientation and signal output. EMBO J 27: 727–735. doi: 10.1038/emboj.2008.10 PMID: 18273062

81. Mazhab-Jafari MT, Marshall CB, Smith MJ, Gasmi-Seabrook GM, Stathopulos PB, Inagaki F, et al. (2015) Oncogenic and RASopathy-associated K-RAS mutations relieve membrane-dependent occlusion of the effector-binding site. Proc Natl Acad Sci U S A 112: 6625–6630. doi: 10.1073/pnas.1419895112 PMID: 25941399

82. Rodriguez-Viciana P, Oses-Prieto J, Burlingame A, Fried M, McCormick F (2006) A phosphatase holoenzyme comprised of Shoc2/Sur8 and the catalytic subunit of PP1 functions as an M-Ras effector to modulate Raf activity. Molecular cell 22: 217–230. doi: 10.1016/j.molcel.2006.03.027 PMID: 16630891

83. Zhou M, Wiener H, Su W, Zhou Y, Liot C, Ahearn I, et al. (2016) VPS35 binds farnesylated N-Ras in the cytosol to regulate N-Ras trafficking. The Journal of cell biology 214: 445–458. doi: 10.1083/jcb.201604061 PMID: 27502489

84. Zheng ZY, Cheng CM, Fu XR, Chen LY, Xu L, Terrillon S, et al. (2012) CHMP6 and VPS4A mediate the recycling of Ras to the plasma membrane to promote growth factor signaling. Oncogene 31: 4630–4638. doi: 10.1038/onc.2011.607 PMID: 22231449

85. Jang H, Abraham SJ, Chavan TS, Hitchinson B, Khavrutskii L, Tarasova NI, et al. (2015) Mechanisms of membrane binding of small GTPase K-Ras4B farnesylated hypervariable region. The Journal of biological chemistry 290: 9465–9477. doi: 10.1074/jbc.M114.620724 PMID: 25713064

86. Lynch SJ, Snitkin H, Gumper I, Philips MR, Sabatini D, Pellicer A (2015) The differential palmitoylation states of N-Ras and H-Ras determine their distinct Golgi subcompartment localizations. J Cell Physiol 230: 610–619. doi: 10.1002/jcp.24779 PMID: 25158650

87. Bivona TG, Quatela SE, Bodemann BO, Ahearn IM, Soskis MJ, Mor A, et al. (2006) PKC regulates a farnesyl-electrostatic switch on K-Ras that promotes its association with Bcl-XL on mitochondria and induces apoptosis. Molecular cell 21: 481–493. doi: 10.1016/j.molcel.2006.01.012 PMID: 16483930

88. Sung PJ, Tsai FD, Vais H, Court H, Yang J, Fehrenbacher N, et al. (2013) Phosphorylated K-Ras limits cell survival by blocking Bcl-xL sensitization of inositol trisphosphate receptors. Proc Natl Acad Sci U S A 110: 20593–20598. doi: 10.1073/pnas.1306431110 PMID: 24297914

89. Wang MT, Holderfield M, Galeas J, Delrosario R, To MD, Balmain A, et al. (2015) K-Ras Promotes Tumorigenicity through Suppression of Non-canonical Wnt Signaling. Cell 163: 1237–1251. doi: 10.1016/j.cell.2015.10.041 PMID: 26590425

90. Rodriguez-Viciana P, McCormick F (2006) Ras ubiquitination: coupling spatial sorting and signal transmission. Cancer Cell 9: 243–244. doi: 10.1016/j.ccr.2006.03.025 PMID: 16616329

91. Jura N, Scotto-Lavino E, Sobczyk A, Bar-Sagi D (2006) Differential modification of Ras proteins by ubiquitination. Molecular cell 21: 679–687. doi: 10.1016/j.molcel.2006.02.011 PMID: 16507365

92. de la Vega M, Burrows JF, McFarlane C, Govender U, Scott CJ, Johnston JA (2010) The deubiquitinating enzyme USP17 blocks N-Ras membrane trafficking and activation but leaves K-Ras

unaffected. The Journal of biological chemistry 285: 12028–12036. doi: 10.1074/jbc.M109.081448 PMID: 20147298

93. Yang MH, Laurent G, Bause AS, Spang R, German N, Haigis MC, et al. (2013) HDAC6 and SIRT2 regulate the acetylation state and oncogenic activity of mutant K-RAS. Molecular cancer research: MCR 11: 1072–1077. doi: 10.1158/1541-7786.MCR-13-0040-T PMID: 23723075

94. Knyphausen P, Lang F, Baldus L, Extra A, Lammers M (2016) Insights into K-Ras 4B regulation by post-translational lysine acetylation. Biol Chem.

95. Yang MH, Nickerson S, Kim ET, Liot C, Laurent G, Spang R, et al. (2012) Regulation of RAS oncogenicity by acetylation. Proc Natl Acad Sci U S A 109: 10843–10848. doi: 10.1073/pnas.1201487109 PMID: 22711838

96. Wurtzel JG, Lee S, Singhal SS, Awasthi S, Ginsberg MH, Goldfinger LE (2015) RLIP76 regulates Arf6-dependent cell spreading and migration by linking ARNO with activated R-Ras at recycling endosomes. Biochemical and biophysical research communications 467: 785–791. doi: 10.1016/j.bbrc.2015.10.064 PMID: 26498519

97. Furuhjelm J, Peranen J (2003) The C-terminal end of R-Ras contains a focal adhesion targeting signal. J Cell Sci 116: 3729–3738. doi: 10.1242/jcs.00689 PMID: 12890755

98. Berzat AC, Brady DC, Fiordalisi JJ, Cox AD (2006) Using inhibitors of prenylation to block localization and transforming activity. Methods Enzymol 407: 575–597. doi: 10.1016/S0076-6879(05)07046-1 PMID: 16757354

99. Oertli B, Han J, Marte BM, Sethi T, Downward J, Ginsberg M, et al. (2000) The effector loop and prenylation site of R-Ras are involved in the regulation of integrin function. Oncogene 19: 4961–4969. doi: 10.1038/sj.onc.1203876 PMID: 11042683

100. Calvo F, Crespo P (2009) Structural and spatial determinants regulating TC21 activation by RasGRF family nucleotide exchange factors. Molecular biology of the cell 20: 4289–4302. doi: 10.1091/mbc.E09-03-0212 PMID: 19692568

101. Holly SP, Larson MK, Parise LV (2005) The unique N-terminus of R-ras is required for Rac activation and precise regulation of cell migration. Molecular biology of the cell 16: 2458–2469. doi: 10.1091/mbc.E03-12-0917 PMID: 15772154

102. Herrmann C, Martin GA, Wittinghofer A (1995) Quantitative analysis of the complex between p21ras and the Ras-binding domain of the human Raf-1 protein kinase. The Journal of biological chemistry 270: 2901–2905. PMID: 7852367

103. Gorman C, Skinner RH, Skelly JV, Neidle S, Lowe PN (1996) Equilibrium and kinetic measurements reveal rapidly reversible binding of Ras to Raf. The Journal of biological chemistry 271: 6713–6719. PMID: 8636091

104. Hwang MC, Sung YJ, Hwang YW (1996) The differential effects of the Gly-60 to Ala mutation on the interaction of H-Ras p21 with different downstream targets. The Journal of biological chemistry 271: 8196–8202. PMID: 8626511

105. Linnemann T, Geyer M, Jaitner BK, Block C, Kalbitzer HR, Wittinghofer A, et al. (1999) Thermodynamic and kinetic characterization of the interaction between the Ras binding domain of AF6 and members of the Ras subfamily. The Journal of biological chemistry 274: 13556–13562. PMID: 10224125

106. Boettner B, Herrmann C, Van Aelst L (2001) Ras and Rap1 interaction with AF-6 effector target. Methods Enzymol 332: 151–168. PMID: 11305093

107. Linnemann T, Zheng YH, Mandic R, Peterlin BM (2002) Interaction between Nef and phosphatidylinositol-3-kinase leads to activation of p21-activated kinase and increased production of HIV. Virology 294: 246–255. doi: 10.1006/viro.2002.1365 PMID: 12009866

108. Gremer L, De Luca A, Merbitz-Zahradnik T, Dallapiccola B, Morlot S, Tartaglia M, et al. (2010) Duplication of Glu37 in the switch I region of HRAS impairs effector/GAP binding and underlies Costello syndrome by promoting enhanced growth factor-dependent MAPK and AKT activation. Human molecular genetics 19: 790–802. doi: 10.1093/hmg/ddp548 PMID: 19995790

109. Sydor JR, Engelhard M, Wittinghofer A, Goody RS, Herrmann C (1998) Transient kinetic studies on the interaction of Ras and the Ras-binding domain of c-Raf-1 reveal rapid equilibration of the complex. Biochemistry 37: 14292–14299. doi: 10.1021/bi980764f PMID: 9760267

110. Sydor JR, Seidel RP, Goody RS, Engelhard M (1999) Cell-free synthesis of the Ras-binding domain of c-Raf-1: binding studies to fluorescently labelled H-ras. FEBS Lett 452: 375–378. PMID: 10386625

111. Vetter IR, Linnemann T, Wohlgemuth S, Geyer M, Kalbitzer HR, Herrmann C, et al. (1999) Structural and biochemical analysis of Ras-effector signaling via RalGDS. FEBS Lett 451: 175–180. PMID: 10371160

112. Rudolph MG, Linnemann T, Grunewald P, Wittinghofer A, Vetter IR, Herrmann C (2001) Thermodynamics of Ras/effector and Cdc42/effector interactions probed by isothermal titration calorimetry. The Journal of biological chemistry 276: 23914–23921. doi: 10.1074/jbc.M011600200 PMID: 11292826

113. Harjes E, Harjes S, Wohlgemuth S, Muller KH, Krieger E, Herrmann C, et al. (2006) GTP-Ras disrupts the intramolecular complex of C1 and RA domains of Nore1. Structure 14: 881–888. doi: 10.1016/j.str.2006.03.008 PMID: 16698549

114. Hunter JC, Manandhar A, Carrasco MA, Gurbani D, Gondi S, Westover KD (2015) Biochemical and Structural Analysis of Common Cancer-Associated KRAS Mutations. Molecular cancer research: MCR 13: 1325–1335. doi: 10.1158/1541-7786.MCR-15-0203 PMID: 26037647

115. Flex E, Jaiswal M, Pantaleoni F, Martinelli S, Strullu M, Fansa EK, et al. (2014) Activating mutations in RRAS underlie a phenotype within the RASopathy spectrum and contribute to leukaemogenesis. Human molecular genetics 23: 4315–4327. doi: 10.1093/hmg/ddu148 PMID: 24705357

116. Herrmann C, Horn G, Spaargaren M, Wittinghofer A (1996) Differential interaction of the ras family GTP-binding proteins H-Ras, Rap1A, and R-Ras with the putative effector molecules Raf kinase and Ral-guanine nucleotide exchange factor. The Journal of biological chemistry 271: 6794–6800. PMID: 8636102

117. Stieglitz B, Bee C, Schwarz D, Yildiz Ö, Moshnikova A, Khokhlatchev A, et al. (2008) Novel type of Ras effector interaction established between tumour suppressor NORE1A and Ras switch II. The EMBO journal 27: 1995–2005. doi: 10.1038/emboj.2008.125 PMID: 18596699

118. Qamra R, Hubbard SR (2013) Structural Basis for the Interaction of the Adaptor Protein Grb14 with Activated Ras. PLoS One 8: e72473. doi: 10.1371/journal.pone.0072473 PMID: 23967305

119. Pai EF, Kabsch W, Krengel U, Holmes KC, John J, Wittinghofer A (1989) Structure of the guanine-nucleotide-binding domain of the Ha-ras oncogene product p21 in the triphosphate conformation. Nature 341: 209–214. doi: 10.1038/341209a0 PMID: 2476675

Supporting information

The RAS-effector interface: Isoform-specific differences in the effector binding regions

H. Nakhaeizadeh, E. Amin, S. Nakhaei-Rad, R. Dvorsky, M. R. Ahmadian
Institute of Biochemistry and Molecular Biology II,
Medical Faculty of the Heinrich-Heine University, Düsseldorf, Germany

Table S1. . Published complexes structures of the RAS and Effector proteins.

Proteins	PDB code	Resolution (Å)	Reference
RAP1A(E30D/K31E)-GppNHp-CRAF-RB	1GUA	2.0	[1]
HRAS-GppNHp-RALGDS	1LFD	2.1	[2]
HRAS(G12V)-GppNHp-PI3Kγ-RB(V223K/V326A)	1HE8	3.0	[3]
HRAS-GDP-CRAF-RB(A85K)	3KUD	2.15	[4]
HRAS-GppNHp-Byr2-RB	1K8R	3.0	[5]
HRAS(G12V)-GTP-PLCε(Y2176L)	2C5L	1.9	[6]
HRAS(D30E/E31K)-GppNHp-RASSF5-RA (L285M/K302D)	3DDC	1.8	[7]
HRAS(G12V)-GTP-GRAB14-RA/PH (K272A/E273A)	4K81	2.4	[8]
HRAS-GppNHp-CRAF-RB	4G0N	2.45	[9]
HRAS(Q61L)-GppNHp-CRAF-RB	4G3X	3.25	[9]
KRAS-GppNHp-ARAF-RB	2MSE	NMR	[10]

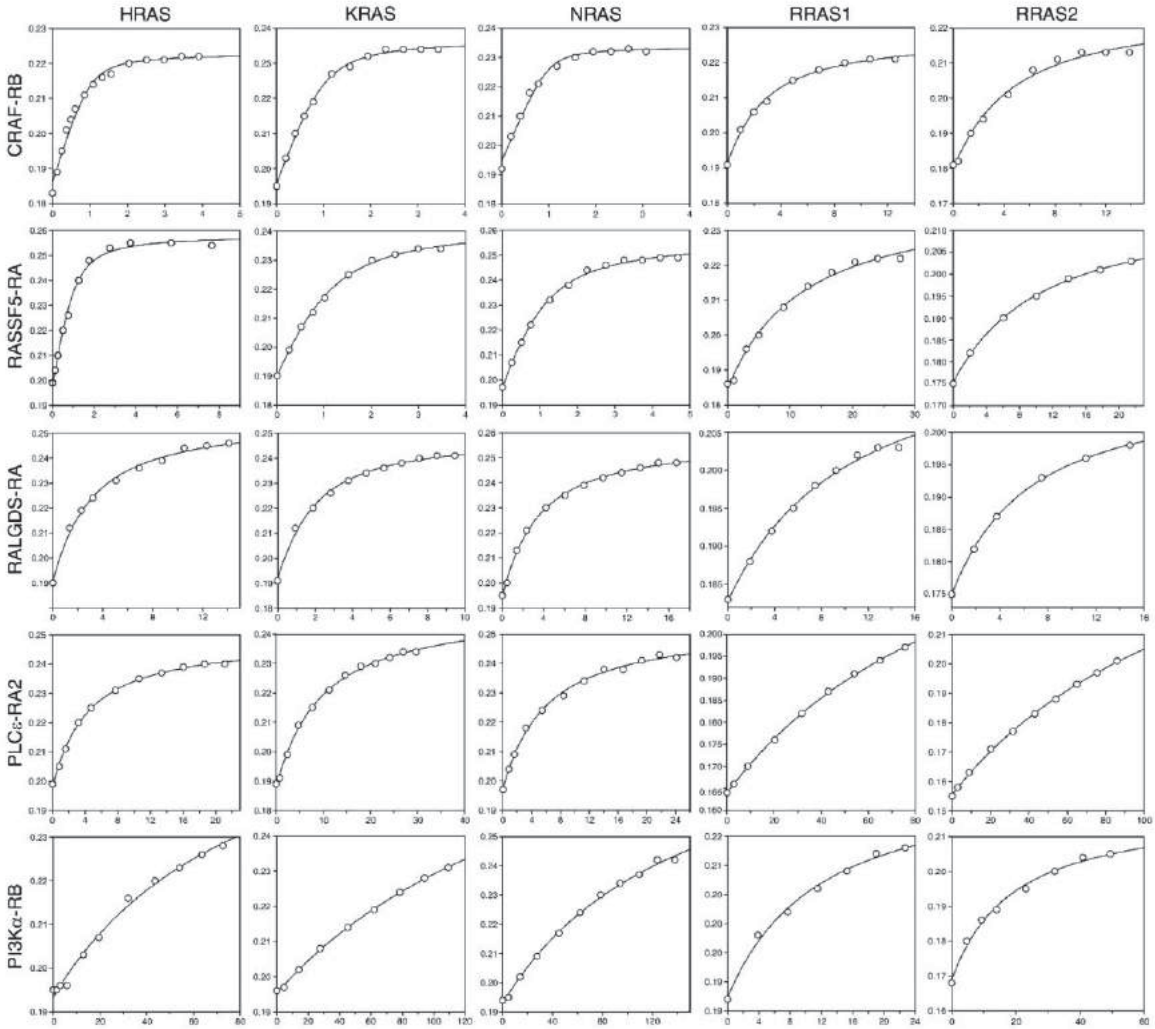

Figure S1. Equilibrium dissociation constants for RAS-effector interaction determined by Fluorescence polarization. Fluorescence polarization experiments were conducted by titrating mGppNHp-bound, active forms of RAS proteins (1 µM, respectively) with increasing concentrations of the respective effector domains, as indicated. The y-axis represents fluorescence polarization and the x-axis the concentration of the effector domain as MBP fusion proteins in µM. Evaluated equilibrium dissociation constants (K_d) are illustrated as bar charts in Figure 2 and summarized in Table 2.

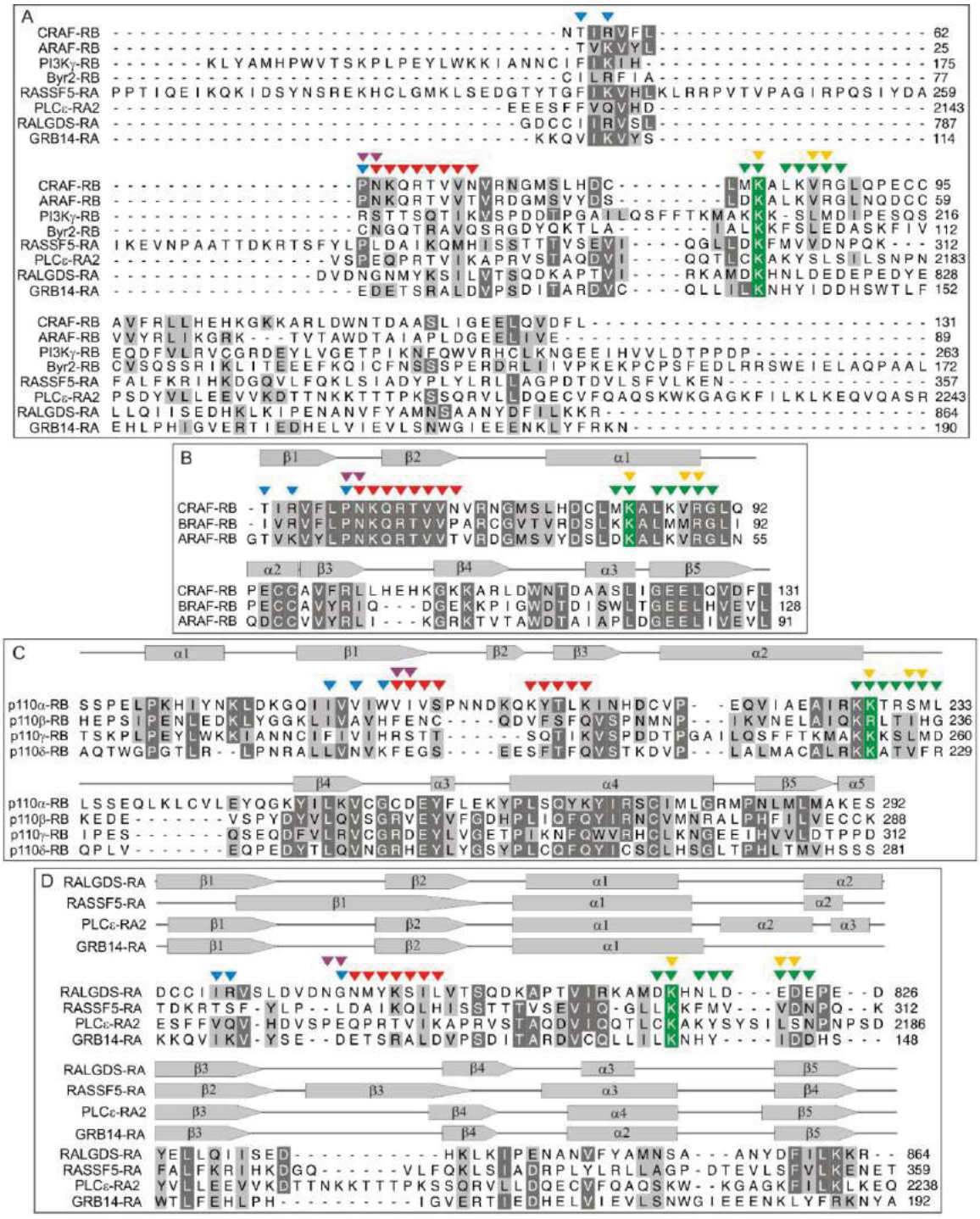

Figure S2. Sequence Alignment of the RAS effector domains. The overall amino acid alignment of RB and RA domains (A) was adjusted with structure alignment to increase the identity score. The latter was clearly increased when we separated RB domains of RAF isoforms (B) and the catalytic subunits of PI3K isoforms (C) from the RA domains (D). The five regions, described in Figure 3, are highlighted as arrowheads: R1 in red, R2 in green, R3 in blue, R4 in orange and R5 in purple. The secondary structure elements, the α helices and β sheets, from the RA domains were deduced from the crystal structures of HRAS complexes with RALGDS (PDB code: 1LFD) [2], RASSF5 (PDB code: 3DDC) [7], PLCε (PDB code: 2C5L) [6], and GRB14 (PDB code: 4K81) [8], respectively.

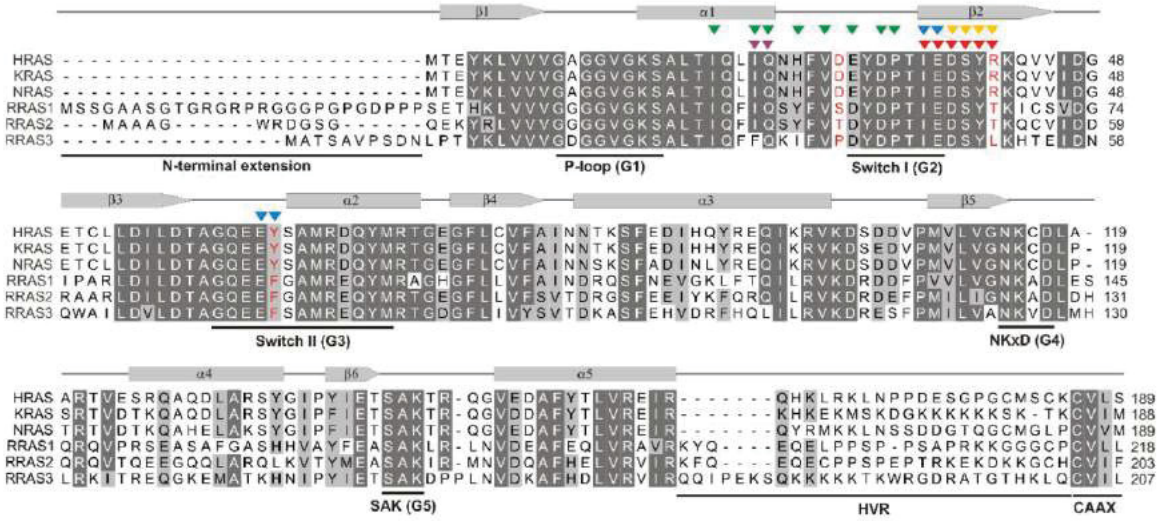

Figure S3. Overall sequence comparison of human RAS proteins. Multiple amino acid sequence alignment of RAS proteins with high similarities has been prepared by clustalW. Interaction regions, R1 to R5, at interface with the RB and RA effector domains are illustrated by arrowhead (color-coding is the same as in Fig. 4: R1 in red; R2 in green; R3 in blue; R4 in purple; R4 in orange). The secondary structure elements, the α helices and β sheets, of the G domain were deduced from the HRAS crystal structure (PDB code: 5P21) [11]. G1 to G5 boxes indicate the presence of five essential GDP/GTP binding (G) motifs. The three amino acid deviations between RAS and RRAS isoforms that are critical selectivity-determining residues for effector binding are highlighted in red.

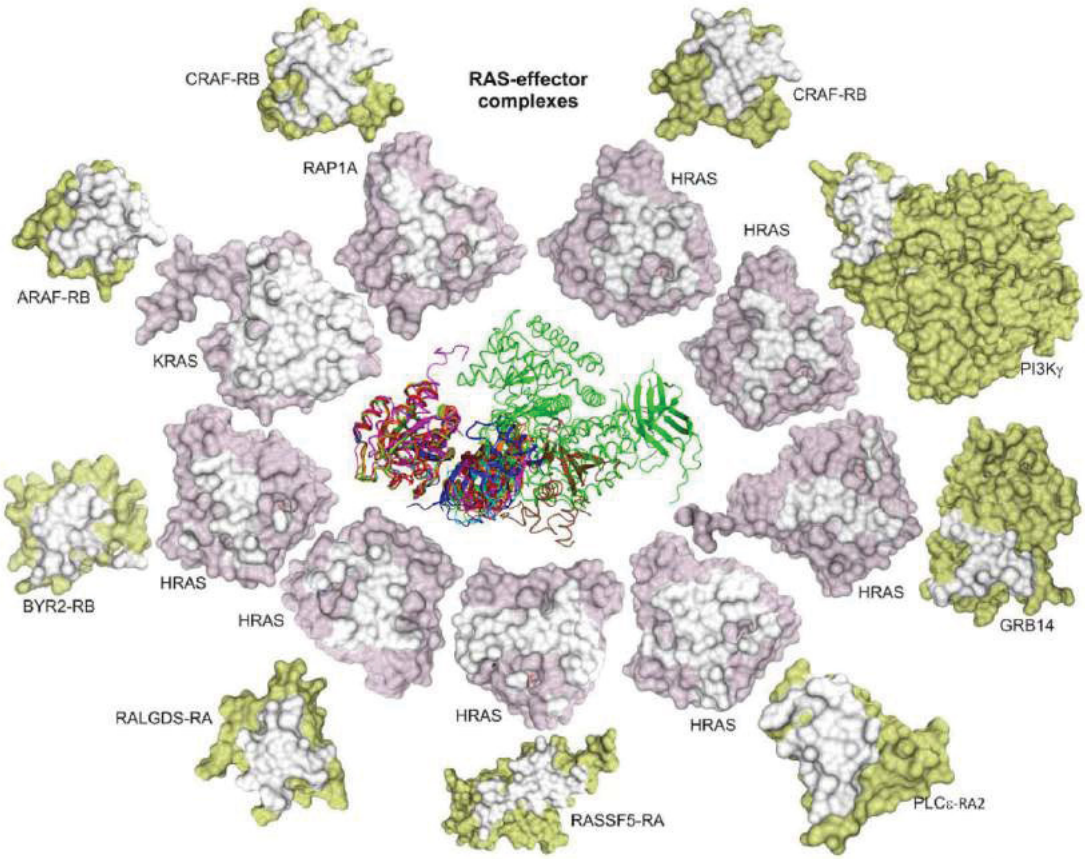

Figure S4. Known structures of the RAS-effector complexes. Nine structures of RAS-effector domain complexes were found in a PDB search, including HRAS-CRAF-RB (PDB code: 4g0n, 4G3X, 3kud), HRAS-BYR2-RB (PDB code: 1k8r), RAP1A-CRAF-RB (PDB code: 1GUA), KRAS-ARAF-RB (PDB code: 2mse), HRAS-RALGDS (PDB code: 1lfd), HRAS-PI3Kγ (PDB code: 1he8), HRAS-PLCε (PDB code: 2c5l), HRAS-RASSF (PDB code: 3ddc), HRAS-GRAB14 (PDB code: 4k81). An overlaid structure in ribbon presentation (central panel) illustrates the overall contacts of these structures (see also Figure 3). The contact sites (with distances of 4 Å or less) were calculated by Pymol and colored in white. RAS proteins are shown in orchid and the effector domains in olive as indicated.

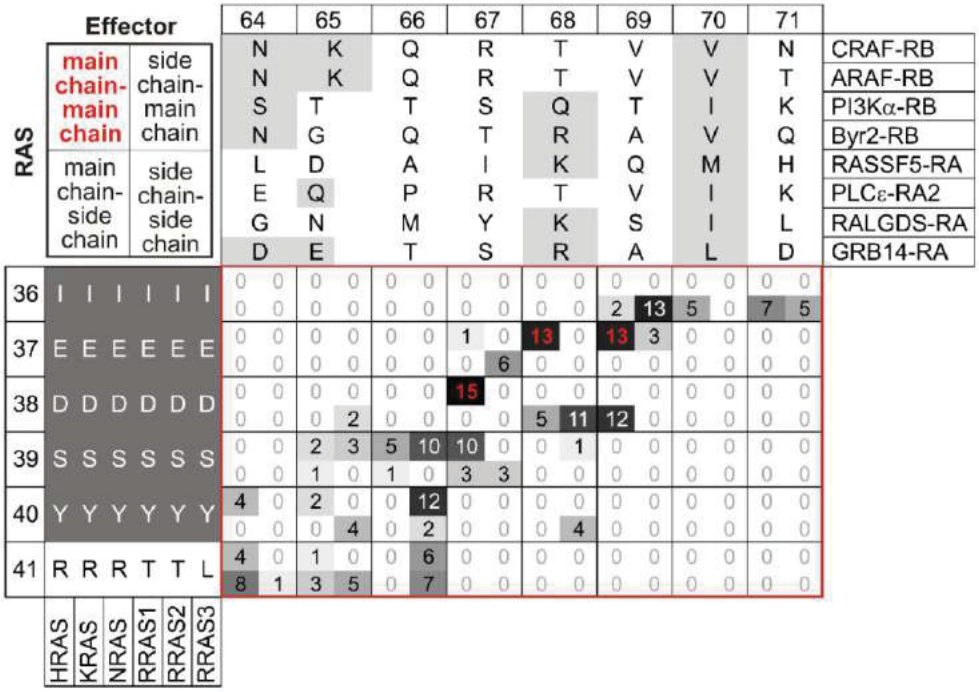

Figure S5. Intermolecular β sheet-β sheet interactions between RAS proteins and their effectors covered by the recognition region R1 in the interaction matrix. Interaction matrix is launched to demonstrate interaction residues in all available structures. Left and upper panels comprises the amino acid sequence alignment of RAS and effector proteins, respectively. Each element corresponds a possible interaction of RAS (row) and effectors (column) residues. Besides, each element involves four sub-elements, which show a combination of main-chain and side-chain interactions, as indicated. Main-chain–main-chain contacts are shown in red.

Supporting References

1. Nassar, N., et al., *Ras/Rap effector specificity determined by charge reversal.* Nat Struct Biol, 1996. **3**(8): p. 723-9.
2. Huang, L., et al., *Structural basis for the interaction of Ras with RalGDS.* Nat Struct Biol, 1998. **5**(6): p. 422-6.
3. Pacold, M.E., et al., *Crystal structure and functional analysis of Ras binding to its effector phosphoinositide 3-kinase gamma.* Cell, 2000. **103**(6): p. 931-43.
4. Filchtinski, D., et al., *What Makes Ras an Efficient Molecular Switch: A Computational, Biophysical, and Structural Study of Ras-GDP Interactions with Mutants of Raf.* Journal of Molecular Biology, 2010. **399**(3): p. 422-435.
5. Scheffzek, K., et al., *The Ras-Byr2RBD complex: structural basis for Ras effector recognition in yeast.* Structure, 2001. **9**(11): p. 1043-50.
6. Bunney, T.D., et al., *Structural and Mechanistic Insights into Ras Association Domains of Phospholipase C Epsilon.* Molecular Cell, 2006. **21**(4): p. 495-507.
7. Stieglitz, B., et al., *Novel type of Ras effector interaction established between tumour suppressor NORE1A and Ras switch II.* The EMBO journal, 2008. **27**(14): p. 1995-2005.
8. Qamra, R. and S.R. Hubbard, *Structural Basis for the Interaction of the Adaptor Protein Grb14 with Activated Ras.* PLoS One, 2013. **8**(8): p. e72473.
9. Fetics, Susan K., et al., *Allosteric Effects of the Oncogenic RasQ61L Mutant on Raf-RBD.* Structure, 2015. **23**(3): p. 505-516.
10. Mazhab-Jafari, M.T., et al., *Oncogenic and RASopathy-associated K-RAS mutations relieve membrane-dependent occlusion of the effector-binding site.* Proceedings of the National Academy of Sciences, 2015. **112**(21): p. 6625-6630.
11. Pai, E.F., et al., *Structure of the guanine-nucleotide-binding domain of the Ha-ras oncogene product p21 in the triphosphate conformation.* Nature, 1989. **341**(6239): p. 209-14.

Chapter IV

The impact of the interaction between Embryonic stem cell-expressed Ras (E-Ras) and Arginase-1 in hepatic stellate cells

Graphica Abstract

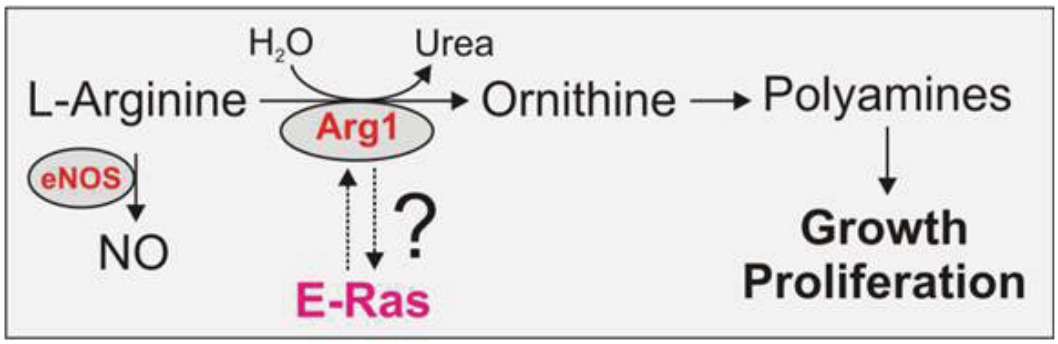

Status: In preparation

Own Proportion to this work: 75%
Site direct mutagenesis
Cloning
Protein purification
Arginase Assay
Pull-down assay
Confocal microscopy
Immunoblotting
Preparing of the manuscript

The impact of the interaction between Embryonic stem cell-expressed Ras (E-Ras) and Arginase-1 in hepatic stellate cells*

Hossein Nakhaeizadeh[1], Saeideh Nakhaei-Rad[1], Jana Lissy[1], Kazem Nuri[1], Ehsan Amin[1], Claus Kordes[2], Dieter Häussinger[2], Mohammad Reza Ahmadian[1@]

[1]Institute of Biochemistry and Molecular Biology II, Medical Faculty of the Heinrich-Heine University, Düsseldorf, Germany; [2]Clinic of Gastroenterology, Hepatology and Infectious Diseases, Medical Faculty of the Heinrich-Heine University, Düsseldorf, Germany.

*Running title: The impact of E-Ras/Arginase interaction

[@]Correspondences should be addressed to:

Mohammad Reza Ahmadian, Ph.D., Institut für Biochemie und Molekularbiologie II, Medizinische Fakultät der Heinrich-Heine-Universität, Universitaetsstr. 1, Gebäude 22.03.03, 40255 Düsseldorf, Germany, phone: 49-211-81 12384, Fax: 49-211-81 12726, e-mail: reza.ahmadian@uni-duesseldorf.de

Key words: Stem cell expressed Ras, E-Ras, Arginase-1, Hepatic stellate cells, L-Aginine

Summary

E-Ras is a member of Ras family specifically expressed in embryonic stem cells and hepatic stellate cells (HSCs). Unlike classical Ras isoforms, E-Ras has an extended 38-amino acid long unique N-terminal region with still unknown functions. A comparative proteome analysis of the N-terminal extension of human and rat E-Ras proteins, which exhibit remarkable sequence deviations, led to the identification of 51 associated proteins (10 with the human E-Ras, 3 with rat E-Ras and 38 with both species). These interactions appear to participate in distinct cellular processes, including cell cycle, transcription, immune response, signal transduction, cell adhesion, cytoskeletal dynamics and metabolism. One of these proteins is the cytosolic Arginase-1(Arg1). which is known to convert L-arginine to L-ornithine. Interaction studies showed that Arg1 physically binds to different E-Ras variants, including isolated E-Ras N-terminus, under cell-free condition using purified proteins and also using lysates of hepatic stellate cells. We also investigated the molecular nature of Arg1 regulation and function by E-Ras, and a correlation between these two proteins in quiescence HSCs. It seems that E-Ras N-terminus directly binds to Arg1 and potentiates its enzymatic activity.

Result

From 51 associated proteins with the N-terminus of E-Ras, which were identified in a proteome analysis, we further characterize the association of Arginase-1 (Arg1), Nucleophosmin-1 (NMP1), Lamin B1 and Vimentin with E-Ras in more detail in HSCs (Fig. 1).

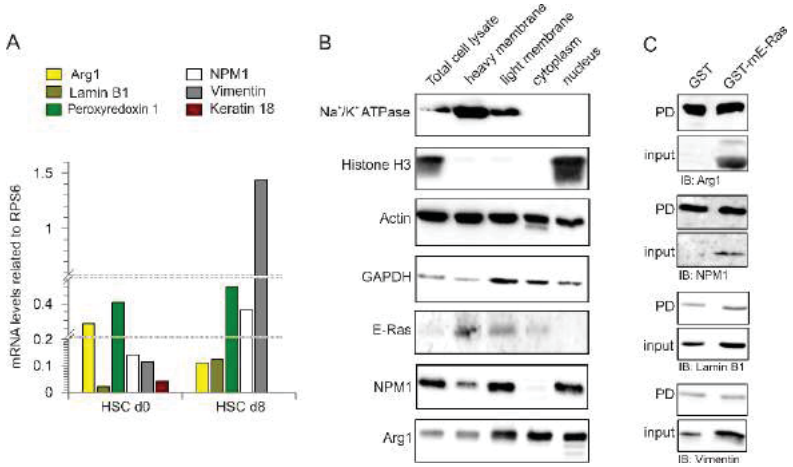

Figure 3: The N-terminal extension of E-Ras appears to be critical for diverse protein-protein interactions. (A) Expression of E-Ras-associating proteins in HSCs. Arg1, NPM1, Lamin B1, Vimentin, Peroxyredoxin 1, and Keratin 18, which were found as E-Ras-associating proteins are differentially expressed in quiescent (d0) and activated (d8) HSCs. (B) Experimental cell fractionation procedure employing several differential centrifugation steps resulted in isolation of six distinct fractions, including heavy membrane (plasma membrane and rough endoplasmic reticulum), light membrane (polysomes, golgi apparatus, smooth endoplasmic reticulum), cytoplasm (cytoplasm and lysosomes), and nucleus. (B) Association of E-Ras with diverse proteins in HSC (d0) was analyzed using GST-fusion of the N-terminal

extension of E-Ras in a pulldown assay and by immunoblotting (IB) with antibodies against Arg1, NPM1, Lamin B1, and Vimentin.

Moreover, we found out that high expression of Arg1 in quiescent HSC, determined by quantitative PCR (Fig. 2A). Arg1 enzymatic activity was analysed in HSC lysates in the quiescent state (Day 0) and in the activated state (day 4 and 8) using L-arginine as ARG1 substrate by measuring generation of urea and L-ornithine at an absorbance of 540 nm (Fig. 2B). The highest activities were observed in day 0, which nicely correlates with the expression of both Arg1 and E-Ras in quiescent HSCs (Chapter 5). Arg1 binds directly to the N-terminus of rat and human E-Ras. However, due to a large amino acid sequence deviation between human and rat species in this region, we found a higher binding affinity of Arg1 for human E-Ras as compared to rat E-Ras (Fig. 2C). An association of Arg1 with endogenous E-Ras is shown in Figure 2D, were Arg1 was co-immunoprecipitated with E-Ras. To address the question of whether E-Ras may have an impact of Arg1 activity we measured the urea production as a functional activity of Arg1 in the presence of increasing E-Ras proteins. Figure 2E shows that the urea production by Arg1 increases in the presence of human E-Ras, which appears to bind Arg1 much tighter as compared to rat E-Ras (Fig. 2C). These data suggests that E-Ras may play a critical role in modulating the enzymatic activity of Arg1 *via* physical interaction.

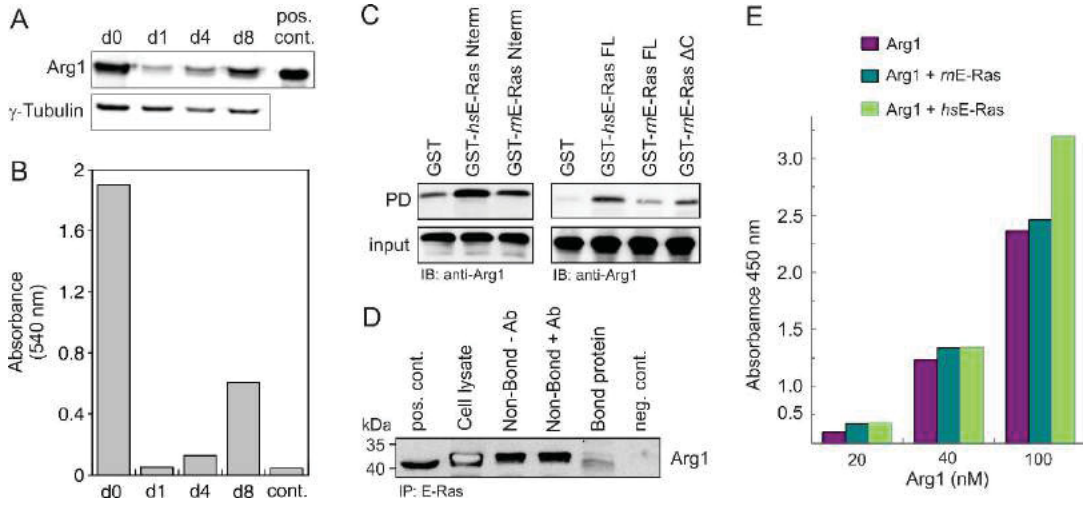

FIGURE 2. Correlation between Arg1 activity in HSCs and its interaction with E-Ras. (A) Arg1 Expression in in HSCs at different days. Purified Arg1 was used as positive control and γ-Tubulin as loading control. (B) Urea production as functional activity of Arg1 in HSCs in different days. (C-D) E-Ras N-terminus directly interacts with Arg1. Pull-down experiments (C) were performed by mixing bacterially purified Arg1 and GST-E-Ras immobilized on glutathione sepharose beads. GST was used as a control. Proteins retained on the beads were resolved by SDS-PAGE Laemmli buffer and processed for SDS-PAGE gel, which was stained using coomassie brilliant blue (CBB) and Western blotting using a monoclonal antibody (M01) against Arg1. Immunoprecipitation (IP) experiments (D) were performed by mixing HSC lysate with monoclonal antibody against E-Ras immobilized on Sepharose beads. (E) E-Ras may potentiate Arg1 activity in HSCs. Urea production was measured as functional activity of Arg1 in the presence of E-Ras proteins.

Conclusion

The N-terminal extension of E-Ras represents an additional modular unit, which may be involved in different cellular functions of E-Ras by undergoing diverse protein-protein interactions. One of these functions appears to binding to and potentiating the enzyme activity of cytosolic Arg1, which in turn competes with NO synthase and converts L-arginine to L-Ornithine and Urea.

Chapter V

The Role of Embryonic Stem Cell-expressed RAS (ERAS) in the Maintenance of Quiescent Hepatic Stellate Cells

Graphical Abstract

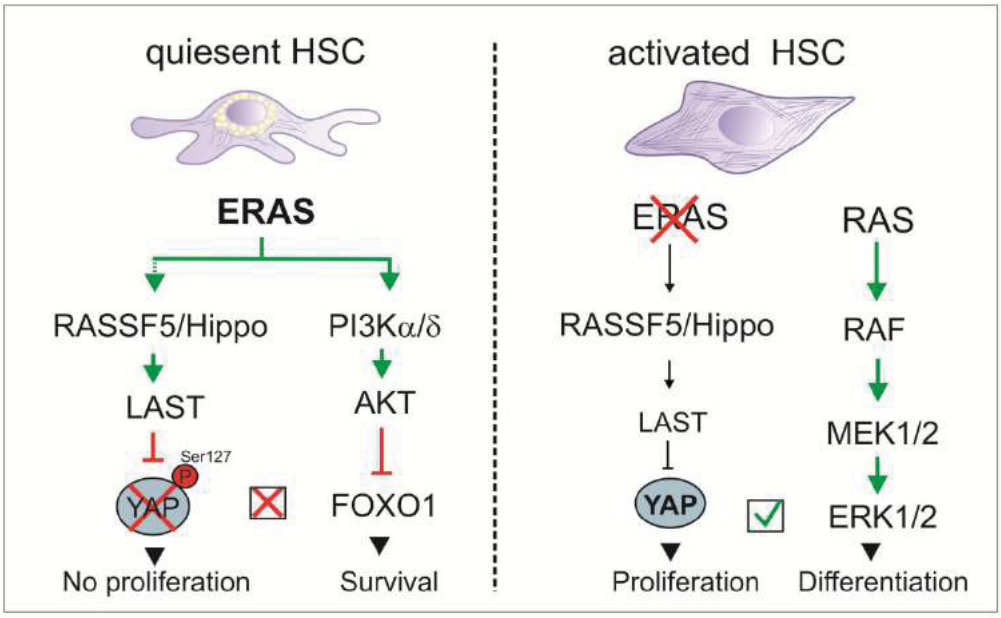

Status: Published in J Biol Chem. 2016 Apr

Impact Factor: 4.25

Own Proportion to this work: 10%

Antibody Purification

Cell fractionation

Immunoblotting

Preparing of the manuscript

THE JOURNAL OF BIOLOGICAL CHEMISTRY VOL. 291, NO. 16, pp. 8399–8413, April 15, 2016

The Role of Embryonic Stem Cell-expressed RAS (ERAS) in the Maintenance of Quiescent Hepatic Stellate Cells*[S]

Received for publication, October 22, 2015, and in revised form, February 13, 2016 Published, JBC Papers in Press, February 16, 2016, DOI 10.1074/jbc.M115.700088

Saeideh Nakhaei-Rad[‡], Hossein Nakhaeizadeh[‡], Silke Götze[§], Claus Kordes[§], Iris Sawitza[§], Michèle J Hoffmann[¶], Manuel Franke[‡], Wolfgang A. Schulz[¶], Jürgen Scheller[‡], Roland P. Piekorz[‡], Dieter Häussinger[§], and Mohammad R. Ahmadian[‡1]

From the [‡]Institute of Biochemistry and Molecular Biology II, Medical Faculty, the [§]Clinic of Gastroenterology, Hepatology, and Infectious Diseases, and the [¶]Department of Urology, Medical Faculty, Heinrich-Heine University, 40225 Düsseldorf, Germany

Hepatic stellate cells (HSCs) were recently identified as liver-resident mesenchymal stem cells. HSCs are activated after liver injury and involved in pivotal processes, such as liver development, immunoregulation, regeneration, and also fibrogenesis. To date, several studies have reported candidate pathways that regulate the plasticity of HSCs during physiological and pathophysiological processes. Here we analyzed the expression changes and activity of the RAS family GTPases and thereby investigated the signaling networks of quiescent HSCs *versus* activated HSCs. For the first time, we report that embryonic stem cell-expressed RAS (ERAS) is specifically expressed in quiescent HSCs and down-regulated during HSC activation via promoter DNA methylation. Notably, in quiescent HSCs, the high level of ERAS protein correlates with the activation of AKT, STAT3, mTORC2, and HIPPO signaling pathways and inactivation of FOXO1 and YAP. Our data strongly indicate that in quiescent HSCs, ERAS targets AKT via two distinct pathways driven by PI3Kα/δ and mTORC2, whereas in activated HSCs, RAS signaling shifts to RAF-MEK-ERK. Thus, in contrast to the reported role of ERAS in tumor cells associated with cell proliferation, our findings indicate that ERAS is important to maintain quiescence in HSCs.

Hepatic stellate cells (HSCs[2]; also called Ito cells, lipocytes, fat storing cells, or perisinusoidal cells) contribute 5–8% of total liver-resident cells and are located between sinusoidal endothelial cells and hepatocytes in the space of Dissé (1, 2). HSCs play pivotal roles in liver development, immunoregulation, regeneration, and pathology. They exhibit a remarkable plasticity in their phenotype, gene expression profile, and cellular function (3). In healthy liver, HSCs remain in a quiescent state and store vitamin A mainly as retinyl palmitate in cytoplasmic membrane-coated vesicles. Moreover, HSCs typically express neural and mesodermal markers (*i.e.* glial fibrillary acidic protein (GFAP) and desmin). They possess characteristics of stem cells, like the expression of Wnt and NOTCH, which are required for developmental fate decisions. Activated HSCs display an expression profile highly reminiscent of mesenchymal stem cells. Due to typical functions of mesenchymal stem cells, such as differentiation into adipocytes and osteocytes as well as support of hematopoietic stem cells, HSCs were identified as liver-resident mesenchymal stem cells (4).

Following liver injury, HSCs become activated and exhibit properties of myofibroblast-like cells. During activation, HSCs release vitamin A, up-regulate various genes, including α-smooth muscle actin and collagen type I, and down-regulate GFAP (2). Activated HSCs are multipotent cells, and recent studies revealed a new aspect of HSCs plasticity (*i.e.* their differentiation into liver progenitor cells during liver regeneration) (5, 6). Physiologically, HSCs represent well known extracellular matrix-producing cells. In some pathophysiological conditions, sustained activation of HSCs causes the accumulation of extracellular matrix in the liver and initiates liver diseases, such as fibrosis, cirrhosis, and hepatocellular carcinoma. Therefore, it is worthwhile to reconsider the impact of different signaling pathways on HSC fate decisions in order to be able to modulate them so that activated HSCs contribute to liver regeneration but not fibrosis. To date, several growth factors (PDGF, TGFβ, and insulin-like growth factor) and signaling pathways have been described to control HSC activation through effector pathways, including Wnt, Hedgehog, NOTCH, RAS-MAPK, PI3K-AKT, JAK-STAT3, and HIPPO-YAP (7–13). However, there is a need to further identify key players that orchestrate HSC activity and to find out how they control as positive and negative regulators HSC activation in

* This work was supported by the Deutsche Forschungsgemeinschaft through Collaborative Research Center 974 (SFB 974), "Communication and System Relevance during Liver Injury and Regeneration." The authors declare that they have no conflicts of interest with the contents of this article.

[S] This article contains supplemental Table S1 and Figs. S1–S4.

[1] To whom correspondence should be addressed: Institut für Biochemie und Molekularbiologie II, Medizinische Fakultät der Heinrich-Heine-Universität, Universitätstr. 1, Gebäude 22.03, 40225 Düsseldorf, Germany. Tel.: 49-211-81-12384; Fax: 49-211-81-12726; E-mail: reza.ahmadian@uni-duesseldorf.de.

[2] The abbreviations used are: HSC, hepatic stellate cell; aa, amino acid(s); CTGF, connective tissue growth factor; RAS, rat sarcoma; ERAS, embryonic stem cell-expressed RAS; EYFP, enhanced YFP; FOXO1, forkhead transcription factor; GAP, GTPase-activating protein; GFAP, glial fibrillary acidic protein; HRAS, Harvey rat sarcoma; KRAS, Kirsten rat sarcoma; MMP, matrix metalloproteinase; MRAS, muscle RAS; mSIN1, mammalian stress-activated MAPK-interacting protein 1; mTORC, mammalian target of rapamycin; NRAS, neuroblastoma RAS; PDK1, 3-phosphoinositide-dependent protein kinase; PLC, phospholipase C; PPARγ, peroxisome proliferative-activator receptor-γ; RBD, RAS-binding domain; RA, RAS association domain; RAL, RAS-like; RALGDS, guanine nucleotide dissociation stimulator; RAP2, RAS-related protein 2; RASSF5, RAS-association domain family; RRAS, related RAS viral; SATB1, special AT-rich binding protein 1; SREBP, sterol regulatory element-binding protein; TSC, tuberous sclerosis; YAP, Yes-associated protein; qPCR, quantitative PCR; 5-AZA, 5-aza-2′-deoxycytidine; LIF, leukemia inhibitory factor; miRNA, microRNA; d, day; p-, phosphorylated.

response to liver injury. Among these pathways, RAS signaling is one of the earliest that was identified to play a role in HSC activation (14) and to act as a node of intracellular signal transduction networking. Therefore, RAS-dependent signaling pathways were the focus of the present study.

Small GTPases of the RAS family are involved in a variety of cellular processes ranging from intracellular metabolisms to proliferation, migration, and differentiation as well as embryogenesis and normal development (15–17). RAS proteins respond to extracellular signals and transform them into intracellular responses through interaction with effector proteins. The activity of RAS proteins is highly controlled through two sets of specific regulators with opposite functions, the guanine nucleotide exchange factors and the GTPase-activating proteins (GAPs), as activators and inactivators of RAS signaling, respectively (18). In the present study, we analyzed the expression profile of different *Ras* isoforms in HSCs and found embryonic stem cell-expressed RAS (*ERas*) specifically expressed in quiescent HSCs. To date, ERAS expression has been reported in undifferentiated embryonic stem cells and in colorectal, pancreatic, breast, gastric, and neuroblastoma cancer cell lines (19–22). Recently, we demonstrated that ERAS represents a unique member of the RAS family with remarkable characteristics. The most profound features of ERAS include its GAP insensitivity (*i.e.* constitutive activity), its unique N terminus among all RAS isoforms, its distinct effector selection properties, and the posttranslational modification site at its C terminus (23).

Here, we investigated in detail the expression, localization, and signaling network of ERAS in quiescent and culture-activated HSCs. During *ex vivo* culture-induced activation of HSCs, the expression of ERAS was significantly down-regulated at the mRNA and protein level, probably due to an increase in promoter DNA methylation. We examined possible interactions and signaling of ERAS via various RAS effectors in HSCs. We found that the PI3Kα/δ-AKT, mTORC2-AKT, and RASSF5 (RAS association domain family)-HIPPO-YAP axis can be considered as downstream targets of ERAS in quiescent HSCs. In contrast, MRAS, RRAS, and RAP2A and also the RAS-RAF-MEK-ERK cascade may control proliferation and differentiation in activated HSCs.

Materials and Methods

Cell Isolation and Culture—Male Wistar rats (500–600 g) were obtained from the local animal facility of Heinrich Heine University (Düsseldorf, Germany). The livers were used for isolation of HSCs as described previously (24). Briefly, rat livers were enzymatically digested with collagenase H (Roche Applied Science) and protease E (Merck) and subjected to density gradient centrifugation to obtain primary cultures of HSCs. Purified HSCs were cultured in Dulbecco's modified Eagle's medium (DMEM) supplemented with 15% fetal calf serum and 50 units of penicillin/streptomycin (Gibco Life Technologies). Other liver cells, such as parenchymal cells, Kupffer cells, and sinusoidal liver endothelial cells were isolated and cultivated as described earlier (25). MDCKII and COS-7 cells were cultured in DMEM supplemented with 10% fetal calf serum. TurboFect transfection reagent (Life Technologies) was used to transfect MDCKII and COS-7 cells according to the manufacturer's protocol.

DNA Methyltransferase and Histone Deacetylase Inhibitor Treatment—Primary rat HSCs at day 3 were treated with 10 μM 5-aza-2′-deoxycytidine (5-AZA) (Decitabine, Sigma catalog no. A3656), a specific DNA methyltransferase inhibitor, for 4 successive days. In parallel, rat HSCs were treated with a 5 μM concentration of the histone deacetylase inhibitor suberoylanilide hydroxamic acid (Vorinostat, Cayman Chemicals catalog no. 10009929) under the same conditions. The control cells were treated with DMSO only. Cells were lysed at day 8 for RNA isolation and quantitative real-time reverse transcriptase polymerase chain reaction (qPCR) analysis.

Reverse Transcriptase Polymerase Chain Reaction—Cells were disrupted by QIAzol lysis reagent (Qiagen, Germany), and total RNA was extracted via the RNeasy Plus kit (Qiagen, Germany) according to the manufacturer's protocol. The quality and quantity of isolated RNA samples were analyzed on 1% agarose gels and using a Nanodrop spectrophotometer, respectively. Possible genomic DNA contaminations were removed using the DNA-free™ DNA removal kit (Ambion, Life Technologies). DNase-treated RNA was transcribed into complementary DNA (cDNA) using the ImProm-II™ reverse transcription system (Promega, Germany). qPCR was performed using TaqMan probes or SYBR Green reagent (Life Technologies). Probes/primers used for qPCR in the Taqman system, including Rn02098893_s1 for *ERas* and Rn01527840_m1 for HPRT1, were purchased from Applied Biosystems (Life Technologies). Primer sequences are listed in supplemental Table S1. The $2^{-\Delta\Delta Ct}$ method was employed for estimating the relative mRNA expression levels and $2^{-\Delta\Delta Ct}$ for mRNA levels. HPRT1 was used for normalization.

Immunostaining—Immunostaining was performed as described previously (23). Briefly, cells were washed twice with ice-cold PBS containing magnesium/calcium and fixed with 4% formaldehyde (Merck) for 20 min at room temperature. To permeabilize cell membranes, cells were incubated in 0.25% Triton X-100/PBS for 5 min. Blocking was done with 3% bovine serum albumin (BSA; Merck) and 2% goat serum diluted in PBS containing 0.25% Triton X-100 for 1 h at room temperature. Incubation with primary antibodies was performed overnight at 4 °C followed by staining at room temperature for 2 h. Cells were washed three times for 10 min with PBS and incubated with secondary antibodies for 2 h at room temperature. Slides were washed three times, and the ProLong® Gold antifade mountant with 4′,6-diamidino-2-phenylindole (DAPI) (Life Technologies) was applied to mount the coverslips. Primary antibodies included rabbit anti-FLAG (catalog no. F7425, Sigma-Aldrich), ERAS clone 6.5.2, and GFAP (catalog no. Z0334, Dako). Secondary antibodies included Alexa488-conjugated goat anti-rabbit IgG (catalog no. A11034), Alexa546-conjugated goat anti-mouse IgG (catalog nos. A11003 and A11008), Alexa633-conjugated goat anti-rabbit IgG (catalog no. A4671), and Alexa488-conjugated goat anti-mouse IgG (catalog no. A11029) (all from Life Technologies). Confocal images were obtained using an LSM 510-Meta microscope (Zeiss, Jena, Germany).

Constructs—Rat *ERas* cDNA was amplified by PCR from a cDNA library of freshly isolated rat hepatic stellate cells and subsequently cloned into pcDNA.3.1 and pEYFP-C1 vectors via the BamHI/XhoI and EcoRI/BamHI restriction sites, respectively. Mutations of G12V in *HRAS* ($HRAS^{V12}$) and C220S/C222S in *ERas* ($ERas^{S/S}$) were introduced by PCR-based site-directed mutagenesis as described earlier (26). To generate the N-terminal truncated *ERas* variants ($ERas^{\Delta N}$ and $ERas^{\Delta N/S/S}$), $ERas^{wt}$ and $ERas^{S/S}$ cDNA was PCR-amplified from amino acid (aa) 39 to 227 and from aa 1 to 227, respectively. Human *HRAS*, *KRAS*, *NRAS*, *TC21*, *MRAS*, and *ERAS* as well as rat *ERas* were cloned in pGEX vectors and used for protein purification for *Escherichia coli* as described previously (27).

Pull-down Assay—FLAG-tagged rat *ERas* and human *HRAS* cDNAs were cloned into pcDNA3.1 vector and overexpressed in COS-7 cells. The RAS-binding/association domains of effector proteins, including CRAF-RBD (aa 51–131), RALGDS-RA (aa 777–872), PLCϵ-RA (aa 2130–2240), p110α-RBD (aa 127–314), and RASSF5-RA (aa 200–358), were constructed as GST fusions in pGEX-4T and transformed in *E. coli*. GST-fused proteins were isolated from total bacterial lysates using glutathione-Sepharose beads. GTP-bound RAS proteins were pulled down from total cell lysates and heated in Laemmli buffer for 10 min at 95 °C.

Immunoblotting—Cell lysates were made with lysis buffer (50 mM Tris-HCl, pH 7.5, 100 mM NaCl, 2 mM $MgCl_2$, 1% Igepal CA-630, 10% glycerol, 20 mM β-glycerolphosphate, 1 mM *ortho*-Na_3VO_4, EDTA-free protease inhibitor (Roche Applied Science)), and protein concentrations were determined with a Bradford assay (Bio-Rad). Equal amounts of cell lysates (ERAS, 120 μg; FOXO1/p-FOXO1, 50 μg; remaining proteins, 15 μg), were subjected to SDS-PAGE. Following electrophoresis, the proteins were transferred to a nitrocellulose membrane by electroblotting and probed with primary antibodies overnight at 4 °C. All antibodies from Santa Cruz Biotechnology, Inc. were diluted 1:200 in 5% nonfat milk (Merck)/TBST (Tris-buffered saline, 0.05% Tween 20), and remaining antibodies were diluted 1:1000. The following antibodies were applied for immunoblotting: rabbit anti-FLAG (catalog no. F7425) and mouse γ-tubulin (catalog no. T5326) from Sigma-Aldrich; rabbit MEK1/2 (catalog no. 9126), rabbit ERK1/2 (catalog no. 9102), rabbit AKT (catalog no. 9272), rabbit phospho-MEK1/2 (Ser-217/Ser-221, catalog no. 9154), rabbit phospho-ERK1/2 (Thr-202/Thr-204, catalog no. 9106), rabbit phospho-AKT (Ser-473, catalog no. 4060; Thr-308, catalog no. 2965), rabbit p110α (catalog no. 4249), mouse STAT3 (catalog no. 9139S), rabbit phospho-STAT3 (catalog no. 9145S), rabbit FOXO1 (catalog no. 2880), and rabbit phospho-FOXO1 (catalog no. 9461) all from Cell Signaling; and antibodies to rabbit p110β (catalog no. sc-602), p110γ (catalog no. sc-7177), and p110δ (catalog no. sc-7176) from Santa Cruz Biotechnology. Mouse α-actin antibody (catalog no. MAB1510) was obtained from Millipore. Membranes were stained with horseradish peroxidase (HRP)-conjugated secondary antibodies (1:5000 dilution). Signals were visualized using ECL (enhanced chemiluminescence) reagent (GE Healthcare).

Expression and Purification of GBD-Nanotrap Beads and Co-immunoprecipitation—For immunoprecipitation studies of overexpressed EYFP-fused HRAS and ERAS in COS-7 cells, we applied a GFP-binding protein coupled to Sepharose beads. The GFP-binding protein used for Nanotrap experiments was designed as described previously (28). Briefly, the GFP-binding V_HH domain was cloned into pET23a-PelB vector adding C-terminal Myc and histidine (His_6) tags and transformed in *E. coli* BL21. An overnight 50-ml *E. coli* preculture with the antibiotic ampicillin was used to inoculate 2000 ml of medium to an A_{600} of 0.8. The expression of recombinant genes was induced with 1 mM isopropyl β-D-1-thiogalactopyranoside overnight at 30 °C. Cells were harvested by centrifugation (2 h, 4 °C, 4000 rpm), and the supernatant was stored at −80 °C. For purification, the supernatant was filtered through a 0.45-μm SFCA NALGENE®Rapid-Flow™ Bottle Top Filter (Thermo Scientific, Waltham, MA) to remove cell debris. Flow-through was mixed 1:1 with PP buffer (500 mM NaCl, 50 mM Na_2HPO_4/NaH_2PO_4, pH 7.4) and loaded on a pre-equilibrated nickel-nitrilotriacetic acid column (GE Healthcare) and purified. His-tagged protein was eluted by PP buffer containing 500 mM imidazole. The protein was concentrated, and imidazole was removed by using Amicon® Ultra-15 10K centrifugal filter devices (Merck Millipore Ltd., Tullagreen, Ireland). To perform pull-down of proteins by the GBD-nanotrap technique, 1 mg of purified protein was covalently coupled to 2 ml of NHS-activated Sepharose 4 Fast Flow (GE Healthcare), according to the manufacturer's instructions. Thereafter, beads were washed three times in ice-cold 1 mM HCl (2 min, 5400 rpm, 4 °C), added to the purified protein, and mixed for 2 h at room temperature under constant agitation. Subsequently, free binding sites of the beads were blocked by adding blocking buffer (0.5 M ethanolamine, 0.5 M NaCl, pH 8.3) for 2 h. Finally, beads were washed twice in 0.1 M Tris-HCl (pH 8). Beads were stored in 20% ethanol. For co-immunoprecipitation, cells were lysed in immunoprecipitation buffer (20 mM Tris-HCl, pH 7.4, 150 mM NaCl, 5 mM $MgCl_2$, 0.5% Nonidet P-40, 10 mM β-glycerolphosphate, 0.5 mM Na_3VO_4, 10% glycerol, EDTA-free protease inhibitor). Immunoprecipitation from total cell lysates was carried out for 2 h at 4 °C with GFP-fused nanobeads. The beads were washed five times with immunoprecipitation buffer lacking Nonidet P-40, and eluted proteins were finally heated in SDS-Laemmli buffer at 95 °C and analyzed by immunoblotting.

RAS Proteins and Monoclonal Antibody against ERAS—All RAS-like proteins, including ERAS, were purified following the same protocol as described (29). The monoclonal anti-ERAS antibody was custom-generated (Biogenes, Berlin, Germany) via immunization of mice with a purified N-terminal peptide of rat ERAS and thereafter purified from the supernatant of the respective hybridoma cell line by a protein A column (GE Healthcare). The concentrated antibody solution (~3 mg/ml) was supplemented with 10% glycerol and stored at −20 °C.

Subcellular Fractionation of HSCs by Differential Centrifugation—A differential centrifugation protocol according to Taha *et al.* (30) was used in this study to fractionate HSCs.

DNA Methylation Analysis of ERAS Promoter—A genome-wide DNA methylation analysis from quiescent and early activated HSCs was used to analyze DNA methylation changes dur-

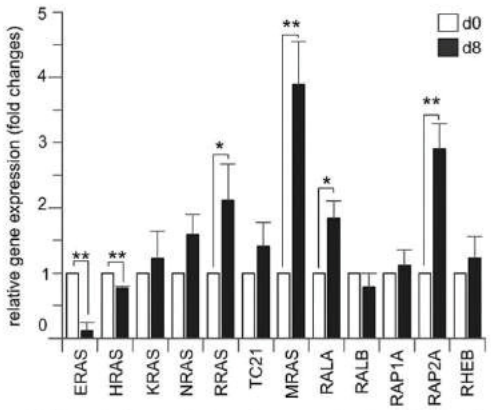

FIGURE 1. **Differential transcription of genes related to the RAS family in quiescent *versus* activated HSCs in primary culture.** qPCR analysis of RAS-related genes in freshly isolated HSCs from rat liver (*d0*) and after *ex vivo* cultivation for 8 days (*d8*) ($n = 3$, *t* test; *, $p < 0.05$; **, $p < 0.001$). *Error bars*, S.E.

ing HSC activation (31). The methylation data were visualized using the UCSC genome browser (University of California, Santa Cruz, CA). Verification of DNA methylation changes was performed by direct bisulfite sequencing. DNA from freshly isolated and cultured HSCs was isolated using the DNeasy blood and tissue kit (Qiagen) and subjected to bisulfite conversion by the EpiTect bisulfite kit (Qiagen). Bisulfite primers for *ERas* were designed using the MethPrimer online tool (32) covering a part of the promoter region (*ERas* 328 bp forward, 5′-GTT GGG GGT AGG GAG TAT TTT AAT-3′; *ERas* 328 bp reverse, 5′-CTC AAA ATT AAA AAA AAA AAA AAA TAA CC-3′). Bisulfite PCR was performed using the Maxima Hot Start PCR Master Mix (Thermo Scientific) together with 20 ng of bisulfite-modified DNA and 0.6 μmol/liter primer. After activation at 95 °C, a PCR protocol with denaturation at 95 °C, annealing at 55 °C, and elongation at 72 °C was used for 40 cycles. The PCR products were purified and sequenced at the DNA sequencing facility of Heinrich-Heine University. DNA methylation was quantified by the Mquant method as described (33). The height of the thymine peak at a CpG dinucleotide was subtracted from the average signal of 10 surrounding thymine peaks to quantify DNA methylation at this site. For the *ERas* methylation analysis, we calculated the mean DNA methylation of five CpG sites in the *ERas* promoter region.

Results

Expression of ERAS in Quiescent but Not Activated HSCs—To investigate the impact of RAS proteins on HSCs, we first investigated the expression profile of various members of the *Ras* family in quiescent *versus* activated rat HSCs by qPCR. Freshly isolated primary HSCs were cultivated on plastic dishes for up to 8 days, where they become activated upon *ex vivo* culture and undergo myofibroblast transition (4). HSCs were analyzed at day 8 (d8) in comparison with unseeded HSCs (d0) as representative of the activated and quiescent state, respectively. Interestingly, among the different members of the *Ras* family, *ERas* was specifically expressed in quiescent HSCs and strongly down-regulated during HSC activation (Fig. 1). In addition, we applied a probe based TaqMan real-time PCR to monitor *ERas* expression at the different time points of HSC cultivation (d0, d1, d2, d4, and d8) and obtained comparable results (supplemental Fig. S1). In contrast, *HRas* expression decreased only slightly in HSCs (d8). In contrast, the gene expressions of *MRas*, *RRas*, *RalA*, and *Rap2A* were up-regulated in activated HSCs, whereas other genes, including *KRas* and *NRas*, were expressed but did not significantly differ between day 0 and day 8 (Fig. 1). Collectively, these data indicate a switch from *ERas* to *MRas*, *RRas*, *RalA*, and *Rap2A* expression during HSC activation.

Generation and Validation of Specific Monoclonal Antibodies against Rat ERAS—ERAS contains an N-terminal extension upstream of its GTP-/GDP-binding (G) domain that is unique among the RAS family (23). As depicted in Fig. 2*A*, there is a significant difference between *Homo sapiens* (*hs*) and *Rattus norvegicus* (*rn*) ERAS proteins regarding their N terminus (Fig. 2*A*). Therefore, we purified the N terminus of *R. norvegicus* ERAS and generated antibodies against this unique ERAS region. Four clones of monoclonal antibodies (mAbs) were obtained and examined for anti-ERAS specificity. Immunoblot analysis of RAS proteins overexpressed in and purified from *E. coli* showed that clone mAb 6.5.2 clearly detected rat ERAS but none of the other members of the RAS family (Fig. 2*B*). The selectivity of mAb 6.5.2 against *H. sapiens* ERAS and *R. norvegicus* ERAS proteins was tested by using COS-7 and MDCKII cell lysates overexpressing *H. sapiens* ERAS and *R. norvegicus* ERAS as EYFP fusion proteins, respectively. As shown in Fig. 2*C*, mAb 6.5.2 only recognized rat ERAS (Fig. 2*A*). We next tested mAb 6.5.2 in confocal immunofluorescence analysis by overexpressing EYFP- and FLAG-tagged ERAS variants in MDCKII cells. As depicted in Fig. 2*D*, mAb 6.5.2 shows a clear specificity against full-length rat ERAS and recognized neither *H. sapiens* ERAS nor *R. norvegicus* ERAS lacking the N-terminal extension (*rn*ERAS$^{\Delta N}$). Taken together, mAb 6.5.2 was validated as a rat-specific anti-ERAS antibody suitable for both immunoblotting and immunofluorescence analysis.

Among Various Rat Liver Cell Types, ERAS Protein Is Only Expressed in Quiescent HSCs—The mAb 6.5.2 was used to analyze the presence of ERAS protein in typical liver cell populations. Therefore, total cell lysates of freshly isolated HSCs, parenchymal cells, Kupffer cells, and sinusoidal liver endothelial cells from rat liver were used for immunoblot analysis. Interestingly, ERAS was detected as a 25 kDa band in HSCs but not in other liver cell types (Fig. 3*A*). Consistent with the mRNA expression data (Fig. 1), the amount of ERAS protein was drastically reduced during the activation process of HSCs, thereby correlating with the loss of GFAP (Fig. 3*B*), which marks quiescent HSCs. In contrast, the myofibroblast marker α-smooth muscle actin became detectable in cultured HSCs from day 4. Moreover, confocal imaging of HSCs revealed that ERAS was mainly cytosolic, which was, in contrast to GFAP, still detectable in cultivated HSCs, although at much lower amounts as compared with day 0 (Fig. 3*C*). Noteworthy, in subcellular fractions of HSCs (d0), ERAS was predominantly found in the light membrane fraction (Golgi apparatus, smooth endoplasmic reticulum, and various organelles) and to a minor extent in the heavy membrane fraction (plasma membrane and rough endoplasmic reticulum) and in the nucleus (Fig. 3*D*). Collectively,

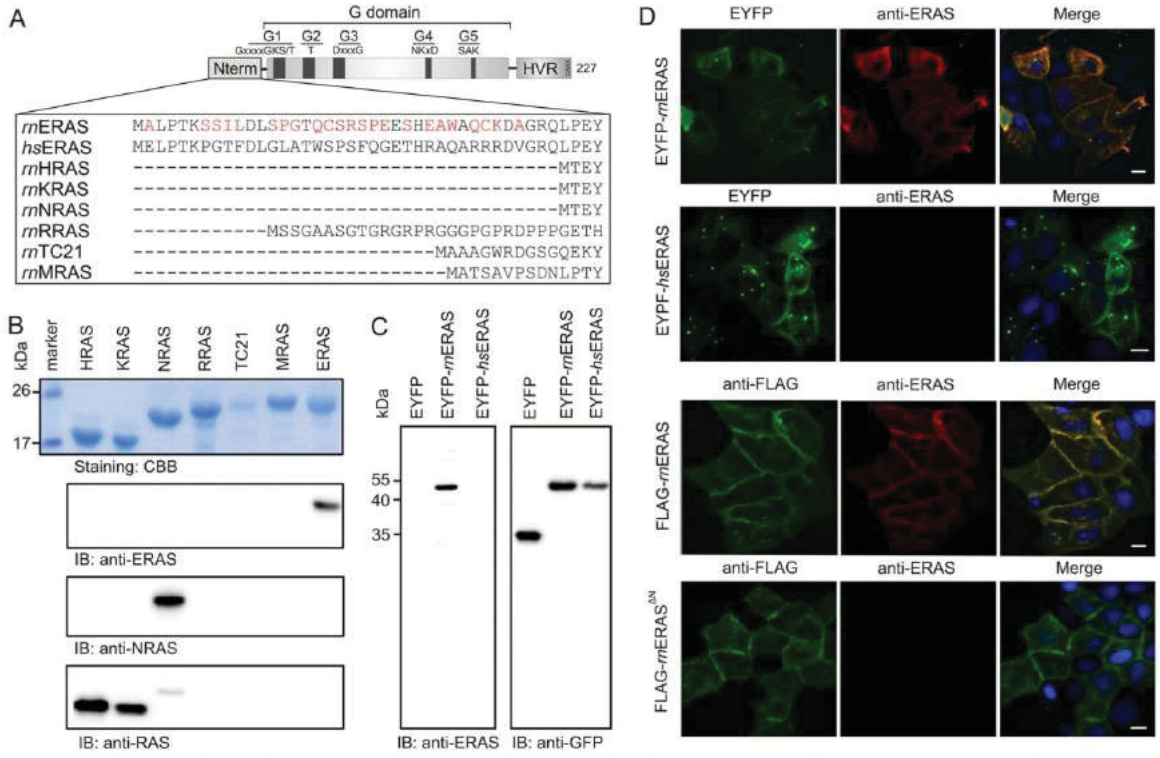

FIGURE 2. **Specification and validation of a monoclonal antibody raised against the rat ERAS N terminus.** *A*, a unique N-terminal extension in ERAS proteins. An amino acid sequence comparison between ERAS and other RAS proteins revealed that ERAS displays an additional region upstream of its G domain that is unique for ERAS in different organisms (23). *H. sapiens* (*hs*) and *R. norvegicus* (*rn*) ERAS (NP_853510.1 and NP_001102845.1, respectively) largely differ within this region (*red letters* in *R. norvegicus* ERAS). *B*, the anti-ERAS monoclonal antibody, clone 6.5.2, only recognized purified ERAS protein and not other RAS family members. Immunoblotting (*IB*) analysis of different RAS proteins, purified from *E. coli*, showed the high specificity of clone 6.5.2 against rat ERAS and exhibited no cross-reactivity against other RAS species. Two other antibodies were used as controls, which only recognized NRAS, HRAS, and KRAS, respectively, and not ERAS. HRAS and KRAS do not contain the hypervariable region (*HVR*) and are therefore smaller as compared, for example, with NRAS. *C* and *D*, anti-ERAS antibody (clone 6.5.2) recognized recombinant *R. norvegicus* ERAS but not *H. sapiens* ERAS, overproduced in COS-7 cells as YFP fusion proteins by immunoblotting (*C*) and in MDCKII cells as FLAG-tagged protein by confocal imaging (*D*). The FLAG-*rn*ERAS$^{\Delta N}$ construct, lacking the N-terminal 38 amino acids of *R. norvegicus* ERAS, was used as a negative control. *Scale bar*, 10 μm. *CBB*, Coomassie Brilliant Blue.

ERAS was detectable in quiescent HSCs, and its protein levels diminished remarkably during HSC activation.

Protein-Protein Interaction Profiling Identifies PI3Kα as a Specific Effector of Rat ERAS—Members of the RAS family GTP-binding proteins act as molecular switches that transduce extracellular signals to intracellular responses via activation of effector proteins. To gain insights into the effector binding specificity downstream of rat ERAS, FLAG-tagged constructs of HRAS and ERAS were overexpressed in COS-7 cells, and total cell lysates were used for pull-down experiments. For pull-down analysis, five major RAS effector proteins were employed (*i.e.* CRAF-RBD, RALGDS-RA, PLCε-RA, PI3Kα-RBD, and RASSF5-RA) (23), which were all produced in *E. coli* as GST fusion proteins. Interestingly, we found that ERAS, in comparison with HRAS, preferentially and most strongly bound to PI3Kα, whereas only a modest interaction was observed with RASSF5 and CRAF (Fig. 4*A*). Unlike HRAS, no ERAS association with RALGDS and PLCε was detectable (Fig. 4*A*). Thus, ERAS and HRAS interact with and probably activate a specifically non-overlapping set of effector proteins.

Similar to HRAS and NRAS, ERAS contains conserved C-terminal motifs for posttranslational modifications, a farnesylation- and palmitoylation-like HRAS (23). ERAS has an N-terminal extension with various motifs and shows a critical amino acid deviation, a serine at position 50 instead of a glycine (Gly-12 in HRAS), which makes ERAS GAP-insensitive (23). These properties may influence physical interaction of ERAS with PI3K and its downstream signaling. Therefore, we generated and analyzed different ERAS variants, lacking either the N terminus (ERAS$^{\Delta N}$) or conserved cysteines for palmitoylation (ERAS$^{S/S}$) or both (ERAS$^{\Delta N/S/S}$) (Fig. 4*B*). First, we investigated binding of ERAS variants to the catalytic subunit of PI3Kα. The obtained data revealed that all ERAS variants were able to associate with PI3Kα-RBD (Fig. 4*C*, *top*). This suggests that the N terminus of ERAS and its C-terminal modification by palmitoylation are not essential for the association of PI3Kα-RBD with the G domain of ERAS.

To examine the signaling activity of ERAS variants toward AKT via PI3K and mTORC2 pathways, we next monitored the phosphorylation states of AKT using specific anti-phospho-AKT (threonine 308 and serine 473) antibodies. It is noteworthy that ERAS strongly activated AKT and induced its phosphorylation at two distinct sites (*i.e.* at Thr-308 by PI3K-PDK1 (p-AKT^{T308}) and at Ser-473 by mTORC2 (p-AKT^{S473}; Fig. 4*C*,

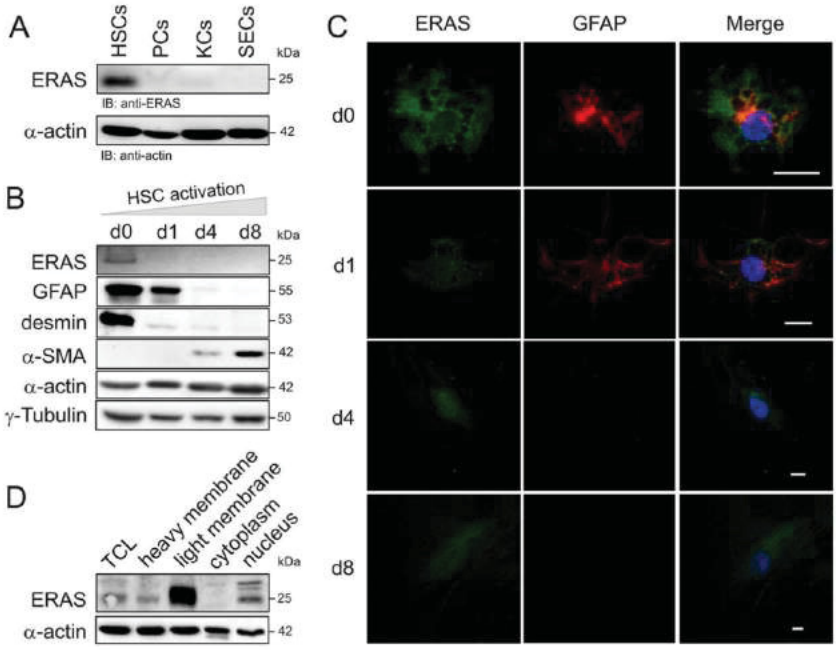

FIGURE 3. **ERAS protein in HSCs.** *A*, immunoblot analysis of isolated liver cell lysates detected ERAS in HSCs but not in other liver cells. *PCs*, parenchymal cell; *KCs*, Kupffer cells; *SECs*, sinusoidal endothelial cells. *B*, immunoblot analysis of ERAS from freshly isolated (*d0*) and activated HSCs maintained in monoculture up to 8 days (*d8*). GFAP and desmin were used as markers for quiescent HSCs (*d0*), and α-smooth muscle actin was used as a marker for activated HSCs (*d8*). α-actin and γ-tubulin served as loading controls. *C*, confocal imaging of ERAS and GFAP in HSC monocultures from d0 to d8. The level of ERAS and also of GFAP is significantly reduced in the course of cell culture with a trace amount of ERAS in the nucleus. *Scale bar*, 10 μm. *D*, ERAS showed a diverse subcellular distribution pattern in HSCs at day 0 as revealed by subcellular fractionation analysis. HSCs were fractionated into four distinct fractions, including heavy membrane (plasma membrane and rough endoplasmic reticulum), light membrane (polysomes, Golgi apparatus, and smooth endoplasmic reticulum), cytoplasm (cytoplasm and lysosomes), and enriched nucleus.

bottom)). Interestingly, in comparison with ERAS wild type (WT), the ERAS variants, most notably the truncated N terminus ($ERAS^{\Delta N}$), the palmitoylation-deficient variants with two cysteines 220 and 222 replaced with serines ($ERAS^{S/S}$), and a combination of both variants ($ERAS^{\Delta N/S/S}$), elicited a significantly reduced AKT phosphorylation, especially of p-AKT^{S473}, which is indicative of mTORC2 activity. These data indicate that both the ERAS N terminus and its plasma membrane anchorage via palmitoylation are essential and critical for AKT activation via the PI3K and mTORC2 axis, although the formation of the GTP-bound state and the interaction with PI3K were not affected.

ERAS-PI3Kα/δ-AKT and mTORC2-AKT Axis Are Highly Activated in Quiescent HSCs—Our findings suggest that the catalytic subunit of PI3K is a candidate effector downstream of ERAS. There are four isoforms of the p110 catalytic subunit of PI3K, p110α, p110β, p110γ, and p110δ, raising a question about the p110 isoform specificity in ERAS-PI3K interaction in HSCs. mRNA expression analysis data revealed that the α isoform of PI3K did not change remarkably between quiescent and activated HSCs, whereas the mRNA levels of the β and δ isoforms increased in the course of the HSC activation (Fig. 4*D*). At the protein level, however, α and γ isoforms were found at clearly higher levels in quiescent HSCs as compared with the β isoform (Fig. 4*E*). Upon HSC activation, the protein levels of β isoforms and, to a certain extent, also δ isoforms increased, whereas a decrease in α and γ isoforms was observed (Fig. 4*E*). Next, we investigated the interaction of ERAS with the four PI3K isoforms in co-immunoprecipitation experiments using ERAS overexpression in COS-7 cells. Wild type and a constitutive active variant of HRAS ($HRAS^{WT}$ and $HRAS^{V12}$) were used as controls. Data shown in Fig. 4*F* demonstrated that not only PI3Kα, but also the δ isoform, co-immunoprecipitated with ERAS. Notably, PI3Kδ appeared to strongly bind $HRAS^{V12}$ (Fig. 4*F*). Thus, cell-based investigations confirmed the interaction between ERAS and PI3Kα, which is consistent with our data obtained under cell-free conditions (Fig. 4*A*).

In the next step, we monitored the AKT phosphorylation states and found that quiescent HSCs at day 0 and, to a certain extent, at day 1, as compared with activated HSCs, exhibited much higher p-AKT^{S473} and p-AKT^{T308} levels, representing mTORC2 and PI3K-PDK1 activity, respectively (Fig. 4*G*). In addition, we also analyzed the phosphorylation states of FOXO1 and STAT3, two other signaling molecules that have been suggested to be downstream of ERAS (34). Interestingly, in ERAS-expressing quiescent HSCs, we observed high levels of STAT3 phosphorylation at Tyr-705 and of FOXO1 phosphorylation at Ser-256 (Fig. 4*G*). Thus, it is obvious that ERAS signaling toward PI3K-PDK1 and mTORC2 pathways activates AKT and maybe also STAT3 but inactivates FOXO1 in order to maintain HSCs in their quiescent state.

ERAS Does Not Actively Impact the MAPK Pathway—In the next step, we investigated the interaction of ERAS with CRAF-RBD and the MAPK pathway in quiescent *versus* activated

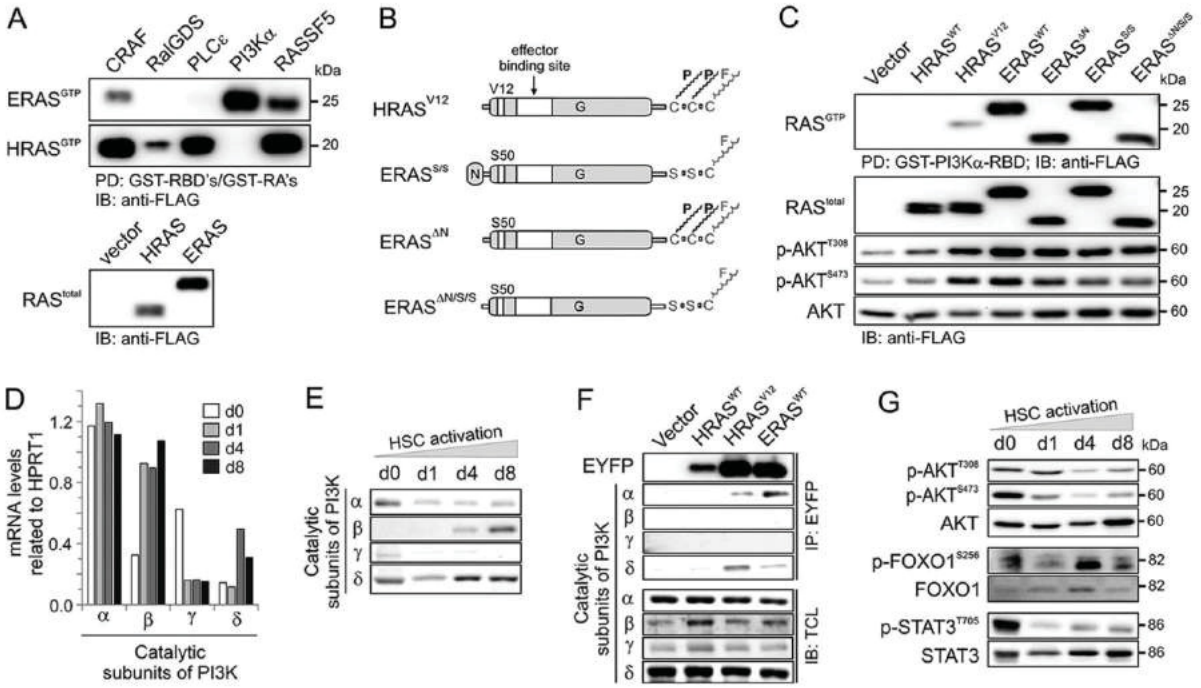

FIGURE 4. **Highly active PI3K-AKT and mTORC2-AKT pathways in quiescent HSCs may be controlled by ERAS.** *A*, transiently expressed FLAG-tagged rat ERAS^{WT} and human HRAS^{WT} were pulled down (*PD*) from COS-7 cell lysates with well known RAS effectors, including CRAF-RBD, RALGDS-RA, PLCε-RA, PI3Kα-RBD, and RASSF5-RA, as GST-fused proteins. Immunoblots (*IB*) of total cell lysates were used as a control to detect FLAG-RAS. *B*, FLAG-tagged RAS constructs used in this study, including ERAS^{WT}, ERAS$^{\Delta N}$ (N-terminal truncated, aa 39–227), ERAS$^{S/S}$ (palmitoylation-deficient), and ERAS$^{\Delta N/S/S}$ (N-terminal truncated and palmitoylation-deficient) as well as HRAS^{WT} and HRAS^{V12} (*G*, G domain). *C*, PI3Kα-RBD-derived pull-down (*PD*) of GTP-bound ERAS variants and their signaling activities were analyzed by immunoblotting of FLAG-tag and AKT phosphorylation (*p-AKT*) at positions Thr-308 and Ser-473. *D*, quantitative mRNA expression analysis of PI3K isoforms α, β, γ, and δ in quiescent and activated HSCs (*d0–d8*). *E*, immunoblot of the PI3K isoforms in quiescent and activated HSCs (*d0–d8*). *F*, co-immunoprecipitation analysis of the PI3K isoforms with ERAS^{WT}, HRAS^{WT}, and HRAS^{V12} overexpressed as EYFP fusion proteins in COS-7 cells. *TCL*, total cell lysate. *G*, immunoblot of the phosphorylated signaling proteins downstream of the PI3K-AKT and mTORC2 axis in quiescent and activated HSCs (*d0–d8*). Total AKT, FOXO1, and STAT3 served as controls.

HSCs. Both wild-type ERAS and its palmitoylation-deficient variant (ERAS$^{S/S}$) strongly bound to CRAF-RBD, although with considerably lower affinity as compared with the constitutive active HRAS^{V12} variant (Fig. 5*A*). This binding was, however, weaker for ERAS$^{\Delta N}$ and ERAS$^{\Delta N/S/S}$, both lacking the N-terminal extension. It is important to note that the latter variants are efficiently expressed and also exist in GTP-bound forms (Fig. 4*C*). The same is true for HRAS^{WT}, which was expressed to a similar level as HRAS^{V12} (Fig. 4*C*). However, its GTP-bound level was much lower due to its ability to hydrolyze GTP normally, therefore resulting in low amounts of HRAS^{WT} in the CRAF-RBD pull-down experiment (Fig. 5*A*). Most remarkably, expression of ERAS^{WT} in COS-7 cells clearly led to a strong reduction of p-MEK1/2 and p-ERK1/2 levels that were far below those obtained with vector control and the HRAS variants (Fig. 5*A*). Notably, similar effects were observed for all ERAS variants analyzed (ERAS$^{\Delta N}$, ERAS$^{S/S}$, and ERAS$^{\Delta N/S/S}$).

In addition, we analyzed the binding property of rat ERAS to cellular RAF isoforms (ARAF, BRAF, and CRAF) by overexpressing and immunoprecipitating EYFP-tagged ERAS from COS-7 total cell lysates. As controls, we used HRAS^{WT} and HRAS^{V12}. Fig. 5*B* shows that ERAS, compared with HRAS^{V12}, bound weakly only to ARAF and CRAF, which is consistent with the data obtained with CRAF-RBD in pull-down experiments (Fig. 5*A*). Thus, we conclude that ERAS can be excluded as an activator of RAF proteins and thus of the MAPK pathway.

The MAPK Pathway Is Highly Dynamic in Activated HSCs—Our data showed that ERAS is endogenously expressed in quiescent HSCs and does not seem to be an activator of the MAPK pathway under overexpression conditions in COS-7 cells. Therefore, we analyzed the activity of the MAPK pathway in HSCs following their activation. First, we analyzed the expression of *Raf*, *MEK*, and *ERK* isoforms in quiescent *versus* activated HSCs by qPCR. As indicated in the legend to Fig. 5*C*, the overall mRNA levels were very similar except for the low expression of *BRaf* in both quiescent and activated HSCs (Fig. 5*C*). For further examination of the role of the MAPK pathway in HSC activation, we looked at the protein levels of phosphorylated (*i.e.* activated) *versus* total MEK1/2 and ERK1/2. As shown in Fig. 5*D*, expression of MEK1/2 increased strongly in the course of the HSC activation as compared with the relatively constant amounts of ERK1/2. The level of ERK1 (44 kDa) was much higher than ERK2 (42 kDa). In contrast, the amounts of the RAF isoforms and total RAS were highest in quiescent HSCs (day 0) and decreased during HSCs activation (Fig. 5*D*). Most remarkably, we observed an increase in p-MEK1/2 and p-ERK1/2, especially p-ERK2, suggesting increased activation of the MAPK pathway in activated HSCs (Fig. 5*D*). In contrast,

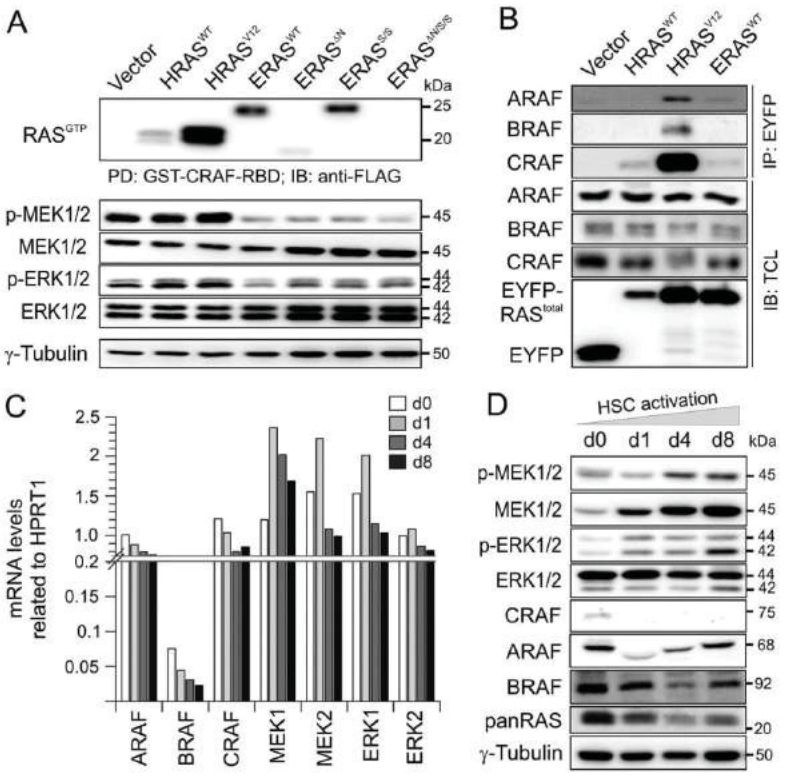

FIGURE 5. **RAF-MEK-ERK signaling in activated HSCs.** *A*, CRAF-RBD-derived pull-down (*PD*) of GTP-bound HRAS and ERAS variants and their signaling activities toward MAPK pathway were analyzed by immunoblotting (*IB*) of the FLAG tag and phosphorylation of MEK1/2 (*p-MEK1/2*) and ERK1/2 (*p-ERK1/2*) using total cell lysates derived from transfected COS-7 cells. γ-Tubulin was used as the loading control. *B*, co-immunoprecipitation analysis (*IP*) of the RAF isoforms with ERAS^{WT}, HRAS^{WT}, and HRAS^{V12} overexpressed as EYFP fusion proteins in COS-7 cells. *TCL*, total cell lysate. *C*, quantitative mRNA expression analysis of the *Raf*, *MEK*, and *ERK* isoforms in quiescent and activated HSCs (*d0–d8*). *D*, immunoblot analysis of the components of the MAPK pathway, including RAF isoforms, p-MEK1/2, and p-ERK1/2 in quiescent and activated HSCs (*d0–d8*). Total RAS was detected using a pan-RAS antibody. Total amounts of MEK1/2 and ERK1/2 as well as γ-tubulin served as loading controls.

the amounts of the RAF isoforms and total RAS were the highest in quiescent HSCs (day 0) and subsequently decreased during HSC activation (Fig. 5*D*). Taken together, it seems that HSCs reciprocally utilize distinct pathways downstream of ERAS to maintain their fate (*i.e.* PI3K-PDK1 and mTORC2 pathways could be activated by ERAS in quiescent HSCs, and the MAPK pathway could be activated by RAS in activated HSCs).

ERAS Contributes to Repression of YAP Activity and Thus May Counteract Activation of Quiescent HSCs—In vitro protein-protein interaction studies revealed that ERAS, like HRAS, directly interacts with RASSF5 (Figs. 4*A* and 6*A*). It has been reported that RASSF5 enables the HIPPO pathway (via MST2/STK3) to respond to and integrate diverse cellular signals by acting as a positive regulator of MST2/STK3 (35). A recent study revealed a role of YAP, the central effector of the HIPPO pathway during HSC activation (13); thus, we analyzed whether ERAS activates the HIPPO pathway, which may lead to phosphorylation and proteolytic degradation of YAP (supplemental Figs. S2 and S3*A*). We further investigated whether YAP and its target genes are expressed in activated rat HSCs. To address the first question, we used COS-7 cells, which normally contain significant amounts of YAP and its phosphorylated form

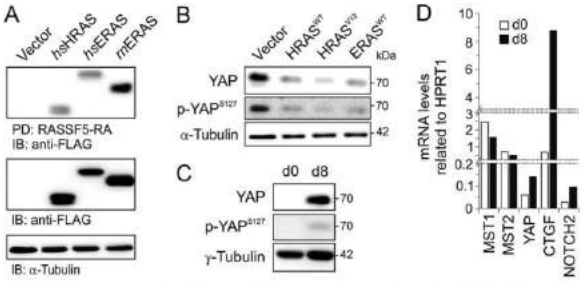

FIGURE 6. **ERAS-RASSF5 interaction may repress YAP that is highly active in activated HSCs.** *A*, RASSF5-RA pull-down (*PD*) of HRAS^{WT}, *H. sapiens* ERAS, and *R. norvegicus* ERAS overexpressed in COS-7 cells. Total amounts of FLAG-tagged RAS proteins as well as α-tubulin were detected as loading controls. *IB*, immunoblotting. *B*, immunoblot of YAP and p-YAP at Ser-127 of COS-7 cell lysate overexpressing wild-type ERAS and HRAS as well as the constitutive active variant of HRAS (HRAS^{V12}). α-Tubulin was used as a loading control. *C*, immunoblot of YAP and p-YAP at Ser-127 of quiescent (*d0*) and activated HSCs (*d8*). γ-Tubulin served as a control. *D*, qPCR analysis of MST1 and -2 as well as YAP and its target genes *Ctgf* and *Notch2* in quiescent (*d0*) *versus* activated HSCs (*d8*).

(p-YAP^{S127}; Fig. 6*B*; see vector control). Interestingly, p-YAP^{S127} and YAP levels were considerably reduced when rat ERAS was overexpressed (Fig. 6*B* and supplemental Fig. S2),

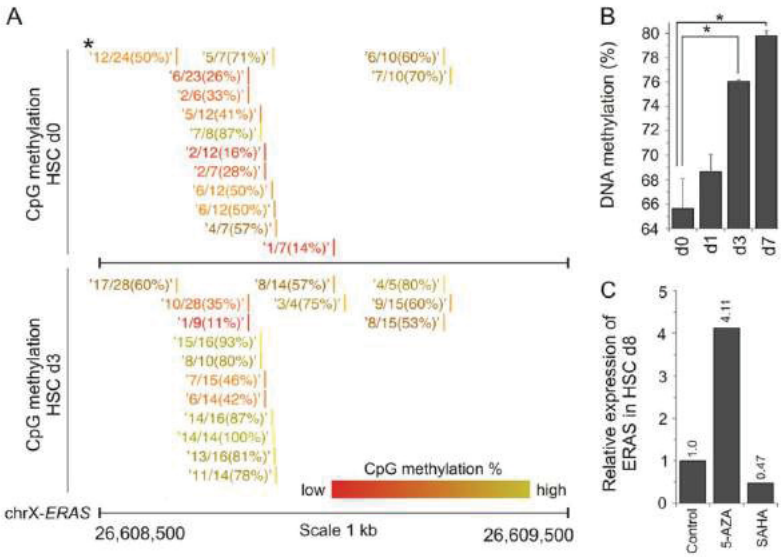

FIGURE 7. **DNA methylation analyses of *ERas* in quiescent and activated primary HSCs.** *A*, results of genome-wide DNA methylation analysis of quiescent HSCs (*d0*) and early activated HSCs (*d3*) at the *ERas* promoter region. DNA methylation of individual CpG dinucleotides is depicted in percent (methylated CpG/total numbers of CpG) and displayed with a *color code* from *red* (0%) to *light green* (100% DNA methylation). *B*, *ERas* promoter methylation analyzed by direct bisulfite sequencing exhibited a significant increase of DNA methylation during HSCs activation ($n = 3$–5, *t* test; *, $p < 0.05$). *C*, HSC (day 3) were treated with 10 μM 5-aza-2′-deoxycytidine (*5-AZA*) and/or 5 μM suberoylanilide hydroxamic acid (*SAHA*) for 4 days, and the expression of *ERas* was analyzed with qPCR at day 8. *Error bars*, S.E.

strongly indicating that ERAS activated the HIPPO pathway in COS-7 cells. Similar results were obtained with the HRAS variants (Fig. 6*B*). Importantly, we next probed YAP and p-YAP^{S127} in HSC lysates and detected them in activated HSCs (day 8) but not in quiescent HSCs (Fig. 6*C*). Consistently, mRNA analysis further revealed that *Mst1/2* (mammalian orthologues of *Hippo*) isoforms were expressed in both states but with more elevated levels of *Mst1* as compared with *Mst2*. *Yap* and its target genes, *Ctgf* (connective tissue growth factor) and *Notch2*, exhibited a distinct increase in their expression levels after HSC activation (Fig. 6*D*). Moreover, the effector binding domain (switch regions) of ERAS differs considerably from those of HRAS in critical residues, which may determine the specificity of ERAS binding to its effectors (23) (supplemental Fig. S3*B*). Interestingly, we found that mutation of two surface-exposed residues (H70Y/Q75E) in the effector binding region of ERAS (ERAS^{SW1}) abolishes the binding affinity for RASSF5 as compared with wild-type ERAS (supplemental Fig. S3*C*). These findings indicate that ERAS needs specific residues that are not conserved within HRAS to interact with RASSF5. To monitor the activity of the ERAS-RASSF5-MST1/2-LATS1/2-YAP cascade downstream of mutated ERAS, we next analyzed the levels of YAP protein in total cell lysates. Consistently, we detected larger amounts of YAP under conditions when the RASSF5 binding-deficient ERAS mutant (ERAS^{SW1}) was overexpressed (supplemental Fig. S3, *D* and *E*). These data further support the idea that ERAS is upstream of the HIPPO-YAP pathway. Collectively, activation of the HIPPO pathway appears to keep HSCs in their quiescent state, whereas YAP clearly may play a role in the activation and eventually further development of HSCs. YAP is obviously repressed in quiescent HSCs potentially mediated through ERAS-RASSF5 signaling.

Increased DNA Methylation of the ERAS Locus Is Associated with ERAS Gene Silencing in Activated HSCs—To characterize possible mechanisms responsible for the down-regulation of *ERas* expression in activated HSCs, epigenetic analysis of the promoter region of the rat *ERas* gene was conducted. Evaluation of a previously performed genome-wide DNA methylation analysis showed an increase of CpG methylation at the *ERas* promoter of ~18% during early HSC activation (Fig. 7*A*). More detailed bisulfite-sequencing analysis during *in vitro* HSC activation revealed a significant increase in promoter DNA methylation, which correlates with the drastic decrease in *ERas* expression in HSCs during their activation (Figs. 1 and 7*B* and supplemental Fig. S1). Of note, the overall degree of promoter DNA methylation increased from 65.5 to ~80% at day 7 of HSC culture. To investigate the functional impact of *ERas* promoter methylation, we examined whether the DNA methyltransferase inhibitor 5-AZA could restore ERAS expression in activated HSC. Therefore, we cultivated primary rat HSC for 3 days, such that the levels of *ERas* mRNA were down-regulated (supplemental Fig. S1). At day 8 of HSC activation (and 4 days of 5-AZA treatment), we analyzed ERAS expression. As indicated in Fig. 7*C*, 5-AZA treatment restored *ERas* expression by ~4-fold in activated HSC. To test whether *ERas* expression is also regulated via histone modifications, such as histone acetylation, we treated HSCs with 5 μM suberoylanilide hydroxamic acid (histone deacetylase inhibitor). As indicated in Fig. 7*C*, suberoylanilide hydroxamic acid treatment alone was not sufficient to rescue *ERas* expression. Taken together, our data indicate that the profound decrease of *ERas* expression but not *NRas* and other *Ras*-related genes, such as *RRas* and *Rap2A* (data not shown), during HSC activation may be caused by epigenetic gene silencing.

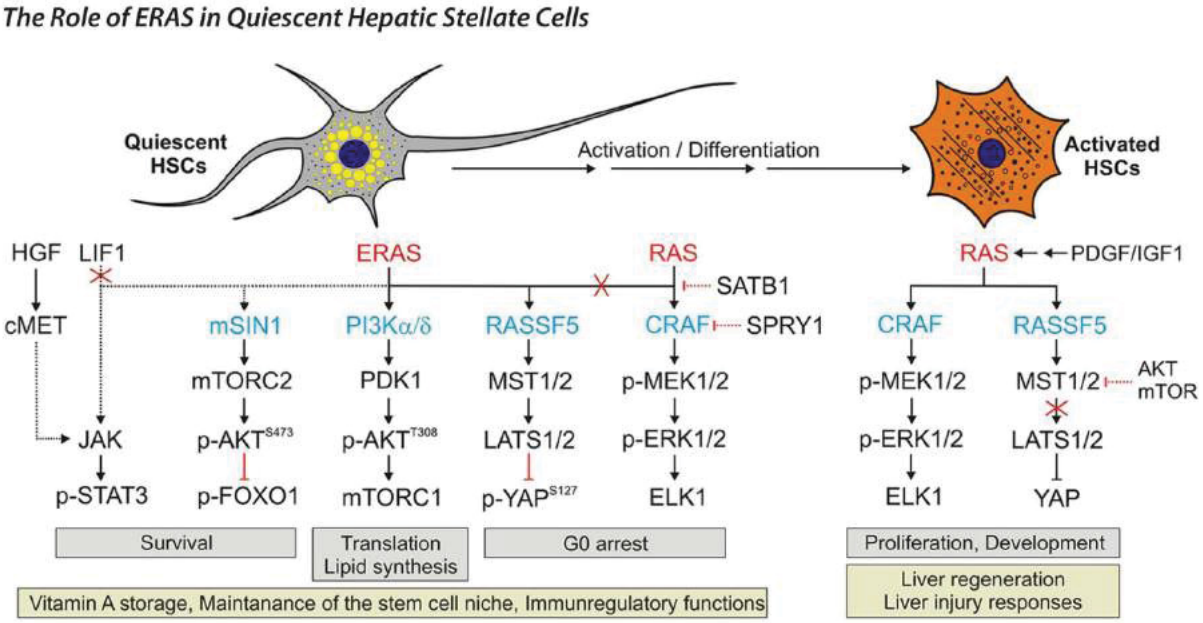

FIGURE 8. **Schematic view of the proposed model on reciprocal ERAS/RAS-dependent signaling pathways in quiescent *versus* activated HSCs (for details, see "Discussion").** *ECM*, extracellular matrix; *IGF*, insulin-like growth factor; *LIF1*, leukemia inhibitory factor; *TSC*, tuberous sclerosis.

Discussion

In this study, we found *ERAS* specifically expressed in one type of liver-resident cells, HSCs. The presence of *ERas* mRNA was detected in quiescent HSCs but not in activated HSCs. In contrast, other RAS-related genes, such as *RRas*, *MRas*, *RalA*, and *Rap2A*, were up-regulated during HSC activation. ERAS protein was detected in quiescent HSCs but not in other liver cell types, and ERAS was considerably down-regulated during HSC activation (d4 and d8). To elucidate the functions of ERAS in quiescent HSCs, we sought ERAS-specific effectors and the corresponding downstream pathways. Interaction analyses with a set of RAS effectors showed that ERAS preferentially interacts with PI3Kα and activates the PI3K-PDK1-AKT axis. The prominent AKT phosphorylation by mTORC2 in quiescent HSCs suggests that mTORC2-AKT acts as a candidate pathway mediates signaling downstream of ERAS. Interestingly, in quiescent HSCs, ERAS does not show any activity toward the MAPK cascade, which is the opposite in activated HSCs. The MST1/2-LATS1/2-YAP (HIPPO pathway) results in inactivation and proteosomal degradation of YAP if activated, for example, by RAS and RASSFs. The fact that YAP was hardly detectable in quiescent HSCs and also in COS-7 cells expressing ERAS, as well as the interaction between ERAS and RASSF5, suggests that ERAS may act as an activator of the HIPPO pathway in quiescent HSCs. Consistently, we detected both YAP protein and its up-regulated target genes in activated HSCs.

Role of the PI3K-AKT-mTORC1 Activity in Quiescent HSCs—Transient expression of ERAS in COS-7 cells and endogenous ERAS expression in quiescent HSCs strongly correlate with high levels of AKT phosphorylated at Thr-308 and Ser-473 through PDK1 and mTORC2, respectively. Protein interaction and immunoprecipitation analysis further revealed that ERAS physically interacts with PI3Kα and also PI3Kδ (Fig. 4, *C* and *F*). Thus, in quiescent HSCs, we propose ERAS as a regulator of the PI3K-PDK1-AKT-mTORC1 axis. This axis is involved in various processes, including cell cycle progression, autophagy, apoptosis, lipid synthesis, and translation (36–40). The latter is controlled by mTOR-mediated activation of S6 kinase, which in turn phosphorylates different substrates, such as ribosomal protein S6, mTOR itself at Ser-2448, and mSIN1 at Thr-86, an upstream component of mTORC2 (Fig. 8) (41–43). Previous studies have shown that quiescent HSCs produce and secrete a significant amount of HGF (44, 45), which is known to regulate hepatocyte survival (46). HGF production and secretion is modulated by the mTORC1-S6 kinase pathway (47). Apart from the retinoid transport from hepatocyte to HSCs, the mTORC1 activity may influence *de novo* lipid synthesis in HSCs. mTORC1 might promote lipid synthesis in HSCs through sterol regulatory element-binding protein (SREBP) and peroxisome proliferative-activator receptor-γ (PPARγ) (48). In this regard, it has been shown that curcumin inhibits SREBP expression in cultured HSCs by modulating the activities of PPARγ and the specificity protein-1 (SP1), thereby repressing LDLR expression, which blocks a proposed LDL-induced HSC activation (49). Thus, the AKT-mTORC1-SREBP/PPARγ pathway appears to play a critical role in lipid metabolism that is obviously required together with other pathways to regulate HSC fate.

Recently, Kwon *et al.* (50) have shown that in mouse embryonic stem cells overexpression of ERAS induces SP1 activation through the JNK pathways. However, it remains to be addressed whether JNK-SP1 signaling is also a downstream target of endogenous ERAS in HSC.

Activity of the mTORC2-AKT-FOXO1 Axis in Quiescent HSCs—In comparison with mTORC1, the regulation of mTORC2 is less understood (51). For example, the TSC1-TSC2 complex can physically associate with mTORC2 but not with

mTORC1, which has been suggested to promote mTORC2 activity (52). Our findings indicate that ERAS may act as an activator of the mTORC2 pathway. Exogenous ERAS has been shown to promote phosphorylation of both AKT (Ser-473) and FOXO1 (Ser-256) in induced pluripotent stem cells generated from mouse embryonic fibroblasts (34). Thus, ERAS-AKT-FOXO1 signaling may be important for somatic cell reprogramming. We detected high levels of p-AKT^{S473} and p-FOXO1^{S256} in quiescent HSCs endogenously expressing ERAS (Fig. 4*G*). Phosphorylated FOXO1, sequestrated in the cytoplasm, cannot translocate to the nucleus, where it binds to gene promoters and induces apoptosis (53). Interestingly, a possible link between ERAS and mTORC2 may be mSIN1, which appears to be an upstream component and modulator of mTORC2 activity (54). It has been reported that mSIN1 contains a RAS-binding domain with some homology to that of CRAF (55). Taken together, the ERAS-mTORC2-AKT-FOXO1 axis may ensure the survival of HSCs in the space of Dissé by interfering with programmed cell death (Fig. 8).

Role of the HGF-JAK-STAT3 Axis in Quiescent HSCs—Ectopic expression of ERAS stimulates phosphorylation of STAT3 probably downstream of leukemia inhibitory factor (LIF) (34). ERAS may compensate for lack of LIF to support the induced pluripotent stem cell generation (34). Moreover, the LIF-STAT3 axis is essential for keeping mouse stem cells undifferentiated in cultures and regulates self-renewal and pluripotency of embryonic stem cells (56). Phosphorylated STAT3 (p-STAT3) has been shown to directly interact with FOXO1/3 transcription factors and regulates their translocation into the nucleus (57). Consistently, we detected high levels of p-STAT3 and p-FOXO1 in quiescent HSCs (Fig. 4*G*), which may control survival, self-renewal, and multipotency of quiescent HSCs. In addition, stimulation of the HGF receptor (c-MET), which is expressed in HSCs, results in JAK activation and phosphorylation of STAT3 (1, 58). Interestingly, HGF is a target gene of IL6-STAT3 signaling (59, 60). Therefore, an autocrine HGF-JAK-STAT3 signaling may also account for STAT3 phosphorylation in quiescent HSCs (Fig. 8). However, determination of the presence and activity of a LIF-STAT3 axis in HSCs requires further investigation.

Quiescent HSCs Display a Locked RAS-MAPK Signaling Pathway—In quiescent HSCs, only basal levels of activated (phosphorylated) MEK and ERK could be observed, although all components of the RAS-RAF-MEK-ERK axis were expressed (Figs. 1 and 5 (*C* and *D*)). There are several explanations for the strongly reduced activity of RAS-MAPK signaling in quiescent HSCs (Fig. 8). (i) External stimuli, such as PDGFA and TGFβ1, are absent in healthy liver. These growth factors are strong activators of the MAPK pathway in activated HSCs (7, 8). (ii) An intracellular inhibitor, like special AT-rich binding protein 1 (SATB1), which is specifically expressed in quiescent HSCs and down-regulated during HSC activation (61), is present. Interestingly, SATB1 has been shown to be a strong inhibitor of the RAS-MAPK pathway that may block this signaling in quiescent HSCs (61). (iii) MicroRNAs (miRNAs), especially miRNA-21, may play a role in the reciprocal regulation of the RAS-MAPK pathway in quiescent *versus* activated HSCs. Up-regulated miRNA-21 in activated HSCs results in MAPK activation, which is based on depletion of SPRY1 (sprouty homolog 1), a target gene of miRNA-21 (62) and a negative regulator of the RAS-MAPK pathway (63).

Biological Functions of PI3K-AKT Pathway Regarding Different p110 Isoforms—The catalytic PI3K isoforms p110α and -β are reported to be ubiquitously expressed, whereas the presence of p110γ and -δ is restricted mainly to hematopoietic cell types (64–67). We identified ERAS as an activator of AKT by interacting with p110α and moderately also with p110δ (Fig. 4*F*). Our RNA and protein analyses indicated high levels of *p110*α/γ in quiescent HSCs and elevated levels of *p110*β/δ in activated HSCs (Fig. 4, *D* and *E*). Wetzker and colleagues (68) reported that retinoic acid treatment can stimulate expression of p110γ, but not p110β/δ, in U937 cells, a myelomonocytic cell line. Quiescent HSCs store high levels of retinoid acids as retinol esters in their lipid droplets, which may elicit the same function in HSCs by up-regulation of p110γ. Khadem *et al.* (69) have shown that HSCs also express the p110δ isoform and that p110δ deficiency in HSCs prevents their activation and their supportive roles in T_{reg} expansion in mice infected with visceral leishmaniasis. Therefore, the high level of the p110δ isoform in activated HSCs may correlate with its immunoregulatory functions.

Epigenetic Regulation of ERAS Expression in HSCs—Unlike other RAS proteins, ERAS is GAP-insensitive and refractory to inactivation by RASGAP proteins (21, 23). This raises the question about the potential mode(s) of ERAS regulation. Because ERAS is not ubiquitously expressed and seems to be limited to a few cell types, we proposed that ERAS is mainly regulated at the transcriptional level as described before for gastric cancers (70). Our epigenetic studies of the *ERas* promoter revealed that its DNA methylation increases (up to 18%) during HSC activation (Fig. 7, *A* and *B*). Moreover, treatment with DNA methyltransferase inhibitor induced re-expression of *ERas* in culture-activated HSCs (Fig. 7*C*). Consistently, *ERas* expression was also induced in certain gastric cell lines by the DNA methyltransferase inhibitor (70). Collectively, our findings clearly indicate that DNA methylation is one of the mechanisms suppressing expression of *ERas* during activation of HSCs. Conceivably, *ERas*-specific microRNAs may also control mRNA degradation and translation of *ERas* when HSC activation is induced.

Cellular Signaling Signature of Activated HSCs—*In vitro* culturing of hepatic stellate cells changes their gene expression profile and cellular properties, thereby stimulating the activation of HSCs (1, 31, 71, 72). HSCs typically lose their lipid droplets and expression of GFAP and elicit the synthesis of collagens, matrix metalloproteinases (MMP2, -9, and -13), and α-smooth muscle actin as important differentiation markers (2, 11). Collectively, during this process, HSCs alter their quiescent characteristics and develop into myofibroblast-like cells, which are recognized as proliferative, multipotent, and migratory cells (6, 73, 74). Comprehensive mRNA analysis of various RAS family members revealed that *RRas*, *MRas*, *RalA*, and *Rap2A* were up-regulated during HSC activation (Fig. 1). These genes may also play a role in the coordination of cellular processes, which are required for activation and differentiation of HSCs, such as polarity, motility, adhesion, and migration. Interestingly, RRAS has been implicated in integrin-dependent cell adhesion (75). Of note, in endothelial cells, the RRAS-RIN2-RAB5 axis stimulates endo-

cytosis of β_1 integrin in a RAC1-dependent manner (76). On the other hand, the muscle RAS oncogene homolog (*MRas*), an RRAS-related protein, is up-regulated during HSC activation. Among the different members of the RAS family, only MRAS can interact with SHOC2 in a ternary complex with protein phosphatase 1, which dephosphorylates autoinhibited CRAF and thereby activates the CRAF-MEK-ERK cascade (77). These findings and data obtained in this study suggest that MRAS may be responsible for the high levels of p-MEK and p-ERK in activated HSCs due to RAF kinase activation. RAP proteins, including RAP2A, are involved in different cellular processes and play pivotal roles in cell motility and cell adhesion (78, 79). Recently, it has been shown that RAP2A represents a novel target gene of p53 and a regulator of cancer cell migration (80). Moreover, expression of RAP2A in cancer cells results in secretion of two matrix metalloproteinases (MMP2 and -9) and AKT phosphorylation at Ser-473, which promotes tumor invasion (80). Notably, p53 is up-regulated in activated HSCs (81). Thus, we speculate that binding of p53 to RAP2A promoter may result in transcription of RAP2A in activated HSCs and may stimulate secretion of MMPs, which remodels the extracellular matrix and facilitates migration of HSCs in the space of Dissé.

Proliferation, Growth, and Differentiation of Activated HSCs—In comparison with quiescent HSCs, activated HSCs are proliferative cells and can pass through cellular checkpoints (82). One of the candidate pathways is the RAF-MEK-ERK cascade that can be stimulated via different growth factors. Consistent with previous studies, we detected high levels of p-MEK and p-ERK in culture-activated HSCs (7, 83). Three scenarios may explain the elevated RAF-MEK-ERK activity in activated HSCs. (i) As discussed above, MRAS with SHOC2 and protein phosphatase 1 is able to activate the CRAF-MEK-ERK pathway (80). Phospho-ERK translocates to the nucleus and phosphorylates different transcriptional factors, including Ets1 and c-Myc, thereby eliciting cell cycle progression and proliferation. The cytoplasmic p-ERK alternatively phosphorylates Mnk1 and p90RSK and thereby promotes protein synthesis and cell growth (84, 85). (ii) PDGF and insulin-like growth factor 1 are the most potent mitogens for activated HSCs and induce activation of MAPK pathways (7, 86). (iii) The expression of SATB1, a cellular inhibitor of the RAS-RAF-MEK-ERK pathway, significantly declines during HSC activation (61).

Putative Role of the ERAS-RASSF5-MST1/2-LATS1/2-YAP Axis in HSCs—We observed a moderate interaction between ERAS and RA of RASSF5A (Fig. 6*A*). Previously, we showed that the switch I region of ERAS is important for ERAS-RASSF5 interaction, and mutation in this region impairs ERAS binding to RASSF5 (23). RASSF proteins are recognized as specific RAS effectors with tumor suppressor function (87, 88). MST1/2, which are expressed in HSCs, interact with and form heterodimers with RASSF1/5A and WW45 through their SARAH (SAV/RASSF/HPO) domain (89). This complex phosphorylates and activates LATS1/2, which in turn promotes phosphorylation, sequestration, and proteasomal degradation of YAP in the cytoplasm (supplemental Fig. S3*A*) (90, 91). YAP is a transcriptional co-activator that promotes transcription of *Ctgf* and *Notch2*, which are involved in cell development and differentiation (92–95). It has been shown that the HIPPO-YAP pathway plays a distinct role in differentiated parenchymal and undifferentiated liver progenitor cells, respectively. Most recently, van Grunsven and colleagues (13) reported that the transcriptional co-activator of YAP controls *in vitro* and *in vivo* activation of HSCs. Consistent with this study, we observed hardly any YAP protein in quiescent HSCs in comparison with activated HSCs (Fig. 6*C*). Thus, our data suggest that YAP degradation through RASSF5-MST1/2-LATS1/2 may be triggered by binding and recruitment of RASSF5 to the plasma membrane via ERAS-GTP (Figs. 6*B* and 8).

Cell Survival and Anti-apoptotic Pathways—One of the most important features of activated HSCs is their survival and anti-apoptotic response during liver injury and regeneration (96). Here, we demonstrated elevated p-AKT levels not only in quiescent but also in activated HSCs, the latter leading to pro-survival responses, such as phosphorylation of FOXO1 (Fig. 4*G*). Additionally, we detected moderate levels of p-STAT3, implying that the JAK1-STAT3-SOCS3 axis may control the anti-apoptotic pathway in activated HSCs.

Last, the high levels of YAP transcriptional activity in activated HSCs, which might result from the inhibitory activities of AKT and mTOR on MST1/2 (97), may contribute to increased cell survival, proliferation, and development of activated HSCs (13) by causing antagonistic effects to the pro-apoptotic RAS-RASSF5-MST1/2-LATS1/2 pathway (Fig. 8).

Functional Similarity between Human and Rat ERAS—We observed sequence deviations between human and rat ERAS, especially at their extended N termini (Fig. 2*A*). Therefore, we compared the signaling activity of different human and rat ERAS variants. However, so far, we did not observe remarkable functional differences (Fig. 4 and supplemental Fig. S4). ERAS function in human diseases is poorly understood. Its expression profile ranges from embryonic stem cells to tumors (20, 21). Yamanaka and colleagues (21) have introduced ERAS as a critical factor for the maintenance of growth of embryonic stem cells. Kaizaki *et al.* (20) reported ERAS expression in 45% of gastric cancer tissues and observed a correlation between ERAS-negative patients and poorer prognosis. In addition, ERAS may promote transforming activity and chemoresistance in neuroblastoma patients (19).

In summary, expression analysis revealed a different pattern of RAS and RAS-signaling components in quiescent *versus* activated HSCs. Among different RAS family members, we identified *ERas*, *p110α*, and *p110γ* to be mainly expressed in quiescent HSCs and *MRas*, *RRas*, *Rap2A*, *RalA*, *p110β*, *p110δ*, *Yap*, *Ctgf*, and *Notch2* expressed in activated HSCs. Our data suggest an increased activity via PI3K-AKT-mTORC1 and HIPPO signaling in quiescent HSCs. Therefore, this study adds ERAS signaling to the remarkable features of quiescent HSCs, and the cellular outcome of these signaling pathways would maintain the quiescent state of HSCs via inhibition of proliferation (HIPPO pathways, G_0 arrest) and apoptosis (PI3K-PDK1 and mTORC2) (see Fig. 8). On the other hand, activated HSCs exhibit YAP-CTGF/NOTCH2 and RAS-RAF-MEK-ERK activity, which are both involved in HSC proliferation and development (Fig. 8). Finally, we would like to point out that our study is based on the *ex vivo* activation of HSCs, which is a known model for the *in vivo* activation process (13, 72). However, there may be some aspects that could be different in the *ex vivo* model

and the *in vivo* situation. Therefore, future studies should also address the ERAS networking in an *in vivo* model of liver injury.

Author Contributions—M. R. A. conceived and coordinated the study. M. R. A. and S. N. R. designed the study and wrote the paper. S. N. R., H. N., S. G., I. S., C. K., M. J. H., and M. F. designed, performed, and analyzed the experiments. All authors reviewed the results and approved the final version of the manuscript.

Acknowledgments—We are grateful to Ehsan Amin, Doreen M. Floss, Alexander Lang, Ilse Meyer, Jens M. Moll, Boris Görg, Kazem Nouri, Claudia Rupprecht, Madhurendra Singh, and Si-Cai Zhang for helpful advice and stimulating discussion.

References

1. Friedman, S. L. (2008) Hepatic stellate cells: protean, multifunctional, and enigmatic cells of the liver. *Physiol. Rev.* **88,** 125–172
2. Kordes, C., and Häussinger, D. (2013) Hepatic stem cell niches. *J. Clin. Invest.* **123,** 1874–1880
3. Yin, C., Evason, K. J., Asahina, K., and Stainier, D. Y. R. (2013) Hepatic stellate cells in liver development, regeneration, and cancer. *J. Clin. Invest.* **123,** 1902–1910
4. Kordes, C., Sawitza, I., Götze, S., and Häussinger, D. (2013) Hepatic stellate cells support hematopoiesis and are liver-resident mesenchymal stem cells. *Cell. Physiol. Biochem.* **31,** 290–304
5. Yang, L., Jung, Y., Omenetti, A., Witek, R. P., Choi, S., Vandongen, H. M., Huang, J., Alpini, G. D., and Diehl, A. M. (2008) Fate-mapping evidence that hepatic stellate cells are epithelial progenitors in adult mouse livers. *Stem Cells* **26,** 2104–2113
6. Kordes, C., Sawitza, I., Götze, S., Herebian, D., and Häussinger, D. (2014) Hepatic stellate cells contribute to progenitor cells and liver regeneration. *J. Clin. Invest.* **124,** 5503–5515
7. Reimann, T., Hempel, U., Krautwald, S., Axmann, A., Scheibe, R., Seidel, D., and Wenzel, K. W. (1997) Transforming growth factor-β1 induces activation of Ras, Raf-1, MEK and MAPK in rat hepatic stellate cells. *FEBS Lett.* **403,** 57–60
8. Carloni, V., Defranco, R. M., Caligiuri, A., Gentilini, A., Sciammetta, S. C., Baldi, E., Lottini, B., Gentilini, P., and Pinzani, M. (2002) Cell adhesion regulates platelet-derived growth factor-induced MAP kinase and PI-3 kinase activation in stellate cells. *Hepatology* **36,** 582–591
9. Kordes, C., Sawitza, I., and Häussinger, D. (2008) Canonical Wnt signaling maintains the quiescent stage of hepatic stellate cells. *Biochem. Biophys. Res. Commun.* **367,** 116–123
10. Lakner, A. M., Moore, C. C., Gulledge, A. A., and Schrum, L. W. (2010) Daily genetic profiling indicates JAK/STAT signaling promotes early hepatic stellate cell transdifferentiation. *World J. Gastroenterol.* **16,** 5047–5056
11. Xie, G., Karaca, G., Swiderska-Syn, M., Michelotti, G. A., Krüger, L., Chen, Y., Premont, R. T., Choi, S. S., and Diehl, A. M. (2013) Cross-talk between Notch and Hedgehog regulates hepatic stellate cell fate in mice. *Hepatology* **58,** 1801–1813
12. de Souza, I. C. C., Meira Martins, L. A., de Vasconcelos, M., de Oliveira, C. M., Barbé-Tuana, F., Andrade, C. B., Pettenuzzo, L. F., Borojevic, R., Margis, R., Guaragna, R., and Guma, F. C. R. (2015) Resveratrol regulates the quiescence-like induction of activated stellate cells by modulating the PPARγ/SIRT1 ratio. *J. Cell. Biochem.* **116,** 2304–2312
13. Mannaerts, I., Leite, S. B., Verhulst, S., Claerhout, S., Eysackers, N., Thoen, L. F. R., Hoorens, A., Reynaert, H., Halder, G., and van Grunsven, L. A. (2015) The Hippo pathway effector YAP controls mouse hepatic stellate cell activation. *J. Hepatol.* **63,** 679–688
14. Parola, M., Robino, G., Marra, F., Pinzani, M., Bellomo, G., Leonarduzzi, G., Chiarugi, P., Camandola, S., Poli, G., Waeg, G., Gentilini, P., and Dianzani, M. U. (1998) HNE interacts directly with JNK isoforms in human hepatic stellate cells. *J. Clin. Invest.* **102,** 1942–1950
15. Nakamura, K., Ichise, H., Nakao, K., Hatta, T., Otani, H., Sakagami, H., Kondo, H., and Katsuki, M. (2008) Partial functional overlap of the three ras genes in mouse embryonic development. *Oncogene* **27,** 2961–2968
16. Karnoub, A. E., and Weinberg, R. A. (2008) Ras oncogenes: split personalities. *Nat. Rev. Mol. Cell Biol.* **9,** 517–531
17. Tidyman, W. E., and Rauen, K. A. (2009) The RASopathies: developmental syndromes of Ras/MAPK pathway dysregulation. *Curr. Opin. Genet. Dev.* **19,** 230–236
18. Hennig, A., Markwart, R., Esparza-Franco, M. A., Ladds, G., and Rubio, I. (2015) Ras activation revisited: role of GEF and GAP systems. *Biol. Chem.* **396,** 831–848
19. Aoyama, M., Kataoka, H., Kubota, E., Tada, T., and Asai, K. (2010) Resistance to chemotherapeutic agents and promotion of transforming activity mediated by embryonic stem cell-expressed Ras (ERas) signal in neuroblastoma cells. *Int. J. Oncol.* **37,** 1011–1016
20. Kaizaki, R., Yashiro, M., Shinto, O., Yasuda, K., Matsuzaki, T., Sawada, T., and Hirakawa, K. (2009) Expression of ERas oncogene in gastric carcinoma. *Anticancer Res.* **29,** 2189–2193
21. Takahashi, K., Mitsui, K., and Yamanaka, S. (2003) Role of ERas in promoting tumour-like properties in mouse embryonic stem cells. *Nature* **423,** 541–545
22. Yasuda, K., Yashiro, M., Sawada, T., Ohira, M., and Hirakawa, K. (2007) ERas oncogene expression and epigenetic regulation by histone acetylation in human cancer cells. *Anticancer Res.* **27,** 4071–4075
23. Nakhaei-Rad, S., Nakhaeizadeh, H., Kordes, C., Cirstea, I. C., Schmick, M., Dvorsky, R., Bastiaens, P. I., Häussinger, D., and Ahmadian, M. R. (2015) The function of embryonic stem cell-expressed Ras (E-Ras), a unique Ras family member, correlates with its additional motifs and its structural properties. *J. Biol. Chem.* **290,** 15892–15903
24. Hendriks, H. F., Verhoofstad, W. A., Brouwer, A., de Leeuw, A. M., and Knook, D. L. (1985) Perisinusoidal fat-storing cells are the main vitamin A storage sites in rat liver. *Exp. Cell Res.* **160,** 138–149
25. Kordes, C., Sawitza, I., Müller-Marbach, A., Ale-Agha, N., Keitel, V., Klonowski-Stumpe, H., and Häussinger, D. (2007) CD133+ hepatic stellate cells are progenitor cells. *Biochem. Biophys. Res. Commun.* **352,** 410–417
26. Ahmadian, M. R., Stege, P., Scheffzek, K., and Wittinghofer, A. (1997) Confirmation of the arginine-finger hypothesis for the GAP-stimulated GTP-hydrolysis reaction of Ras. *Nat. Struct. Biol.* **4,** 686–689
27. Gremer, L., Merbitz-Zahradnik, T., Dvorsky, R., Cirstea, I. C., Kratz, C. P., Zenker, M., Wittinghofer, A., and Ahmadian, M. R. (2011) Germline KRAS mutations cause aberrant biochemical and physical properties leading to developmental disorders. *Hum. Mutat.* **32,** 33–43
28. Rothbauer, U., Zolghadr, K., Muyldermans, S., Schepers, A., Cardoso, M. C., and Leonhardt, H. (2008) A versatile nanotrap for biochemical and functional studies with fluorescent fusion proteins. *Mol. Cell. Proteomics* **7,** 282–289
29. Ahmadian, M. R., Hoffmann, U., Goody, R. S., and Wittinghofer, A. (1997) Individual rate constants for the interaction of Ras proteins with GTPase-activating proteins determined by fluorescence spectroscopy. *Biochemistry* **36,** 4535–4541
30. Taha, M. S., Nouri, K., Milroy, L. G., Moll, J. M., Herrmann, C., Brunsveld, L., Piekorz, R. P., and Ahmadian, M. R. (2014) Subcellular fractionation and localization studies reveal a direct interaction of the fragile X mental retardation protein (FMRP) with nucleolin. *PLoS One* **9,** e91465
31. Götze, S., Schumacher, E. C., Kordes, C., and Häussinger, D. (2015) Epigenetic changes during hepatic stellate cell activation. *PLoS One* **10,** e0128745
32. Li, L. C., and Dahiya, R. (2002) MethPrimer: designing primers for methylation PCRs. *Bioinformatics* **18,** 1427–1431
33. Leakey, T. I., Zielinski, J., Siegfried, R. N., Siegel, E. R., Fan, C. Y., and Cooney, C. A. (2008) A simple algorithm for quantifying DNA methylation levels on multiple independent CpG sites in bisulfite genomic sequencing electropherograms. *Nucleic Acids Res.* **36,** e64
34. Yu, Y., Liang, D., Tian, Q., Chen, X., Jiang, B., Chou, B.-K., Hu, P., Cheng, L., Gao, P., Li, J., and Wang, G. (2014) Stimulation of somatic cell reprogramming by ERas-Akt-FoxO1 signaling axis. *Stem Cells* **32,** 349–363
35. Ni, L., Li, S., Yu, J., Min, J., Brautigam, C. A., Tomchick, D. R., Pan, D., and Luo, X. (2013) Structural basis for autoactivation of human Mst2 kinase

and its regulation by RASSF5. *Structure* **21,** 1757–1768
36. Kim, J. B., and Spiegelman, B. M. (1996) ADD1/SREBP1 promotes adipocyte differentiation and gene expression linked to fatty acid metabolism. *Genes Dev.* **10,** 1096–1107
37. Kim, J. B., Wright, H. M., Wright, M., and Spiegelman, B. M. (1998) ADD1/SREBP1 activates PPARγ through the production of endogenous ligand. *Proc. Natl. Acad. Sci. U.S.A.* **95,** 4333–4337
38. Wang, R. C., Wei, Y., An, Z., Zou, Z., Xiao, G., Bhagat, G., White, M., Reichelt, J., and Levine, B. (2012) Akt-mediated regulation of autophagy and tumorigenesis through Beclin 1 phosphorylation. *Science* **338,** 956–959
39. Tzivion, G., Dobson, M., and Ramakrishnan, G. (2011) FoxO transcription factors: regulation by AKT and 14-3-3 proteins. *Biochim. Biophys. Acta* **1813,** 1938–1945
40. Prasad, S. B., Yadav, S. S., Das, M., Modi, A., Kumari, S., Pandey, L. K., Singh, S., Pradhan, S., and Narayan, G. (2015) PI3K/AKT pathway-mediated regulation of p27(Kip1) is associated with cell cycle arrest and apoptosis in cervical cancer. *Cell. Oncol.* **38,** 215–225
41. Chiang, G. G., and Abraham, R. T. (2005) Phosphorylation of mammalian target of rapamycin (mTOR) at Ser-2448 is mediated by p70S6 kinase. *J. Biol. Chem.* **280,** 25485–25490
42. Liu, P., Guo, J., Gan, W., and Wei, W. (2014) Dual phosphorylation of Sin1 at T86 and T398 negatively regulates mTORC2 complex integrity and activity. *Protein Cell* **5,** 171–177
43. Ma, X. M., Yoon, S. O., Richardson, C. J., Jülich, K., and Blenis, J. (2008) SKAR links pre-mRNA splicing to mTOR/S6K1-mediated enhanced translation efficiency of spliced mRNAs. *Cell* **133,** 303–313
44. Schirmacher, P., Geerts, A., Pietrangelo, A., Dienes, H. P., and Rogler, C. E. (1992) Hepatocyte growth factor/hepatopoietin A is expressed in fat-storing cells from rat liver but not myofibroblast-like cells derived from fat-storing cells. *Hepatology* **15,** 5–11
45. Maher, J. J. (1993) Cell-specific expression of hepatocyte growth factor in liver: up-regulation in sinusoidal endothelial cells after carbon tetrachloride. *J. Clin. Invest.* **91,** 2244–2252
46. Wang, X., DeFrances, M. C., Dai, Y., Pediaditakis, P., Johnson, C., Bell, A., Michalopoulos, G. K., and Zarnegar, R. (2002) A mechanism of cell survival: sequestration of Fas by the HGF receptor Met. *Mol. Cell* **9,** 411–421
47. Tomiya, T., Nishikawa, T., Inoue, Y., Ohtomo, N., Ikeda, H., Tejima, K., Watanabe, N., Tanoue, Y., Omata, M., and Fujiwara, K. (2007) Leucine stimulates HGF production by hepatic stellate cells through mTOR pathway. *Biochem. Biophys. Res. Commun.* **358,** 176–180
48. Porstmann, T., Santos, C. R., Griffiths, B., Cully, M., Wu, M., Leevers, S., Griffiths, J. R., Chung, Y. L., and Schulze, A. (2008) SREBP activity is regulated by mTORC1 and contributes to Akt-dependent cell growth. *Cell Metab.* **8,** 224–236
49. Kang, Q., and Chen, A. (2009) Curcumin inhibits srebp-2 expression in activated hepatic stellate cells *in vitro* by reducing the activity of specificity protein-1. *Endocrinology* **150,** 5384–5394
50. Kwon, Y.-W., Jang, S., Paek, J.-S., Lee, J.-W., Cho, H.-J., Yang, H.-M., and Kim, H.-S. (2015) E-Ras improves the efficiency of reprogramming by facilitating cell cycle progression through JNK–Sp1 pathway. *Stem Cell Res.* **15,** 481–494
51. Oh, W. J., and Jacinto, E. (2011) mTOR complex 2 signaling and functions. *Cell Cycle* **10,** 2305–2316
52. Huang, J., Wu, S., Wu, C. L., and Manning, B. D. (2009) Signaling events downstream of mammalian target of rapamycin complex 2 are attenuated in cells and tumors deficient for the tuberous sclerosis complex tumor suppressors. *Cancer Res.* **69,** 6107–6114
53. Wang, Y., Zhou, Y., and Graves, D. T. (2014) FOXO transcription factors: their clinical significance and regulation. *Biomed. Res. Int.* **2014,** 925350
54. Huang, K., and Fingar, D. C. (2014) Growing knowledge of the mTOR signaling network. *Semin. Cell Dev. Biol.* **36,** 79–90
55. Schroder, W. A., Buck, M., Cloonan, N., Hancock, J. F., Suhrbier, A., Sculley, T., and Bushell, G. (2007) Human Sin1 contains Ras-binding and pleckstrin homology domains and suppresses Ras signalling. *Cell. Signal.* **19,** 1279–1289
56. Stuhlmann-Laeisz, C., Lang, S., Chalaris, A., Krzysztof, P., Enge, S., Eichler, J., Klingmüller, U., Samuel, M., Ernst, M., Rose-John, S., and Scheller, J. (2006) Forced dimerization of gp130 leads to constitutive STAT3 activation, cytokine-independent growth, and blockade of differentiation of embryonic stem cells. *Mol. Biol. Cell* **17,** 2986–2995
57. Oh, H. M., Yu, C. R., Golestaneh, N., Amadi-Obi, A., Lee, Y. S., Eseonu, A., Mahdi, R. M., and Egwuagu, C. E. (2011) STAT3 protein promotes T-cell survival and inhibits interleukin-2 production through up-regulation of Class O Forkhead transcription factors. *J. Biol. Chem.* **286,** 30888–30897
58. Boccaccio, C., Andò, M., Tamagnone, L., Bardelli, A., Michieli, P., Battistini, C., and Comoglio, P. M. (1998) Induction of epithelial tubules by growth factor HGF depends on the STAT pathway. *Nature* **391,** 285–288
59. Hung, W., and Elliott, B. (2001) Co-operative effect of c-Src tyrosine kinase and Stat3 in activation of hepatocyte growth factor expression in mammary carcinoma cells. *J. Biol. Chem.* **276,** 12395–12403
60. Nakagawa, K., Takasawa, S., Nata, K., Yamauchi, A., Itaya-Hironaka, A., Ota, H., Yoshimoto, K., Sakuramoto-Tsuchida, S., Miyaoka, T., Takeda, M., Unno, M., and Okamoto, H. (2013) Prevention of Reg I-induced beta-cell apoptosis by IL-6/dexamethasone through activation of HGF gene regulation, *Biochim. Biophys. Acta* **1833,** 2988–2995
61. He, J., Gong, J., Ding, Q., Tan, Q., Han, P., Liu, J., Zhou, Z., Tu, W., Xia, Y., Yan, W., and Tian, D. (2015) Suppressive effect of SATB1 on hepatic stellate cell activation and liver fibrosis in rats. *FEBS Lett.* **589,** 1359–1368
62. Coll, M., El Taghdouini, A., Perea, L., Mannaerts, I., Vila-Casadesús, M., Blaya, D., Rodrigo-Torres, D., Affò, S., Morales-Ibanez, O., Graupera, I., Lozano, J. J., Najimi, M., Sokal, E., Lambrecht, J., Ginès, P., et al. (2015) Integrative miRNA and gene expression profiling analysis of human quiescent hepatic stellate cells. *Sci. Rep.* **5,** 11549
63. Mason, J. M., Morrison, D. J., Basson, M. A., and Licht, J. D. (2006) Sprouty proteins: multifaceted negative-feedback regulators of receptor tyrosine kinase signaling. *Trends Cell Biol.* **16,** 45–54
64. Vanhaesebroeck, B., Ali, K., Bilancio, A., Geering, B., and Foukas, L. C. (2005) Signalling by PI3K isoforms: insights from gene-targeted mice. *Trends Biochem. Sci.* **30,** 194–204
65. Kok, K., Geering, B., and Vanhaesebroeck, B. (2009) Regulation of phosphoinositide 3-kinase expression in health and disease. *Trends Biochem. Sci.* **34,** 115–127
66. Fritsch, R., de Krijger, I., Fritsch, K., George, R., Reason, B., Kumar, M. S., Diefenbacher, M., Stamp, G., and Downward, J. (2013) RAS and RHO families of GTPases directly regulate distinct phosphoinositide 3-kinase isoforms. *Cell* **153,** 1050–1063
67. Fritsch, R., and Downward, J. (2013) SnapShot: class I PI3K isoform signaling. *Cell* **154,** 940–940.e1
68. Baier, R., Bondeva, T., Klinger, R., Bondev, A., and Wetzker, R. (1999) Retinoic acid induces selective expression of phosphoinositide 3-kinase γ in myelomonocytic U937 cells. *Cell Growth Differ.* **10,** 447–456
69. Khadem, F., Gao, X., Mou, Z., Jia, P., Movassagh, H., Onyilagha, C., Gounni, A. S., Wright, M. C., and Uzonna, J. E. (2016) Hepatic stellate cells regulate liver immunity to visceral leishmaniasis through p110delta-dependent induction and expansion of Tregs in mice. *Hepatology* **63,** 620–632
70. Yashiro, M., Yasuda, K., Nishii, T., Kaizaki, R., Sawada, T., Ohira, M., and Hirakawa, K. (2009) Epigenetic regulation of the embryonic oncogene ERas in gastric cancer cells. *Int. J. Oncol.* **35,** 997–1003
71. Jiang, F., Parsons, C. J., and Stefanovic, B. (2006) Gene expression profile of quiescent and activated rat hepatic stellate cells implicates Wnt signaling pathway in activation. *J. Hepatol.* **45,** 401–409
72. De Minicis, S., Seki, E., Uchinami, H., Kluwe, J., Zhang, Y., Brenner, D. A., and Schwabe, R. F. (2007) Gene expression profiles during hepatic stellate cell activation in culture and *in vivo*. *Gastroenterology* **132,** 1937–1946
73. Bitencourt, S., Mesquita, F., Basso, B., Schmid, J., Ferreira, G., Rizzo, L., Bauer, M., Bartrons, R., Ventura, F., Rosa, J. L., Mannaerts, I., van Grunsven, L. A., and Oliveira, J. (2014) Capsaicin modulates proliferation, migration, and activation of hepatic stellate cells. *Cell Biochem. Biophys.* **68,** 387–396
74. Dong, S., Wu, C., Hu, J., Wang, Q., Chen, S., Zhirong, W., and Xiong, W. (2015) Wnt5a Promotes Cytokines Production and Cell Proliferation in Human Hepatic Stellate Cells Independent of Canonical Wnt Pathway. *Clin. Lab.* **61,** 537–547
75. Kinbara, K., Goldfinger, L. E., Hansen, M., Chou, F. L., and Ginsberg, M. H.

(2003) Ras GTPases: integrins' friends or foes? *Nat. Rev. Mol. Cell Biol.* **4,** 767–776
76. Sandri, C., Caccavari, F., Valdembri, D., Camillo, C., Veltel, S., Santambrogio, M., Lanzetti, L., Bussolino, F., Ivaska, J., and Serini, G. (2012) The R-Ras/RIN2/Rab5 complex controls endothelial cell adhesion and morphogenesis via active integrin endocytosis and Rac signaling. *Cell Res.* **22,** 1479–1501
77. Rodriguez-Viciana, P., Oses-Prieto, J., Burlingame, A., Fried, M., and McCormick, F. (2006) A phosphatase holoenzyme comprised of Shoc2/Sur8 and the catalytic subunit of PP1 functions as an M-Ras effector to modulate Raf activity. *Mol. Cell* **22,** 217–230
78. Torti, M., and Lapetina, E. G. (1994) Structure and function of rap proteins in human platelets. *Thromb. Haemost.* **71,** 533–543
79. Paganini, S., Guidetti, G. F., Catricalà, S., Trionfini, P., Panelli, S., Balduini, C., and Torti, M. (2006) Identification and biochemical characterization of Rap2C, a new member of the Rap family of small GTP-binding proteins. *Biochimie* **88,** 285–295
80. Wu, J.-X., Zhang, D.-G., Zheng, J.-N., and Pei, D.-S. (2015) Rap2a is a novel target gene of p53 and regulates cancer cell migration and invasion. *Cell. Signal.* **27,** 1198–1207
81. Saile, B., Matthes, N., El Armouche, H., Neubauer, K., and Ramadori, G. (2001) The bcl, NFκB and p53/p21WAF1 systems are involved in spontaneous apoptosis and in the anti-apoptotic effect of TGF-β or TNF-α on activated hepatic stellate cells. *Eur. J. Cell Biol.* **80,** 554–561
82. Soliman, E. M., Rodrigues, M. A., Gomes, D. A., Sheung, N., Yu, J., Amaya, M. J., Nathanson, M. H., and Dranoff, J. A. (2009) Intracellular calcium signals regulate growth of hepatic stellate cells via specific effects on cell cycle progression. *Cell Calcium* **45,** 284–292
83. Gu, X., Wang, Y., Xiang, J., Chen, Z., Wang, L., Lu, L., and Qian, S. (2013) Interferon-γ triggers hepatic stellate cell-mediated immune regulation through MEK/ERK signaling pathway. *Clin. Dev. Immunol.* 10.1155/2013/389807
84. Fukunaga, R., and Hunter, T. (1997) MNK1, a new MAP kinase-activated protein kinase, isolated by a novel expression screening method for identifying protein kinase substrates. *EMBO J.* **16,** 1921–1933
85. Pereira, A., Zhang, B., Malcolm, P., and Sundram, S. (2013) Clozapine regulation of p90RSK and c-Fos signaling via the ErbB1-ERK pathway is distinct from olanzapine and haloperidol in mouse cortex and striatum. *Prog. Neuropsychopharmacol. Biol. Psychiatry* **40,** 353–363
86. Iwamoto, H., Nakamuta, M., Tada, S., Sugimoto, R., Enjoji, M., and Nawata, H. (2000) Platelet-derived growth factor receptor tyrosine kinase inhibitor AG1295 attenuates rat hepatic stellate cell growth. *J. Lab. Clin. Med.* **135,** 406–412
87. Vavvas, D., Li, X., Avruch, J., and Zhang, X. F. (1998) Identification of Nore1 as a potential Ras effector. *J. Biol. Chem.* **273,** 5439–5442
88. van der Weyden, L., and Adams, D. J. (2007) The Ras-association domain family (RASSF) members and their role in human tumourigenesis. *Biochim. Biophys. Acta* **1776,** 58–85
89. Scheel, H., and Hofmann, K. (2003) A novel interaction motif, SARAH, connects three classes of tumor suppressor. *Curr. Biol.* **13,** R899–R900
90. Ramos, A., and Camargo, F. D. (2012) The Hippo signaling pathway and stem cell biology. *Trends Cell Biol.* **22,** 339–346
91. Rawat, S. J., and Chernoff, J. (2015) Regulation of mammalian Ste20 (Mst) kinases. *Trends Biochem. Sci.* **40,** 149–156
92. Camargo, F. D., Gokhale, S., Johnnidis, J. B., Fu, D., Bell, G. W., Jaenisch, R., and Brummelkamp, T. R. (2007) YAP1 increases organ size and expands undifferentiated progenitor cells. *Curr. Biol.* **17,** 2054–2060
93. Avruch, J., Zhou, D., Fitamant, J., and Bardeesy, N. (2011) Mst1/2 signalling to Yap: gatekeeper for liver size and tumour development. *Br. J. Cancer* **104,** 24–32
94. Lu, L., Li, Y., Kim, S. M., Bossuyt, W., Liu, P., Qiu, Q., Wang, Y., Halder, G., Finegold, M. J., Lee, J. S., and Johnson, R. L. (2010) Hippo signaling is a potent *in vivo* growth and tumor suppressor pathway in the mammalian liver. *Proc. Natl. Acad. Sci. U.S.A.* **107,** 1437–1442
95. Yimlamai, D., Christodoulou, C., Galli, G. G., Yanger, K., Pepe-Mooney, B., Gurung, B., Shrestha, K., Cahan, P., Stanger, B. Z., and Camargo, F. D. (2014) Hippo pathway activity influences liver cell fate. *Cell* **157,** 1324–1338
96. Saxena, N. K., Titus, M. A., Ding, X., Floyd, J., Srinivasan, S., Sitaraman, S. V., and Anania, F. A. (2004) Leptin as a novel profibrogenic cytokine in hepatic stellate cells: mitogenesis and inhibition of apoptosis mediated by extracellular regulated kinase (Erk) and Akt phosphorylation. *FASEB J.* **18,** 1612–1614
97. Chiang, J., and Martinez-Agosto, J. A. (2012) Effects of mTOR inhibitors on components of the Salvador-Warts-Hippo pathway. *Cells* **1,** 886–904

Supplementary Information

The role of embryonic stem cell-expressed RAS (ERAS) in the maintenance of quiescent hepatic stellate cells *

Saeideh Nakhaei-Rad[1], Hossein Nakhaeizadeh[1], Silke Götze[2], Claus Kordes[2], Iris Sawitza[2], Michèle J Hoffmann[3], Manuel Franke[1], Wolfgang A. Schultz[3], Jürgen Scheller[1], Roland P. Piekorz[1], Dieter Häussinger[2], Mohammad R. Ahmadian[1@]

[1]Institute of Biochemistry and Molecular Biology II, Medical Faculty, Heinrich-Heine University, Düsseldorf, Germany; [2]Clinic of Gastroenterology, Hepatology and Infectious Diseases, Heinrich-Heine University, Düsseldorf, Germany; [3]Department of Urology, Medical Faculty, Heinrich Heine University Düsseldorf, Düsseldorf, Germany

Supplementary TABLE S1. Primer sequences (5´ to 3´) for qPCR using the SYBR Green system obtained from PrimerBank (http://pga.mgh.harvard.edu/primerbank) and modified to match with rat sequences.

Genes	Forward primers	Reverse primers
ARAF	CCTCCTGCTAGTGGGGCT	GAGTCATAGACACTCATGCCATCC
BRAF	TTTCCTGGCTTACTGGAGAGG	GAAGTTGTGGGTTGTCAGAGG
CRAF	GATGGCAAACTCACGGATTCTT	TGCAAGCTCATCCCATTCCG
CTGF	GACCCAACTATGATGCGAGCC	CCCATCCCACAGGTCTTAGAAC
ERAS	CCTTGCCAACAAAGTCTAGCATC	GCCAGCATCTTTGCATTGTGC
ERK1	ACCACATTCTAGGTATACTGGGT	AGTTTCGGGCCTTCATGTTAAT
ERK2	GGTTGTTCCCAAACGCTGACT	CAACTTCAATCCTCTTGTGAGGG
HPRT1	AAGTGTTGGATACAGGCCAGA	GGCTTTGTACTTGGCTTTTCC
HRAS	CGTGAGATTCGGCAGCATAAA	GACAGCACACACTTGCAGCT
KRAS	CAAGAGTGCCTTGACGATACA	CCAAGAGACAGGTTTCTCCATC
MEK1	AATGGTGGAGTGGTGTTCAAG	CGGATTGCGGGTTTGATCTC
MEK2	GTTACCGGCACTCACCATCAAC	CCTCCAGCCGCTTCCTCTG
MRAS	TGTTCCCAGTGACAACCTTCCC	GGGTCGTAGTCAGGCACGAA
MST1	CAGTGATAGGGACACCGTTTTG	GGGCTTTCCTTCAGCCATTTC
MST2	CCGGCGCCCAAGAGTAAG	GCAACAACTTGACCAGATTCCT
NOTCH2	GAGAAGAACCGCTGTCAGAATGG	GGTCGAGTATTGGCAGTCCTC
NRAS	ACTGAGTACAAACTGGTGGTGG	TCGGTAAGAATCCTCTATGGTGG
PIK3CA p110α	CCACGACCATCTTCGGGTG	ACGGAGGCATTCTAAAGTCACT
PIK3CA p110β	CTATGGCAGACACCCTTGACAT	CTTCCCGGGGTACTTCCAACT
PIK3CA p110γ	CACTGGAGTCACCGGCTAC	GACACTGTGAAAACGCTCTCG
PIK3CA p110δ	GTAAACGACTTCCGCACTAAGA	GCTGACATGCAATAAGCCA
RALA	AGGAAGACTACGCTGCAATTAGA	GTAGCTGCAAAGGACTCCATC
RALB	AGCCCTGACGCTCCAGTTC	GGCTGTGTCCAGGATGTCTATCT
RAP1A	ATGCGTGAGTACAAGCTAGTG	AATCTACTTCGACTTGCTTTCTGT
RAP2A	ATGCGCGAGTACAAAGTGGT	GCGACGAGTCCACCTCGAT
RHEB	AAGTCCCGGAAGATCGCCA	GGTTGGATCGTAGGAATCAACAA
RRAS	GACCCCACCATTGAGGATTCC	CTGTCGTTAATGGCAAACACCA
TC21	TGTGACGGACTATGATCCAACC	ACTGCTCTCTCATGGCTCCAA
YAP	TGAGATCCCTGATGATGTACCAT	ATGTTGTTGTCTGATCATTGTGATT

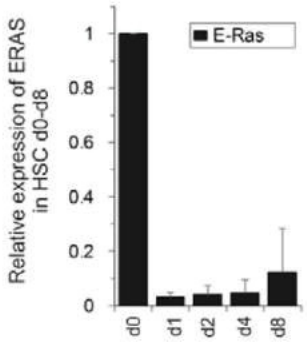

Supplementary FIGURE S1. *ERAS* re-expression in culture-activated hepatic stellate cells. *Ex-vivo* cultivation of HSCs resulted in a strong decrease in *ERAS* expression.

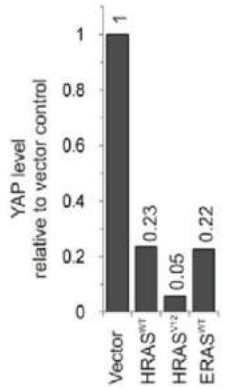

Supplementary FIGURE S2. ERAS and HRAS overexpression led to an overall reduction of the YAP protein. Densitometric quantification (ImageJ software) of YAP immunoblots (Fig. 6B) showed that ERAS expression resulted in a significant reduction of the YAP protein level in the same extend as observed for wild-type HRAS.

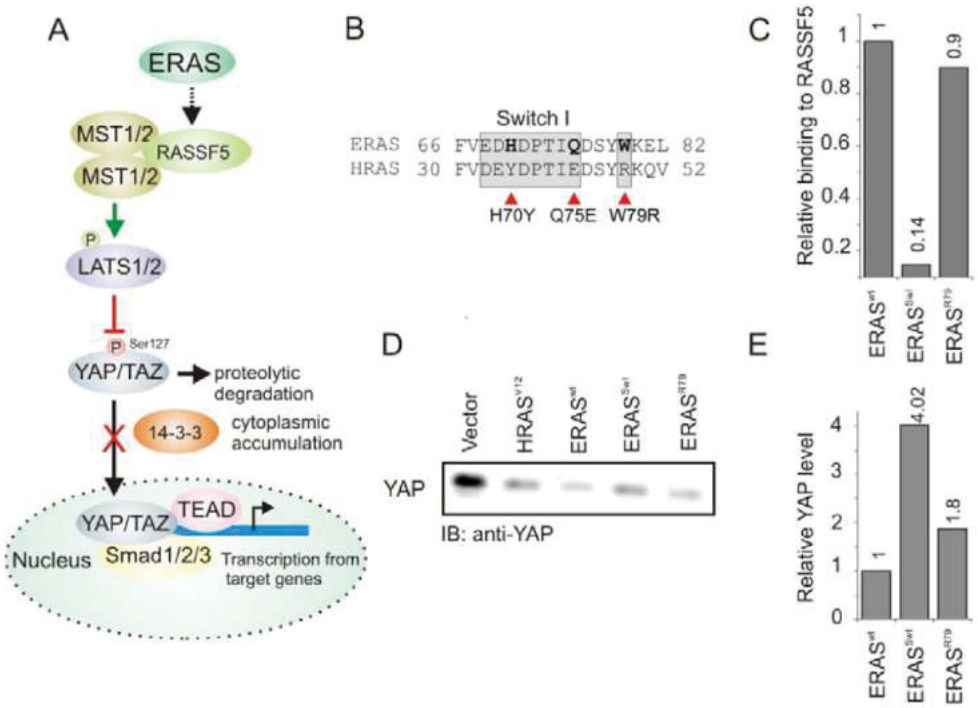

Supplementary FIGURE S3. ERAS-mediated activation of the HIPPO pathway may be mediated by its physical interaction with RASSF5. (A) Schematic view of the ERAS-RASSF5-MST1/2-LATS1/2-YAP pathway. (B) Sequence deviations and generated mutations (arrow heads) in the switch 1 and the interswitch regions of ERAS and HRAS. (C) Densitometric evaluations (ImageJ software) of the pull-down experiment of the $ERAS^{wt}$, $ERAS^{SwI}$ and $ERAS^{R79}$ by the RAS association domain of RASSF5 (Fig. 6A) revealed that the mutations in ERAS switch I region affects its interaction with RASSF5. (D) Overexpression of the ERAS and the HRAS variants in COS-7 cells differentially affect YAP degradation. (E) Densitometric evaluations (ImageJ software) of YAP immunoblot (Fig. S3D) revealed the weaker impact of the switch 1 mutations on the YAP protein degradation where more YAP protein (i.e., less HIPPO activity) was observed.

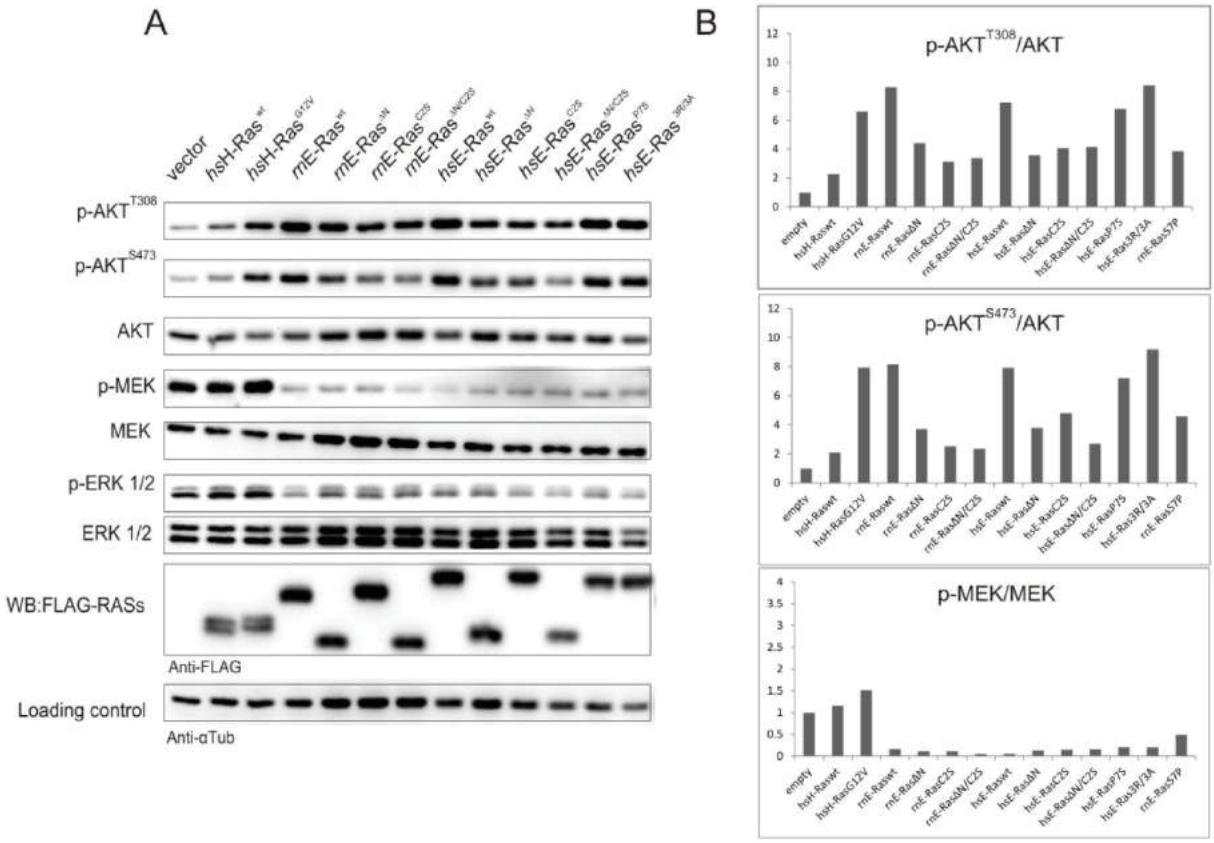

Supplementary FIGURE S4. Comparison of the signaling activity of human and rat ERAS variants. Immunoblot analysis of total cell lysates were derived from transfected COS-7 cells with FLAG-tagged human and rat ERAS variants, $HRAS^{WT}$ and $HRAS^{Val12}$. Total cell lysates were analyzed for the phosphorylation level of AKT (p-AKTT^{308} and p-AKT^{S473}), MEK1/2 (p-MEK1/2) and ERK1/2 (p-ERK1/2). Total amounts of AKT, MEK1/2, and ERK1/2 were applied as loading controls. (B) Densitometry analysis (ImageJ software) revealed that N-terminal truncated and palmitoylation-dead variants of rat and human ERAS showed lower levels of p-AKT^{T308} and p-AKT^{S473}.

Chapter VI

Galectin-1 dimers can scaffold Raf-effectors to increase H-ras nanoclustering

Graphical Abstract

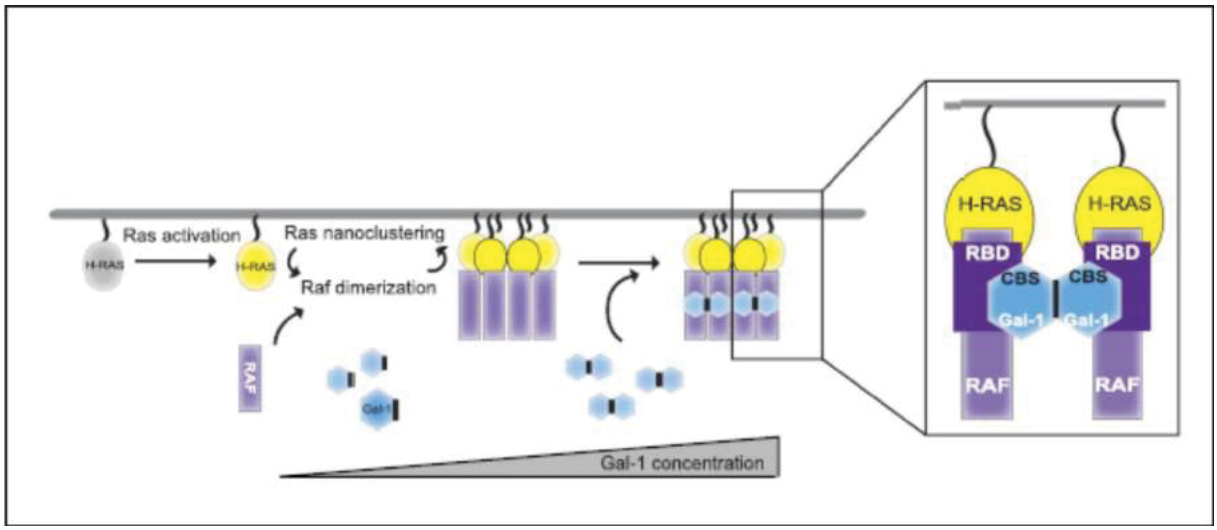

Status: Published in Sci Rep. 2016 Apr 18;6:24165. doi: 10.1038/srep24165
Impact Factor: 5.22
Own Proportion to this work: 10%
Protein purification
Pull-down assay
Immunoblotting

www.nature.com/scientificreports

SCIENTIFIC REPORTS

OPEN

Galectin-1 dimers can scaffold Raf-effectors to increase H-ras nanoclustering

Received: 29 May 2015
Accepted: 22 March 2016
Published: 18 April 2016

Olga Blaževitš[1,*], Yonatan G. Mideksa[1,*], Maja Šolman[1], Alessio Ligabue[1], Nicholas Ariotti[2], Hossein Nakhaeizadeh[3], Eyad K. Fansa[4], Anastassios C. Papageorgiou[1], Alfred Wittinghofer[4], Mohammad R. Ahmadian[3] & Daniel Abankwa[1]

Galectin-1 (Gal-1) dimers crosslink carbohydrates on cell surface receptors. Carbohydrate-derived inhibitors have been developed for cancer treatment. Intracellularly, Gal-1 was suggested to interact with the farnesylated C-terminus of Ras thus specifically stabilizing GTP-H-ras nanoscale signalling hubs in the membrane, termed nanoclusters. The latter activity may present an alternative mechanism for how overexpressed Gal-1 stimulates tumourigenesis. Here we revise the current model for the interaction of Gal-1 with H-ras. We show that it indirectly forms a complex with GTP-H-ras via a high-affinity interaction with the Ras binding domain (RBD) of Ras effectors. A computationally generated model of the Gal-1/C-Raf-RBD complex is validated by mutational analysis. Both cellular FRET as well as proximity ligation assay experiments confirm interaction of Gal-1 with Raf proteins in mammalian cells. Consistently, interference with H-rasG12V-effector interactions basically abolishes H-ras nanoclustering. In addition, an intact dimer interface of Gal-1 is required for it to positively regulate H-rasG12V nanoclustering, but negatively K-rasG12V nanoclustering. Our findings suggest stacked dimers of H-ras, Raf and Gal-1 as building blocks of GTP-H-ras-nanocluster at high Gal-1 levels. Based on our results the Gal-1/effector interface represents a potential drug target site in diseases with aberrant Ras signalling.

The small GTPase Ras is a major signal transducer, which relays mitogenic signals across the membrane into the cell. Its central role during cell proliferation and differentiation is underscored by the high frequency of Ras mutations in cancer[1]. GTP-loaded Ras adopts different conformations, enabling it to interact with downstream effector proteins, such as the Raf kinases. The three Ras isoforms, H-, N- and K-ras, are frequently mutated on codons 12, 13 and 61 in cancer[1]. These mutations render Ras insensitive to GTPase activating protein (GAP) mediated GTP hydrolysis. As a result, Ras is left constitutively GTP-bound and therefore active, as Ras itself is a poor GTPase[2]. Two splice isoforms of K-ras4A and K-ras4B, are both expressed in cancer[3]. However, historically, K-ras4B (hereafter K-ras) has received most attention. While K-ras is considered the most significant Ras isoform, due to its association with many aggressive cancers, recent insight into the origin of cancer cells warrants further investigation of the specific functions of all three Ras isoforms[4].

Ras proteins are highly similar in sequence and vary mostly in their C-terminal hypervariable region (hvr). This part undergoes post-translational farnesylation and palmitoylation (the latter for H- and N-ras) allowing Ras to dynamically insert into cellular membranes[5]. Ras is actively transported to the plasma membrane, where it is further organised into nanoscale signalling hubs, called nanoclusters. A Ras nanocluster comprises 6–8 Ras proteins, which in the case of the active Ras becomes transiently immobilized[6–8]. Nanoclusters are the exclusive sites of effector recruitment thus constituting highly dynamic epicentres of the Ras signalling cascade[9,10]. Nanoclustering is driven by the C-terminal membrane anchor of Ras, which also largely dictates their lateral segregation into isoform specific nanoclusters[11,12]. Importantly, these features are shared with Ras dimers, which appear to constitute the smallest 'nanocluster'[13]. Thus laterally segregated, Ras isoform specific nanoscale

[1]Turku Centre for Biotechnology, Åbo Akademi University, Tykistökatu 6B, 20520 Turku, Finland. [2]Institute for Molecular Bioscience, The University of Queensland, St. Lucia, QLD 4072, Australia. [3]Institute of Biochemistry and Molecular Biology II, Medical Faculty, Heinrich-Heine-University, Düsseldorf, Germany. [4]Max Planck Institute for Molecular Physiology, 44227 Dortmund, Germany. *These authors contributed equally to this work. Correspondence and requests for materials should be addressed to D.A. (email: daniel.abankwa@btk.fi)

oligomeric clusters constitute an important experimental observable that correlates with the structural and functional divergence of the different Ras proteins and the emergence of Ras signalling complexes.

Only very few endogenous regulators of Ras nanoclustering, so called nanocluster scaffolds, are known. These include galectin-3[14], nucleophosmin[15], caveolae[16] and GTP-H-ras[17] for K-ras, and galectin-1 (Gal-1)[9,10,18] for GTP-H-ras. Amongst these, Gal-1 is the best-characterised nanocluster scaffold. Gal-1 is a prototypic member of the family of β-galactoside binding lectins (galectins), of which there are 15 in humans[19]. Galectins are small (*ca.* 15 kDa for a prototypical single carbohydrate binding monomer) proteins formed by two antiparallel β-sheets. The carbohydrate is coordinated by the highly conserved carbohydrate binding site[20]. Gal-1 localizes to the cytoplasm and nucleus and is also secreted by an unknown pathway[21]. Due to oxidation of free cysteines in the protein, secreted Gal-1 loses lectin-binding activity, unless it binds as a dimer to glycoconjugates on the outside of the cell[22,23].

Gal-1 is upregulated in many tumours and associated with more progressive and invasive cancer stages[24,25], as well as radio-[26] and drug-resistance[27,28]. A number of inhibitors against galectins are under development, which are typically competitors of the natural carbohydrate ligands[29–32].

The current model for the nanocluster scaffolding activity of Gal-1 suggests that it directly binds to the C-terminal farnesyl of active H-ras to modulate its intracellular membrane organisation[33,34]. Augmented nanoclustering then increases effector recruitment thus potentiating MAPK signalling output[9,35,36]. Importantly, the Gal-1/GTP-H-ras interaction is suggested to be the target of the anti-Ras drug Salirasib (developed as farnesylthiosalicylic acid, FTS), which is currently assessed preclinically and in clinical trials for the treatment of cancer[37].

Förster Resonance Energy Transfer (FRET) was amongst the first methods to be used to study the nanoscale membrane organisation of proteins in the intact cell[13]. In FRET a donor fluorophore transfers part of its energy to an acceptor fluorophore, when they are as close as <10 nm, such as in nanoclusters. In addition, FRET is frequently used to measure protein-protein interactions and conformational changes[38]. In particular fluorescence lifetime imaging microscopy (FLIM) allows the fast and precise quantitation of FRET[39]. In FLIM-FRET, FRET is observed by the decrease of the donor fluorescence lifetime.

Using a wide spectrum of quantitative *in vitro* and cellular assays as well as computational modelling we show here that Gal-1 does not directly bind to H-ras, but instead to the Ras binding domain (RBD) of Ras effectors, such as Raf. This explains how Gal-1 specifically recognizes active (GTP-)Ras. We furthermore show that while Gal-1 positively regulates GTP-H-ras nanoclustering, it has the opposite effect on GTP-K-ras and both of these activities depend on its intact dimer interface. We present an entirely revised model of the mechanism of action of Gal-1 as a nanocluster scaffold and briefly discuss implications for Gal-1 and Ras drug development.

Results

Galectin-1 does not directly bind to H-ras. Galectin-1 (Gal-1) specifically stabilizes nanoclusters of active (GTP-)H-ras, thus augmenting H-ras signalling output[10,36]. According to the current model, Gal-1 interacts directly with the farnesyl-moiety of Ras in a way analogous to the binding of RhoGDI to the geranylgeranyl-moiety of Rho proteins[33]. Gal-1 should therefore effectively function as a chaperone that solubilizes farnesylated proteins and by a structurally unknown mechanism also as a nanocluster scaffold. The stage II (ClinicalTrials.gov identifier NCT00531401) drug farnesylthiosalicylic acid (Salirasib) is a farnesyl-derivative, which was undergoing clinical trials for lung cancer treatment[40]. It was initially found to disrupt the H-ras/Gal-1-interaction in biochemical experiments[35]. It is therefore of high translational relevance to understand this interaction in molecular-mechanistic detail.

In cellular FRET experiments we observed that H-ras and Gal-1 are in a complex in the cytoplasm, even after farnesylation of Ras is blocked by statin treatment or mutation of the cysteine in the C-terminal CAAX-box of Ras that normally undergoes farnesylation (Supplementary Fig. 1A,B). Likewise, the recently described mutation K28T (K29T according to our numbering) on Gal-1, which was shown to block farnesyl-recognition[41], did not abolish FRET between H-rasG12V and Gal-1 (Supplementary Fig. 1B). These observations were at variance with the previously proposed farnesyl-dependent interaction model by Rotblat *et al.*[33].

In an effort to explain this contradictory observation, we scrutinized the structural basis of the specific Gal-1/H-ras interaction. We first studied their complex formation in solution outside of the membrane. In order to test whether Gal-1 could indeed bind farnesylated Ras-proteins, we employed a fluorescence polarization binding assay that was recently used to demonstrate the ability of the Ras trafficking chaperone PDEδ to solubilize farnesylated proteins[42]. Incubation of a fluorescently labelled peptide derived from the Ras-family protein Rheb with increasing concentrations of PDEδ increased the polarization signal, in agreement with binding of the rotationally highly mobile peptide to the relatively immobile PDEδ protein (Fig. 1A). By contrast, no change in polarization was observed, if the peptide was incubated with purified Gal-1 at concentrations up to 50 μM (Fig. 1B), confirming very recently published results[43].

Gal-1 specifically recognizes active H-ras and should therefore in addition to the farnesylated C-terminal hypervariable region (hvr) of Ras also recognize its G-domain[35]. We therefore next investigated whether Gal-1 directly binds to this major part of H-ras. Following the N-terminal labelling rational from cellular FRET-experiments[12], we produced H-ras and Gal-1 proteins with an N-terminal acyl carrier protein (ACP)-tag, A1[44], that is amenable to specific fluorescent labelling[45] (Supplementary Fig. 1C). Both the purified His-A1-tagged Gal-1, as well as the final processed A1-tagged Gal-1, retained their lectin-binding ability in a hemagglutination assay (Supplementary Fig. 1D). As expected, we found a significant increase in FRET upon incubation of ATTO-488-labelled GTPγS-H-ras with the DY-547-labelled Ras Binding Domain (hereafter RBD) of the Ras effector C-Raf, which is known to bind to Ras and here served as a positive control. By contrast, incubation with Gal-1 under the same conditions did not show any increase in FRET, as compared to control samples of GDP-H-ras with the C-Raf-RBD or Gal-1, or of fluorophore-only controls (Fig. 1C).

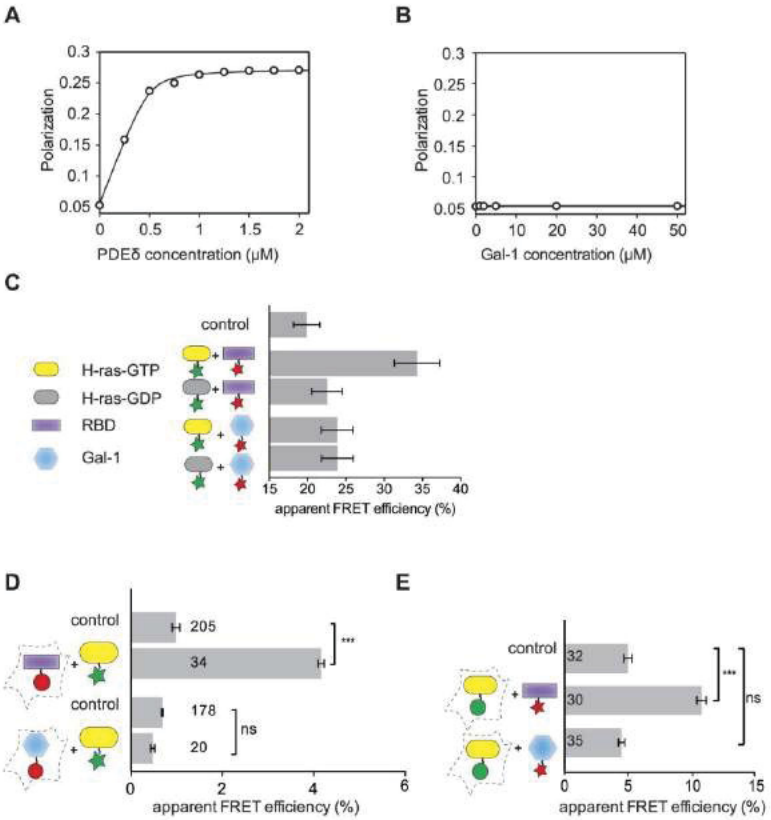

Figure 1. Galectin-1 neither binds to a farnesylated Ras-peptide nor to H-ras in solution experiments. (**A,B**) Fluorescence polarization binding assay of 0.25 μM fluorescein labelled and farnesylated Rheb peptide titrated with increasing concentrations of (**A**) the farnesyl-binding protein PDEδ or (**B**) purified Gal-1. (**C**) Sensitized acceptor FRET binding experiment of 250 nM H-ras and 250 nM Gal-1 or 250 nM C-Raf–RBD (RBD) fluorescently labelled using the ACP-tag technology. The legend to the left shows interaction partners schematically. H-ras was either GTPγS (GTP) or GDP loaded, as indicated. Fluorescent labelling substrates, coenzyme A (CoA)-linked ATTO-488 as a FRET-donor and DY-547 as FRET-acceptor, are represented by green and red stars, respectively. Control sample was a 1:1 mix of fluorescent labelling substrates each at 100 nM. Error bars indicate measurement error. (**D,E**) Interaction between H-ras and Gal-1 or the C-Raf-RBD (RBD) as indicated by the legend in (**C**) was determined by FLIM-FRET. Purified proteins as in (**C**) were incubated with fluorescent protein tagged proteins derived from BHK21 cell lysates (indicated with dotted cell outline). (**D**) Proteins from cell lysates were mRFP-tagged (red circle). (**E**) H-rasG12V labelled with mGFP (green circle) from lysates was used. Control is either mRFP-tagged C-Raf-RBD (upper column) or Gal-1 (lower column) incubated with 1 μM of CoA-488 in (**D**) and mGFP-H-rasG12V incubated with 1 μM of CoA-547 label in (**E**). (**C–E**) Binding of GTP-H-ras and the C-Raf-RBD served as a positive control. (**D,E**) Plotted values correspond to the mean ± SEM from three independent biological repeats. Numbers inside or above the bars indicate total number of imaged regions. The Methods section describes indicated statistical comparisons (ns, non-significant; ***$p < 0.001$).

In order to rule out that any missing stable posttranslational modification on either protein or other stable unknown cellular components prevented the GTP-H-ras/Gal-1 interaction, we performed FRET-experiments with A1-tagged purified proteins that were fluorescently labelled and fluorescent-protein tagged proteins obtained from crude mammalian cell lysates. While purified A1-labelled GTPγS-H-ras showed high FRET with lysates from BHK21 cells expressing mRFP-labelled C-Raf-RBD, no FRET was observed with mRFP-Gal-1 lysates (Fig. 1D). Note that the mRFP-tag did not abolish the ability of wt Gal-1 to bind to its ligand lactose (Supplementary Fig. 1E). Binding was only abolished once mutation N47D,W69L[46,47] was in addition introduced, which inactivates the carbohydrate binding site (Supplementary Fig. 1E). In the inverse FRET situation, predominantly GTP-loaded mGFP-H-rasG12V from cell lysates showed significantly increased FRET with

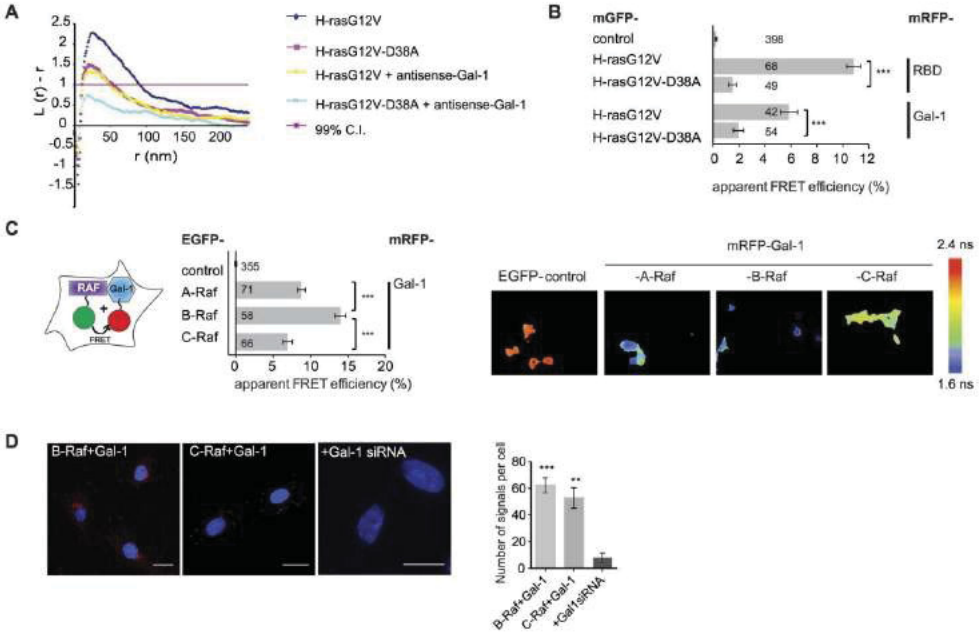

Figure 2. H-rasG12V nanoclustering largely depends on effector interactions, while Gal-1 interacts with Raf-effectors. (**A**) Electron microscopic nanoclustering analysis of mGFP-H-rasG12V and mGFP-H-rasG12V-D38A with or without antisense-mediated knockdown of Gal-1 in BHK21 cells. Normalized univariate K-functions, where maximal $L(r)$-r values above the 99% CI for complete spatial randomness indicate clustering at that value of r (number of membrane sheets analysed per condition, $n \geq 10$). (**B**) Complexation between indicated mGFP-tagged H-ras mutants and mRFP-tagged C-Raf-RBD or Gal-1 was determined using FLIM-FRET in HEK293-EBNA cells transiently expressing above constructs (two independent biological repeats). (**C**) Complexation between indicated EGFP-tagged full-length Raf proteins and mRFP-tagged Gal-1 measured by FLIM-FRET in HEK293-EBNA cells (three independent biological repeats). Examples of FLIM-FRET images of cells, coexpressing indicated FRET-pairs or EGFP-tagged C-Raf-RBD as donor-only control. Image colour look-up table on the right shows fluorescence lifetimes. (**B,C**) Plotted values correspond to the mean ± SEM. Numbers inside and above the bars indicate total number of cells imaged. The Methods section describes the indicated statistical comparisons (***$p < 0.001$). Samples with coexpressed fluorescent proteins mGFP and mRFP (**B**), or EGFP and mRFP (**C**) served as FRET controls. Note that non-control sample FRET-values were all significantly different from the (FRET-)control sample. (**D**) Analysis of the interaction between endogenous Raf isoforms and Gal-1 in BHK21 cells using *in situ* proximity ligation assay (PLA). Representative confocal microscopy images of indicated proteins are shown. The sample with siRNA-mediated Gal-1 depletion served as a negative control. Cell nuclei were stained with DAPI. Red foci indicate positive signals for protein interactions and their quantification is shown in the graph. Scale bar is 21 μm.

DY-547-labeled C-Raf-RBD, while the identically labelled Gal-1 did not show any FRET above background (Fig. 1E). Here, we observed a higher background FRET signal, due to the CoA-547 label, as demonstrated in control experiments (Supplementary Fig. 1F).

In conclusion, these experiments did not support the direct binding of Gal-1 to farnesylated Ras-peptides or active H-ras, thus confirming our initial observations. Hence an alternative model to the one describing a direct, farnesyl-dependent GTP-H-ras/Gal-1 interaction was required.

Galectin-1 indirectly interacts with active H-ras via the RBD of Ras effectors. When studying nanoclustering of H-rasG12V mutants, we serendipitously found that the effector-site mutation D38A[48] reduced nanoclustering to a similar extent as knockdown of Gal-1, and a complete loss of nanoclustering was observed when knockdown and mutation were combined (Fig. 2A). We therefore tested, whether residue D38A, which is at the centre of the Ras/RBD interface[48], affects the FRET between mRFP-Gal-1 and mGFP-H-rasG12V in HEK293-EBNA cells. Indeed, the Ras effector-site mutation did not only abrogate FRET between H-rasG12V and the C-Raf-RBD, but also of H-rasG12V and Gal-1 (Fig. 2B). Note that FRET-levels were significantly lower than those of the non-farnesylatable CAAX-mutant (Supplementary Fig. 1B), supporting that farnesylation was not required for an interaction with either the RBD or Gal-1 in cells, while an intact effector-site on H-ras was

required. These data therefore indicated that GTP-H-ras/Gal-1 complex formation depends on binding of an effector to H-ras and may therefore proceed indirectly.

Gal-1 overexpression was previously shown to increase and prolong EGF-stimulated signalling output of Raf, while apparently suppressing that of PI3K, the other major Ras effector[36]. We therefore tested, whether Gal-1 forms FRET-competent complexes with the Raf kinases (Supplementary Fig. 2A), which could bridge the interaction to active Ras. We coexpressed EGFP-tagged Raf paralogs and mRFP-tagged Gal-1 and monitored their interaction in HEK293-EBNA cells grown under normal serum levels using FRET. As compared to the H-rasG12V interaction with Gal-1 (Fig. 2B), all Raf paralogs showed similar FRET with Gal-1, with B-Raf displaying the highest FRET (Fig. 2C). Moreover, Proximity Ligation Assay (PLA) in BHK21 cells confirmed interaction of endogenous Gal-1 with B- and C-Raf (Fig. 2D).

In agreement with a significant requirement of Raf-proteins for mediating Gal-1 induced H-rasG12V-nanoclustering, knockdown of B-Raf abolished the Gal-1 induced increase in FRET (Supplementary Fig. 2B), indicating a significant role of B-Raf in H-rasG12V nanoclustering. Interestingly, knockdown of A-Raf significantly decreased nanoclustering of H-rasG12V in the presence of Gal-1 below control levels (Supplementary Fig. 2B). These data may suggest an important role for A-Raf in independently scaffolding GTP-H-ras nanocluster or preventing a negative effect on these nanocluster in the presence of Gal-1.

Next, we wanted to identify the minimal domain of Raf that mediates the interaction with Gal-1. The D38A mutation reduces the affinity of GTP-H-ras to the C-Raf-RBD by approximately 100-fold to 1300 nM, thus basically abrogating their interaction[48]. Based on our observations that this mutation also blocks H-rasG12V complexation with Gal-1 (Fig. 2B), we reasoned that RBD containing Raf-fragments would bind to Gal-1. Indeed, both the C-Raf-RBD and the same extended by the cysteine rich domain (CRD) showed identically high FRET with Gal-1 when expressed in BHK21 cells (Fig. 3A). Moreover, the structurally related RBD from PI3Kα showed FRET with Gal-1, albeit significantly less than the C-Raf-RBD (Fig. 3A, Supplementary Fig. 3B), suggesting that Gal-1 directly interacts with the Ras binding domain of effectors. In order to confirm these FRET results, we performed co-immunoprecipitation experiments, which showed that GST-labelled RBD-fragments were able to pull-down bacterially purified Gal-1 (Fig. 3B) or *vice versa* (Supplementary Fig. 2D). Finally, we provided evidence for direct binding of Gal-1 to the RBD. We purified Gal-1 and the C-Raf-RBD, both with N-terminal A1-tags in order to label them fluorescently for FRET-based binding experiments (Fig. 3C). Analysis of our FRET-binding data established a dissociation constant for Gal-1/C-Raf-RBD of $K_d = 106 \pm 40$ nM.

In conclusion, our results demonstrate that Gal-1 binds directly and with submicromolar affinity to the Ras-binding domain of effectors. This binding mode finally explains how Gal-1 selectively recognizes active Ras, namely by co-recruitment with effectors to active Ras.

Loss of galectin-1 binding by mutating D117 in the RBD provides tentative support for a computational model of the galectin-1/RBD complex. In order to have an experimentally testable model of the complex between Gal-1 and the C-Raf-RBD, we conducted computational docking using the existing crystal structural data of Gal-1 and the C-Raf-RBD (Fig. 4A).

The Global RAnge Molecular Matching (GRAMM) methodology, validated on the docking benchmark set and through the Critical Assessment of PRedicted Interactions blind prediction challenge (CAPRI), was employed to build 20 Gal-1 (carbohydrate ligand-bound and -unbound) complexes with the C-Raf-RBD that were ranked highest amongst 1000 docking poses. The software ranks poses by energy minimization and taking the clustering in same local energy minima into account. Highest ranked poses satisfying post-processing experimental constraint filters that are described below, were further refined locally in the RosettaDock web interface for the best fit between the two binding partners.

In order to filter for candidate poses that could represent testable models for the Gal-1/C-Raf-RBD complex, we took three sets of experimental data into account. Firstly, the interface should be common to Gal-1 and galectin-3 (Gal-3; Supplementary Fig. 3B,C), i.e. close to the conserved carbohydrate binding site (CBS), but possibly not identical, as a thiodigalactoside-derived inhibitor of Gal-1 and Gal-3 with submicromolar affinity to Gal-3 ($K_d = 29 \pm 7$ nM)[49] did not affect cellular FRET between Gal-1 and the C-Raf-RBD (Supplementary Fig. 3A). Importantly, this suggests that classical inhibitors of galectins that compete with the β-galactoside-ligand do not interfere with the Gal-1/RBD-interaction. In agreement with this, also H-rasG12V nanoclustering remained unaffected by the compound (Supplementary Fig. 3A). Secondly, Gal-1 interacts with both the C-Raf- and the PI3Kα-RBD (Fig. 3A), suggesting that the interface must span conserved regions of these two proteins (Supplementary Fig. 2C). Thirdly, the Gal-1 interface with the RBDs cannot overlap with their Ras binding region, as Gal-1, RBD and Ras would form concurrently a complex.

An initial complex of the Gal-1 monomer in the ligand bound state (i.e. prepared from dimeric, lactose bound Gal-1, PDB ID: *1GZW*)[50] and the C-Raf-RBD (PDB ID: *1RFA*)[51] was made in GRAMM compiler and iteratively refined (Supplementary Fig. 3D). Based on this model we generated Gal-1- and RBD-mutants, in order to experimentally validate the Gal-1/C-Raf-RBD interaction surface (Supplementary Table 1). Three initial mutants of the C-Raf-RBD from the lowest energy poses of Gal-1 with the C-Raf-RBD that did not undergo subsequent refinement in RosettaDock predominantly localized to the nucleus, unlike their wt counterpart (Supplementary Fig. 3E), which obviated further Gal-1 interaction analysis. Sequence analysis revealed that previously unrecognized nuclear localization- (NLS) and nuclear export signals (NES) appear to be localized in the C-terminal part of the RBD of C-Raf (Supplementary Fig. 2C). Two Gal-1 mutants that were generated based on this first, ligand-bound Gal-1 pose (Supplementary Fig. 3D) localized normally, but did not show any loss of function (Supplementary Fig. 3F,G).

Considering that there are no known intracellular carbohydrate ligands, we used a Gal-1 monomer in the ligand unbound (apo-) state prepared from dimeric Gal-1 (PDB ID: *3W58*) docked with the C-Raf-RBD (PDB ID: *1C1Y*)[52] to build an alternative lowest-energy refined pose (Fig. 4A). Here, residues D113 and D117 formed

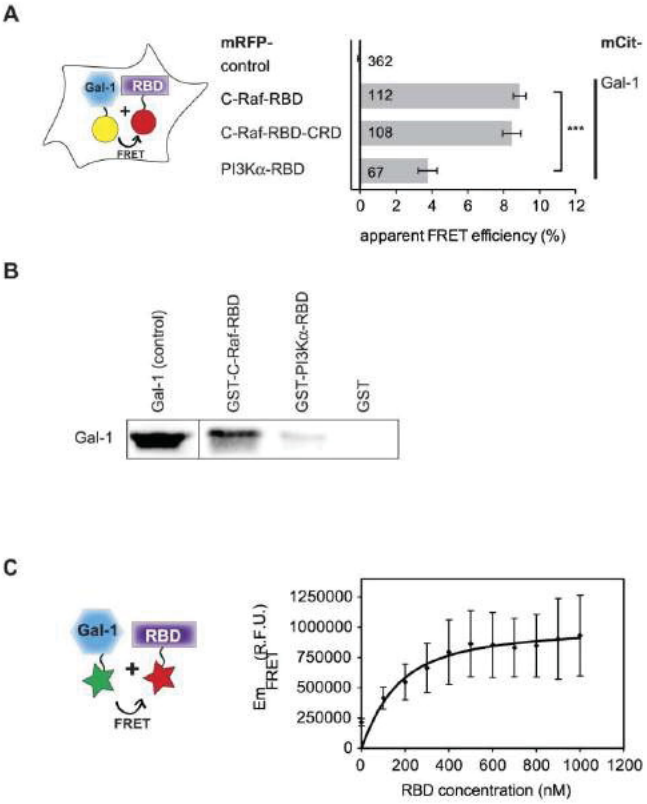

Figure 3. Galectin-1 directly binds to the Ras binding domain of effectors. (**A**) Interaction of Gal-1 with fragments of C-Raf (as can be derived from Supplementary Fig. 2A) or with the RBD of PI3Kα studied by FLIM-FRET in BHK21 cells, transiently expressing mCit-tagged Gal-1 and mRFP-tagged RBD-constructs (three independent biological repeats). Fluorescence lifetimes of FRET-samples were all significantly different from the donor-control. Plotted values correspond to the mean ± SEM. Numbers inside and above the bars indicate total number of cells imaged. The Methods section describes the indicated statistical comparisons (***$p < 0.001$). Samples with coexpressed fluorescent proteins mRFP and mCit served as FRET controls. Note that non-control sample FRET-values were all significantly different from the (FRET-)control sample. (**B**) GST pull-down experiments were performed by mixing bacterially purified Gal-1 with GST, GST-C-Raf-RBD or GST-PI3Kα-RBD immobilized on glutathione sepharose beads. GST was used as a negative control. Proteins retained on the beads were resolved by SDS-PAGE and Western blotted using a monoclonal antibody (M01) against Gal-1 for detection. (**C**) Corrected sensitized acceptor emission FRET data of 100 nM ATTO-488-labelled Gal-1 titrated with increasing concentrations of DY-547-labelled C-Raf-RBD (scheme on the left). Both proteins were purified from bacteria and labelled with the ACP-tag method. The dissociation constant (K_d) was determined from the shown curve fit on the dataset of Em_{FRET} as described in the Methods section. Plotted values correspond to the mean ± SEM.

ionic and hydrogen bonds with Gal-1's R74 and Q73, respectively. In addition R100 from the RBD formed an ionic bond with Gal-1's D103. From both structural models (Fig. 4A, Supplementary Fig. 3A), three C-Raf-RBD mutants could thus be derived, RBD-D113A, D117A and RBD-D117A, as well as the charge reversing counterpart RBD-D117R. All of them localized to the cytoplasm and nucleus like the parent, wild type (wt) C-Raf-RBD (Fig. 4B). Analysis of their interaction with Gal-1 in cells using FRET revealed a significant loss of function in their interaction with Gal-1 (Fig. 4C). Importantly, mutation D117A or D117R in the C-Raf-RBD was sufficient to desensitize it for Gal-1 enhanced recruitment to H-rasG12V (Fig. 4D).

The mutation of Arg 100, another residue in the modelled interface (Fig. 4A) to Asp did already affect the RBD-recruitment FRET to H-rasG12V (Supplementary Fig. 3H). This suggested that overall properties of the RBD affinity to Ras were compromised. Indeed, a previous report stated that only if R100 was mutated to Ala, would the affinity of the RBD for H-ras be basically unaffected[53]. Mutational analysis of the Gal-1 interface was inconclusive, as the mutation Q73A did not have an effect (Supplementary Fig. 3G).

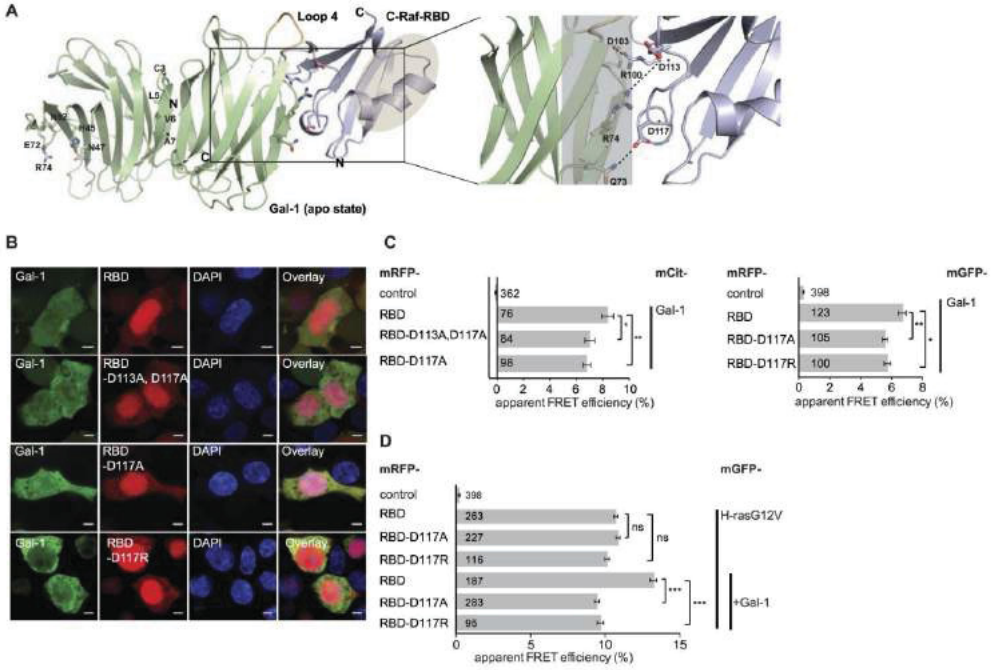

Figure 4. Computational modelling and mutational validation of the Galectin-1/RBD complex. (**A**) Computational representation of a monomer of Gal-1 (*3W58*) and C-Raf-RBD (*1C1Y*: herein RBD)[52] complex from an optimized low energy molecular docking pose superimposed with dimeric Gal-1 from the same PDB deposition. Numbering of residues is according to sequences deposited in UniProt (P09382 – Gal-1_*Homo sapiens*, P04049 – C-Raf_*Homo sapiens*). The loop (loop 4) that undergoes major conformational and stereo-chemical changes between apo- and liganded Gal-1 is coloured orange (Supplementary Fig. 3A). *Left:* Note that the Gal-1 dimer interface, marked by the four mutated residues, is to the left near the N-terminus (N) of Gal-1. Residues forming the CBS are shown on the left monomer. The grey oval marks the region on the C-Raf-RBD that contacts Ras. *Enlarged panel to the right* shows a close-up view into the putative protein-protein interface and major interactions. Residues that were mutated in the RBD and showed an effect are marked with asterisks. The uncertainty regarding the interacting surface on Gal-1 is indicated by the translucent grey box. (**B**) Representative confocal images of HEK293-EBNA cells co-transfected with mGFP-Gal-1 and mRFP-C-Raf-RBD (RBD) mutated in the indicated residues. Columns represent imaged fluorescent channels, appropriate for the indicated construct. The nucleus is stained by DAPI. Overlay images show superposition of images to the left. Scale bar is 5 μm. (**C**) Interaction between mCit-Gal-1 (left) or mGFP-Gal-1 (right) and mRFP-tagged C-Raf-RBD and derived interfacial mutants studied using FLIM-FRET in HEK293-EBNA cells transiently expressing indicated constructs (three independent biological experiments). (**D**) Interaction between mGFP-H-rasG12V and mRFP-tagged C-Raf-RBD and derived interfacial mutants with or without coexpressed non-labelled Gal-1 (+Gal-1) studied using FLIM-FRET in HEK293-EBNA cells transiently expressing indicated constructs (three independent biological experiments). (**C,D**) Plotted values correspond to the mean ± SEM. Numbers inside the bars indicate total number of cells imaged. The Methods section describes indicated statistical comparisons (ns, non significant; $^{*}p < 0.05$; $^{**}p < 0.01$; $^{***}p < 0.001$). Samples with coexpressed fluorescent proteins mCit and mRFP (**C**) or mGFP and mRFP (**C,D**) served as a FRET control. Note that non-control sample FRET-values were all significantly different from the (FRET-)control sample.

In conclusion, a structural docking derived C-Raf-RBD mutant that is deficient in Gal-1 binding is also insensitive to Gal-1-dependent (nanoclustering mediated) enhanced recruitment to active H-ras[10]. These data support the C-Raf-RBD interface of our tentative structural model, while that of Gal-1 remains unclear. Therefore only high-resolution structural approaches (of full length proteins in the context of the membrane) can resolve the actual details of the complex, and we wish to clarify that our model represents merely a proposition of how Gal-1 and the C-Raf-RBD might interact, based on our experimental data.

The galectin-1 dimer interface is required to modulate positively GTP-H-ras-, and negatively GTP-K-ras-nanoclustering. Inhibitors of Raf that induce its dimerization were recently shown to increase Ras nanoclustering. Likewise an artificial tandem-fusion protein of the B- and C-Raf RBD-CRD was sufficient to

stabilize Ras nanoclustering[54]. Given the very similar nanoscale organization of the effector Raf with Ras[9,55], it is plausible to assume that dimeric Gal-1 stabilizes effector dimers to augment nanoclustering.

We therefore tested the hypothesis that an intact Gal-1 dimer-interface is necessary for H-rasG12V-nanoclustering and -signalling promotion. Mutations at the N-terminus of Gal-1 were previously described in two dimerization compromised mutants (Gal-1-C3S,L5Q,V6D,A7S; $K_d \approx 250\,\mu M$ and Gal-1-V6D; $K_d \approx 60\,\mu M$)[56]. However, the single mutation of residue V6D, did not lead to a loss of dimerization-FRET in HEK293-EBNA cells (Supplementary Fig. 4A). By contrast, the mutant that combined all N-terminal mutations, here named N-Gal-1, showed significantly decreased dimerization-FRET in HEK293-EBNA cells as compared to the non-mutated parent (Supplementary Fig. 4A), as well as reduced amounts of the dimer in a native gel analysis (Supplementary Fig. 4B).

While wt Gal-1 significantly increased H-rasG12V nanoclustering (Fig. 5A) and RBD-effector recruitment to H-rasG12V (Fig. 5B) as observed before[10], N-Gal-1 did not support either increase (Fig. 5A,B). Of note, FRET between the C-Raf-RBD and N-Gal-1 was significantly increased in cells (Supplementary Fig. 4C). This observation rules out that a loss in affinity for the C-Raf-RBD is responsible for the loss in RBD recruitment. Consistent with this loss-of-function in supporting H-rasG12V nanoclustering and RBD recruitment, N-Gal-1 did not potentiate EGF-induced ppERK-signalling when H-ras was overexpressed (Fig. 5C). Hence, our data show that an intact Gal-1 dimer interface is required for H-ras nanocluster augmentation.

In addition to H-rasG12V, K-rasG12V was also originally described to co-immunoprecipitate with Gal-1, opening up the possibility that K-ras nanoclustering could also be affected by Gal-1[36]. Based on FRET-experiments, we could confirm that like H-rasG12V (Supplementary Fig. 1A) both K- and N-rasG12V are in close, FRET-competent complexes with Gal-1 in BHK21 cells, even if the cells were treated with compactin to block farnesylation (Supplementary Fig. 4D). However, when we studied the effect of Gal-1 on Ras nanoclustering in BHK21 cells, we observed that increasing concentrations of Gal-1 had no effect on N-rasG12V, while they negatively regulated K-rasG12V nanoclustering-FRET (Fig. 5D). Consistent with a dimerization dependent negative activity of Gal-1 on K-rasG12V nanoclustering, N-Gal-1 was also less efficient in reducing K-rasG12V nanoclustering than wt Gal-1 (Fig. 5E).

In conclusion, efficient Gal-1 dimerization is required to positively regulate H-rasG12V nanocluster and negatively regulate K-rasG12V nanocluster.

Discussion

Ras nanoclustering is indispensable for Ras signalling[8] and we have recently described it as target of cancer associated Ras-mutations[57], underscoring its significance for the signalling architecture of Ras. Only a handful of nanocluster regulators, so called Ras nanocluster scaffolds are known, and Gal-1 has so far been the one scaffold that was functionally and mechanistically best understood. We here presented data, which question the existing model of Gal-1 binding directly to the farnesyl-lipid on the C-terminus of Ras proteins (Fig. 6A). We did neither observe binding of Gal-1 to a farnesylated Ras-peptide, nor directly to the G-domain of Ras (Fig. 1). Instead, we found that Gal-1 indirectly couples to Ras via a direct association with the RBD-domain of effectors (Figs 2–4) and that an intact Gal-1 dimer interface is required for Gal-1 to modulate Ras nanoclustering (Fig. 5).

Others previously suggested binding of farnesylated proteins to Gal-1. Two different mutations were described that abrogated binding to farnesyl, K28T (according to our numbering K29T)[41] and L11A (L12A, likewise)[33]. These mutants were brought in agreement by proposing a farnesyl-binding pocket along the N-terminal or dimer interface part of Gal-1[41]. However, we did not observe any effect of the former mutation on the complexation of Gal-1 and H-rasG12V (Supplementary Fig. 1B). It is conceivable that the L11A mutation near the dimer interface of Gal-1 affects the ability of Gal-1 to dimerize and thus H-ras-GTP nanoclustering. However, this has not been shown so far.

With our new model (Fig. 6B), we resolve inconsistencies of the previous model, such as how specificity for active Ras is mediated and incorporate recent findings, which demonstrated that Raf dimer-inducing compounds do also increase Ras nanoclustering[54]. Thus we propose the following revised mechanistic model for the function of Gal-1 as a nanocluster scaffold (Fig. 6B): upon Ras activation and recruitment of the effectors to Ras, Gal-1 binds with high affinity to the accessible part of the RBD of effectors. Note that according to our data with non-farnesylated H-rasG12V (Supplementary Fig. 1A,B), it is possible that Gal-1 and effectors directly bind to each other in the cytoplasm. As Gal-1 can dimerize at μM concentrations that can be found in mammalian cells[10], it could stabilize effector dimers, such as e.g. Raf-dimers. We therefore here propose that the Raf-dimers are the actual nanocluster stabilizer. This is supported by our data showing that loss of the effector binding capability of H-rasG12V-D38A (Fig. 2B) and knockdown of A- and B-Raf (Supplementary Fig. 2A) can dramatically reduce Gal-1 supported H-rasG12V nanoclustering. This model is furthermore consistent with the activity of artificially fused dimeric RBD-CRD to stabilize nanocluster[54]. Our model is also in agreement with data that revealed a clustered organisation of Raf on the membrane[18,55]. Thus the idea is corroborated that Ras-nanoclusters represent dynamic signalling hubs of Ras and its effectors.

Our new model brings about a 'chicken-and-egg' problem, namely whether nanoclustering enhances effector recruitment[10] or effector binding to Ras enhances nanoclustering. Given the dense 'lattice' of nanoclustered Ras, effectors and scaffolds on the inner side of the plasma membrane, allosteric or configurational cooperativity may at least transiently emerge in Ras nanoclusters, which could resolve this apparent paradox. Effector dimerization most likely leads to the cooperative growth of Ras nanocluster, which conversely increases the recruitment probability of more effectors. The activity of this system would be strictly limited by the highly dynamic nature of the Ras-effector interaction (high off-rate of effectors) and ultimately by the GTP/GDP-exchange cycle of Ras.

This model may also explain the observation that Gal-1 apparently shifts the H-ras activity from the PI3K to the Raf pathway. The higher effective affinity (i.e. as judged by our cellular FRET-experiments) of Gal-1 for the

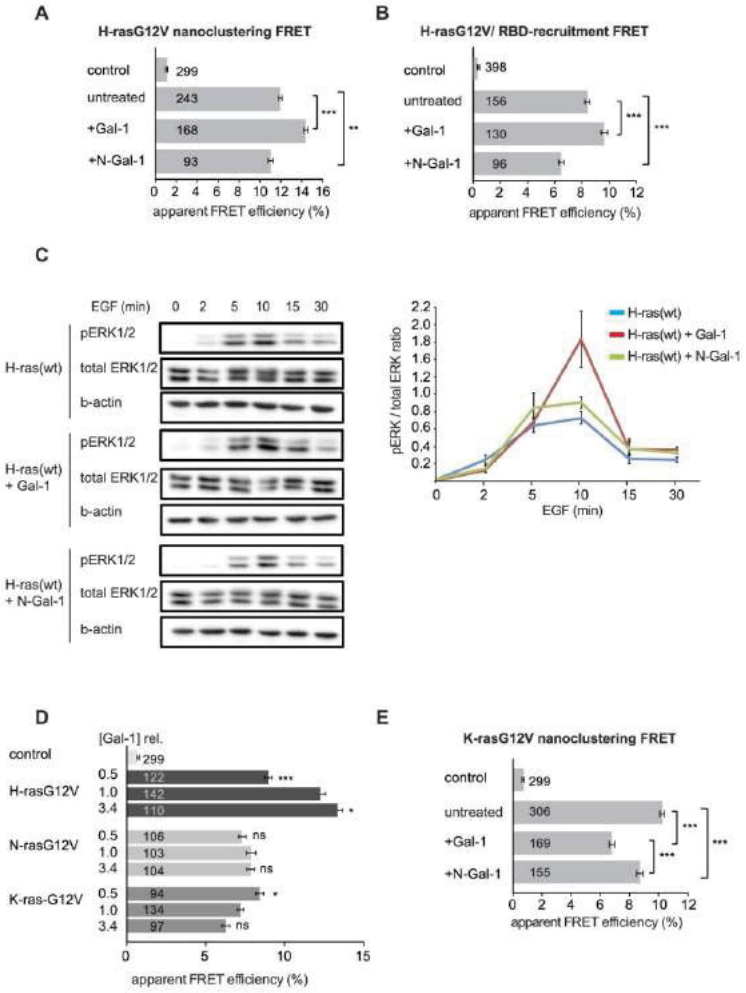

Figure 5. A dimerization deficient Galectin-1 mutant loses its effect on Ras nanoclustering and signalling. (**A**) Nanoclustering-FRET response of H-rasG12V in dependence of Gal-1 or its dimerization deficient mutant N-Gal-1 in HEK293-EBNA cells expressing mGFP-/mCherry-H-rasG12V. (**B**) RBD-recruitment FRET response of H-rasG12V in dependence of Gal-1 or its dimerization deficient mutant N-Gal-1 (mGFP-H-rasG12V and mRFP-C-Raf-RBD expressed in HEK293-EBNA) to assess effector translocation from the cytoplasm to active H-ras in plasma membrane nanoclusters. (**C**) Left, Western blot analysis of HEK293-EBNA lysates expressing mGFP-tagged H-ras and mRFP-tagged Gal-1 constructs as indicated. Serum-starved cells were stimulated with 100 ng/ml EGF for the indicated times. Total ERK and phospho-ERK (pERK) levels were then determined by immunoblotting. β-actin is the loading control. Right, Quantification of three independent repeats of Western blot data as shown on left. The pERK-signal was normalized to the total ERK-signal. (**D**) The nanoclustering-FRET response of H-rasG12V, N-rasG12V and K-rasG12V with increasing concentration of Gal-1. BHK21 cells were transiently co-transfected with mGFP-/and mCherry-tagged Ras constructs alone (1.0) or with antisense-Gal-1 (0.5) or non-labelled Gal-1 (3.4). The cellular total Gal-1 concentration relative to endogenous Gal-1 in control BHK21 cells ([Gal-1]rel.) is displayed to the left of the data. (**E**) The nanoclustering-FRET response of K-rasG12V. HEK293-EBNA cells transiently expressed mGFP-/mCherry-K-rasG12V and if indicated non-labelled Gal-1 or N-Gal-1. Note that in (**D**) the FRET-levels for K-rasG12V are lower than in (**E**), due to the higher Gal-1 level in BHK21 as compared to HEK293-EBNA cells (Supplementary Fig. 4E). (**A,B,D,E**) Plotted values correspond to the mean ± SEM of three independent biological experiments. Numbers inside the bars indicate total number of cells imaged. The Methods section describes the indicated statistical comparisons (ns, non significant; $^{*}p < 0.05$; $^{***}p < 0.001$); comparisons in (**D**) were done against the 1.0 parent-control. Samples with coexpressed fluorescent proteins mGFP and mCherry (**A,E**) or mGFP and mRFP (**B**) served as a FRET control. Note that non-control sample FRET-values were all significantly different from the (FRET-)control sample.

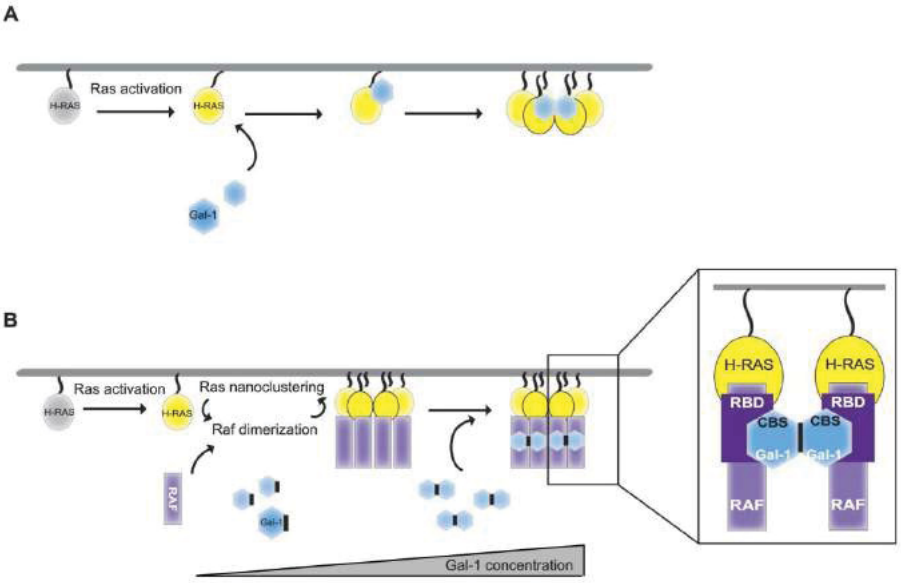

Figure 6. Comparison of current and our new model for the mechanism of action of Gal-1 as a nanocluster scaffold. (**A**) Current model. Direct interaction of active H-ras and Gal-1 stabilizes nanocluster. H-ras (depicted as yellow oval) activation supposedly makes the C-terminal farnesyl chain of H-ras more accessible for the prenyl-binding pocket of Gal-1 (depicted as a blue hexagon). This mechanistic step has not been described for other, similar trafficking chaperones, such as GDIs or PDEδ. Instead the spontaneous, activation state independent dissociation from the membrane is the basis for complexation by such chaperones in the cytoplasm[74,75]. (**B**) In the new model proposed here, Raf effectors (depicted as violet rectangles) are recruited to active H-ras in nanoclusters on the plasma membrane. At higher concentrations Gal-1 can dimerize. Gal-1 binds directly to the Ras binding domain (RBD) of effectors, such as Raf. Thus, dimeric Gal-1 could stabilize effector (Raf)-dimers, which then act as the actual 'scaffold' for H-ras nanocluster. Note that effector and Gal-1 can form complexes already in the cytoplasm. Stacked dimers of H-ras + effector (Raf) + Gal-1 (box to right) would be nucleating the growth of H-ras nanocluster, a process that may be supported by the membrane environment.

RBD of C-Raf *vs.* PI3Kα (Fig. 3A) could explain, how Gal-1 shifts the signalling output relatively from PI3K to Raf, an effect that could be potentiated in a nanocluster.

However, our model still cannot explain how selectivity for H-ras is realized. We propose that the H-ras-effector-Gal-1 complex is conformationally favoured, given that H-, N- and K-ras exhibit apparently distinct reorientation properties on the plasma membrane, with GTP-H-ras contacting the membrane via its helix α4[12,58]. Likewise, certain effectors or effector paralogs might be favoured by different conformational mechanisms. From our data one might speculate that A- and B-Raf are particularly relevant for H-ras nanoclustering, a constellation, which would be somewhat complementary to the apparent preference of N- and K-ras nanocluster for B- and C-Raf[54].

How does Gal-1 negatively impact on K-ras nanoclustering? It is important to note that the dimer-interface mutant N-Gal-1 does not lead to an increase of K-ras nanoclustering as compared to Gal-1 depletion (compare Fig. 5D,E). This means that the N-Gal-1 mutant is just less potent than the wt Gal-1 to affect K-ras nanoclustering, while another component upstream may actually mediate the effect on K-ras. We therefore propose that the effect of Gal-1 on K-ras nanoclustering depends on GTP-H-ras, which was recently shown to negatively regulate K-ras nanoclustering by redistributing phosphatidyl-serine in the plasma membrane[17]. Thus GTP-H-ras nanocluster would negatively regulate K-ras, an intriguing antagonistic constellation of these two Ras isoforms, which might be associated with the very different mutation rates of these elemental switches in cancer.

Currently a number of inhibitors for galectins are being developed[29,32,59]. However, their intended mechanism of action is exclusively focused on the functions of galectins in the extracellular space. Most of these compounds are β-galactoside analogs that are often not cell permeable and would compete with natural ligands of galectins in the extracellular space. Our current data show that a cell-permeable inhibitor of that type does not interfere with the binding of Gal-1 to the C-Raf-RBD, opening up the possibility of a distinctly targetable interface. Another interesting aspect is that this new interaction site would overlap with the NWGR anti-death motif in Gal-3[60]. However, we have not investigated Gal-3 further in the current study.

Finally, our data suggest that Salirasib may have a different molecular target than Gal-1 to exert its anti-cancer activity (e.g. PDEδ could be a candidate). Given Salirasib's success to progress in clinical trials, it may be crucial to establish its true target in order to support the development of similar therapeutic approaches in the future.

Methods

Plasmids and molecular cloning. Different expression plasmids for *in vitro* and cellular experiments were used. We obtained plasmid pEGFP-C-Raf as a kind gift from Prof. Krishnaraj Rajalingam, pEGFP-A-Raf from Dr. Angela Baljuls and pEGFP-B-Raf from Prof. John F Hancock.

Plasmids pmRFP-Gal-1, pmRFP-C-Raf-RBD, pmRFP-PI3Kα-RBD, pmRFP-C-Raf-RBD-CRD and pmGFP-H-rasG12V were described in ref. 12,58, while plasmids pcDNA3-antisense-Gal-1 and pcDNA3-Gal-1 in ref. 35. Plasmids pQE-A1, pQE-A1-H-ras(wt) and pQE-A1-C-Raf-RBD were described in ref. 10. Plasmids pmGFP-H-ras(wt), pmCherry-H-rasG12V, pmGFP-K-rasG12V, pmCherry-K-rasG12V, pmGFP-N-rasG12V and pmCherry-N-rasG12V were described elsewhere[57]. Plasmid pmGFP-H-rasG12V-D38A was prepared by mutating the H-rasG12V parent. pmCit-Gal-3, pmCit-Gal-1 were generated by cloning galectins from the mRFP-vectors into the pmCit-C1 vector. To generate construct pQE-A1-Gal-1, sequence of Gal-1 was first amplified from plasmid pmRFP-Gal-1 by PCR using forward primer 5′-TCAGATCTCATGGCCTGTGGTCTGGTC- 3′ and reverse primer 5′- GAGGTACCTTTATCACTCAAAGGCCACACAC -3′ (Sigma-Aldrich). Amplified PCR product was purified and sub-cloned into pCR™ II-Blunt-TOPO (Invitrogen). From there, the Gal-1 sequence was sub-cloned into BglII and KpnI restriction sites of the pQE-A1 vector. Plasmid pmRFP-C-Raf-RBD served as a template to which mutations were introduced by site-directed mutagenesis (GenScript USA Inc.) in order to generate plasmids pmRFP-C-Raf-RBD-W114,T116A,L121A (C3A); pmRFP-C-Raf-RBD-K109A,W114A,T116A (N3A); pmRFP-C-Raf-RBD- K109A,W114A,T116A,L121A,E124A,L126A (6A); pmRFP-C-Raf-RBD-D117A, pmRFP-C-Raf-RBD-D113A,D117A, pmRFP-C-Raf-RBD-D117R and pmRFP-C-Raf-RBD-R100D. Gal-1 mutants pmRFP-Gal-1-S63A; pmRFP-Gal-1-S63A,D65A; pmRFP-Gal-1-C3S,L5Q,V6D,A7S (pmRFP-N-Gal-1), pmRFP-Gal-1-V6D, pmRFP-Gal-1-K28T and pmRFP-Gal-1-N47D,W69L were constructed by site-directed mutagenesis on the plasmid pmRFP-Gal-1 (GenScript USA Inc.). pmGFP-H-rasG12V-C186S was generated on the plasmid pmGFP-H-rasG12V (GenScript USA Inc.). To generate plasmid pcDNA3-N-Gal-1, the N-Gal-1 sequence from pmRFP-N-Gal-1 was sub-cloned into the HindIII and BamHI sites of the plasmid pcDNA3-Gal-1. All constructs were verified by sequencing (GATC Biotech and GenScript USA Inc.).

Protein preparation and protein fluorescent labelling for *in vitro* studies. A1-tagged proteins H-ras, Gal-1 and C-Raf-RBD proteins were expressed in *Escherichia coli* using the pQE-expression system (Qiagen, Hilden, Germany) and purified as described[10]. The Ras-binding domains (RBDs) of C-Raf (aa 51–131) and p110α (aa 127–314), the catalytic subunit of PI3Kα, and full-length Gal-1 were produced as glutathione S-transferase (GST) fusion proteins in *E. coli*. The proteins were purified and the GST-tag was cleaved using TEV protease as described before[61]. All proteins were purified and nucleotide exchange for GDP or GTPγS on the H-ras molecule was done as described previously[10].

The labelling of A1-tagged purified proteins (H-ras, Gal-1 and RBD) was conducted with photostable fluorescent substrates, derivatives of coenzyme A (CoA) (NEB). CoA substrates are based on the ATTO-TEC dye ATTO-488 (CoA-488) or Dyomics dye DY-547 (CoA547) correspondingly and used to label ACP or A1-tagged fusion proteins. The labelling of the fusion proteins with the CoA substrates was performed according to the labelling procedure of the commercial protocol using ACP synthase (NEB, P9301S) from New England Biolabs (NEB). The unreacted substrate was removed by 5 times wash using Amicon® Ultra-2 filters (Millipore). The fluorescent labelling was quantified with Nano Drop 2000c (Thermo Scientific).

Fluorescence anisotropy. The proteins PDEδ and Gal-1 were expressed in *E. coli* and purified as described[10,62]. Rheb peptide (purity > 90%) was purchased from JPT GmbH (Germany). Fluorescence polarization measurements were carried out using a Fluoromax-4 spectrophotometer (HORIBA Jobin Yvon, Munich, Germany). All measurements were carried out at 20 °C in buffer containing 30 mM Tris, 150 mM NaCl and 3 mM Dithiothreitol (DTT) at 495 nm excitation and 520 nM emission wavelengths. Data were analysed using Grafit 5.0 (Erithacus Software, East Grinstead, UK).

Preparation of cell lysates for protein interaction measurement by FLIM-FRET. BHK21 cells were transiently transfected with the respective plasmids (pmGFP-H-rasG12V, pmRFP-C-Raf-RBD or pmRFP-Gal-1 constructs using JetPRIME transfection reagent (Polyplus-transfection). 24 h after transfection cells were lysed according to the procedure described by Dimauro *et al.* with some modifications[63]. In brief, 4×10^5 cells were washed with phosphate buffer saline and harvested with lysis buffer (50 mM Tris-HCl, 250 mM sucrose, 5 mM $MgCl_2$, 3 mM DTT, EDTA-free inhibitor cocktail), incubated on ice for 30 min upon sonication and vortexed for 15 s. The cell debris was pelleted by centrifugation at 800 g for 10 min and total protein amount was measured using the Bradford method (Bio-Rad). The precleared lysates containing overexpressed mGFP-H-ras were mixed with either fluorescently labelled protein DY-547-Gal-1 or DY-547-RBD of final concentration of 1 μM for the latters. The FRET-pair combinations of free fluorescent labels or fluorescent proteins at concentration of 1 μM were used as controls. The supernatants containing overexpressed mRFP-Gal-1 or mRFP-RBD were mixed with H-ras labelled with ATTO-488 and freshly loaded with GTPγS at the final concentration of 1 μM. The final protein/cell lysate mixtures were incubated for 30 min at 4 °C and the samples were measured by FLIM-FRET.

GST pull-down assay for protein interaction studies. GST pull-down experiments were conducted by adding 30 μM Gal-1 to 30 μM of the GST-fused RBDs of C-Raf and p110α (the catalytic subunit of PI3Kα) immobilized on 30 μl glutathione-conjugated Sepharose 4B beads (Macherey-Nagel, Duren, Germany). The mixture

was incubated at 4 °C for 45 min in buffer, containing 30 mM Tris-HCl, pH 7.5, 150 mM NaCl, 3 mM DTT. After washing for three times with the same buffer proteins retained on the beads were resolved by SDS-PAGE and processed for immunoblotting using a monoclonal antibody (M01) against Gal-1 (Abnova). GST was used as a negative control.

FRET assay *in vitro*. An *in vitro* FRET assay was used to measure FRET between GDP- or GTPγS-loaded H-ras and C-Raf-RBD or Gal-1 in solution. Equal amount of GTPγS-loaded/GDP and ATTO-488-labeled 250 nM H-ras (donors) and 250 nM Dy-547-labeled Gal-1 or RBD (acceptors) as a positive control were used. Measurements were conducted at room temperature in the buffer containing 25 mM Hepes, 100 mM NaCl, 3 mM DTT and 3 mM $MgCl_2$, pH 7.2. Fluorescence spectra were collected from 550 nm to 640 nm after excitation at 470 nm using a Synergy H1 hybrid fluorescence plate-reader (BioTek).

Efficiency of FRET was calculated by measuring the sensitized emission of the acceptor according to

$$E = \frac{\varepsilon_A}{\varepsilon_D} * \left(\frac{I_{AD}}{I_A} - 1\right),$$

where ε_A and ε_D are the molar extinction coefficients of the acceptor and donor, respectively, at the wavelength of excitation, I_{AD} is the emission of the acceptor in the presence of the donor and I_A is the fluorescence of the acceptor-only sample.

FRET assay *in vitro* was also used to determine the affinity between Gal-1 and RBD in solution. Normally, 100 nM of purified and ATTO-488 labeled Gal-1 was titrated with increasing concentrations (100 nM to 1000 nM) of purified and labelled DY-547-labelled C-Raf-RBD in 25 mM HEPES, 100 mM NaCl, 3 mM $MgCl_2$, 3 mM DTT pH 7.2 buffer. FRET measurements were performed in a 96-well plate (Perkin-Elmer) with a Synergy H1 hybrid fluorescence plate reader (BioTek, Winooski, VT). Two excitation wavelengths were used: 470 nm to excite ATTO-488-Gal-1 (donor), and 550 nm to excite DY-547-RBD (acceptor). Free dyes ATTO-488 and DY-547 were used as negative control. FRET was measured by sensitized emission of the acceptor using fluorescence spectra collected from 550 nm to 640 nm after excitation at 470 nm. FRET emission of DY-547-RBD (Em_{FRET}) was calculated from the total emission of the acceptor in presence of donor by subtraction of the direct emission of donor (donor only) and direct emission of acceptor (acceptor only) according to Song *et al.*[64]. Data processing was done using Gen5 software (version 2.01, BioTek), and K_d values were determined as described[64] using GraphPad Prism 6 software (GraphPad Software Inc., La Jolla, CA). The final Em FRET values were corrected by subtracting background FRET of the free fluorescent dyes.

Cellular FLIM-FRET analysis. BHK21 or HEK293-EBNA cells were transfected with indicated mGFP- or mCit- tagged donor construct and mCherry- or mRFP-tagged acceptor construct using JetPRIME transfection reagent (Polyplus transfection). For the inhibitor studies cells were treated for 2 h with either control (DMSO 0.2% (v/v)) or 20 μM Di-(3-deoxy-3-(4-((butylamino)carbonyl)-1H-1,2,3- triazol-1-yl)-β-D-galactopyranosyl)sulfane, IC-26-147-1 (batch PRV0312, Galecto Biotech)[49]. DMSO concentration in the final samples was under 0.2% (v/v). Co-transfection with pcDNA3-Gal-1, pcDNA3-N-Gal-1, pcDNA3-Gal-1-V6D or pcDNA3-antisense-Gal-1 was done in order to overexpress Gal-1, N-Gal-1 or Gal-1-V6D or to knockdown Gal-1. Cells were fixed with 4% PFA and mounted with Mowiol 4-88 (Sigma-Aldrich). To knock-down specific Raf paralogs, transfection with 50 nM A-Raf (L 003563-00), B-Raf (L003460-00), C-Raf (L 003601-00) siRNA or scrambled control (D 00181001-05, Dharmacon, GE Healthcare) using JetPRIME transfection reagent was done. Cells were fixed after 48 h. Fluorescence lifetimes of mGFP/mCit (intact cells) or ATTO-488 (cell lysates) were measured using a fluorescence lifetime imaging attachment (Lambert Instruments) on an inverted microscope (Zeiss AXIO Observer D1) as described in ref. 10. Fluorescein (0.01 mM, pH 9) was used as a lifetime reference. Three biological repeats were performed and averages of fluorescence lifetimes from at least 21 cells were calculated. The apparent FRET efficiency was calculated from obtained fluorescence lifetimes[10].

Cell culture and confocal imaging. Baby Hamster Kidney (BHK) 21 and Human Embryonic Kidney (HEK) 293-EBNA cells were obtained from ATCC repository. They were grown in Dulbecco's modified Eagle medium (DMEM) supplemented with 10% FBS, L-glutamine, penicillin (100 U/ml) and streptomycin (100 μg/mL). Both cell lines were grown to a confluency of 80% (8×10^7 cells/ml) and then sub-cultured every 2–3 days.

Subcellular distribution of Gal-1 and RBD mutants was imaged using confocal microscopy. HEK293-EBNA cells, coexpressing mRFP-tagged RBD or Gal-1 mutant with mGFP-tagged wild-type Gal-1 or RBD respectively, were imaged using Zeiss LSM 780 (63×, NA 1.2 water immersion objective, mGFP excitation at 488 nm and mCherry excitation at 543 nm).

Western blot analysis of ERK activation. HEK293-EBNA cells were transfected with pmGFP-H-ras(wt) alone or co-transfected with pmRFP-Gal-1 or pmRFP-N-Gal-1 using JetPRIME transfection reagent (Polyplus transfection). After 24 h cells, which were previously serum starved for 5 h, were stimulated with 100 ng/ml EGF (Sigma-Aldrich) for 0 min, 2 min, 5 min, 10 min, 15 min and 30 min and lysed using SDS lysis buffer. Cell lysates were separated by SDS-PAGE and blotted using pERK (Cell Signalling, #9106), total ERK (Cell Signalling, #9102) and β-actin (Sigma Aldrich, A1978) antibodies. The Chemidoc MP system (Bio-Rad Laboratories) was used to detect the band intensities, which were then quantified by densitometry in ImageJ software. Band intensities of pERK were normalized to the ones of total ERK. Averages from three different biological repeats were calculated.

Electron microscopic Ras-nanoclustering analysis. Apical plasma membrane sheets were prepared from BHK cells transiently expressing mGFP-H-rasG12V or mGFP-H-rasG12V-D38A alone or with

antisense-Gal-1. mGFP in the plasma membrane sheets was then labelled with 4.5 nm (diameter) gold nano-particles coupled to anti-GFP antibody and digital images were taken at 100,000 × magnification in an electron microscope (Jeol 1011). From the obtained images spatial mapping of the gold particles was performed as described previously[65]. For each sample at least 10 plasma membrane sheets were imaged and analysed. The statistical significance of differences was determined between replicated point patterns using bootstrap test as described in ref. 66.

Computational modelling and mutational validation. *Protein Structure and Sequence search.* Full length and domain-specific amino acid sequence queries were retrieved from UniProt (http://www.uniprot.org/). X-ray crystal structures for human Gal-1 (*1GZW*, *3W58*), C-Raf-RBD (*1C1Y*) and NMR structure of C-Raf-RBD (*1RFA*) were collected from the RCSB Protein Data Bank. The Invitrogen Vector NTI AlignX module was used for amino acid alignment of human Gal-1 with Gal-3 and of RAS-binding domains (RBDs) of Raf kinases and PI3Kα. Automatic alignments were critically analysed and compared with structure-based alignments in PyMOL.

Computational analysis for prediction of NLS and NES stretches. Here we identified nuclear localization signals from target sequences using cNLS mapper predictor model ensuring incorporation of non-canonical NLSs with activity score threshold of 3[67]. Further characterization of the sequences involved prediction of export signals on machine learned NetNES 1.1 server (http://www.cbs.dtu.dk/services/NetNES/). Both approaches (artificial neural networks and hidden Markov models) displayed on the signal plot from which the NES score is calculated were closely inspected for possible mispredictions. The use of point mutations disrupting nuclear exclusion signals and fluorescent cell imaging further confirmed this experimentally.

In silico approach to locate protein binding interfaces (PBIs). For the initial Gal-1/C-Raf-RBD model, global search of the best rigid body conformations was performed according to high-resolution generic docking parameters (Geometric docking[68]). The first stage in GRAMM-X docking starts with searching shape complementarity between the two proteins. This involves simplifying the protein structure as a rigid body representation on a 3D Cartesian grid then searching for degrees of overlap between the pairs of grids with a Fast Fourier Transform (FFT) approach to perform the docking. Next a softened Lennard-Jones potential function is employed to model conformational changes that take place during protein-protein binding[69]. To select for the best conformation from generated hundred to a thousand complexes GRAMM-X re-ranks poses by local minimization with soft van der Waals interaction, clustering of predictions within the same local minima, and rescoring with the target function combining Lennard-Jones[70] in the second stage of docking. No refinement that allows side-chain or backbone flexibility is available during the GRAMM-X docking steps. GRAMM-X displays final top scoring models based on soft Lennard-Jones potential, evolutionary conservation of predicted interface, statistical residue-residue preference, volume of the minimum, empirical binding free energy and atomic contact energy[69,70]. The web based GRAMM-X software (http://vakser.compbio.ku.edu/resources/gramm/grammx/) with default parameters was used for the optimized model. Both low-energy (high scoring) models have been refined locally in RosettaDock server[71]. Output PDB entries were further analysed for interface complementarity, area, and residue interactions using the PISA server (http://www.ebi.ac.uk/pdbe/prot_int/pistart.html) or manually in Discovery Studio (version 4.0, www.accelrys.com).

***In Situ* Proximity Ligation Assay (PLA).** BHK21 cells cultured on coverslips were transfected with scrambled control (D 00181001-05, Dharmacon, GE Healthcare) or siRNAs targeting Gal-1 (FlexiTube, GS3956, Qiagen) at a final concentration of 50 nM. After 48 h cells were serum starved for 5 h and then stimulated with 100 ng/ml EGF (Sigma-Aldrich) for 10 min before they were fixed with ice-cold methanol. Samples were incubated with mouse monoclonal anti C-Raf (H-8, lot #H0712, Santa Cruz Biotechnology) or anti B-Raf (F-7, lot #B271, Santa Cruz Biotechnology) antibodies and rabbit polyclonal anti Gal-1 antibody (PeproTech USA) for 120 min. Proximity ligation was carried out with the Duolink II *in situ* PLA kit (Sigma Aldrich) according to the instructions of the manufacturer (Olink Biosciences, Sweden). Coverslips were mounted on glass slides using Duolink® *in situ* mounting medium containing DAPI (Sigma Aldrich). At least three confocal images of each sample were acquired using a Zeiss LSM 780 (63×, NA 1.2 water immersion objective, DAPI excitation at 360 nm, detection 461 nm and Duolink® *in situ* detection reagent Red excitation at 594 nm, detection 624 nm). The protein interaction signal per cell was analysed in ImageJ software. In brief, the total number of PLA signal foci were counted and normalized to the number of cells (identified by DAPI stained nuclei).

Lactose-binding activity of mRFP-Gal-1 (Lactose agarose affinity assay). HEK293-EBNA cells transiently expressing mRFP-Gal-1(wt) and mRFP-Gal-1-N47D,W69L[46,47] constructs were harvested with lysis buffer (25 mM HEPES, 100 mM NaCl, 5 mM EDTA, 0.5% Triton, pH 7.5) without DTT and immobilized on lactose agarose beads (Vector Laboratories, Inc.) for 1 h following the equilibration, binding, and washing steps in the protocol for immunoprecipitation of GFP-fusion proteins using GFP-Trap®_A (ChromoTek GmbH, Germany). 250 mM lactose (10 mM HEPES, 150 mM NaCl, pH 7.5) was used to displace the retained fraction of Gal-1. Samples were resolved by SDS-PAGE and blotted with human Gal-1 antibody (PeproTech USA).

Lectin activity of purified Gal-1 variants (Hemagglutination assay). Mouse red blood cells were prepared and suspended in PBS buffer according to a published assay protocol (Guillaume, St-Pierre, Valérie, M., Sachiko, S., Purification of recombinant human galectin-1(Gal-1). Available at: http://jcggdb.jp/GlycoPOD (2014)). Purified A1-Gal-1 and His-A1-Gal-1 (Supplementary Fig. 1C) were quality checked for any sign of

degradation on Coomassie stained SDS-PAGE gels. Both proteins were serially diluted (1:2) into a V-shaped 96-well microtiter plate in the buffer containing 25 mM HEPES, 100 mM NaCl, 2 mM DTT and 3 mM $MgCl_2$, pH 7.2, starting from 10 mM Gal-1 concentration. An increasing gradient (20–45 µl) of the red blood cell suspension is then added to the wells to evaluate the optimal volume and avoid false positives. Similarly diluted (1:2 dilution with 10 mM starting concentration) concanavalin A was a positive control in this experiment, while equivalent volume of buffer without a lectin acted as a negative control. Instead of presenting the observed formation of spread out agglutinated red blood cells (positive result) versus a clearly defined sediment of non-agglutinated cells (negative outcome), we quantitated the agglutination effect using spectral absorbance[72] between 400–800 nm after 24 h incubation at 4 °C. The mean maximum OD value from two peaks in that wavelength range was recorded with a Synergy H1 hybrid fluorescence plate reader (BioTek) to determine and compare the agglutination capacity of His-A1-Gal-1 and A1-Gal-1 against concanavalin A mean maximum OD values. Overlapping OD values at desired concentration ranges showing galectin-induced versus concanavalin A hemagglutination were displayed for 30 µl red blood cell suspension.

Galectin-1 dimer/monomer equilibrium detection by native PAGE. HEK293-EBNA cells transiently expressing untagged Gal-1, mRFP-Gal-1(wt) and mRFP-N-Gal-1 constructs were harvested with lysis buffer (25 mM HEPES, 100 mM NaCl, 5 mM EDTA, 0.5% Triton, pH 7.5) without DTT and were resolved by native PAGE as described in ref. 73. In brief, stacking and resolving gels were prepared using 1.5 M Tris- buffer without SDS. For running/electrode buffer 100 mM Tris-tricine without SDS was used. Membranes were blotted with human Gal-1 antibody (PeproTech USA).

Statistical analysis. For experimental data statistical differences were determined using an analysis of variance (one-way ANOVA) complemented by Tukey's honest significant difference test (Tukey's HSD). The software GraphPad Prism 6 (GraphPad Prism Software Inc., La Jolla, CA) was used to perform these analyses. Confidence p-levels above columns indicated by asterisks are given with annotation as ns - non significant, i.e. $^{*}p < 0.05$, $^{**}p < 0.01$, $^{***}p < 0.001$.

References

1. Prior, I. A., Lewis, P. D. & Mattos, C. A comprehensive survey of ras mutations in cancer. *Cancer Res.* **72,** 2457–2467 (2012).
2. Vetter, I. R. & Wittinghofer, A. The guanine nucleotide-binding switch in three dimensions. *Science* **294,** 1299–1304 (2001).
3. Tsai, F. D. *et al.* K-Ras4A splice variant is widely expressed in cancer and uses a hybrid membrane-targeting motif. **112,** 779–784 (2015).
4. Quinlan, M. P. & Settleman, J. Explaining the preponderance of Kras mutations in human cancer: An isoform-specific function in stem cell expansion. *Cell Cycle* **7,** 1332–1335 (2008).
5. Ahearn, I. M., Haigis, K., Bar-Sagi, D. & Philips, M. R. Regulating the regulator: post-translational modification of RAS. *Nat. Rev. Mol. Cell Biol.* **13,** 39–51 (2012).
6. Hancock, J. F. & Parton, R. G. Ras plasma membrane signalling platforms. *Biochem. J.* **389,** 1–11 (2005).
7. Abankwa, D., Gorfe, A. A. & Hancock, J. F. Ras nanoclusters: molecular structure and assembly. *Semin. Cell Dev. Biol.* **18,** 599–607 (2007).
8. Tian, T. *et al.* Plasma membrane nanoswitches generate high-fidelity Ras signal transduction. *Nat. Cell Biol.* **9,** 905–914 (2007).
9. Rotblat, B. *et al.* H-Ras nanocluster stability regulates the magnitude of MAPK signal output. *Plos ONE* **5,** e11991 (2010).
10. Guzmán, C. *et al.* The efficacy of Raf kinase recruitment to the GTPase H-ras depends on H-ras membrane conformer-specific nanoclustering. *J. Biol. Chem.* **289,** 9519–9533 (2014).
11. Henis, Y. I., Hancock, J. F. & Prior, I. A. Ras acylation, compartmentalization and signaling nanoclusters (Review). *Mol. Membr. Biol.* **26,** 80–92 (2009).
12. Abankwa, D., Gorfe, A. A., Inder, K. & Hancock, J. F. Ras membrane orientation and nanodomain localization generate isoform diversity. *Proc. Natl. Acad. Sci. USA* **107,** 1130–1135 (2010).
13. Zhou, Y. & Hancock, J. F. Ras nanoclusters: Versatile lipid-based signaling platforms. *Biochim. Biophys. Acta-Molecular Cell Research* **1853(4),** 841–849 (2014).
14. Shalom-Feuerstein, R. *et al.* K-ras nanoclustering is subverted by overexpression of the scaffold protein galectin-3. *Cancer Res.* **68,** 6608–6616 (2008).
15. Inder, K. L. *et al.* Nucleophosmin and Nucleolin Regulate K-Ras Plasma Membrane Interactions and MAPK Signal Transduction. *J. Biol. Chem.* **284,** 28410–28419 (2009).
16. Ariotti, N. *et al.* Caveolae regulate the nanoscale organization of the plasma membrane to remotely control Ras signaling. *J. Cell Biol.* **204,** 777–792 (2014).
17. Zhou, Y. *et al.* Signal Integration by Lipid-Mediated Spatial Cross Talk between Ras Nanoclusters. *Mol. Cell. Biol.* **34,** 862–876 (2014).
18. Belanis, L., Plowman, S. J., Rotblat, B., Hancock, J. F. & Kloog, Y. Galectin-1 is a novel structural component and a major regulator of h-ras nanoclusters. *Mol. Biol. Cell* **19,** 1404–1414 (2008).
19. Camby, I., Le Mercier, M., Lefranc, F. & Kiss, R. Galectin-1: a small protein with major functions. *Glycobiology* **16,** 137R–157R (2006).
20. López-Lucendo, M. F. *et al.* Growth-regulatory human galectin-1: crystallographic characterisation of the structural changes induced by single-site mutations and their impact on the thermodynamics of ligand binding. *J. Mol. Biol.* **343,** 957–970 (2004).
21. Seelenmeyer, C., Stegmayer, C. & Nickel, W. Unconventional secretion of fibroblast growth factor 2 and galectin-1 does not require shedding of plasma membrane-derived vesicles. *FEBS Letters* **582,** 1362–1368 (2008).
22. Scott, S. A., Bugarcic, A. & Blanchard, H. Characterisation of oxidized recombinant human galectin-1. *Protein Pept. Lett.* **16,** 1249–1255 (2009).
23. Stowell, S. R. *et al.* Galectin-1 induces reversible phosphatidylserine exposure at the plasma membrane. *Mol. Biol. Cell* **20,** 1408–1418 (2009).
24. Astorgues-Xerri, L. *et al.* Unraveling galectin-1 as a novel therapeutic target for cancer. *Cancer Treatment Reviews* **40,** 307–319 (2014).
25. Ebrahim, A. H. *et al.* Galectins in cancer: carcinogenesis, diagnosis and therapy. *Ann. Transl. Med.* **2,** 88 (2014).
26. Huang, E.-Y. *et al.* A novel radioresistant mechanism of galectin-1 mediated by H-Ras-dependent pathways in cervical cancer cells. *Cell Death Dis* **3,** e251 (2012).

27. Chung, L.-Y. *et al.* Galectin-1 promotes lung cancer progression and chemoresistance by upregulating p38 MAPK, ERK and cyclooxygenase-2. *Clin. Cancer Res.* **18(15),** 4037–4047 (2012).
28. Zhang, P. *et al.* Galectin-1 overexpression promotes progression and chemoresistance to cisplatin in epithelial ovarian cancer. *Cell Death Dis* **5,** e991 (2014).
29. Rabinovich, G. A. *et al.* Synthetic lactulose amines: novel class of anticancer agents that induce tumor-cell apoptosis and inhibit galectin-mediated homotypic cell aggregation and endothelial cell morphogenesis. *Glycobiology* **16,** 210–220 (2006).
30. Iurisci, I. *et al.* Synthetic inhibitors of galectin-1 and -3 selectively modulate homotypic cell aggregation and tumor cell apoptosis. *Anticancer Res.* **29,** 403–410 (2009).
31. Collins, P. M., Oberg, C. T., Leffler, H., Nilsson, U. J. & Blanchard, H. Taloside inhibitors of galectin-1 and galectin-3. *Chem Biol Drug Des* **79,** 339–346 (2012).
32. Blanchard, H., Yu, X., Collins, P. M. & Bum-Erdene, K. Galectin-3 inhibitors: a patent review (2008-present). *Expert Opin Ther Pat* **24,** 1053–1065 (2014).
33. Rotblat, B. *et al.* Galectin-1(L11A) predicted from a computed galectin-1 farnesyl-binding pocket selectively inhibits Ras-GTP. *Cancer Res.* **64,** 3112–3118 (2004).
34. Ashery, U. *et al.* Spatiotemporal organization of Ras signaling: rasosomes and the galectin switch. *Cell. Mol. Neurobiol.* **26,** 471–495 (2006).
35. Paz, A., Haklai, R., Elad-Sfadia, G., Ballan, E. & Kloog, Y. Galectin-1 binds oncogenic H-Ras to mediate Ras membrane anchorage and cell transformation. *Oncogene* **20,** 7486–7493 (2001).
36. Elad-Sfadia, G., Haklai, R., Ballan, E., Gabius, H.-J. & Kloog, Y. Galectin-1 augments Ras activation and diverts Ras signals to Raf-1 at the expense of phosphoinositide 3-kinase. *J. Biol. Chem.* **277,** 37169–37175 (2002).
37. Laheru, D. *et al.* Integrated preclinical and clinical development of S-trans, trans-Farnesylthiosalicylic Acid (FTS, Salirasib) in pancreatic cancer. *Invest New Drugs* **30,** 2391–2399 (2012).
38. Grecco, H. E. & Verveer, P. J. FRET in Cell Biology: Still Shining in the Age of Super-Resolution? **12,** 484–490 (2010).
39. Guzman, C., Oetken-Lindholm, C. & Abankwa, D. Automated High-Throughput Fluorescence Lifetime Imaging Microscopy to Detect Protein-Protein Interactions. *J. Lab. Autom.* 1–8 (2015).
40. Riely, G. J. *et al.* A phase II trial of Salirasib in patients with lung adenocarcinomas with KRAS mutations. **6,** 1435–1437 (2011).
41. Yu, X. *et al.* Redox state influence on human galectin-1 function. *Biochimie* **116,** 8–16 (2015).
42. Ismail, S. A. *et al.* Arl2-GTP and Arl3-GTP regulate a GDI-like transport system for farnesylated cargo. *Nat Chem Biol* **7,** 942–949 (2011).
43. Mejuch, T., van Hattum, H., Triola, G., Jaiswal, M. & Waldmann, H. Specificity of Lipoprotein Chaperones for the Characteristic Lipidated Structural Motifs of their Cognate Lipoproteins. *Chembiochem* (2015).
44. Zhou, Z. *et al.* Genetically encoded short peptide tags for orthogonal protein labeling by Sfp and AcpS phosphopantetheinyl transferases. *ACS Chem. Biol.* **2,** 337–346 (2007).
45. George, N., Pick, H., Vogel, H., Johnsson, N. & Johnsson, K. Specific labeling of cell surface proteins with chemically diverse compounds. **126,** 8896–8897 (2004).
46. Hirabayashi, J. & Kasai, K. Effect of amino acid substitution by sited-directed mutagenesis on the carbohydrate recognition and stability of human 14-kDa beta-galactoside-binding lectin. *J. Biol. Chem.* **266,** 23648–23653 (1991).
47. Abbott, W. M. & Feizi, T. Soluble 14-kDa beta-galactoside-specific bovine lectin. Evidence from mutagenesis and proteolysis that almost the complete polypeptide chain is necessary for integrity of the carbohydrate recognition domain. *J. Biol. Chem.* **266,** 5552–5557 (1991).
48. Herrmann, C., Martin, G. A. & Wittinghofer, A. Quantitative analysis of the complex between p21ras and the Ras-binding domain of the human Raf-1 protein kinase. *J. Biol. Chem.* **270,** 2901–2905 (1995).
49. Salameh, B. A., Cumpstey, I., Sundin, A., Leffler, H. & Nilsson, U. J. 1H-1,2,3-triazol-1-yl thiodigalactoside derivatives as high affinity galectin-3 inhibitors. *Bioorg. Med. Chem.* **18,** 5367–5378 (2010).
50. López-Lucendo, M. F. *et al.* Gene design, expression, crystallization and preliminary diffraction analysis of two isolectins from the fungus Coprinus cinereus: a model for studying functional diversification of galectins in the same organism and their evolutionary pathways. *Acta Crystallogr. D Biol. Crystallogr.* **60,** 721–724 (2004).
51. Emerson, S. D. *et al.* Solution structure of the Ras-binding domain of c-Raf-1 and identification of its Ras interaction surface. *Biochemistry* **34,** 6911–6918 (1995).
52. Nassar, N. *et al.* The 2.2 A crystal structure of the Ras-binding domain of the serine/threonine kinase c-Raf1 in complex with Rap1A and a GTP analogue. *Nature* **375,** 554–560 (1995).
53. Campbell-Valois, F.-X., Tarassov, K. & Michnick, S. W. Massive sequence perturbation of a small protein. *Proc. Natl. Acad. Sci. USA* **102,** 14988–14993 (2005).
54. Cho, K.-J. *et al.* Raf Inhibitors Target Ras Spatiotemporal Dynamics. *Curr. Biol.* **22(11),** 945–955 (2012).
55. Nan, X. *et al.* Single-molecule superresolution imaging allows quantitative analysis of RAF multimer formation and signaling. *Proc. Natl. Acad. Sci. USA* **110,** 18519–18524 (2013).
56. Cho, M. & Cummings, R. D. Characterization of monomeric forms of galectin-1 generated by site-directed mutagenesis. *Biochemistry* **35(40),** 13081–13088 (1996).
57. Šolman, M. *et al.* Specific cancer-associated mutations in the switch III region of Ras increase tumorigenicity by nanocluster augmentation. *Elife* **4,** (2015).
58. Abankwa, D. *et al.* A novel switch region regulates H-ras membrane orientation and signal output. *EMBO J.* **27,** 727–735 (2008).
59. Astorgues-Xerri, L. *et al.* OTX008, a selective small-molecule inhibitor of galectin-1, downregulates cancer cell proliferation, invasion and tumour angiogenesis. *Eur. J. Cancer* **50,** 2463–2477 (2014).
60. Fukumori, T., Kanayama, H.-O. & Raz, A. The role of galectin-3 in cancer drug resistance. *Drug Resist. Updat.* **10,** 101–108 (2007).
61. Gremer, L. *et al.* Germline KRAS mutations cause aberrant biochemical and physical properties leading to developmental disorders. *Hum. Mutat.* **32(1),** 33–43 (2011).
62. Linari, M., Hanzal-Bayer, M. & Becker, J. The delta subunit of rod specific cyclic GMP phosphodiesterase, PDE δ, interacts with the Arf-like protein Arl3 in a GTP specific manner. *FEBS Letters* **458,** 55–59 (1999).
63. Dimauro, I., Pearson, T., Caporossi, D. & Jackson, M. J. A simple protocol for the subcellular fractionation of skeletal muscle cells and tissue. *BMC Research Notes* **5,** 1–1 (2012).
64. Song, Y., Rodgers, V. G. J., Schultz, J. S. & Liao, J. Protein interaction affinity determination by quantitative FRET technology. *Biotechnol. Bioeng.* **109,** 2875–2883 (2012).
65. Prior, I. A., Parton, R. G. & Hancock, J. F. Observing cell surface signaling domains using electron microscopy. *Sci. Signal.* **2003(177),** PL9 (2003).
66. Plowman, S. J., Muncke, C., Parton, R. G. & Hancock, J. F. H-ras, K-ras, and inner plasma membrane raft proteins operate in nanoclusters with differential dependence on the actin cytoskeleton. *Proc. Natl. Acad. Sci. USA* **102,** 15500–15505 (2005).
67. Kosugi, S., Hasebe, M., Tomita, M. & Yanagawa, H. Systematic identification of cell cycle-dependent yeast nucleocytoplasmic shuttling proteins by prediction of composite motifs. *Proc. Natl. Acad. Sci. USA* **106,** 13142–13142 (2009).
68. Vakser, I. A. Long-distance potentials: An approach to the multiple-minima problem in ligand-receptor interaction. *Protein Eng.* **9(1),** 37–41 (1996).

69. Tovchigrechko, A. & Vakser, I. A. GRAMM-X public web server for protein-protein docking. *Nucleic Acids Res.* **34** (suppl 2), W310–4 (2006).
70. Tovchigrechko, A. & Vakser, I. A. Development and testing of an automated approach to protein docking. *Proteins* **60,** 296–301 (2005).
71. The RosettaDock server for local protein–protein docking. *Nucleic Acids Res.* **36** (suppl 2), W233–W238 (2008).
72. Iwasaka, M., Miyakoshi, J. & Ueno, S. Optical absorbance of hemoglobin and red blood cell suspensions under magnetic fields. *IEEE Trans. Magn.* **37(4),** 2906–2908 (2001).
73. Haider, S. R., Sharp, B. L. & Reid, H. J. A comparison of Tris-glycine and Tris-tricine buffers for the electrophoretic separation of major serum proteins. *J Sep Sci* **34,** 2463–2467 (2011).
74. Silvius, J. R., Bhagatji, P., Leventis, R. & Terrone, D. K-ras4B and prenylated proteins lacking 'second signals' associate dynamically with cellular membranes. *Mol. Biol. Cell* **17,** 192–202 (2006).
75. Rocks, O., Peyker, A. & Bastiaens, P. I. H. Spatio-temporal segregation of Ras signals: one ship, three anchors, many harbors. *Curr. Opin. Cell Biol.* **18,** 351–357 (2006).

Acknowledgements

We thank Dr. Camilo Guzman for assistance with *in vitro* FRET experiment analysis. Plasmids encoding pEGFP-C-Raf, pEGFP-A-Raf and pEGFP-B-Raf were kindly provided by Prof. Krishnaraj Rajalingam, Dr. Angela Baljuls and Prof. John F Hancock, respectively. Gal-1 inhibitor IC-26-177-1 was kindly supplied by Dr. Ulf Nilsson (Galecto Biotech, Sweden). We are grateful to Prof. Alemayehu Gorfe for initial advice on protein docking, Dr. Tina Salminen and Dr. Radovan Dvorsky for the help with validation of docking steps and Prof. Rob Parton for insightful comments on the manuscript. The authors are grateful for support from the cell imaging core (CIC). HN and MRA were supported by the German Research Foundation (DFG) through the Collaborative Research Center 974 (SFB 974 Communication and Systems Relevance during Liver Injury and Regeneration). EKF and AW received funding by the Sonder- forschungsbereich-DFG (SFB 642). This work was supported by the Academy of Finland fellowship grant, the Sigrid Juselius Foundation, the Cancer Society of Finland, the Marie-Curie Reintegration Grant and the Jane and Aatos Erkko Foundation grants to D.A. M.S. was supported by the TUBS graduate school.

Author Contributions

D.A. conceived the project. O.B. conducted FRET experiments in cell lysates and *in vitro*, acquired and analysed cellular FRET data, purified and fluorescently labelled proteins, performed Western blot experiments for MAPK signalling, performed PLA experiment and native gel analysis. Y.G.M. conducted computational docking, performed bioinformatics sequence analysis, acquired and analysed FRET cellular data, validated lectin-binding activity of tagged-galectins and performed Western blot experiments. M.S. acquired and analysed cellular FRET data, acquired confocal microscopy images, performed Western blot experiments for MAPK signalling. A.L. acquired and analysed *in vitro* FRET data, purified and fluorescently labelled proteins. N.A. acquired and analysed EM data. M.R.A. and H.N. planned and carried out pull-down experiments. A.W. and E.K.F. performed and analysed anisotropy assays. A.C.P. assisted in computational docking. All authors contributed to writing and discussion of the manuscript. O.B, Y.G.M. and D.A. designed the experiments and wrote the manuscript.

Additional Information

Supplementary information accompanies this paper at http://www.nature.com/srep

Competing financial interests: The authors declare no competing financial interests.

How to cite this article: Blazevits, O. *et al.* Galectin-1 dimers can scaffold Raf-effectors to increase H-ras nanoclustering. *Sci. Rep.* **6**, 24165; doi: 10.1038/srep24165 (2016).

Chapter VII

Classical RHO proteins: biochemistry of molecular switch function

Graphical Abstract

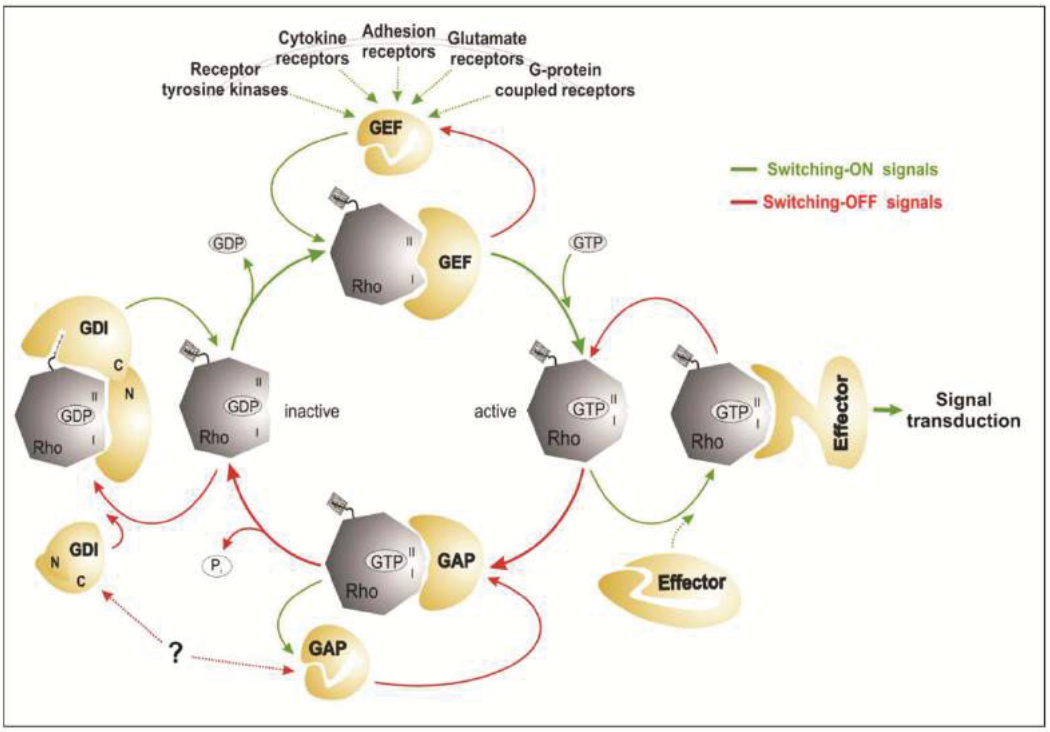

Status: Springer Vienna
Impact factor: Book chapter (not available)
Own Proportion to this work: 10 %
Writing the manuscript

Chapter 14
Classical Rho Proteins: Biochemistry of Molecular Switch Function and Regulation

Si-Cai Zhang, Kazem Nouri, Ehsan Amin, Mohamed S. Taha, Hossein Nakhaeizadeh, Saeideh Nakhaei-Rad, Radovan Dvorsky, and Mohammad Reza Ahmadian

Abstract Rho family proteins are involved in an array of cellular processes by modulating cytoskeletal organization, transcription, and cell cycle progression. The signaling functions of Rho family proteins are based on the formation of distinctive protein–protein complexes with their regulators and effectors. A necessary precondition for such differential interactions is an intact molecular switch function, which is a hallmark of most members of the Rho family. Such classical Rho proteins cycle between an inactive GDP-bound state and an active GTP-bound state. They specifically interact via a consensus-binding sites called switch I and II with three structurally and functionally unrelated classes of regulatory proteins, such as guanine nucleotide dissociation inhibitors (GDIs), guanine nucleotide exchange factors (GEFs), and GTPase-activating proteins (GAPs). Extensive studies in the last 25 years have provided invaluable insights into the molecular mechanisms underlying regulation and signal transduction of the Rho family proteins. In this chapter, we will review common features of Rho protein regulations and highlight specific aspects of their structure–function relationships.

Keywords Effector • GAP • GDI • GEF • Rho GTPase • Switch region

Abbreviations

A	Aliphatic amino acid
Bcr	Breakpoint cluster region protein
C	Cysteine
CZH	CDM-zizimin homology

S.-C. Zhang • K. Nouri • E. Amin • M.S. Taha • H. Nakhaeizadeh • S. Nakhaei-Rad • R. Dvorsky • M.R. Ahmadian (✉)
Institute of Biochemistry and Molecular Biology II, Medical Faculty, Heinrich-Heine-University, 40225 Düsseldorf, Germany
e-mail: reza.ahmadian@uni-duesseldorf.de

A. Wittinghofer (ed.), *Ras Superfamily Small G Proteins: Biology and Mechanisms 1*, DOI 10.1007/978-3-7091-1806-1_14, © Springer-Verlag Wien 2014

Db1	Diffuse B-cell lymphoma
DH	Dbl homology domain
DHR1&2	DOCK-homology regions 1 and 2
ERM	Ezrin/radixin/moesin
GAPs	GTPase-activating proteins
GDIs	Guanine nucleotide dissociation inhibitors
GDP	Guanosine diphosphate
GEFs	Guanine nucleotide exchange factors
Gln	Glutamine
Gly	Glycine
GTP	Guanosine triphosphate
$p75^{NTR}$	Neurotrophin receptor p75
PAK1	p21-activated kinase 1
PH	Pleckstrin homology domain
PKA	Protein kinase A
PKC	Protein kinase C
P-loop	Phosphate-binding loop
X	Any amino acid

14.1 General Introduction

The role of the Rho family proteins as signaling molecules in controlling a large number of fundamental cellular processes is largely dependent on a functional molecular switch between a GDP-bound, inactive state and a GTP-bound, active state (Dvorsky and Ahmadian 2004). This function underlies a so-called GTPase cycle consisting of two different, slow biochemical reactions, the GDP/GTP exchange and the GTP hydrolysis. The cellular regulation of this cycle involves guanine nucleotide exchange factors (GEFs), which accelerate the intrinsic nucleotide exchange, and GTPase-activating proteins (GAPs), which stimulate the intrinsic GTP hydrolysis activity (Cherfils and Zeghouf 2013). Rho protein function requires both posttranslational modification by isoprenyl groups and membrane association. Therefore, Rho proteins underlie a third control mechanism that directs their membrane targeting to specific subcellular sites. This mechanism is achieved by the function of guanine nucleotide dissociation inhibitors (GDIs), which bind selectively to prenylated Rho proteins and control their cycle between cytosol and membrane. Activation of Rho proteins results in their association with effector molecules that subsequently activate a wide variety of downstream signaling cascades (Bishop and Hall 2000; Burridge and Wennerberg 2004), thereby regulating many important physiological and pathophysiological processes in eukaryotic cells (Etienne-Manneville and Hall 2002; Heasman and Ridley 2008) (see Chap. 16). In the following, the biochemical properties of the Rho proteins and their regulatory cycles will be described in detail. Figure 14.1 schematically summarizes the regulatory mechanism of the Rho proteins.

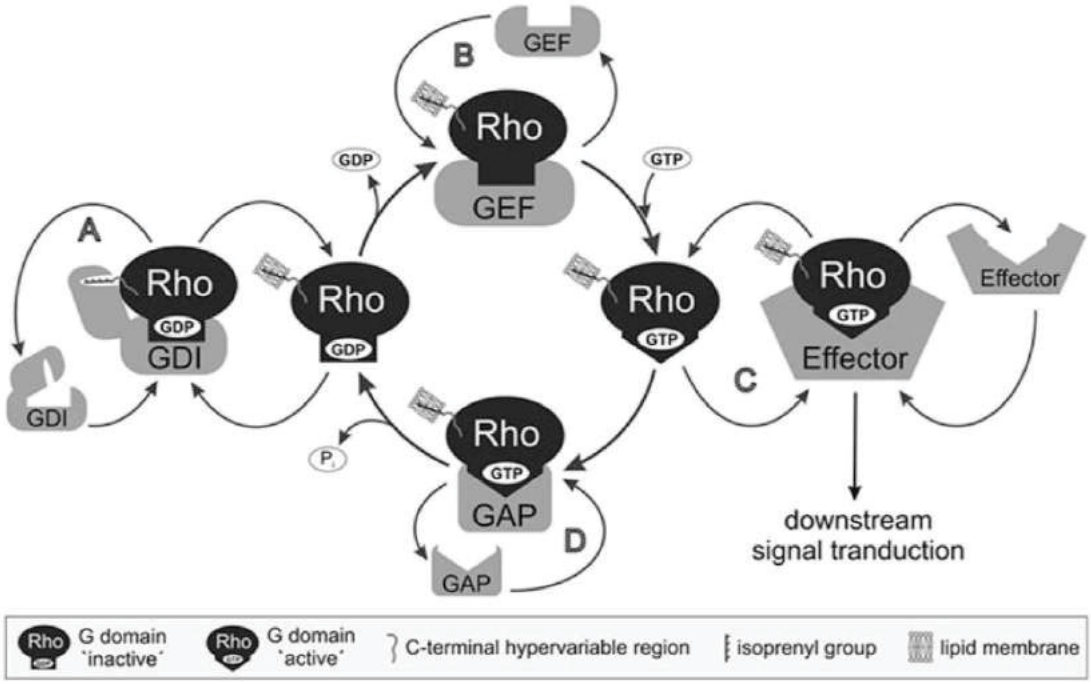

Fig. 14.1 Molecular principles of regulation and signaling of Rho Proteins. Most members of the Rho family act as molecular switches by cycling between an inactive, GDP-bound state and an active GTP-bound state. They interact specifically with four structurally and functionally unrelated classes of proteins: (**a**) In resting cells, guanine nucleotide dissociation inhibitors (GDIs) sequestrate the Rho proteins from the membrane by binding to the lipid anchor and create an inactivated cytosolic pool. (**b**) In stimulated cells, different classes of membrane receptors activate guanine nucleotide exchange factors (GEFs), which in turn activate their substrate Rho proteins by accelerating the slow intrinsic exchange of GDP for GTP and turn on the signal transduction. (**c**) The active GTP-bound Rho proteins interact with and activate their targets (the downstream effectors) to evoke a variety of intracellular responses. (**d**) GTPase-activating proteins (GAPs) negatively regulate the switch by stimulating the slow intrinsic GTP hydrolysis activity of the Rho proteins and turn off the signal transduction

14.2 Rho Family and the Molecular Switch Mechanism

Members of the GTP-binding proteins of the Rho family have emerged as key regulatory molecules that couple changes in the extracellular environment to intracellular signal transduction pathways. So far, 20 human members of the Rho family have been identified, which can be divided into six distinct subfamilies based on their sequence homology: (1) Rho (RhoA, RhoB, RhoC); (2) Rac (Rac1, Rac1b, Rac2, Rac3, RhoG); (3) Cdc42 (Cdc42, G25K, TC10, TCL, RhoU/Wrch1, RhoV/Chp); (4) RhoD (RhoD, Rif); (5) Rnd (Rnd1, Rnd2, Rnd3); (6) RhoH/TTF (Boureux et al. 2007; Jaiswal et al. 2013a, b; Wennerberg and Der 2004).

Rho family proteins are approximately 21–25 kDa in size typically containing a conserved GDP/GTP-binding domain (called G domain) and a C-terminal hypervariable region ending with a consensus sequence known as CAAX (C is cysteine, A is any aliphatic amino acid, and X is any amino acid). The G domain consists of five conserved sequence motifs (G1-G5) that are involved in nucleotide binding and

hydrolysis (Wittinghofer and Vetter 2011). In the cycle between the inactive and active states at least two regions of the protein, switch I (G2) and Switch II (G3), undergo structural rearrangements and transmit the "OFF" to "ON" signal to downstream effectors (Fig. 14.1) (Dvorsky and Ahmadian 2004). Subcellular localization of Rho proteins at different cellular membranes, that is known to be critical for their biological activity, is achieved by a series of posttranslational modifications at a cysteine residue in the CAAX motif, including isoprenylation (geranylgeranyl or farnesyl), endoproteolysis, and carboxyl methylation (Roberts et al. 2008).

A characteristic region of Rho family GTPases is the insert helix (amino acids 124–136, RhoA numbering) that may play a role in effector activation and downstream process (Thapar et al. 2002). Although the function of the insert helix has not been elucidated yet, it has been reported to be involved in the Rho-dependent activation of ROCK (Zong et al. 2001), phospholipase D (Walker and Brown 2002) and mDia (Lammers et al. 2008; Rose et al. 2005), and in the Rac-dependent activation of p67phox (Joneson and Bar-Sagi 1997; Karnoub et al. 2001; Nisimoto et al. 1997) and Plexin B1 (Bouguet-Bonnet and Buck 2008).

Although the majority of the Rho family proteins are remarkably inefficient GTP hydrolyzing enzymes, in quiescent cells they rest in an inactive state because the GTP hydrolysis is in average two orders of magnitude faster than the GDP/GTP exchange (Jaiswal et al. 2013a, b). Such different intrinsic activities provide the basis for a two-state molecular switch mechanism, which highly depends on the regulatory functions of GEFs and GAPs that directly control ON and OFF states of classical type of Rho proteins (Fig. 14.1). Eleven out of twenty members of the Rho family belong to these classical molecular switches, namely RhoA, RhoB, RhoC, Rac1, Rac2, Rac3, RhoG, Cdc42, G25K, TC10, and TCL (Jaiswal et al. 2013a, b).

The atypical Rho family members, including Rnd1, Rnd2, Rnd3, Rac1b, RhoH/TTF, Wrch1, RhoD, and Rif, have been proposed to accumulate in the GTP-bound form in cells due to various biochemical properties (Jaiswal et al. 2013a, b). Rnd1, Rnd2, Rnd3, and RhoH/TTF represent a completely distinct group of proteins within the Rho family (Riou et al. 2010; Troeger et al. 2013), as they do not share several conserved and essential amino acids, including Gly-12 (Rac1 numbering) in the G1 motif (also called phosphate-binding loop or P-loop) and Gln-61 (Rac1 numbering) in the G3 motif or switch II region. The role of these residues in GTP hydrolysis is well described for Ras oncogene in human cancers (Chaps. 6 and 7). Thus, they can be considered as GTPase-deficient Rho-related GTP-binding proteins (Fiegen et al. 2002; Garavini et al. 2002; Gu et al. 2005; Li et al. 2002) (see also Chap. 15). Another example is Rac1b, which is an alternative splice variant of Rac1 and contains a 19-amino acid insertion next to the switch II region (Jordan et al. 1999). Rac1b exhibits different biochemical properties as compared to the other Rac isoforms (Fiegen et al. 2004; Haeusler et al. 2006), including an accelerated GEF-independent GDP/GTP exchange and an impaired GTP hydrolysis (Fiegen et al. 2004). RhoD and Rif are involved in the regulation of actin dynamics (Fan and Mellor 2012; Gad and Aspenstrom 2010) and exhibit a strikingly faster nucleotide exchange than GTP hydrolysis similarly to Rac1b and thus persist

mainly in the active state under resting conditions (Jaiswal et al. 2013a, b). Wrch1, a Cdc42-like protein that has been reported to be a fast cycling protein (Shutes et al. 2006), resembles in this context Rac1b, RhoD, and Rif (Jaiswal et al. 2013a, b). These atypical members of the Rho family with their distinctive biochemical features do not follow the classical switch mechanism and may thus require additional forms of regulation.

14.3 Guanine Nucleotide Dissociation Inhibitors

Multiple functions have been originally described for the Rho-specific GDIs, including the inhibition of the GDP/GTP exchange (Hiraoka et al. 1992; Ohga et al. 1989), the intrinsic and GAP-stimulated GTP hydrolysis (Chuang et al. 1993; Hancock and Hall 1993; Hart et al. 1992), and the interaction with the downstream effectors (Pick et al. 1993). However, it is generally accepted that in resting cells, RhoGDIs target the isoprenyl anchor and sequester Rho proteins from their site of action at the membrane in the cytosol (Boulter and Garcia-Mata 2010; Garcia-Mata et al. 2011).

RhoGDIs undergo a high affinity interaction with the Rho proteins using an N-terminal regulatory arm contacting the switch regions and a C-terminal domain binding the isoprenyl group (Tnimov et al. 2012). In contrast to the large number of RhoGEFs and RhoGAPs, there are only three known RhoGDIs in human (DerMardirossian and Bokoch 2005). RhoGDI-1 (also called RhoGDIα) is ubiquitously expressed (Fukumoto et al. 1990), whereas RhoGDI-2 (also called RhoGDIβ, LyGDI, or D4GDI) is predominantly found in hematopoietic tissues and lymphocytes (Leonard et al. 1992; Scherle et al. 1993) and RhoGDI-3 (also called RhoGDIγ) in lung, brain, and testis (Adra et al. 1997; Zalcman et al. 1996).

Despite intensive research over the last two decades, the molecular basis by which GDI proteins associate and extract the Rho GTPases from the membrane remains to be investigated. The neurotrophin receptor p75 ($p75^{NTR}$) and ezrin/radixin/moesin (ERM) proteins have been proposed to displace the Rho proteins from the RhoGDI complex resulting in reassociation with the cell membrane (Takahashi et al. 1997; Yamashita and Tohyama 2003). Another regulatory mechanism is RhoGDI phosphorylation. RhoGDI has been shown to be phosphorylated by serine/threonine p21-activated kinase 1 (PAK1), protein kinase A (PKA), protein kinase C (PKC), and the tyrosine kinase Src, thereby decreasing the ability of RhoGDI to form a complex with the Rho proteins, including RhoA, Rac1, and Cdc42 (DerMardirossian et al. 2004, 2006).

14.4 Guanine Nucleotide Exchange Factors

GEFs are able to selectively bind to their respective Rho proteins and accelerate the exchange of tightly bound GDP for GTP. A common mechanism utilized by GEFs is to strongly reduce the affinity of the bound GDP, leading to its displacement and the subsequent association with GTP (Cherfils and Chardin 1999; Guo et al. 2005). This reaction involves several stages, including an intermediate state of the GEF in the complex with the nucleotide-free Rho protein. This intermediate does not accumulate in the cell and rapidly dissociates because of the high intracellular GTP concentration leading to the formation of the active Rho·GTP complex. The main reason therefore is that the binding affinity of nucleotide-free Rho protein is significantly higher for GTP than for the GEF proteins (Cherfils and Chardin 1999; Hutchinson and Eccleston 2000). Cellular activation of the Rho proteins and their cellular signaling can be selectively uncoupled from the GEFs by overexpressing dominant negative mutants of the Rho proteins (e.g., threonine 17 in Rac1 and Cdc42 or threonine 19 in RhoA to asparagine) (Heasman and Ridley 2008). Such mutations decrease the affinity of the Rho protein to nucleotide resulting in a so-called dominant negative behavior (Rossman et al. 2002). As a consequence, dominant negative mutants form a tight complex with their cognate GEFs and thus prevent them from activating the endogenous Rho proteins.

RhoGEFs of the diffuse B-cell lymphoma (Dbl) family directly activate the proteins of the Rho family (Cook et al. 2013; Jaiswal et al. 2013a, b). The prototype of this GEF family is the Dbl protein, which was isolated as an oncogenic product from diffuse B-cell lymphoma cells in an oncogene screen (Eva et al. 1988; Srivastava et al. 1986), and has been later reported to act on Cdc42 (Hart et al. 1991). The Dbl family consists of 74 members in human (Jaiswal et al. 2013a, b) with evolutionary conserved orthologs in fly (23 members), yeast (6 members), worm (18 members) (Schmidt and Hall 2002; Venter et al. 2001), and slime mold (45 members) (Vlahou and Rivero 2006). Human Dbl family proteins have recently been grouped into functionally distinct categories based on both their catalytic efficiencies and their sequence–structure relationship (Jaiswal et al. 2013a, b). The members of the Dbl family are characterized by a unique Dbl homology (DH) domain (Aittaleb et al. 2010; Erickson and Cerione 2004; Hoffman and Cerione 2002; Jaiswal et al. 2011; Viaud et al. 2012). The DH domain is a highly efficient catalytic machine (Rossman et al. 2005) that is able to accelerate the nucleotide exchange of Rho proteins up to 10^7-fold (Jaiswal et al. 2011, 2013a, b), as efficiently as the RanGEF RCC1 (Klebe et al. 1995) and *Salmonella typhimurium* effector SopE (see below) (Bulgin et al. 2010; Rudolph et al. 1999). The DH domain is often preceded by a pleckstrin homology (PH) domain indicating an essential and conserved function. A model for PH domain-assisted nucleotide exchange has been proposed for some GEFs, such as Dbl, Dbs, and Trio (Rossman et al. 2005). Herein the PH domain serves multiple roles in signaling events anchoring GEFs to the membrane (via phosphoinositides) and directing them

towards their interacting GTPases which are already localized to the membrane (Rossman et al. 2005).

In addition to the DH-PH tandem, Dbl family proteins are highly diverse and contain additional domains with different functions, including SH2, SH3, CH, RGS, PDZ, and IQ domains for interaction with other proteins; BAR, PH FYVE, C1, and C2 domains for interaction with membrane lipids; and other functional domains like Ser/Thr kinase, RasGEF, RhoGAP, and RanGEF (Cook et al. 2013). These additional domains have been implicated in autoregulation, subcellular localization, and connection to upstream signals (Dubash et al. 2007; Rossman et al. 2005). Spatiotemporal regulation of the Dbl proteins has been implicated to specifically initiate activation of substrate Rho proteins (Jaiswal et al. 2013a, b) and to control a broad spectrum of normal and pathological cellular functions (Dubash et al. 2007; Hall and Lalli 2010; Mulinari and Hacker 2010; Mulloy et al. 2010; Schmidt and Hall 2002). Thus, it is evident that members of the Dbl protein family are attractive therapeutic targets for a variety of diseases (Bos et al. 2007; Loirand et al. 2008; Vigil et al. 2010).

Apart from conventional Dbl family RhoGEFs there are two additional proteins families, which do not share any sequence and structural similarity with each other. The dedicator of cytokinesis (DOCK) or CDM-zizimin homology (CZH) family RhoGEFs are characterized by two conserved regions, known as the DOCK-homology regions 1 and 2 (DHR1 and DHR2) domains (Meller et al. 2005; Rittinger 2009). This type of GEFs employs their DHR2 domain to activate specially Rac and Cdc42 proteins (Meller et al. 2005). Another Rho protein-specific GEF family, represented by the SopE/WxxxE-type exchange factors, is classified as type III effector proteins of bacterial pathogens (Bulgin et al. 2010). They mimic functionally, but not structurally, eukaryotic GEFs by efficiently activating Rac1 and Cdc42 and thus induce "the trigger mechanism of cell entry" (see Chap. 4) (Bulgin et al. 2010; Rudolph et al. 1999).

14.5 GTPase-Activating Proteins

Hydrolysis of the bound GTP is the timing mechanism that terminates signal transduction of the Rho family proteins and returns them to their GDP-bound inactive state (Jaiswal et al. 2012). The intrinsic GTP hydrolysis (GTPase) reaction is usually slow, but can be stimulated by several orders of magnitude through interaction with Rho-specific GAPs (Eberth et al. 2005; Fidyk and Cerione 2002; Zhang and Zheng 1998). The RhoGAP family is defined by the presence of a conserved catalytic GAP domain which is sufficient for the interaction with Rho proteins and mediating accelerated catalysis (Scheffzek and Ahmadian 2005). The GAP domain supplies a conserved arginine residue, termed "arginine finger", into the GTP-binding site of the cognate Rho protein, in order to stabilize the transition state and catalyze the GTP hydrolysis reaction (Nassar et al. 1998; Rittinger et al. 1997). A similar mechanism is utilized by other small GTP-binding proteins

(Scheffzek and Ahmadian 2005), including Ras, Rab, and Arf, although the sequence and folding of the respective GAP families are different (Ismail et al. 2010; Pan et al. 2006; Scheffzek et al. 1997). Masking the catalytic arginine finger is an elegant mechanism for the inhibition of the GAP activity. This has been recently shown for the tumor suppressor protein DLC1, a RhoGAP, which is competitively and selectively inhibited by the SH3 domain of p120RasGAP (Jaiswal et al. 2014).

RhoGAP insensitivity can be achieved by the substitution of either the catalytic arginine of the GAP domain (Fidyk and Cerione 2002; Graham et al. 1999) or amino acids critical for the GTP hydrolysis in Rho proteins, e.g., Glycine 12 and Glutamine 61 in Rac1 and Cdc42 or Glycine 14 and Glutamine 63 in RhoA, which are known as the constitutive active mutants (Ahmadian et al. 1997; Graham et al. 1999). Most remarkably, a similar mechanistic strategy has been mimicked by bacterial GAPs (see Chap. 4), such as the *Salmonella typhimurium* virulence factor SptP, the *Pseudomonas aeruginosa* cytotoxin ExoS, and *Yersinia pestis* YopE, even though they do not share any sequence or structural similarity to eukaryotic RhoGAP domains (Evdokimov et al. 2002; Stebbins and Galan 2000; Wurtele et al. 2001).

The first RhoGAP, p50RhoGAP, was identified by biochemical analysis of human spleen cell extracts in the presence of recombinant RhoA (Garrett et al. 1989). Since then more than 80 RhoGAP containing proteins have been identified in eukaryotes, ranging from yeast to human (Lancaster et al. 1994; Moon and Zheng 2003). The RhoGAP domain (also known as Bcr-homology, BH domain) containing proteins are present throughout the genome and rarely cluster in specific chromosomal regions (Peck et al. 2002). The majority of the RhoGAP family members are frequently accompanied by several other functional domains and motifs implicated in tight regulation and membrane targeting (Eberth et al. 2009; Moon and Zheng 2003; Tcherkezian and Lamarche-Vane 2007). Numerous mechanisms have been shown to affect the specificity and the catalytic activity of the RhoGAPs, e.g., intramolecular autoinhibition (Eberth et al. 2009), posttranslational modification (Minoshima et al. 2003), and regulation by interaction with lipid membrane (Ligeti et al. 2004) and proteins (Yang et al. 2009).

14.6 Conclusions

Abnormal activation of Rho proteins has been shown to play a crucial role in cancer, infectious and cognitive disorders, and cardiovascular diseases. However, several tasks have to be yet accomplished in order to understand the complexity of Rho proteins signaling: (1) The Rho family comprises of 20 signaling proteins, of which only RhoA, Rac1, and Cdc42 have been comprehensively studied so far. The functions of the other less-characterized members of this protein family await detailed investigation. (2) Despite intensive research over the last two decades, the mechanisms by which RhoGDIs associate and extract the Rho proteins from the

membrane and the factors displacing the Rho protein from the complex with RhoGDI remain to be elucidated. (3) For the regulation of the 22 Rho proteins, a tremendous number of their regulatory proteins (>74 GEFs and >80 GAPs) exist in the human genome. How these regulators selectively recognize their Rho protein targets is not well understood and majority of GEFs and GAPs in humans so far remain uncharacterized. (4) Most of the GEFs and GAPs themselves need to be regulated and require activation through the relief of autoinhibitory elements (Chow et al. 2013; Eberth et al. 2009; Jaiswal et al. 2011; Mitin et al. 2007; Moskwa et al. 2005; Rojas et al. 2007; Yohe et al. 2008). With a few exceptions (Cherfils and Zeghouf 2013; Mayer et al. 2013), it is conceptually still unclear how such autoregulatory mechanisms are operated. A better understanding of the specificity and the mode of action of these regulatory proteins is not only fundamentally important for many aspects of biology but is also a master key for the development of drugs against a variety of diseases caused by aberrant functions of Rho proteins.

References

Adra CN, Manor D, Ko JL et al (1997) RhoGDIgamma: a GDP-dissociation inhibitor for Rho proteins with preferential expression in brain and pancreas. Proc Natl Acad Sci USA 94:4279–4284

Ahmadian MR, Mittal R, Hall A et al (1997) Aluminum fluoride associates with the small guanine nucleotide binding proteins. FEBS Lett 408:315–318

Aittaleb M, Boguth CA, Tesmer JJ (2010) Structure and function of heterotrimeric G protein-regulated Rho guanine nucleotide exchange factors. Mol Pharmacol 77:111–125

Bishop AL, Hall A (2000) Rho GTPases and their effector proteins. Biochem J 348(Pt 2):241–255

Bos JL, Rehmann H, Wittinghofer A (2007) GEFs and GAPs: critical elements in the control of small G proteins. Cell 129:865–877

Bouguet-Bonnet S, Buck M (2008) Compensatory and long-range changes in picosecond-nanosecond main-chain dynamics upon complex formation: 15N relaxation analysis of the free and bound states of the ubiquitin-like domain of human plexin-B1 and the small GTPase Rac1. J Mol Biol 377:1474–1487

Boulter E, Garcia-Mata R (2010) RhoGDI: a rheostat for the Rho switch. Small GTPases 1:65–68

Boureux A, Vignal E, Faure S et al (2007) Evolution of the Rho family of ras-like GTPases in eukaryotes. Mol Biol Evol 24:203–216

Bulgin R, Raymond B, Garnett JA et al (2010) Bacterial guanine nucleotide exchange factors SopE-like and WxxxE effectors. Infect Immun 78:1417–1425

Burridge K, Wennerberg K (2004) Rho and Rac take center stage. Cell 116:167–179

Cherfils J, Chardin P (1999) GEFs: structural basis for their activation of small GTP-binding proteins. Trends Biochem Sci 24:306–311

Cherfils J, Zeghouf M (2013) Regulation of small GTPases by GEFs, GAPs, and GDIs. Physiol Rev 93:269–309

Chow CR, Suzuki N, Kawamura T et al (2013) Modification of p115RhoGEF Ser(330) regulates its RhoGEF activity. Cell Signal 25:2085–2092

Chuang TH, Xu X, Knaus UG et al (1993) GDP dissociation inhibitor prevents intrinsic and GTPase activating protein-stimulated GTP hydrolysis by the Rac GTP-binding protein. J Biol Chem 268:775–778

Cook DR, Rossman KL, Der CJ (2013) Rho guanine nucleotide exchange factors: regulators of Rho GTPase activity in development and disease. Oncogene 16:362

DerMardirossian C, Bokoch GM (2005) GDIs: central regulatory molecules in Rho GTPase activation. Trends Cell Biol 15:356–363

DerMardirossian C, Schnelzer A, Bokoch GM (2004) Phosphorylation of RhoGDI by Pak1 mediates, dissociation of Rac GTPase. Mol Cell 15:117–127

DerMardirossian C, Rocklin G, Seo JY et al (2006) Phosphorylation of RhoGDI by Src regulates Rho GTPase binding and cytosol-membrane cycling. Mol Biol Cell 17:4760–4768

Dubash AD, Wennerberg K, Garcia-Mata R et al (2007) A novel role for Lsc/p115 RhoGEF and LARG in regulating RhoA activity downstream of adhesion to fibronectin. J Cell Sci 120:3989–3998

Dvorsky R, Ahmadian MR (2004) Always look on the bright site of Rho: structural implications for a conserved intermolecular interface. EMBO Rep 5:1130–1136

Eberth A, Dvorsky R, Becker CF et al (2005) Monitoring the real-time kinetics of the hydrolysis reaction of guanine nucleotide-binding proteins. Biol Chem 386:1105–1114

Eberth A, Lundmark R, Gremer L et al (2009) A BAR domain-mediated autoinhibitory mechanism for RhoGAPs of the GRAF family. Biochem J 417:371–377

Erickson JW, Cerione RA (2004) Structural elements, mechanism, and evolutionary convergence of Rho protein-guanine nucleotide exchange factor complexes. Biochemistry 43:837–842

Etienne-Manneville S, Hall A (2002) Rho GTPases in cell biology. Nature 420:629–635

Eva A, Vecchio G, Rao CD et al (1988) The predicted DBL oncogene product defines a distinct class of transforming proteins. Proc Natl Acad Sci USA 85:2061–2065

Evdokimov AG, Tropea JE, Routzahn KM et al (2002) Crystal structure of the Yersinia pestis GTPase activator YopE. Protein Sci 11:401–408

Fan L, Mellor H (2012) The small Rho GTPase Rif and actin cytoskeletal remodelling. Biochem Soc Trans 40:268–272

Fidyk NJ, Cerione RA (2002) Understanding the catalytic mechanism of GTPase-activating proteins: demonstration of the importance of switch domain stabilization in the stimulation of GTP hydrolysis. Biochemistry 41:15644–15653

Fiegen D, Blumenstein L, Stege P et al (2002) Crystal structure of Rnd3/RhoE: functional implications. FEBS Lett 525:100–104

Fiegen D, Haeusler LC, Blumenstein L et al (2004) Alternative splicing of Rac1 generates Rac1b, a self-activating GTPase. J Biol Chem 279:4743–4749

Fukumoto Y, Kaibuchi K, Hori Y et al (1990) Molecular-cloning and characterization of a novel type of regulatory protein (Gdi) for the Rho proteins, Ras P21-Like small Gtp-binding proteins. Oncogene 5:1321–1328

Gad AK, Aspenstrom P (2010) Rif proteins take to the RhoD: Rho GTPases at the crossroads of actin dynamics and membrane trafficking. Cell Signal 22:183–189

Garavini H, Riento K, Phelan JP et al (2002) Crystal structure of the core domain of RhoE/Rnd3: a constitutively activated small G protein. Biochemistry 41:6303–6310

Garcia-Mata R, Boulter E, Burridge K (2011) The 'invisible hand': regulation of RHO GTPases by RHOGDIs. Nat Rev Mol Cell Biol 12:493–504

Garrett MD, Self AJ, van Oers C et al (1989) Identification of distinct cytoplasmic targets for ras/R-ras and rho regulatory proteins. J Biol Chem 264:10–13

Graham DL, Eccleston JF, Lowe PN (1999) The conserved arginine in rho-GTPase-activating protein is essential for efficient catalysis but not for complex formation with Rho.GDP and aluminum fluoride. Biochemistry 38:985–991

Gu Y, Zheng Y, Williams DA (2005) RhoH GTPase: a key regulator of hematopoietic cell proliferation and apoptosis? Cell Cycle 4:201–202

Guo Z, Ahmadian MR, Goody RS (2005) Guanine nucleotide exchange factors operate by a simple allosteric competitive mechanism. Biochemistry 44:15423–15429

Haeusler LC, Hemsath L, Fiegen D et al (2006) Purification and biochemical properties of Rac1, 2, 3 and the splice variant Rac1b. Methods Enzymol 406:1–11

Hall A, Lalli G (2010) Rho and Ras GTPases in axon growth, guidance, and branching. Cold Spring Harb Perspect Biol 2:a001818

Hancock JF, Hall A (1993) A novel role for RhoGDI as an inhibitor of GAP proteins. EMBO J 12:1915–1921

Hart MJ, Eva A, Evans T et al (1991) Catalysis of guanine nucleotide exchange on the CDC42Hs protein by the dbl oncogene product. Nature 354:311–314

Hart MJ, Maru Y, Leonard D et al (1992) A GDP dissociation inhibitor that serves as a GTPase inhibitor for the Ras-like protein CDC42Hs. Science 258:812–815

Heasman SJ, Ridley AJ (2008) Mammalian Rho GTPases: new insights into their functions from in vivo studies. Nat Rev Mol Cell Biol 9:690–701

Hiraoka K, Kaibuchi K, Ando S et al (1992) Both stimulatory and inhibitory GDP/GTP exchange proteins, smg GDS and rho GDI, are active on multiple small GTP-binding proteins. Biochem Biophys Res Commun 182:921–930

Hoffman GR, Cerione RA (2002) Signaling to the Rho GTPases: networking with the DH domain. FEBS Lett 513:85–91

Hutchinson JP, Eccleston JF (2000) Mechanism of nucleotide release from Rho by the GDP dissociation stimulator protein. Biochemistry 39:11348–11359

Ismail SA, Vetter IR, Sot B et al (2010) The structure of an Arf-ArfGAP complex reveals a Ca2+ regulatory mechanism. Cell 141:812–821

Jaiswal M, Gremer L, Dvorsky R et al (2011) Mechanistic insights into specificity, activity, and regulatory elements of the regulator of G-protein signaling (RGS)-containing Rho-specific guanine nucleotide exchange factors (GEFs) p115, PDZ-RhoGEF (PRG), and leukemia-associated RhoGEF (LARG). J Biol Chem 286:18202–18212

Jaiswal M, Dubey BN, Koessmeier KT et al (2012) Biochemical assays to characterize Rho GTPases. Methods Mol Biol 827:37–58

Jaiswal M, Dvorsky R, Ahmadian MR (2013a) Deciphering the molecular and functional basis of Dbl family proteins: a novel systematic approach toward classification of selective activation of the Rho family proteins. J Biol Chem 288:4486–4500

Jaiswal M, Fansa EK, Dvorsky R et al (2013b) New insight into the molecular switch mechanism of human Rho family proteins: shifting a paradigm. Biol Chem 394:89–95

Jaiswal M, Dvorsky R, Amin E et al (2014) Functional crosstalk between Ras and Rho pathways: p120RasGAP competitively inhibits the RhoGAP activity of Deleted in Liver Cancer (DLC) tumor suppressors by masking its catalytic arginine finger. J Biol Chem 289:6839–6849

Joneson T, Bar-Sagi D (1997) Ras effectors and their role in mitogenesis and oncogenesis. J Mol Med (Berl) 75:587–593

Jordan P, Brazao R, Boavida MG et al (1999) Cloning of a novel human Rac1b splice variant with increased expression in colorectal tumors. Oncogene 18:6835–6839

Karnoub AE, Der CJ, Campbell SL (2001) The insert region of Rac1 is essential for membrane ruffling but not cellular transformation. Mol Cell Biol 21:2847–2857

Klebe C, Prinz H, Wittinghofer A et al (1995) The kinetic mechanism of Ran–nucleotide exchange catalyzed by RCC1. Biochemistry 34:12543–12552

Lammers M, Meyer S, Kuhlmann D et al (2008) Specificity of interactions between mDia isoforms and Rho proteins. J Biol Chem 283:35236–35246

Lancaster CA, Taylor-Harris PM, Self AJ et al (1994) Characterization of rhoGAP. A GTPase-activating protein for rho-related small GTPases. J Biol Chem 269:1137–1142

Leonard D, Hart MJ, Platko JV et al (1992) The identification and characterization of a GDP-dissociation inhibitor (GDI) for the CDC42Hs protein. J Biol Chem 267:22860–22868

Li X, Bu X, Lu B et al (2002) The hematopoiesis-specific GTP-binding protein RhoH is GTPase deficient and modulates activities of other Rho GTPases by an inhibitory function. Mol Cell Biol 22:1158–1171

Ligeti E, Dagher MC, Hernandez SE et al (2004) Phospholipids can switch the GTPase substrate preference of a GTPase-activating protein. J Biol Chem 279:5055–5058

Loirand G, Scalbert E, Bril A et al (2008) Rho exchange factors in the cardiovascular system. Curr Opin Pharmacol 8:174–180

Mayer S, Kumar R, Jaiswal M et al (2013) Collybistin activation by GTP-TC10 enhances postsynaptic gephyrin clustering and hippocampal GABAergic neurotransmission. Proc Natl Acad Sci USA 110:20795–20800

Meller N, Merlot S, Guda C (2005) CZH proteins: a new family of Rho-GEFs. J Cell Sci 118:4937–4946

Minoshima Y, Kawashima T, Hirose K et al (2003) Phosphorylation by aurora B converts MgcRacGAP to a RhoGAP during cytokinesis. Dev Cell 4:549–560

Mitin N, Betts L, Yohe ME et al (2007) Release of autoinhibition of ASEF by APC leads to CDC42 activation and tumor suppression. Nat Struct Mol Biol 14:814–823

Moon SY, Zheng Y (2003) Rho GTPase-activating proteins in cell regulation. Trends Cell Biol 13:13–22

Moskwa P, Paclet MH, Dagher MC et al (2005) Autoinhibition of p50 Rho GTPase-activating protein (GAP) is released by prenylated small GTPases. J Biol Chem 280:6716–6720

Mulinari S, Hacker U (2010) Rho-guanine nucleotide exchange factors during development: Force is nothing without control. Small GTPases 1:28–43

Mulloy JC, Cancelas JA, Filippi MD et al (2010) Rho GTPases in hematopoiesis and hemopathies. Blood 115:936–947

Nassar N, Hoffman GR, Manor D et al (1998) Structures of Cdc42 bound to the active and catalytically compromised forms of Cdc42GAP. Nat Struct Biol 5:1047–1052

Nisimoto Y, Freeman JL, Motalebi SA et al (1997) Rac binding to p67(phox). Structural basis for interactions of the Rac1 effector region and insert region with components of the respiratory burst oxidase. J Biol Chem 272:18834–18841

Ohga N, Kikuchi A, Ueda T et al (1989) Rabbit intestine contains a protein that inhibits the dissociation of GDP from and the subsequent binding of GTP to rhoB p20, a ras p21-like GTP-binding protein. Biochem Biophys Res Commun 163:1523–1533

Pan X, Eathiraj S, Munson M et al (2006) TBC-domain GAPs for Rab GTPases accelerate GTP hydrolysis by a dual-finger mechanism. Nature 442:303–306

Peck J, Douglas Gt WCH et al (2002) Human RhoGAP domain-containing proteins: structure, function and evolutionary relationships. FEBS Lett 528:27–34

Pick E, Gorzalczany Y, Engel S (1993) Role of the rac1 p21-GDP-dissociation inhibitor for rho heterodimer in the activation of the superoxide-forming NADPH oxidase of macrophages. Eur J Biochem 217:441–455

Riou P, Villalonga P, Ridley AJ (2010) Rnd proteins: multifunctional regulators of the cytoskeleton and cell cycle progression. Bioessays 32:986–992

Rittinger K (2009) Snapshots form a big picture of guanine nucleotide exchange. Sci Signal 2:pe63

Rittinger K, Walker PA, Eccleston JF et al (1997) Structure at 1.65 A of RhoA and its GTPase-activating protein in complex with a transition-state analogue. Nature 389:758–762

Roberts PJ, Mitin N, Keller PJ et al (2008) Rho Family GTPase modification and dependence on CAAX motif-signaled posttranslational modification. J Biol Chem 283:25150–25163

Rojas RJ, Yohe ME, Gershburg S et al (2007) Galphaq directly activates p63RhoGEF and Trio via a conserved extension of the Dbl homology-associated pleckstrin homology domain. J Biol Chem 282:29201–29210

Rose R, Weyand M, Lammers M et al (2005) Structural and mechanistic insights into the interaction between Rho and mammalian Dia. Nature 435:513–518

Rossman KL, Worthylake DK, Snyder JT et al (2002) Functional analysis of cdc42 residues required for Guanine nucleotide exchange. J Biol Chem 277:50893–50898

Rossman KL, Der CJ, Sondek J (2005) GEF means go: turning on RHO GTPases with guanine nucleotide-exchange factors. Nat Rev Mol Cell Biol 6:167–180

Rudolph MG, Weise C, Mirold S et al (1999) Biochemical analysis of SopE from Salmonella typhimurium, a highly efficient guanosine nucleotide exchange factor for RhoGTPases. J Biol Chem 274:30501–30509

Scheffzek K, Ahmadian MR (2005) GTPase activating proteins: structural and functional insights 18 years after discovery. Cell Mol Life Sci 62:3014–3038

Scheffzek K, Ahmadian MR, Kabsch W et al (1997) The Ras-RasGAP complex: structural basis for GTPase activation and its loss in oncogenic Ras mutants. Science 277:333–338

Scherle P, Behrens T, Staudt LM (1993) Ly-GDI, a GDP-dissociation inhibitor of the RhoA GTP-binding protein, is expressed preferentially in lymphocytes. Proc Natl Acad Sci USA 90:7568–7572

Schmidt A, Hall A (2002) Guanine nucleotide exchange factors for Rho GTPases: turning on the switch. Genes Dev 16:1587–1609

Shutes A, Berzat AC, Chenette EJ et al (2006) Biochemical analyses of the Wrch atypical Rho family GTPases. Methods Enzymol 406:11–26

Srivastava SK, Wheelock RH, Aaronson SA et al (1986) Identification of the protein encoded by the human diffuse B-cell lymphoma (dbl) oncogene. Proc Natl Acad Sci USA 83:8868–8872

Stebbins CE, Galan JE (2000) Modulation of host signaling by a bacterial mimic: structure of the Salmonella effector SptP bound to Rac1. Mol Cell 6:1449–1460

Takahashi K, Sasaki T, Mammoto A et al (1997) Direct interaction of the Rho GDP dissociation inhibitor with ezrin/radixin/moesin initiates the activation of the Rho small G protein. J Biol Chem 272:23371–23375

Tcherkezian J, Lamarche-Vane N (2007) Current knowledge of the large RhoGAP family of proteins. Biol Cell 99:67–86

Thapar R, Karnoub AE, Campbell SL (2002) Structural and biophysical insights into the role of the insert region in Rac1 function. Biochemistry 41:3875–3883

Tnimov Z, Guo Z, Gambin Y et al (2012) Quantitative analysis of prenylated RhoA interaction with its chaperone, RhoGDI. J Biol Chem 287:26549–26562

Troeger A, Chae HD, Senturk M et al (2013) A unique carboxyl-terminal insert domain in the hematopoietic-specific, GTPase-deficient Rho GTPase RhoH regulates post-translational processing. J Biol Chem 288:36451–36462

Venter JC, Adams MD, Myers EW et al (2001) The sequence of the human genome. Science 291:1304–1351

Viaud J, Gaits-Iacovoni F, Payrastre B (2012) Regulation of the DH-PH tandem of guanine nucleotide exchange factor for Rho GTPases by phosphoinositides. Adv Biol Regul 52:303–314

Vigil D, Cherfils J, Rossman KL et al (2010) Ras superfamily GEFs and GAPs: validated and tractable targets for cancer therapy? Nat Rev Cancer 10:842–857

Vlahou G, Rivero F (2006) Rho GTPase signaling in Dictyostelium discoideum: insights from the genome. Eur J Cell Biol 85:947–959

Walker SJ, Brown HA (2002) Specificity of Rho insert-mediated activation of phospholipase D1. J Biol Chem 277:26260–26267

Wennerberg K, Der CJ (2004) Rho-family GTPases: it's not only Rac and Rho (and I like it). J Cell Sci 117:1301–1312

Wittinghofer A, Vetter IR (2011) Structure-function relationships of the G domain, a canonical switch motif. Annu Rev Biochem 80:943–971

Wurtele M, Wolf E, Pederson KJ et al (2001) How the Pseudomonas aeruginosa ExoS toxin downregulates Rac. Nat Struct Biol 8:23–26

Yamashita T, Tohyama M (2003) The p75 receptor acts as a displacement factor that releases Rho from Rho-GDI. Nat Neurosci 6:461–467

Yang XY, Guan M, Vigil D et al (2009) p120Ras-GAP binds the DLC1 Rho-GAP tumor suppressor protein and inhibits its RhoA GTPase and growth-suppressing activities. Oncogene 28:1401–1409

Yohe ME, Rossman K, Sondek J (2008) Role of the C-terminal SH3 domain and N-terminal tyrosine phosphorylation in regulation of Tim and related Dbl-family proteins. Biochemistry 47:6827–6839

Zalcman G, Closson V, Camonis J et al (1996) RhoGDI-3 is a new GDP dissociation inhibitor (GDI). Identification of a non-cytosolic GDI protein interacting with the small GTP-binding proteins RhoB and RhoG. J Biol Chem 271:30366–30374

Chapter VIII

Discussion

Ras proteins share a highly conserved GTP-binding (G) domain with five essential motifs, termed G1 to G5 (Bourne *et al.*, 1990; Bourne *et al.*, 1991). G2 and G3, also referred to as switch I and switch II, respectively, are dynamic regions that sense the nucleotide state and provide the regulator and effector-binding sites (Bourne et al., 1990; Bourne et al., 1991). Classical Ras proteins (H-, N-, and K-Ras4B) share an identical effector binding regions suggesting that they may share the same downstream effectors. In contrast, E-Ras, revealed significant differences in the effector binding regions. This implicates that it may utilize other effectors as compared with known H-Ras effectors and may consequently have different cellular functions. R-Ras proteins (R-Ras, TC21 and M-Ras) additionally show some deviations in their switch regions in comparison to classical Ras proteins, which might be the reason for different binding affinities of Ras effectors for these three proteins.

This doctoral thesis has focused on the structure-function relationship of Ras proteins and their interaction with other proteins, including downstream effectors, enzymes and scaffold proteins. In addition to the G domain interactions, we also investigated the role of extended N termini, as found some of Ras protein, such as E-RAS and R-Ras. This may provide a putative interaction site for a new group of proteins, which may determine their subcellular localization. For instance, E-Ras contains a PXXP motif that may serve as a putative binding motif for interaction with Src homology 3-containing proteins.Scaffold proteins, like Gal-1, has been shown to be critical for subcellular localization and nanoclustering of the Ras proteins. We found Gal-1 associated with a Ras effector, *e.g.*, C-Raf. In conclusion, there are many components operating on Ras proteins and their downstream pathways, which will be discuss in more details in following pages.

N-terminal Extension of E-RAS participate in protein-protein interaction

Sequence comparison between E-Ras and other Ras proteins highlighted additional regions and motifs, such as the unique N-terminus of E-RAS. However, the function of such an additional region with various putative motifs (PXXP and RRR) remained unclear. Therefore, we proposed that interaction of N-terminal extension of E-Ras might modulate its localization, signaling and/or cellular metabolism through interaction with potential adaptor/scaffold proteins.

We investigated the impact of N-terminus of E-Ras regarding cellular localization MDCK-II cells by of overexpressing different E-Ras variants. Data obtained showed no significant differences in localization of an N-terminal truncated E-Ras ($E\text{-}Ras^{\Delta N}$) as compared with $E\text{-}Ras^{WT}$. In contrast, our cell-based studies revealed that the N-terminal extension of E-Ras is critical for PI3K-AKT-mTORC activation, as $E\text{-}Ras^{\Delta N}$ remarkably revealed a significantly lower signaling activity of this pathway (Chapter 2). One explanation may be the role of the unique N terminus in the lateral segregation of E-Ras across the membrane that consequently specifies association with and activation of its effectors in

a manner reminiscent to microdomain localization of H-Ras that regulates its interaction with effector proteins of RAF1 and PI3K (Jaumot *et al.*, 2002). In addition, E-Ras was found in membrane ruffles, which may be induced by Rac1 activated by the E- RAS-PI3K-PIP3-RacGEF axis (Innocenti *et al.*, 2003; Inabe *et al.*, 2002; Dillon *et al.*, 2015). Such a scenario has been reported for the R-Ras N-terminal 26-amino acid extension, which has been proposed to positively regulate Rac1 activation and cell spreading (Holly *et al.*, 2005).

Another explanation could be the role of E-Ras N-terminus as a platform for protein-protein interaction required for the cell metabolism. Comparative proteome analysis revealed that E-Ras is associated with 51 proteins (10 with human E-Ras, 3 with rat E-Ras and 38 with both species), participating in various cellular processes, including cell cycle, transcription, immune response, signal transduction, cell adhesion, cytoskeletal dynamics and metabolism (Chapter 4). Among this pool of binding partners we found that different E-Ras variants, including isolated E-Ras N-terminus physically binds to Arginase-1 (Arg1) under cell-free condition using purified proteins. Cytosolic Arg1 is well-known to convert L-arginine to L-ornithine (Curran *et al.*, 2006). Enzymatic measurement of the Arg1 activity in the presence and in the absence of human and rat E-Ras revealed that in contrast to rat E-Ras, human E-Ras considerably potentiates the Arg1 activity. Moreover, Arginase is a critical component of the urea cycle because ornithine, the product of Arg1 activity, is the precursor of the biosynthesis of proline and polyamines (Janne *et al.*, 1991; Mezl and Knox, 1977). On the other hand, L-arginine is a substrate of both Arg1 and nitric oxide (NO) synthase. The latter catalyzes the formation of NO, which is involved in a variety of biological functions, for example, it is an established neurotransmitter in the nervous system (Durante *et al.*, 2007). Endothelial NO acts as a regulator of blood pressure and is a potent anti-microbial, cytotoxic and inflammatory mediator (Corraliza *et al.*, 1994; Hibbs *et al.*, 1988). Arginine is, at the same time, a substrate of polyamines that is required for cell proliferation, whereas No synthesis has cytostatic and cytolytic effects. In this sense, all agents controlling the relative rates of L-arginine flux between Arg1 and NO synthase may play a significant role in the regulation of cellular growth (Corraliza *et al.*, 1994). Thus, it is conceivable the observed effect of E-Ras on the Arg1 activity indirectly control cell metabolism and the balance between NO and proline synthesis.

Tryptophan-79 of E-Ras dictates its physical association with effector proteins

Ras proteins transduce extracellular signals to a variety of intracellular signaling pathways through the interaction with a wide spectrum of effector proteins. Upon GDP to GTP exchange, Ras proteins undergo conformational changes at two critical regions, switch I and II. Notably, the GTP-bound form of Ras interacts with their target effectors

through switch regions and thereby activates various pathways (Karnoub and Weinberg, 2008).

A detailed study on structure-sequence relationships revealed a distinctive effector-binding region for E-Ras in comparison to classical Ras proteins (H-, N-, and K-Ras). Subsequent interaction analysis with five different Ras effectors revealed that effector binding profile of E-Ras significantly differs from H-Ras. E-Ras^{WT} tightly bound to PI3Kα and revealed very low affinity for other Ras effectors (Chapter 2). In contrast, H-Ras showed an opposite pattern with the highest affinity for RAF1. These data were confirmed by investigating the respective downstream signaling cascades (PI3K-AKT-mTORC and RAF1-MEK1/2-ERK1/2) at the level of phosphorylated AKT, MEK1/2, and ERK1/2. Our results are consistent with a previous study of Yamanaka and co-workers (Takahashi *et al.*, 2003), who applied another PI3K isoform (PI3Kδ) and observed differences between H-RAS and E-RAS. It seems probable that E-Ras and H-Ras possess a different affinity for distinct PI3K isoforms, α, β, γ, and δ, and this may account for their specific biological outputs (Vanhaesebroeck *et al.*, 2010). Consistently, the catalytic subunit of the PI3Kγ isoform, PI3Kγ, interacts with switch I of H-Ras in anti-parallel β-sheet fashion (Pacold *et al.*, 2000). Substitutions of E-Ras residues in the switch I and II and interswitch regions with corresponding residues in H-Ras provided several interesting aspects and new insights. One is a shift in effector selection of E-Ras from PI3K to RAF1, RALGDS and PLCε. RAF1-RBD undergoes contacts with the switch I and the interswitch regions (Nassar *et al.*, 1996; Filchtinski *et al.*, 2010). However, E-Ras^{SwI}, which has an almost identical switch I when compared with H-Ras, showed a reduced binding to RAF1 that was clearly elevated when this was combined with the interswitch mutation W79R (E-RAS$^{SwI/Arg-79}$). Consistently, the major difference was observed with E-Ras^{Arg-79}, where a tryptophan was replaced by an arginine (Arg-41 in H-Ras). This variant led to increase in RAF1 binding and partly rescued the low affinity of the wild type and the switch variants (ERas$^{SwI/Arg-79}$ and E-Ras$^{SwI/Arg-79/SwII}$). According to the crystal structure (Nassar *et al.*, 1996) Arg-41 in H-Ras (Trp-79 in E-Ras) interestingly forms a hydrogen bond with the backbone oxygen of Asn-64 in RAF1-RBD that very likely enabled E-Ras^{Arg-79} to make additional electrostatic contacts with RAF1. In addition, E-Ras shares a glutamate with H-Ras (Glu-3). Glu-3 interacts in intermolecular fashion with Arg-41 and stabilizes the H-Ras-RAF1 complex formation. Accordingly, mutation of W79R in E-Ras reconstitutes such intermolecular interaction between Glu-41 and Arg-79, thus increasing significantly the interaction between E-Ras^{Arg-79} and RAF1. Another important contribution to effector binding concerning Trp-79 originates very likely in its expulsion from the above-mentioned Glu-41 and the ability of bound effector protein to accommodate altered conformation of Trp-79. As mentioned before, Arg-41 of H-Ras interact with Asn-64 in RAF1 in its complex structure. The space where the tryptophan can be accommodated and hydrophobically interact with the effector is thus limited resulting in diminished affinity of these effectors to E-Ras^{WT}. Moreover, switch II quadruple mutation of E-Ras (E-Ras^{SwII}) showed the largest impairment in RAF1 binding.

This was not expected especially because the structural data, reported previously (Filchtinski *et al.*, 2010; Nassar *et al.*, 1996), have shown that RAF1-RBD does not physically contact the switch II of Ras. Again, E-Ras$^{Arg\text{-}79/SwII}$ partially restored the loss of RAF1 binding but most remarkably not the E-Ras$^{SwI/SwII}$ variant that actually is almost identical to H-Ras regarding the amino acid sequence of its switch I and II regions. Even though E-Ras$^{Arg\text{-}79}$ binds more tightly to RAF1, it still does not activate the MAPK pathway like E-Ras^{WT}. Note that there was no increase in MEK and ERK phosphorylation, and we detected even the opposite, namely a significant decrease in pMEK1/2 and pERK1/2 as compared with the vector control. An explanation for the absence of E-Ras$^{Arg\text{-}79}$ signaling toward the MAPK pathway is that most probably the additional component, including scaffold proteins such as SHOC2 (Matsunaga-Udagawa *et al.*, 2010; Cordeddu *et al.*, 2009; Rodriguez-Viciana *et al.*, 2006), may not exist in the E-RAS-Arg79-RAF1 complex. This provides the assumption that E-Ras localizes to a different membrane region then, for example, the H-Ras, RAF1, and the components of the MAPK pathway.

PI3K is a well-known effector of classical Ras proteins and promotes cellular survival (Vanhaesebroeck *et al.*, 2010). In comparison with H-Ras, E-Ras interacts more strongly with PI3Kα-RBD and activates the PI3K-AKT-mTORC cascade. Mutagenesis at switch and interswitch regions (E-Ras^{SwI}, E-Ras$^{Arg\text{-}79}$, and E-Ras^{SwII}), attenuated binding of E-Ras to PI3Kα-RBD, demonstrating the role of critical E-Ras residues at effector binding regions. These data are consistent with a previous study that has shown that PI3Kα-RBD contacts both switch I and switch II regions of H-RAS (Pacold *et al.*, 2000). Interestingly, W79R mutation of E-Ras (Arg-41 H-Ras), which has increased binding to RAF1, PLCε, and Ral-GDS, dramatically reduced the binding to PI3Kα. The affinity of this E-Ras mutant (E-Ras$^{Arg\text{-}79}$) for PI3Kα-RBD appears similar to that of H-Ras$^{Val\text{-}12}$. We think that the strong interaction between E-Ras and PI3K stems from the ability of structure to accommodate altered conformation of Trp-79 and from its hydrophobic contact to PI3K. In contrast, W79R mutation in E-Ras enables Glu-41 to attract Arg-79 and to interfere with this hydrophobic interaction, resulting in a significant reduction of the binding affinity between PI3K and E-Ras. In the same line of evidence, we also observed E-Ras$^{Arg\text{-}79}$ deficient at the activation of Ras-PI3K-AKTmTORC2 pathway (Cirstea *et al.*, 2013) as monitored with Ser-473 phosphorylation of AKT. Thus, Trp-79 in E-Ras represents a specificity-determining residue for the proper binding to and activation of PI3K.

Critical determinants for RAS-effector interaction

We have quantitatively analysed the interaction between five effector proteins and five Ras proteins, including R-Ras isoforms, under the same conditions (Chapter 3). Our measurements reveal that the Ras isoforms (H-Ras, K-Ras and N-Ras) behave similarly toward each effector but very differently as compared to R-Ras isoforms (R-Ras1 and R-Ras2), in spite of their high sequence identity. A previous study has reported that Ras isoforms much stronger activate the MAPK pathway via the RAF kinase as compared to

R-Ras isoforms (Rodriguez-Viciana *et al.*, 2004). These data are consistent with K_d values determined in our study for Ras (0.048-0.142 μM) and R-Ras (2.29-4.09 μM) isoforms. Notably, R-Ras isoforms bind, except for PLCε, similarly to all tested effector domains with an up to 4-fold difference in binding affinities compare to RAS isoforms. Interestingly, they significantly interacted with PI3Kα but not with PLCε, which is in agreement with the cell-based data reported previously (Rodriguez-Viciana *et al.*, 2004). In particular, the RAS isoforms, which exhibit high selectivity for CRAF followed by RASSF5, RALGDS and PLCε, seem not to retain its affinity for PI3Kα. It could be argued that isolated RB domain of PI3Kα, consisting of the amino acids 169-301, may lack additional binding determinants, in comparison to a 50-fold higher affinity obtained with isolated RB domain of PI3Kγ, consisting of the amino acids 144-1102 (Tables 1 and 2 chapter3) (Pacold *et al.*, 2000). As we discussed before RB domain of PI3Kα (aa 127–314) is sufficient to bind to E-Ras, but obviously not to H-Ras. However, the immunoprecipitation studies have revealed the endogenous PI3K isoforms α and γ interact with almost same affinity with both E-Ras and H-Ras (Chapter 5). These data suggest that RB domain of PI3Kα is sufficient for a tight interaction with E-Ras but obviously requires additional capacity to properly associate with H-Ras. Sequence deviations in effector binding regions may be critical for determining the minimal binding regions of Ras-effectors. It is, therefore, assumable that E-Ras and R-Ras isoforms but not Ras isoforms efficiently interact with RB domain of PI3Ks and Ras isoforms need a second binding region or alternatively a scaffold protein. Similar to the Ras isoforms, which have identical effector binding regions, the R-Ras isoforms, also including R-Ras3, revealed a very high sequence identity in these regions.Among the amino acid deviations between the Ras and R-Ras isoforms, there is a critical residue (Arg-41 in RAS isoforms substituted by Thr/Leu in RRAS isoforms residues). It probably determine effector selectivity between these isoforms, as confirmed for E-Ras that has a tryptophan (Trp-79) at the corresponding position of Arg-41 in H-Ras and has exhibited a higher selectivity for PI3K than CRAF.

The RB and RA domains share higher sequence homologies if they are aligned individually. However, there is no common consensus sequence for Ras binding if they are aligned together, particularly in the Ras binding regions R1 to R5. Therefore there is no identical patch on RAS effector proteins. However, intermolecular β-sheet interactions between Ras proteins and their effectors are conserved and seem to supply the role of identical patch, or in this special case a stretch, of homologous amino acid residues. The analysis of complex structures showed that these interactions, covered by the recognition region R1 in the interaction matrix, are prevailing and occur in almost all structures. In following, we have analysed the proximity of effector binding residues in different Ras isoforms in the same way as of residues involved in β-sheet interactions and summarized the results as matrices. Introduction of four different interaction types in the matrix with high scores of separated main-chain and side-chain Ras-effector interactions allowed a detailed inspection of central R1 region. Strikingly, there are three

hotspots, which largely undergo main-chain/main-chain interactions (Glu-37 of Ras proteins with effector residues at position 68 and 69, respectively Asp-38 with residues at position 67). These observations confirm the central role of R1 in the association of Ras proteins with their effectors and strongly suggest that the main-chain/main-chain interactions within this region are crucial for the recognition of these classes of proteins. Finally, we note that interactions in R1 also dependent, to certain extend, on side chains of accompanying amino acids. They indirectly support the formation of β-sheet on both sides of complexes. However, they also utilize their side chains in intramolecular interactions significantly contributing to the complex formation. In this way, Asp-38 interacts by its side chain exclusively with the effector residues at positions 68 and 69 within R1. Side chains of Glu-37 and Ile-37 undergo contacts with residues at positions 57 and 59 outside of the effector β-strand within the region R3. On the effector side of complexes, there are only two positions that contain identical or highly homologous amino acids, namely the position 59 and 84. They are in both cases populated by positively charged residues, with exception of PLCε that has a Gln at position 59. These residues interact with negatively charged residues on Ras proteins (Glu-37 and Asp-33) and strongly contribute to the formation of complexes. However, no unique and/or particular residue of effectors can be attributed to overall differences observed for their association with Ras proteins. Effectors interacting residues are so variable at almost all interacting spots that only their concerted action is likely to explain measured diversity.

Previous studies have shown that Ras mutants (Thr-35, Glu-37, Asp-38 and Tyr-40) including also residues mentioned above, preferentially interact with some effectors but not others (Khosravi-Far *et al.*, 1996; Khwaja *et al.*, 1997; Vavvas *et al.*, 1998; White *et al.*, 1995).The invariant Thr-35 of Ras was not gated in one of the three main regions in the matrix as it is mainly burden in Ras structure and does not directly interact with RAF1. However, Spoerner and colleagues have shown that T35S mutation drastically reduces H-Ras affinity for effectors, including CRAF-RB (60-fold) and RALGDS-RA (>100-fold) (Spoerner *et al.*, 2001). On the other hand E37G mutation results in loss of PI3K and CRAF binding, but is able to interact with RA domain-containing effectors, such as RALGDS, RASSF5 and BYR2 (White *et al.*, 1995). Our interaction matrix shows contacts between E37G of H-Ras and positively charged residues 61 and 69- and main-chain interactions with residue 69, and 70 of effectors. D38A mutation has been shown to retain CRAF binding but to lose interaction with PI3K, RALGDS and RASSF5 (Katz and McCormick, 1997; Vavvas *et al.*, 1998). Among different effector binding mutants, Y40C selectively activates PI3K but is unable to activate other effectors, such as RAF1, RALGDS, RASSF5 and BYR2 (Rodriguez-Viciana *et al.*, 1997). H-RasG12V/Y40C and H-RasG12V/E37G have been reported to cooperatively induce cell transformation via PI3K and RALGDS, respectively, but not via CRAF (Khosravi-Far *et al.*, 1996). Vandal and colleagues have observed that K-RasG12V/Y40C-PI3K has shown the largest impact on an increase in tumour size whereas K-RasG12V/E38G-CRAF resulted in a decrease in tumour

size but an increase of the number of tumors when combined with BRAFV600E (Vandal *et al.*, 2014).

Being central elements of R1, R3 and R4, our analysis not only confirms a prominent role of Glu-37, Asp-38 and Tyr-40 in effector binding but gives also hints for the mode of their interaction, which relies on the main-chain main-chain interaction. As this interaction is in the first rank independent on 8 accompanied side chains, it can be considered as conserved also in effectors. Consequently, it supplies thus the role of homologous residues found to be essential for the recognition of regulator proteins by Rho GTPases. Hence we state, that these Ras residues are responsible with their main-chain atoms for the recognition of effectors. On the other hand, side chains of these residues are still influential on the binding with effectors. Either indirectly affecting the structure of Ras switch I or directly interacting with effector residues within the regions R3 and R4 of our interaction matrix.

In conclusion, our data collectively support previous observations that the specificity in the signaling properties and biological functions of the various Ras proteins arises from the specific combination of effector pathways they regulate in each cell type. Considering the identity of interacting residues of different types of isoforms, a uniform association of Ras isoforms or rather R-Ras isoforms can be expected with a particular effector. An interesting issue, which is increasingly appreciated, is a RAS-membrane interface that appears to generate Ras isoform specificity with respect to effector interactions (Abankwa *et al.*, 2008; Mazhab-Jafari *et al.*, 2015; Parker and Mattos, 2015).This is likely achieved by Ras-specific scaffold proteins, including CaM, GAL1, GAL3, IQGAPs, NPM1, NCL, SHOC2/SUR8 (Abraham *et al.*, 2009; Rodriguez-Viciana *et al.*, 2006) which may modulate isoform specificity at specific site of the cell. Another critical aspect is sorting/trafficking of the isoforms (Zhou *et al.*, 2016; Zheng *et al.*, 2012) that has recently been shown to be highly specific for the respective Ras proteins and dependents on specific posttranslational modifications, including prenylation and acylation (Jang *et al.*, 2015; Lynch *et al.*, 2015), phosphorylation (Bivona *et al.*, 2006; Sung *et al.*, 2013), ubiquitination (Wang *et al.*, 2015; Rodriguez-Viciana and McCormick, 2006; Jura *et al.*, 2006; de la Vega *et al.*, 2010) and acetylation (Yang *et al.*, 2013; Knyphausen *et al.*, 2016; Yang *et al.*, 2012). Similar characteristics have been reported for the R-Ras isoforms, including protein-protein interaction required for subcellular localization, e.g., at focal adhesion or recycling endosomes, (Wurtzel *et al.*, 2015; Furuhjelm and Peranen, 2003), and posttranslational modifications (Berzat *et al.*, 2006; Oertli *et al.*, 2000; Calvo and Crespo, 2009). In addition, they contain extended N-termini that has been shown to be critical for R-Ras1 in cell migration (Holly *et al.*, 2005).The N-terminus of E-Ras, which undergoes multiple interaction with other proteins (chapter 4), contains similar to R-Ras1, putative SH3-binding motifs. These motifs may provide additional mechanisms for sorting and trafficking to specific subcellular sites.

Biological role of endogenous E-RAS in hepatic stellate cells (HSCs)

We analyzed the biochemical and proposed the binding partner of E-Ras in vitro and overexpression system. To investigate the biological functions of E-Ras we need a normal cell line or primary cells that endogenously express E-Ras. For the first time we showed the expression of E-Ras in HSCs. To date, E-Ras expression was only reported in few cancer cell lines and embryonic stem cells. The presence of E-Ras mRNA was detected in quiescent HSCs but not in activated HSCs. In contrast, other Ras-related genes, such as R-Ras, M-Ras, RalA, and Rap2A, were up-regulated E-Ras level decreased during HSC activation. At the protein level, E-Ras protein was detected in quiescent HSCs but not in other liver cell types and E-Ras was considerably down-regulated during HSC activation (d4 and d8 of cultivation). To elucidate the functions of E-Ras in quiescent HSCs, we sought E-Ras specific effectors and the corresponding downstream pathways. Interaction analyses with a set of Ras effectors showed that E-Ras preferentially interacts with PI3Kα and activates the PI3K-PDK1-AKT axis. The prominent AKT phosphorylation by mTORC2 in quiescent HSCs suggests that mTORC2-AKT acts as a candidate pathway mediates signaling downstream of E-Ras. Transient expression of E-Ras in COS-7 cells and endogenous E-Ras expression in quiescent HSCs strongly correlate with high levels of AKT phosphorylated at Thr-308 and Ser-473 through PDK1 and mTORC2, respectively. Protein interaction and immunoprecipitation analysis further revealed that E-Ras physically interacts with PI3Kα and also PI3Kγ (Chapter 5).

Activity of the mTORC2-AKT-FOXO1 axis in quiescent HSCs

Our findings indicate that E-RAS may act as an activator of the mTORC2 pathway. Exogenous E-Ras has been shown to promote phosphorylation of both AKT (Ser-473) and FOXO1 (Ser-256) in induced pluripotent stem cells generated from mouse embryonic fibroblasts (Yu *et al.*, 2014). Thus, E-Ras-AKT-FOXO1 signaling may be important for somatic cell reprogramming. We detected high levels of p-AKT^{S473} and p-FOXO1^{S256} in quiescent HSCs endogenously expressing E-Ras (Chapter 5). Phosphorylated FOXO1, sequestrated in the cytoplasm, cannot translocate to the nucleus, where it binds to gene promoters and induces apoptosis (Wang *et al.*, 2014). Interestingly, a possible link between E-Ras and mTORC2 may be mSIN1, which appears to be an upstream component and modulator of mTORC2 activity (Huang and Fingar, 2014). It has been reported that mSIN1 contains a Ras-binding domain with some homology to that of CRAF (Schroder *et al.*, 2007). Taken together, the E-Ras-mTORC2-AKTFOXO1 axis may ensure the survival of HSCs in the space of Dissé by interfering with programmed cell death.

Biological Functions of PI3K-AKT Pathway Regarding Different p110 Isoforms

The catalytic PI3K isoforms p110α and β are reported to be ubiquitously expressed, whereas the presence of p110γ and -δ is restricted mainly to hematopoietic cell types

(Vanhaesebroeck *et al.*, 2005; Kok *et al.*, 2009; Fritsch *et al.*, 2013; Fritsch and Downward, 2013). We identified E-Ras as an activator of AKT by interacting with p110α and moderately also with p110δ (Chapter 5). Our RNA and protein analyses indicated high levels of *p110*α/γ in quiescent HSCs and elevated levels of *p110*β/δ in activated HSCs. Wetzker and colleagues (Baier *et al.*, 1999) reported that retinoic acid treatment can stimulate expression of p110γ, but not p110β/δ, in U937 cells, a myelomonocytic cell line. Quiescent HSCs store high levels of retinoid acids as retinol esters in their lipid droplets, which may elicit the same function in HSCs by up-regulation of p110γ. Khadem et al. (Khadem *et al.*, 2016) have shown that HSCs also express the p110δ isoform and that p110δ deficiency in HSCs prevents their activation and their supportive roles in T_{reg} expansion in mice infected with visceral leishmaniasis. Therefore, the high level of the p110δ isoform in activated HSCs may correlate with its immunoregulatory functions.

Role of GAL-1 as scaffolding protein on Ras-effector binding

As we already mentioned the function of Ras proteins can be affected by other binding proteins, these proteins probably effect on localization of Ras proteins and also on the interaction of Ras proteins with their effectors and regulators. In the other hand some protein binds with effectors and changes the affinity of effectors to Ras proteins.

Ras proteins are highly similar in sequence and vary mostly in their C-terminal hypervariable region (HVR). This part undergoes post-translational farnesylation and palmitoylation modifications (the latter for H- and N-Ras) allowing Ras to dynamically insert into cellular membranes (Ahearn *et al.*, 2012). Ras is actively transported to the plasma membrane, where it is further organized into nanoscale signaling hubs, called nanoclusters. A Ras nanocluster comprises 6-8 Ras proteins, which in the case of the active Ras becomes transiently immobilized (Hancock and Parton, 2005; Abankwa *et al.*, 2007; Tian *et al.*, 2007). Nanoclusters are the exclusive sites of effector recruitment thus constituting highly dynamic epicentres of the Ras signaling cascade (Rotblat *et al.*, 2010; Guzman *et al.*, 2014). Nanoclustering is driven by the C-terminal membrane anchor of Ras, which also largely dictates their lateral segregation into isoform specific nanoclusters (Henis *et al.*, 2009; Abankwa *et al.*, 2010). Importantly, these features are shared with Ras dimers, which appear to constitute the smallest 'nanocluster' (Zhou and Hancock, 2015). Thus laterally segregated, Ras isoform specific nanoscale oligomeric clusters constitute an important experimental observable that correlates with the structural and functional divergence of the different Ras proteins and the emergence of Ras signaling complexes.

Only very few endogenous regulators of Ras nanoclustering, so called nanocluster scaffolds, are known. These include galectin-3 (Shalom-Feuerstein *et al.*, 2008), nucleophosmin (Inder *et al.*, 2009), caveolae (Ariotti *et al.*, 2014) and H-Ras-GTP (Zhou *et al.*, 2014) for K-Ras, and galectin-1 (Gal-1) (Belanis *et al.*, 2008; Guzman *et al.*, 2014; Rotblat *et al.*, 2010) for H-Ras-GTP. Amongst these, Gal-1 is the best-characterized

nanocluster scaffold. Gal-1 is upregulated in many tumors and associated with more progressive and invasive cancer stages (Astorgues-Xerri *et al.*, 2014; Ebrahim *et al.*, 2014).

Ras nanoclustering is indispensable for Ras signaling (Tian *et al.*, 2007), underscoring its significance for the signaling architecture of Ras. Only a handful of nanocluster regulators, so called Ras nanocluster scaffolds are known, and Gal-1 has so far been the one scaffold that was functionally and mechanistically best understood. The former model for the nanocluster scaffolding activity of Gal-1 suggests that it directly binds to the C-terminal farnesyl of active H-Ras to modulate its intracellular membrane organization (Rotblat *et al.*, 2004; Ashery *et al.*, 2006). We here presented data, which question the existing model of Gal-1 binding directly to the farnesyl-lipid on the C-terminus of Ras proteins. We did neither observe binding of Gal-1 to a farnesylated Ras-peptide, nor directly to the G-domain of Ras. Instead, we found that Gal-1 indirectly couples to Ras via a direct association with the RBD-domain of effectors (Chapter 6) and that an intact Gal-1 dimer interface is required for Gal-1 to modulate Ras nanoclustering. Others previously suggested binding of farnesylated proteins to Gal-1. Two different mutations were described that abrogated binding to farnesyl, K28T and L11A (Rotblat *et al.*, 2004). These mutants were brought in agreement by proposing a farnesyl-binding pocket along the N-terminal or dimer interface part of Gal-141. However, we did not observe any effect of the former mutation on the complexation of Gal-1 and H- Ras^{G12V}. It is conceivable that the L11A mutation near the dimer interface of Gal-1 affects the ability of Gal-1 to dimerize and thus H- Ras-GTP nanoclustering. However, this has not been shown so far.

With our new model, we resolve inconsistencies of the previous model, such as how specificity for active Ras is mediated and incorporate recent findings, which demonstrated that Raf dimer-inducing compounds do also increase Ras nanoclustering (Cho *et al.*, 2012). Thus we propose the following revised mechanistic model for the function of Gal-1 as a nanocluster scaffold: upon Ras activation and recruitment of the effectors to Ras, Gal-1 binds with high affinity to the accessible part of the RBD of effectors. Note that according to our data with non-farnesylated H- Ras^{G12V}, it is possible that Gal-1 and effectors directly bind to each other in the cytoplasm. As Gal-1 can dimerize at µM concentrations that can be found in mammalian cells (Guzman *et al.*, 2014), it could stabilize effector dimers, such as e.g. Raf-dimers. We therefore here propose that the Raf-dimers are the actual nanocluster stabilizer. This is supported by our data showing that loss of the effector binding capability of H- $Ras^{G12V-D38A}$ and knockdown of A- and B-Raf can dramatically reduce Gal-1 supported H-Ras^{G12V}nanoclustering. This model is furthermore consistent with the activity of artificially fused dimeric RBD-CRD to stabilize nanocluster (Cho *et al.*, 2012). Our model is also in agreement with data that revealed a clustered organization of Raf on the membrane (Belanis *et al.*, 2008; Nan *et al.*, 2013). Thus, the idea is corroborated that Ras-nanoclusters represent dynamic signaling hubs of Ras and its effectors.

This model may also explain the observation that Gal-1 apparently shifts the H-Ras activity from the PI3K to the Raf pathway. The higher effective affinity (i.e. as judged by our cellular FRET-experiments) of Gal-1 for the RBD of C-Raf *vs.* PI3Kα could explain, how Gal-1 shifts the signaling output relatively from PI3K to Raf, an effect that could be potentiated in a nanocluster.

Refrences

Abankwa, D., Gorfe, A. A. &Hancock, J. F. (2007). Ras nanoclusters: molecular structure and assembly. *Seminars in cell & developmental biology* 18(5): 599-607.

Abankwa, D., Gorfe, A. A., Inder, K. &Hancock, J. F. (2010). Ras membrane orientation and nanodomain localization generate isoform diversity. *Proceedings of the National Academy of Sciences of the United States of America* 107(3): 1130-1135.

Abankwa, D., Hanzal-Bayer, M., Ariotti, N., Plowman, S. J., Gorfe, A. A., Parton, R. G., McCammon, J. A. &Hancock, J. F. (2008). A novel switch region regulates H-ras membrane orientation and signal output. *EMBO J* 27(5): 727-735.

Abraham, S. J., Nolet, R. P., Calvert, R. J., Anderson, L. M. &Gaponenko, V. (2009). The hypervariable region of K-Ras4B is responsible for its specific interactions with calmodulin. *Biochemistry* 48(32): 7575-7583.

Ahearn, I. M., Haigis, K., Bar-Sagi, D. &Philips, M. R. (2012). Regulating the regulator: post-translational modification of RAS. *Nature reviews. Molecular cell biology* 13(1): 39-51.

Ahmadian, M. R. (2002). Prospects for anti-ras drugs. *Br J Haematol* 116(3): 511-518.

Ahuja, H. G., Foti, A., Zhou, D. J. &Cline, M. J. (1990). Analysis of proto-oncogenes in acute myeloid leukemia: loss of heterozygosity for the Ha-ras gene. *Blood* 75(4): 819-822.

Alexa, A., Varga, J. &Remenyi, A. (2010). Scaffolds are 'active' regulators of signaling modules. *The FEBS journal* 277(21): 4376-4382.

Almoguera, C., Shibata, D., Forrester, K., Martin, J., Arnheim, N. &Perucho, M. (1988). Most human carcinomas of the exocrine pancreas contain mutant c-K-ras genes. *Cell* 53(4): 549-554.

Apolloni, A., Prior, I. A., Lindsay, M., Parton, R. G. &Hancock, J. F. (2000). H-ras but not K-ras traffics to the plasma membrane through the exocytic pathway. *Mol Cell Biol* 20(7): 2475-2487.

Ariotti, N., Fernandez-Rojo, M. A., Zhou, Y., Hill, M. M., Rodkey, T. L., Inder, K. L., Tanner, L. B., Wenk, M. R., Hancock, J. F. &Parton, R. G. (2014). Caveolae regulate the nanoscale organization of the plasma membrane to remotely control Ras signaling. *The Journal of cell biology* 204(5): 777-792.

Ash, D. E. (2004). Structure and function of arginases. *J Nutr* 134(10 Suppl): 2760S-2764S; discussion 2765S-2767S.

Ashery, U., Yizhar, O., Rotblat, B., Elad-Sfadia, G., Barkan, B., Haklai, R. &Kloog, Y. (2006). Spatiotemporal organization of Ras signaling: rasosomes and the galectin switch. *Cellular and molecular neurobiology* 26(4-6): 471-495.

Astorgues-Xerri, L., Riveiro, M. E., Tijeras-Raballand, A., Serova, M., Neuzillet, C., Albert, S., Raymond, E. &Faivre, S. (2014). Unraveling galectin-1 as a novel therapeutic target for cancer. *Cancer treatment reviews* 40(2): 307-319.

Ayllon, V. &Rebollo, A. (2000). Ras-induced cellular events (review). *Mol Membr Biol* 17(2): 65-73.

Bagi, Z., Feher, A., Dou, H. &Broskova, Z. (2013). Selective up-regulation of arginase-1 in coronary arteries of diabetic patients. *Frontiers in immunology* 4: 293.

Baier, R., Bondeva, T., Klinger, R., Bondev, A. &Wetzker, R. (1999). Retinoic acid induces selective expression of phosphoinositide 3-kinase gamma in myelomonocytic U937 cells. *Cell Growth Differ* 10(6): 447-456.

Barbacid, M. (1990). ras oncogenes: their role in neoplasia. *Eur J Clin Invest* 20(3): 225-235.

Beaupre, D. M. &Kurzrock, R. (1999). RAS inhibitors in hematologic cancers: biologic considerations and clinical applications. *Investigational new drugs* 17(2): 137-143.

Belanis, L., Plowman, S. J., Rotblat, B., Hancock, J. F. &Kloog, Y. (2008). Galectin-1 is a novel structural component and a major regulator of h-ras nanoclusters. *Molecular biology of the cell* 19(4): 1404-1414.

Berzat, A. C., Brady, D. C., Fiordalisi, J. J. &Cox, A. D. (2006). Using inhibitors of prenylation to block localization and transforming activity. *Methods Enzymol* 407: 575-597.

Bivona, T. G., Quatela, S. E., Bodemann, B. O., Ahearn, I. M., Soskis, M. J., Mor, A., Miura, J., Wiener, H. H., Wright, L., Saba, S. G., Yim, D., Fein, A., Perez de Castro, I., Li, C., Thompson, C. B., Cox, A. D. &Philips, M. R. (2006). PKC regulates a farnesyl-electrostatic switch on K-Ras that promotes its association with Bcl-XL on mitochondria and induces apoptosis. *Molecular cell* 21(4): 481-493.

Blazevits, O., Mideksa, Y. G., Solman, M., Ligabue, A., Ariotti, N., Nakhaeizadeh, H., Fansa, E. K., Papageorgiou, A. C., Wittinghofer, A., Ahmadian, M. R. &Abankwa, D. (2016). Galectin-1 dimers can scaffold Raf-effectors to increase H-ras nanoclustering. *Scientific reports* 6: 24165.

Blidner, A. G., Mendez-Huergo, S. P., Cagnoni, A. J. &Rabinovich, G. A. (2015). Re-wiring regulatory cell networks in immunity by galectin-glycan interactions. *FEBS Lett* 589(22): 3407-3418.

Bos, J. L. (1989). ras oncogenes in human cancer: a review. *Cancer Res* 49(17): 4682-4689.

Bourne, H. R., Sanders, D. A. &McCormick, F. (1990). The GTPase superfamily: a conserved switch for diverse cell functions. *Nature* 348(6297): 125-132.

Bourne, H. R., Sanders, D. A. &McCormick, F. (1991). The GTPase superfamily: conserved structure and molecular mechanism. *Nature* 349(6305): 117-127.

Bunney, T. D., Harris, R., Gandarillas, N. L., Josephs, M. B., Roe, S. M., Sorli, S. C., Paterson, H. F., Rodrigues-Lima, F., Esposito, D., Ponting, C. P., Gierschik, P., Pearl, L. H., Driscoll, P. C. &Katan, M. (2006). Structural and mechanistic insights into ras association domains of phospholipase C epsilon. *Molecular cell* 21(4): 495-507.

Burmer, G. C. &Loeb, L. A. (1989). Mutations in the KRAS2 oncogene during progressive stages of human colon carcinoma. *Proc Natl Acad Sci U S A* 86(7): 2403-2407.

Calvo, F. &Crespo, P. (2009). Structural and spatial determinants regulating TC21 activation by RasGRF family nucleotide exchange factors. *Molecular biology of the cell* 20(20): 4289-4302.

Cama, E., Colleluori, D. M., Emig, F. A., Shin, H., Kim, S. W., Kim, N. N., Traish, A. M., Ash, D. E. &Christianson, D. W. (2003). Human arginase II: crystal structure and physiological role in male and female sexual arousal. *Biochemistry* 42(28): 8445-8451.

Camby, I., Le Mercier, M., Lefranc, F. &Kiss, R. (2006). Galectin-1: a small protein with major functions. *Glycobiology* 16(11): 137R-157R.

Cantley, L. C. (2002). The phosphoinositide 3-kinase pathway. *Science* 296(5573): 1655-1657.

Carnero, A. (2010). The PKB/AKT pathway in cancer. *Curr Pharm Des* 16(1): 34-44.

Castellano, E. &Downward, J. (2011). RAS Interaction with PI3K: More Than Just Another Effector Pathway. *Genes & cancer* 2(3): 261-274.

Cederbaum, S. D., Yu, H., Grody, W. W., Kern, R. M., Yoo, P. &Iyer, R. K. (2004). Arginases I and II: do their functions overlap? *Molecular genetics and metabolism* 81 Suppl 1: S38-44.

Chan, J. J. &Katan, M. (2013). PLCvarepsilon and the RASSF family in tumour suppression and other functions. *Advances in biological regulation* 53(3): 258-279.

Chien, U. H., Lai, M., Shih, T. Y., Verma, I. M., Scolnick, E. M., Roy-Burman, P. &Davidson, N. (1979). Heteroduplex analysis of the sequence relationships between the genomes of Kirsten and Harvey sarcoma viruses, their respective parental murine leukemia viruses, and the rat endogenous 30S RNA. *J Virol* 31(3): 752-760.

Cho, K. J., Kasai, R. S., Park, J. H., Chigurupati, S., Heidorn, S. J., van der Hoeven, D., Plowman, S. J., Kusumi, A., Marais, R. &Hancock, J. F. (2012). Raf inhibitors target ras spatiotemporal dynamics. *Curr Biol* 22(11): 945-955.

Cirstea, I. C., Gremer, L., Dvorsky, R., Zhang, S. C., Piekorz, R. P., Zenker, M. &Ahmadian, M. R. (2013). Diverging gain-of-function mechanisms of two novel KRAS mutations associated with Noonan and cardio-facio-cutaneous syndromes. *Human molecular genetics* 22(2): 262-270.

Cordeddu, V., Di Schiavi, E., Pennacchio, L. A., Ma'ayan, A., Sarkozy, A., Fodale, V., Cecchetti, S., Cardinale, A., Martin, J., Schackwitz, W., Lipzen, A., Zampino, G., Mazzanti, L., Digilio, M. C., Martinelli, S., Flex, E., Lepri, F., Bartholdi, D., Kutsche, K., Ferrero, G. B., Anichini, C., Selicorni, A., Rossi, C., Tenconi, R., Zenker, M., Merlo, D., Dallapiccola, B., Iyengar, R., Bazzicalupo, P., Gelb, B. D. &Tartaglia, M. (2009). Mutation of SHOC2 promotes aberrant protein N-myristoylation and causes Noonan-like syndrome with loose anagen hair. *Nature genetics* 41(9): 1022-1026.

Corraliza, I. M., Campo, M. L., Soler, G. &Modolell, M. (1994). Determination of arginase activity in macrophages: a micromethod. *J Immunol Methods* 174(1-2): 231-235.

Cox, A. D. &Der, C. J. (2003). The dark side of Ras: regulation of apoptosis. *Oncogene* 22(56): 8999-9006.

Curran, J. N., Winter, D. C. &Bouchier-Hayes, D. (2006). Biological fate and clinical implications of arginine metabolism in tissue healing. *Wound repair and regeneration : official publication of the Wound Healing Society [and] the European Tissue Repair Society* 14(4): 376-386.

de la Vega, M., Burrows, J. F., McFarlane, C., Govender, U., Scott, C. J. &Johnston, J. A. (2010). The deubiquitinating enzyme USP17 blocks N-Ras membrane trafficking and activation but leaves K-Ras unaffected. *The Journal of biological chemistry* 285(16): 12028-12036.

Der, C. J. (1989). The ras family of oncogenes. *Cancer Treat Res* 47: 73-119.

Der, C. J., Krontiris, T. G. &Cooper, G. M. (1982). Transforming genes of human bladder and lung carcinoma cell lines are homologous to the ras genes of Harvey and Kirsten sarcoma viruses. *Proc Natl Acad Sci U S A* 79(11): 3637-3640.

Desideri, E., Cavallo, A. L. &Baccarini, M. (2015). Alike but Different: RAF Paralogs and Their Signaling Outputs. *Cell* 161(5): 967-970.

Dillon, L. M., Bean, J. R., Yang, W., Shee, K., Symonds, L. K., Balko, J. M., McDonald, W. H., Liu, S., Gonzalez-Angulo, A. M., Mills, G. B., Arteaga, C. L. &Miller, T. W. (2015). P-REX1 creates a positive feedback loop to activate growth factor receptor, PI3K/AKT and MEK/ERK signaling in breast cancer. *Oncogene* 34(30): 3968-3976.

Dowling, D. P., Di Costanzo, L., Gennadios, H. A. &Christianson, D. W. (2008). Evolution of the arginase fold and functional diversity. *Cellular and molecular life sciences : CMLS* 65(13): 2039-2055.

Durante, W., Johnson, F. K. &Johnson, R. A. (2007). Arginase: a critical regulator of nitric oxide synthesis and vascular function. *Clin Exp Pharmacol Physiol* 34(9): 906-911.

Ebrahim, A. H., Alalawi, Z., Mirandola, L., Rakhshanda, R., Dahlbeck, S., Nguyen, D., Jenkins, M., Grizzi, F., Cobos, E., Figueroa, J. A. &Chiriva-Internati, M. (2014). Galectins in cancer: carcinogenesis, diagnosis and therapy. *Annals of translational medicine* 2(9): 88.

Evellin, S., Nolte, J., Tysack, K., vom Dorp, F., Thiel, M., Weernink, P. A., Jakobs, K. H., Webb, E. J., Lomasney, J. W. &Schmidt, M. (2002). Stimulation of phospholipase C-epsilon by the M3 muscarinic acetylcholine receptor mediated by cyclic AMP and the GTPase Rap2B. *The Journal of biological chemistry* 277(19): 16805-16813.

Feig, L. A. &Buchsbaum, R. J. (2002). Cell signaling: life or death decisions of ras proteins. *Curr Biol* 12(7): R259-261.

Ferro, E. &Trabalzini, L. (2010). RalGDS family members couple Ras to Ral signalling and that's not all. *Cellular signalling* 22(12): 1804-1810.

Filchtinski, D., Sharabi, O., Ruppel, A., Vetter, I. R., Herrmann, C. &Shifman, J. M. (2010). What makes Ras an efficient molecular switch: a computational, biophysical, and structural study of Ras-GDP interactions with mutants of Raf. *Journal of molecular biology* 399(3): 422-435.

Frias, M. A., Thoreen, C. C., Jaffe, J. D., Schroder, W., Sculley, T., Carr, S. A. &Sabatini, D. M. (2006). mSin1 is necessary for Akt/PKB phosphorylation, and its isoforms define three distinct mTORC2s. *Current biology : CB* 16(18): 1865-1870.

Friedman, S. L. (2008). Hepatic stellate cells: protean, multifunctional, and enigmatic cells of the liver. *Physiological reviews* 88(1): 125-172.

Fritsch, R., de Krijger, I., Fritsch, K., George, R., Reason, B., Kumar, M. S., Diefenbacher, M., Stamp, G. &Downward, J. (2013). RAS and RHO families of GTPases directly regulate distinct phosphoinositide 3-kinase isoforms. *Cell* 153(5): 1050-1063.

Fritsch, R. &Downward, J. (2013). SnapShot: Class I PI3K isoform signaling. *Cell* 154(4): 940-940 e941.

Furuhjelm, J. &Peranen, J. (2003). The C-terminal end of R-Ras contains a focal adhesion targeting signal. *J Cell Sci* 116(Pt 18): 3729-3738.

Geering, B., Cutillas, P. R. &Vanhaesebroeck, B. (2007). Regulation of class IA PI3Ks: is there a role for monomeric PI3K subunits? *Biochemical Society transactions* 35(Pt 2): 199-203.

Geerts, A. (2004). On the origin of stellate cells: mesodermal, endodermal or neuro-ectodermal? *Journal of Hepatology* 40(2): 331-334.

Gentry, L. R., Martin, T. D., Reiner, D. J. &Der, C. J. (2014). Ral small GTPase signaling and oncogenesis: More than just 15minutes of fame. *Biochimica et biophysica acta* 1843(12): 2976-2988.

Gresset, A., Sondek, J. &Harden, T. K. (2012). The phospholipase C isozymes and their regulation. *Sub-cellular biochemistry* 58: 61-94.

Guerrero, I. &Pellicer, A. (1987). Mutational activation of oncogenes in animal model systems of carcinogenesis. *Mutat Res* 185(3): 293-308.

Guzman, C., Solman, M., Ligabue, A., Blazevits, O., Andrade, D. M., Reymond, L., Eggeling, C. &Abankwa, D. (2014). The efficacy of Raf kinase recruitment to the

GTPase H-ras depends on H-ras membrane conformer-specific nanoclustering. *The Journal of biological chemistry* 289(14): 9519-9533.

Hancock, J. F. &Parton, R. G. (2005). Ras plasma membrane signalling platforms. *Biochem J* 389(Pt 1): 1-11.

Harjes, E., Harjes, S., Wohlgemuth, S., Muller, K. H., Krieger, E., Herrmann, C. &Bayer, P. (2006). GTP-Ras disrupts the intramolecular complex of C1 and RA domains of Nore1. *Structure* 14(5): 881-888.

Heiss, C., Rodriguez-Mateos, A. &Kelm, M. (2015). Central role of eNOS in the maintenance of endothelial homeostasis. *Antioxidants & redox signaling* 22(14): 1230-1242.

Henis, Y. I., Hancock, J. F. &Prior, I. A. (2009). Ras acylation, compartmentalization and signaling nanoclusters (Review). *Molecular membrane biology* 26(1): 80-92.

Hennig, A., Markwart, R., Esparza-Franco, M. A., Ladds, G. &Rubio, I. (2015). Ras activation revisited: role of GEF and GAP systems. *Biol Chem* 396(8): 831-848.

Hibbs, J. B., Jr., Taintor, R. R., Vavrin, Z. &Rachlin, E. M. (1988). Nitric oxide: a cytotoxic activated macrophage effector molecule. *Biochemical and biophysical research communications* 157(1): 87-94.

Hirsch-Ginsberg, C., LeMaistre, A. C., Kantarjian, H., Talpaz, M., Cork, A., Freireich, E. J., Trujillo, J. M., Lee, M. S. &Stass, S. A. (1990). RAS mutations are rare events in Philadelphia chromosome-negative/bcr gene rearrangement-negative chronic myelogenous leukemia, but are prevalent in chronic myelomonocytic leukemia. *Blood* 76(6): 1214-1219.

Holly, S. P., Larson, M. K. &Parise, L. V. (2005). The unique N-terminus of R-ras is required for Rac activation and precise regulation of cell migration. *Molecular biology of the cell* 16(5): 2458-2469.

Huang, K. &Fingar, D. C. (2014). Growing knowledge of the mTOR signaling network. *Seminars in cell & developmental biology* 36: 79-90.

Huang, L., Hofer, F., Martin, G. S. &Kim, S. H. (1998). Structural basis for the interaction of Ras with RalGDS. *Nat Struct Biol* 5(6): 422-426.

Inabe, K., Ishiai, M., Scharenberg, A. M., Freshney, N., Downward, J. &Kurosaki, T. (2002). Vav3 modulates B cell receptor responses by regulating phosphoinositide 3-kinase activation. *J Exp Med* 195(2): 189-200.

Inder, K. L., Lau, C., Loo, D., Chaudhary, N., Goodall, A., Martin, S., Jones, A., van der Hoeven, D., Parton, R. G., Hill, M. M. &Hancock, J. F. (2009). Nucleophosmin and nucleolin regulate K-Ras plasma membrane interactions and MAPK signal transduction. *The Journal of biological chemistry* 284(41): 28410-28419.

Innocenti, M., Frittoli, E., Ponzanelli, I., Falck, J. R., Brachmann, S. M., Di Fiore, P. P. &Scita, G. (2003). Phosphoinositide 3-kinase activates Rac by entering in a complex with Eps8, Abi1, and Sos-1. *The Journal of cell biology* 160(1): 17-23.

Jang, H., Abraham, S. J., Chavan, T. S., Hitchinson, B., Khavrutskii, L., Tarasova, N. I., Nussinov, R. &Gaponenko, V. (2015). Mechanisms of membrane binding of small GTPase K-Ras4B farnesylated hypervariable region. *The Journal of biological chemistry* 290(15): 9465-9477.

Janne, J., Alhonen, L. &Leinonen, P. (1991). Polyamines: from molecular biology to clinical applications. *Ann Med* 23(3): 241-259.

Janssen, J. W., Steenvoorden, A. C., Lyons, J., Anger, B., Bohlke, J. U., Bos, J. L., Seliger, H. &Bartram, C. R. (1987). RAS gene mutations in acute and chronic myelocytic

leukemias, chronic myeloproliferative disorders, and myelodysplastic syndromes. *Proc Natl Acad Sci U S A* 84(24): 9228-9232.

Jaumot, M., Yan, J., Clyde-Smith, J., Sluimer, J. &Hancock, J. F. (2002). The linker domain of the Ha-Ras hypervariable region regulates interactions with exchange factors, Raf-1 and phosphoinositide 3-kinase. *The Journal of biological chemistry* 277(1): 272-278.

Jura, N., Scotto-Lavino, E., Sobczyk, A. &Bar-Sagi, D. (2006). Differential modification of Ras proteins by ubiquitination. *Molecular cell* 21(5): 679-687.

Kaizaki, R., Yashiro, M., Shinto, O., Yasuda, K., Matsuzaki, T., Sawada, T. &Hirakawa, K. (2009). Expression of ERas oncogene in gastric carcinoma. *Anticancer Res* 29(6): 2189-2193.

Kanyo, Z. F., Chen, C. Y., Daghigh, F., Ash, D. E. &Christianson, D. W. (1992). Crystallization and oligomeric structure of rat liver arginase. *Journal of molecular biology* 224(4): 1175-1177.

Karnoub, A. E. &Weinberg, R. A. (2008). Ras oncogenes: split personalities. *Nature reviews. Molecular cell biology* 9(7): 517-531.

Katz, M. E. &McCormick, F. (1997). Signal transduction from multiple Ras effectors. *Current opinion in genetics & development* 7(1): 75-79.

Kelley, G. G., Reks, S. E., Ondrako, J. M. &Smrcka, A. V. (2001). Phospholipase C(epsilon): a novel Ras effector. *EMBO J* 20(4): 743-754.

Khadem, F., Gao, X., Mou, Z., Jia, P., Movassagh, H., Onyilagha, C., Gounni, A. S., Wright, M. C. &Uzonna, J. E. (2016). Hepatic stellate cells regulate liver immunity to visceral leishmaniasis through P110delta-dependent induction and expansion of regulatory T cells in mice. *Hepatology* 63(2): 620-632.

Khosravi-Far, R., White, M. A., Westwick, J. K., Solski, P. A., Chrzanowska-Wodnicka, M., Van Aelst, L., Wigler, M. H. &Der, C. J. (1996). Oncogenic Ras activation of Raf/mitogen-activated protein kinase-independent pathways is sufficient to cause tumorigenic transformation. *Mol Cell Biol* 16(7): 3923-3933.

Khwaja, A., Rodriguez-Viciana, P., Wennstrom, S., Warne, P. H. &Downward, J. (1997). Matrix adhesion and Ras transformation both activate a phosphoinositide 3-OH kinase and protein kinase B/Akt cellular survival pathway. *EMBO J* 16(10): 2783-2793.

Knyphausen, P., Lang, F., Baldus, L., Extra, A. &Lammers, M. (2016). Insights into K-Ras 4B regulation by post-translational lysine acetylation. *Biol Chem*.

Kok, K., Geering, B. &Vanhaesebroeck, B. (2009). Regulation of phosphoinositide 3-kinase expression in health and disease. *Trends Biochem Sci* 34(3): 115-127.

Kordes, C. &Haussinger, D. (2013). Hepatic stem cell niches. *The Journal of clinical investigation* 123(5): 1874-1880.

Kordes, C., Sawitza, I., Gotze, S. &Haussinger, D. (2013). Hepatic stellate cells support hematopoiesis and are liver-resident mesenchymal stem cells. *Cellular physiology and biochemistry : international journal of experimental cellular physiology, biochemistry, and pharmacology* 31(2-3): 290-304.

Kordes, C., Sawitza, I., Gotze, S., Herebian, D. &Haussinger, D. (2014). Hepatic stellate cells contribute to progenitor cells and liver regeneration. *The Journal of clinical investigation* 124(12): 5503-5515.

Kordes, C., Sawitza, I., Gotze, S., Schumacher, E. &Haussinger, D. (2015). Beyond fibrosis: stellate cells as liver stem cells. *Z Gastroenterol* 53(12): 1425-1431.

Kurig, B., Shymanets, A., Bohnacker, T., Prajwal, Brock, C., Ahmadian, M. R., Schaefer, M., Gohla, A., Harteneck, C., Wymann, M. P., Jeanclos, E. &Nurnberg, B. (2009). Ras is an indispensable coregulator of the class IB phosphoinositide 3-kinase p87/p110gamma. *Proceedings of the National Academy of Sciences of the United States of America* 106(48): 20312-20317.

Laheru, D., Shah, P., Rajeshkumar, N. V., McAllister, F., Taylor, G., Goldsweig, H., Le, D. T., Donehower, R., Jimeno, A., Linden, S., Zhao, M., Song, D., Rudek, M. A. &Hidalgo, M. (2012). Integrated preclinical and clinical development of S-trans, trans-Farnesylthiosalicylic Acid (FTS, Salirasib) in pancreatic cancer. *Investigational new drugs* 30(6): 2391-2399.

Laplante, M. &Sabatini, D. M. (2009). mTOR signaling at a glance. *Journal of cell science* 122(Pt 20): 3589-3594.

Lavoie, H. &Therrien, M. (2015). Regulation of RAF protein kinases in ERK signalling. *Nature reviews. Molecular cell biology* 16(5): 281-298.

Lee, U. E. &Friedman, S. L. (2011). Mechanisms of hepatic fibrogenesis. *Best practice & research. Clinical gastroenterology* 25(2): 195-206.

Leevers, S. J., Vanhaesebroeck, B. &Waterfield, M. D. (1999). Signalling through phosphoinositide 3-kinases: the lipids take centre stage. *Curr Opin Cell Biol* 11(2): 219-225.

Liu, P., Gan, W., Inuzuka, H., Lazorchak, A. S., Gao, D., Arojo, O., Liu, D., Wan, L., Zhai, B., Yu, Y., Yuan, M., Kim, B. M., Shaik, S., Menon, S., Gygi, S. P., Lee, T. H., Asara, J. M., Manning, B. D., Blenis, J., Su, B. &Wei, W. (2013). Sin1 phosphorylation impairs mTORC2 complex integrity and inhibits downstream Akt signalling to suppress tumorigenesis. *Nature cell biology* 15(11): 1340-1350.

Lynch, S. J., Snitkin, H., Gumper, I., Philips, M. R., Sabatini, D. &Pellicer, A. (2015). The differential palmitoylation states of N-Ras and H-Ras determine their distinct Golgi subcompartment localizations. *J Cell Physiol* 230(3): 610-619.

Makbul, C., Constantinescu Aruxandei, D., Hofmann, E., Schwarz, D., Wolf, E. &Herrmann, C. (2013). Structural and thermodynamic characterization of Nore1-SARAH: a small, helical module important in signal transduction networks. *Biochemistry* 52(6): 1045-1054.

Matallanas, D., Birtwistle, M., Romano, D., Zebisch, A., Rauch, J., von Kriegsheim, A. &Kolch, W. (2011). Raf family kinases: old dogs have learned new tricks. *Genes & cancer* 2(3): 232-260.

Matozaki, T., Nakanishi, H. &Takai, Y. (2000). Small G-protein networks: their crosstalk and signal cascades. *Cellular signalling* 12(8): 515-524.

Matsunaga-Udagawa, R., Fujita, Y., Yoshiki, S., Terai, K., Kamioka, Y., Kiyokawa, E., Yugi, K., Aoki, K. &Matsuda, M. (2010). The scaffold protein Shoc2/SUR-8 accelerates the interaction of Ras and Raf. *The Journal of biological chemistry* 285(10): 7818-7826.

Mazhab-Jafari, M. T., Marshall, C. B., Smith, M. J., Gasmi-Seabrook, G. M., Stathopulos, P. B., Inagaki, F., Kay, L. E., Neel, B. G. &Ikura, M. (2015). Oncogenic and RASopathy-associated K-RAS mutations relieve membrane-dependent occlusion of the effector-binding site. *Proc Natl Acad Sci U S A* 112(21): 6625-6630.

Mezl, V. A. &Knox, W. E. (1977). Metabolism of arginine in lactating rat mammary gland. *Biochem J* 166(1): 105-113.

Morris, S. M., Jr. (2009). Recent advances in arginine metabolism: roles and regulation of the arginases. *British journal of pharmacology* 157(6): 922-930.

Mott, H. R. &Owen, D. (2015). Structures of Ras superfamily effector complexes: What have we learnt in two decades? *Critical reviews in biochemistry and molecular biology* 50(2): 85-133.

Nakhaei-Rad, S., Nakhaeizadeh, H., Gotze, S., Kordes, C., Sawitza, I., Hoffmann, M. J., Franke, M., Schulz, W. A., Scheller, J., Piekorz, R. P., Haussinger, D. &Ahmadian, M. R. (2016). The Role of Embryonic Stem Cell-expressed RAS (ERAS) in the Maintenance of Quiescent Hepatic Stellate Cells. *The Journal of biological chemistry* 291(16): 8399-8413.

Nan, X., Collisson, E. A., Lewis, S., Huang, J., Tamguney, T. M., Liphardt, J. T., McCormick, F., Gray, J. W. &Chu, S. (2013). Single-molecule superresolution imaging allows quantitative analysis of RAF multimer formation and signaling. *Proceedings of the National Academy of Sciences of the United States of America* 110(46): 18519-18524.

Nassar, N., Horn, G., Herrmann, C., Block, C., Janknecht, R. &Wittinghofer, A. (1996). Ras/Rap effector specificity determined by charge reversal. *Nat Struct Biol* 3(8): 723-729.

Nassar, N., Horn, G., Herrmann, C., Scherer, A., McCormick, F. &Wittinghofer, A. (1995). The 2.2 A crystal structure of the Ras-binding domain of the serine/threonine kinase c-Raf1 in complex with Rap1A and a GTP analogue. *Nature* 375(6532): 554-560.

Neel, N. F., Martin, T. D., Stratford, J. K., Zand, T. P., Reiner, D. J. &Der, C. J. (2011). The RalGEF-Ral Effector Signaling Network: The Road Less Traveled for Anti-Ras Drug Discovery. *Genes & cancer* 2(3): 275-287.

Oertli, B., Han, J., Marte, B. M., Sethi, T., Downward, J., Ginsberg, M. &Hughes, P. E. (2000). The effector loop and prenylation site of R-Ras are involved in the regulation of integrin function. *Oncogene* 19(43): 4961-4969.

Pacold, M. E., Suire, S., Perisic, O., Lara-Gonzalez, S., Davis, C. T., Walker, E. H., Hawkins, P. T., Stephens, L., Eccleston, J. F. &Williams, R. L. (2000). Crystal structure and functional analysis of Ras binding to its effector phosphoinositide 3-kinase gamma. *Cell* 103(6): 931-943.

Parada, L. F., Tabin, C. J., Shih, C. &Weinberg, R. A. (1982). Human EJ bladder carcinoma oncogene is homologue of Harvey sarcoma virus ras gene. *Nature* 297(5866): 474-478.

Parker, J. A. &Mattos, C. (2015). The Ras-Membrane Interface: Isoform-specific Differences in The Catalytic Domain. *Molecular cancer research : MCR* 13(4): 595-603.

Paz, A., Haklai, R., Elad-Sfadia, G., Ballan, E. &Kloog, Y. (2001). Galectin-1 binds oncogenic H-Ras to mediate Ras membrane anchorage and cell transformation. *Oncogene* 20(51): 7486-7493.

Repasky, G. A., Chenette, E. J. &Der, C. J. (2004a). Renewing the conspiracy theory debate: does Raf function alone to mediate Ras oncogenesis? *Trends Cell Biol* 14(11): 639-647.

Repasky, G. A., Chenette, E. J. &Der, C. J. (2004b). Renewing the conspiracy theory debate: does Raf function alone to mediate Ras oncogenesis? *Trends in cell biology* 14(11): 639-647.

Rocks, O., Peyker, A., Kahms, M., Verveer, P. J., Koerner, C., Lumbierres, M., Kuhlmann, J., Waldmann, H., Wittinghofer, A. &Bastiaens, P. I. (2005). An acylation cycle

regulates localization and activity of palmitoylated Ras isoforms. *Science* 307(5716): 1746-1752.

Rodriguez-Viciana, P. &McCormick, F. (2006). Ras ubiquitination: coupling spatial sorting and signal transmission. *Cancer Cell* 9(4): 243-244.

Rodriguez-Viciana, P., Oses-Prieto, J., Burlingame, A., Fried, M. &McCormick, F. (2006). A phosphatase holoenzyme comprised of Shoc2/Sur8 and the catalytic subunit of PP1 functions as an M-Ras effector to modulate Raf activity. *Molecular cell* 22(2): 217-230.

Rodriguez-Viciana, P., Sabatier, C. &McCormick, F. (2004). Signaling specificity by Ras family GTPases is determined by the full spectrum of effectors they regulate. *Mol Cell Biol* 24(11): 4943-4954.

Rodriguez-Viciana, P., Warne, P. H., Khwaja, A., Marte, B. M., Pappin, D., Das, P., Waterfield, M. D., Ridley, A. &Downward, J. (1997). Role of phosphoinositide 3-OH kinase in cell transformation and control of the actin cytoskeleton by Ras. *Cell* 89(3): 457-467.

Rojas, A. M., Fuentes, G., Rausell, A. &Valencia, A. (2012). The Ras protein superfamily: evolutionary tree and role of conserved amino acids. *The Journal of cell biology* 196(2): 189-201.

Roskoski, R., Jr. (2010). RAF protein-serine/threonine kinases: structure and regulation. *Biochemical and biophysical research communications* 399(3): 313-317.

Rotblat, B., Belanis, L., Liang, H., Haklai, R., Elad-Zefadia, G., Hancock, J. F., Kloog, Y. &Plowman, S. J. (2010). H-Ras nanocluster stability regulates the magnitude of MAPK signal output. *PloS one* 5(8): e11991.

Rotblat, B., Niv, H., Andre, S., Kaltner, H., Gabius, H. J. &Kloog, Y. (2004). Galectin-1(L11A) predicted from a computed galectin-1 farnesyl-binding pocket selectively inhibits Ras-GTP. *Cancer Res* 64(9): 3112-3118.

Santos, E., Tronick, S. R., Aaronson, S. A., Pulciani, S. &Barbacid, M. (1982). T24 human bladder carcinoma oncogene is an activated form of the normal human homologue of BALB- and Harvey-MSV transforming genes. *Nature* 298(5872): 343-347.

Scheele, J. S., Ripple, D. &Lubbert, M. (2000). The role of ras and other low molecular weight guanine nucleotide (GTP)-binding proteins during hematopoietic cell differentiation. *Cellular and molecular life sciences : CMLS* 57(13-14): 1950-1963.

Scheffzek, K. &Ahmadian, M. R. (2005). GTPase activating proteins: structural and functional insights 18 years after discovery. *Cellular and molecular life sciences : CMLS* 62(24): 3014-3038.

Scheffzek, K., Ahmadian, M. R. &Wittinghofer, A. (1998). GTPase-activating proteins: helping hands to complement an active site. *Trends Biochem Sci* 23(7): 257-262.

Schroder, W. A., Buck, M., Cloonan, N., Hancock, J. F., Suhrbier, A., Sculley, T. &Bushell, G. (2007). Human Sin1 contains Ras-binding and pleckstrin homology domains and suppresses Ras signalling. *Cellular signalling* 19(6): 1279-1289.

Seelenmeyer, C., Stegmayer, C. &Nickel, W. (2008). Unconventional secretion of fibroblast growth factor 2 and galectin-1 does not require shedding of plasma membrane-derived vesicles. *FEBS Lett* 582(9): 1362-1368.

Shalom-Feuerstein, R., Plowman, S. J., Rotblat, B., Ariotti, N., Tian, T., Hancock, J. F. &Kloog, Y. (2008). K-ras nanoclustering is subverted by overexpression of the scaffold protein galectin-3. *Cancer research* 68(16): 6608-6616.

Shih, T. Y., Weeks, M. O., Troxler, D. H., Coffin, J. M. &Scolnick, E. M. (1978). Mapping host range-specific oligonucleotides within genomes of the ecotropic and mink cell focus-inducing strains of Moloney murine leukemia virus. *J Virol* 26(1): 71-83.

Shymanets, A., Prajwal, Bucher, K., Beer-Hammer, S., Harteneck, C. &Nurnberg, B. (2013). p87 and p101 subunits are distinct regulators determining class IB phosphoinositide 3-kinase (PI3K) specificity. *The Journal of biological chemistry* 288(43): 31059-31068.

Spoerner, M., Herrmann, C., Vetter, I. R., Kalbitzer, H. R. &Wittinghofer, A. (2001). Dynamic properties of the Ras switch I region and its importance for binding to effectors. *Proc Natl Acad Sci U S A* 98(9): 4944-4949.

Sung, P. J., Tsai, F. D., Vais, H., Court, H., Yang, J., Fehrenbacher, N., Foskett, J. K. &Philips, M. R. (2013). Phosphorylated K-Ras limits cell survival by blocking Bcl-xL sensitization of inositol trisphosphate receptors. *Proc Natl Acad Sci U S A* 110(51): 20593-20598.

Takahashi, K., Mitsui, K. &Yamanaka, S. (2003). Role of ERas in promoting tumour-like properties in mouse embryonic stem cells. *Nature* 423(6939): 541-545.

Takahashi, K., Nakagawa, M., Young, S. G. &Yamanaka, S. (2005). Differential membrane localization of ERas and Rheb, two Ras-related proteins involved in the phosphatidylinositol 3-kinase/mTOR pathway. *The Journal of biological chemistry* 280(38): 32768-32774.

Tian, T., Harding, A., Inder, K., Plowman, S., Parton, R. G. &Hancock, J. F. (2007). Plasma membrane nanoswitches generate high-fidelity Ras signal transduction. *Nat Cell Biol* 9(8): 905-914.

Vandal, G., Geiling, B. &Dankort, D. (2014). Ras effector mutant expression suggest a negative regulator inhibits lung tumor formation. *PloS one* 9(1): e84745.

Vanhaesebroeck, B., Ali, K., Bilancio, A., Geering, B. &Foukas, L. C. (2005). Signalling by PI3K isoforms: insights from gene-targeted mice. *Trends Biochem Sci* 30(4): 194-204.

Vanhaesebroeck, B., Guillermet-Guibert, J., Graupera, M. &Bilanges, B. (2010). The emerging mechanisms of isoform-specific PI3K signalling. *Nature reviews. Molecular cell biology* 11(5): 329-341.

Vasta, G. R., Feng, C., Bianchet, M. A., Bachvaroff, T. R. &Tasumi, S. (2015). Structural, functional, and evolutionary aspects of galectins in aquatic mollusks: From a sweet tooth to the Trojan horse. *Fish & shellfish immunology* 46(1): 94-106.

Vavvas, D., Li, X., Avruch, J. &Zhang, X. F. (1998). Identification of Nore1 as a potential Ras effector. *The Journal of biological chemistry* 273(10): 5439-5442.

Vetter, I. R. &Wittinghofer, A. (2001). The guanine nucleotide-binding switch in three dimensions. *Science* 294(5545): 1299-1304.

Volinia, S., Hiles, I., Ormondroyd, E., Nizetic, D., Antonacci, R., Rocchi, M. &Waterfield, M. D. (1994). Molecular cloning, cDNA sequence, and chromosomal localization of the human phosphatidylinositol 3-kinase p110 alpha (PIK3CA) gene. *Genomics* 24(3): 472-477.

Wang, M. T., Holderfield, M., Galeas, J., Delrosario, R., To, M. D., Balmain, A. &McCormick, F. (2015). K-Ras Promotes Tumorigenicity through Suppression of Non-canonical Wnt Signaling. *Cell* 163(5): 1237-1251.

Wang, Y., Zhou, Y. &Graves, D. T. (2014). FOXO transcription factors: their clinical significance and regulation. *BioMed research international* 2014: 925350.

Wennerberg, K., Rossman, K. L. &Der, C. J. (2005). The Ras superfamily at a glance. *Journal of cell science* 118(Pt 5): 843-846.

White, M. A., Nicolette, C., Minden, A., Polverino, A., Van Aelst, L., Karin, M. &Wigler, M. H. (1995). Multiple Ras functions can contribute to mammalian cell transformation. *Cell* 80(4): 533-541.

Wohlgemuth, S., Kiel, C., Kramer, A., Serrano, L., Wittinghofer, F. &Herrmann, C. (2005). Recognizing and defining true Ras binding domains I: biochemical analysis. *Journal of molecular biology* 348(3): 741-758.

Wurtzel, J. G., Lee, S., Singhal, S. S., Awasthi, S., Ginsberg, M. H. &Goldfinger, L. E. (2015). RLIP76 regulates Arf6-dependent cell spreading and migration by linking ARNO with activated R-Ras at recycling endosomes. *Biochemical and biophysical research communications* 467(4): 785-791.

Yang, M. H., Laurent, G., Bause, A. S., Spang, R., German, N., Haigis, M. C. &Haigis, K. M. (2013). HDAC6 and SIRT2 regulate the acetylation state and oncogenic activity of mutant K-RAS. *Molecular cancer research : MCR* 11(9): 1072-1077.

Yang, M. H., Nickerson, S., Kim, E. T., Liot, C., Laurent, G., Spang, R., Philips, M. R., Shan, Y., Shaw, D. E., Bar-Sagi, D., Haigis, M. C. &Haigis, K. M. (2012). Regulation of RAS oncogenicity by acetylation. *Proc Natl Acad Sci U S A* 109(27): 10843-10848.

Yin, C., Evason, K. J., Asahina, K. &Stainier, D. Y. (2013). Hepatic stellate cells in liver development, regeneration, and cancer. *The Journal of clinical investigation* 123(5): 1902-1910.

Yu, Y., Liang, D., Tian, Q., Chen, X., Jiang, B., Chou, B. K., Hu, P., Cheng, L., Gao, P., Li, J. &Wang, G. (2014). Stimulation of somatic cell reprogramming by ERas-Akt-FoxO1 signaling axis. *Stem cells* 32(2): 349-363.

Zheng, Z. Y., Cheng, C. M., Fu, X. R., Chen, L. Y., Xu, L., Terrillon, S., Wong, S. T., Bar-Sagi, D., Songyang, Z. &Chang, E. C. (2012). CHMP6 and VPS4A mediate the recycling of Ras to the plasma membrane to promote growth factor signaling. *Oncogene* 31(43): 4630-4638.

Zhou, M., Wiener, H., Su, W., Zhou, Y., Liot, C., Ahearn, I., Hancock, J. F. &Philips, M. R. (2016). VPS35 binds farnesylated N-Ras in the cytosol to regulate N-Ras trafficking. *The Journal of cell biology* 214(4): 445-458.

Zhou, Y. &Hancock, J. F. (2015). Ras nanoclusters: Versatile lipid-based signaling platforms. *Biochimica et biophysica acta* 1853(4): 841-849.

Zhou, Y., Liang, H., Rodkey, T., Ariotti, N., Parton, R. G. &Hancock, J. F. (2014). Signal integration by lipid-mediated spatial cross talk between Ras nanoclusters. *Mol Cell Biol* 34(5): 862-876.

Acknowledgment

Foremost, I would like to express my sincere gratitude to my advisor Prof. Dr. Mohammad Reza Ahmadian for the continuous support of my Ph.D. study and research, for his patience, motivation, enthusiasm, and immense knowledge. His guidance helped me in all the time of research and writing of this thesis. This journey would not have been possible without his support.

Also my deep appreciation and thanks goes to my co-supervisor Prof. Dr. Dieter Willbold for his precious support.

I am especially grateful to Prof. Dr. Jürgen Scheller and Dr. Roland Piekorz for their support, and advices.

My sincere thanks go to all my friends in Düsseldorf, specially Saeideh Nakhaei-Rad, Ehsan Amin, and Kazem Nouri for support and a very fruitful collaboration.
My thanks also go to all my colleagues in the Institute of Biochemistry and Molecular biology II, especially Petra Opree, Ilse Meyer, Freshteh Kamrani, and Zeynap Tokyurek for helping me in this way.

I would like to give special thanks to Dr. Radovan Dvorsky for his time and invaluable support.

I give my very special thanks to my daughter Bahar and my wife Neda for emotionally supporting and encouraging me in all my pursuits and inspiring me to follow my dreams.
Finally I dedicate this thesis to my mother and the soul of my father who place is in my heart.

Curriculum Vitae

Personal data

Date of Birth: 9th August 1969
Sex: Male
Country of Birth: Iran
Address: Institute of Biochemistry and Molecular Biology II, University Hospital Dusseldorf, Universität Str.1, Building 22.03, 40225 Düsseldorf, Germany.
Address (home): Reisholzer Str. 12, Dusseldorf, Germany
Telephone (mobile): +4917641730545
E-Mail Address: Hossein.Nakhaeizadeh@uni-duesseldorf.de
Marital Status: Married, one child

Academic education

2009-2011, M.Sc. in Cellular Molecular Biology, Ferdowsi University of Mashhad, Mashhad, Iran
Thesis Title: Investigating the cytotoxic and DNA damaging effects of sesquiterpene ferutinin on several carcinoma cell lines
Supervised by Dr. M. Matin
1994-1998, B.Sc. in Microbiology, Isfahan University, Isfahan, Iran

Career summary

1998-2012 supervisor of quality control section in Daroo-Sazi Samen pharmaceutical Co., Mashhad, Iran

List of publications

Nakhaei-Rad S, **Nakhaeizadeh H**, Kordes C, Cirstea IC, Schmick M, Dvorsky R, Bastiaens PI, Häussinger D, Ahmadian MR. The Function of Embryonic Stem Cell-expressed RAS (E-RAS), a Unique RAS Family Member, Correlates with Its Additional Motifs and Its Structural Properties. J Biol Chem. 2015 Jun 19; 290(25):15892-903

Blazevits O, Mideksa YG, Solman M, Ligabue A, Ariotti N, **Nakhaeizadeh H**, Fansa EK, Papageorgiou AC, Wittinghofer A, Ahmadian MR, Abankwa D. Galectin-1 dimers can scaffold Raf-effectors to increase H-Ras nanoclustering. Sci Rep Sci Rep. 2016 Apr 18;6:24165.

Nakhaei-Rad N, **Nakhaeizadeh H**, Götze S, Kordes C, Sawitza I, Franke M, Scheller J, Piekorz RP, Häussinger D, Ahmadian MR. Expression, epigenetical regulation and signaling network of embryonic stem cell-expressed RAS in hepatic stellate cells J Biol Chem. 2016 Apr 15;291(16):8399-413.

Matin MM, **Nakhaeizadeh H**, Bahrami AR, Iranshahi M, Arghiani N, Rassouli FB. Ferutinin, an apoptosis inducing terpenoid from Ferula ovina. Asian Pac J Cancer Prev. 2014;15(5):2123-8

The RAS-effector interface: Isoform-specific differences in the effector binding regions **Hossein Nakhaeizadeh**, Ehsan Amin, Saeideh Nakhaei-Rad, Radovan Dvorsky, Mohammad Reza Ahmadian PLoS One 11:e0167145

Nakhaeizadeh H, Nakhaei-Rad N, Amin E, Nouri K, Dvorsky R, Kordes C, Häussinger D, Ahmadian MR. The impact of the interaction between Embryonic stem cell-expressed Ras (E-Ras) and Arginase-1 in hepatic stellate cells (in preparation)

Eidesstattliche Erklärung zur Dissertation

Hiermit versichere ich, dass die vorliegende Dissertation von mir selbstständig und ohne unzulässige fremde Hilfe unter Beachtung der Grundsätze zur Sicherung guter wissenschaftlicher Praxis an der Heinrich-Heine-Universität Düsseldorf verfasst worden ist. Die Dissertation wurde in der vorgelegten oder in ähnlicher Form noch bei keiner anderen Institution eingereicht. Ich habe bisher keine erfolglosen Promotionsversuche unternommen.
Düsseldorf, den 17.10.2016

Hossein Nakhaeizadeh